Integration of circadian clocks and metabolism in the hypothalamus

A thesis submitted to the University of Manchester for the degree of Doctor of Philosophy in the Faculty of Biology, Medicine and Health

2018

Adam G. Watson

School of Medical Sciences, Division of Diabetes, Endocrinology and Gastroenterology

Table of Contents

Final word count: 73,560

Abbreviations

ACTH	Adrenocorticotropic hormone
ADP50	Half-duration of action potential
AgRP	Agouti-related peptide
AMPAR	α-amino-3-hydroxy-5-methyl-4-isoxazolepropionic acid receptor
αMSH	α-melanocyte stimulating hormone
AP5	2-Amino-5-phosphonopentanoic acid
AP	Action potential
ARC	Arcuate nucleus of the hypothalamus
ATP	Adenosine triphosphate
BBB	Blood-brain barrier
BK	Big conductance calcium-dependent potassium channels
Bmal1	Brain and Muscle ARNT-Like 1
CCGs	Clock controlled genes`
CK1ε	Casein kinase 1 epsilon
CNQX	6-Cyano-7-nitroquinoxaline-2,3-dione
CNS	Central nervous system
Cry	Cryptochrome
CT	Circadian time
DD	Constant darkness
DLAMO	Depolarised low amplitude membrane oscillations
DMH	Dorsomedial hypothalamus
ECs	Endothelial cells
EPSC	Excitatory postsynaptic current
FAA	Food anticipatory activity
GABA	Gamma-aminobutyric acid
GAD	Glutamic acid decarboxylase
GFAP	Glial fibrillary acidic protein
GFP	Green fluorescent protein
GHSR	Growth hormone secretagogue receptor
GIRK	G-protein-linked inwardly rectifying potassium channel
Hb	Habenula
ipRGCs	Intrinsically photosensitive retinal ganglion cells
IPSC	Inhibitory postsynaptic current
IR	Immunoreactivity
ISI	Interspike interval
KATP	ATP-sensitive potassium channel
latARC	Lateral ARC
LD	Light-dark cycle
LepRb	Long isoform leptin receptor
mARC	Medial ARC
MBH	Mediobasal hypothalamus
MC4R	Melanocortin receptor type 4
ME	Median eminence

MUA	Multiunit activity
NMDAR	N-methyl-D-aspartate receptor
NPY	Neuropeptide-Y
Per	Period
PER2::LUC	PERIOD2::LUCIFERASE reporter
pMEA	Perforated multielectrode array
POMC	Proopiomelanocortin
PVN	Paraventricular nucleus of the hypothalamus
SCN	Suprachiasmatic nucleus
rAAV	Recombinant Adeno-associated virus
RFS	Restricted feeding schedule
R_{input}	Input resistance
RMP	Resting membrane potential
SAP	Saporin
SFR	Spontaneous firing rate
TEA	Tetraethyl ammonium
TH	Tyrosine hydroxylase
TTFL	Transcription-translation feedback loop
VMH	Ventromedial hypothalamus
TTX	Tetrodotoxin
VGAT	Vesicular GABA transporter
VGLUT	Vesicular glutamate transporter
Y2	NPY receptor isoform 2
ZT	Zeitgeber time
3V	Third ventricle
4-AP	4-Aminopyridine

Interaction of circadian clocks and metabolism in the hypothalamus

Adam G. Watson, PhD Neuroscience, 2018

Recent evidence implicates circadian disruption in the increasing prevalence of obesity. This disruption is thought to occur partly due to aberrant circadian regulation in brain regions that are critical to feeding. The transcription-translation feedback loop (TTFL) drives suprachiasmatic neurons in the mammalian master clock to depolarise and increase action potential (AP) firing during the day and to hyperpolarise and reduce AP firing at night. Intriguingly, core components of the TTFL such as *Period1* (*Per1*) and *Cryptochrome1/2* (*Cry1/2*) are also rhythmically expressed in other brain regions including the arcuate nuclei of the hypothalamus (ARC). ARC neurons are critical sensors of metabolic information and project to downstream brain regions to influence appetite and feeding homeostasis. However, it is currently unknown whether local oscillations in the molecular clockwork drive daily rhythms in ARC neuronal activity.

Using a mouse in which *Per1* promoter activity is reported by Venus protein (*Per1*::Venus), electrophysiological recordings were made from *Per1*::Venus positive ARC neurons maintained in acute adult brain slices. *Per1*::Venus positive neurons were significantly more active at night, firing APs at ~4Hz, compared to ~2Hz during the day and received more frequent GABAergic input during the day than at night. Importantly, daily variation in firing rate was only observed in neurons located in lateral areas of the ARC. We postulate that rhythmic inhibitory GABA is responsible for generating daily and circadian changes in latARC electrical output, and that this signal originates from a population of GABAergic neurons within the ARC.

To establish whether the day-night change in firing of ARC neurons is dependent on an intact TTFL, we made whole-cell recordings from slices prepared from mice lacking *Cry1/2* (*Cry1*$^{-/-}$*Cry2*$^{-/-}$), and found daily variations in firing rate to be absent. Notably, the activity of *Cry1*$^{-/-}$*Cry2*$^{-/-}$ ARC neurons was constitutively elevated across the day-night cycle, which highlights the role of the circadian molecular clockwork in setting excitability in neurons with an intact clock. To confirm that expression of core clock components locally in ARC is responsible for driving daily rhythms we performed bilateral microinjection of rAAV2-Cre-GFP (or control rAAV2-GFP) viral vectors into the ARC of *Bmal1*$^{fl/fl}$ mice, which led to a cre-dependent increase in daytime firing. We also employed whole-cell methods to record the firing activity of neuropeptide-Y-expressing neurons (NPY-humanised Renilla Green Fluorescent Protein; NPY-hrGFP), which play an established role as stimulators of appetite. However, NPY-hrGFP neurons fired APs at a consistent rate across the day. Collectively, these results demonstrate that the TTFL drives daily changes in electrical activity in a unique sub-population of ARC neurons that not does not overlap with those that express NPY. This study has key implications for our understanding of how the TTFL influences the excitability of neurons in an extra-SCN oscillator with well-established role in feeding homeostasis. Ultimately, this study begins to elucidate how one critical brain area may contribute to a network of circadian oscillators which are important for normal body weight control.

Declaration

No portion of the work referred to in the thesis has been submitted in support of an application for another degree or qualification of this or any other university or other institute of learning.

A part of the work presented in Chapter 1 was conducted by Dr. Mino Belle, The University of Manchester. For the specific contribution please refer to Chapter 1 results.

Copyright statement

Acknowledgements

As I near the end of my PhD, I reflect on the generous support of all those who made this time so scientifically stimulating and enjoyable. First of all I would like to extend my thanks to the BBSRC for funding this project and my studies through award of a studentship grant to Prof. Hugh Piggins and Dr. David Bechtold. This project was also supported by the Mark Younger scholarship which was awarded to me by a university alumnus with passion for supporting blue skies physiological research. Thanks Mark for your support - it was a pleasure meeting with you and keeping you up to date with our progress.

I would like to express a huge thank you to my supervisor Prof. Hugh Piggins for his advice, help and support over the last 4 years as a doctoral student, and for his comments on this thesis. I feel that the successes of this project are largely attributable to our fantastic working relationship. I thoroughly enjoyed our scientific discussions and am grateful for his support with conference trips, which I feel will be of great personal benefit to me in the future. I would also like to thank my co-supervisor Dr. David Bechtold who has offered invaluable advice and support to me throughout this project. His expertise has greatly complemented that of Prof. Hugh Piggins and together they have formed an excellent supervisory team.

I am hugely indebted to Dr. Mino Belle for his training and assistance with electrophysiological methods employed for the work presented in this thesis. I place great value on his advice and friendship over the past years. It was a pleasure to work with him.

Thanks to Dr. Sven Wegner for spending weeks of his own precious time to take me through the fundamentals of whole-cell electrophysiology at the start of my studies. I would next like to extend thanks to the rest of the Piggins lab, past and present, who have helped me in some way. In no particular order; thanks to Dr. Alun Hughes, Dr. Bea Otalora, Rebecca Northeast, Cheryl Petit, Natasza Klas, Dr. Alok Joshi, Carla Santos, Ms. Rayna Samuels, Dr. Joe Timothy, Mohamed Mansour, Lukasz Chrobok, Taghreed Almansouri, Adriana Basnakova and Abi Pienaar.

I am also grateful to Dr. Lauren Walmsley for training and assistance with the *in vivo* methods presented in the second results chapter of this thesis.

On a personal level I would give a special mention to my friends who have provided unwavering support throughout my time in Manchester. There are too many to list, however I would like to give a special mention to Alex Palmer, Mike Shipton, Elliot Gerrard, Becca Northeast, Jack Reed and Nick Keith for supporting me through my studies. Also thanks to all my friends from Thame for your support.

I have outstandingly supportive parents without whom I would definitely not be where I am today. My mum Fran Watson, guided me through early academic struggles at school and has continued to support me in everything I do to this day. My dad Mark Watson has always provided me with exceptional advice and always has a beer ready for when I return home. My parents, both scientists themselves, have always supported their kids in whatever they have wanted to do, be it studying for a PhD, becoming a world-class flautist, a Thames Valley Police Officer or on the brink of becoming the next top sports coach. On that note, thanks to my siblings Suzie, Mash, Dave and Sully for always asking me what circadian means. If they ever read this (hopefully), they're sure to understand what it means by the end.

Last but certainly not least, I would like to send special thanks to Ms. Beth Morgan for your kindness and love throughout this process. You have given me the support that any person would dream of. Without a doubt my successes during this project are attributable to your loving support. Thank you!

As a student in year 13 I was asked to answer some short questions for entry into the yearbook, which was to serve as a memento as we all went off to find jobs or seek further study. One question stood out for me in particular - "what/where will you be in 10years time?" My answer - PhD Neuroscience. Thanks to everybody has helped me on my journey towards achieving this.

Introduction

Introduction

An almost ubiquitous range of eukaryotic and prokaryotic organisms have evolved an innate biological timekeeping mechanism to counteract the selective pressures introduced by the periodic cycling of day and night (Bell-Pedersen et al., 2005, Johnson et al., 1996, Dunlap, 1999). In parallel with daily changes in environmental conditions, behaviour and physiological processes are rhythmically partitioned into temporal niches to exploit optimal conditions. In humans and most mammalian species, there are ~24-hour rhythms in circulating hormones, metabolism, blood pressure and body temperature as well as many other physiological parameters (Honma et al., 1983, Cameron et al., 2008, Eckel-Mahan and Sassone-Corsi, 2009). Ultimately, the adaptive advantage conveyed in the ability to temporally compartmentalise behaviour and physiology increases an organisms health, survival and reproductive success (Gachon et al., 2004, Fu and Lee, 2003).

Circadian (derived from approximately – *circa*; a day - *diem*) rhythms rely upon the function of an internal clockwork collectively coined the circadian system, that continues to free-run under constant environmental conditions (Stephan and Zucker, 1972, Panda et al., 2002b, Mrosovsky et al., 1989). Robust temporal precision is an inherent property of the circadian system, but the phase of rhythms in output behaviour and physiology flexibly responds to external time cues or zeitgebers. While light exposure is the primary entrainment signal for the circadian system, numerous other zeitgebers including food intake, social interaction and exercise adjust the phase of the internal clockwork and resulting output circadian rhythms (Hastings et al., 1992, Mrosovsky, 1996, Maywood et al., 1997, Mohawk et al., 2012, Hughes and Piggins, 2012).

Captivating progress in the field has sparked intense experimentation into the underlying molecular and neurophysiological mechanisms responsible for the generation of circadian rhythms in a range of model organisms. Parallel to studying the fundamental rhythm-generating machinery, another challenge is how the circadian system may interact with disease states in a causal and consequential manner as a broad range of health

conditions, including metabolic disturbances, are associated with disrupted physiological rhythms (Foster et al., 2013, Turek et al., 2005).

An approximate location for the mammalian circadian clock was suggested as early as 1965 by Curt Richter, and was subsequently confirmed in 1972 when two groups simultaneously published results demonstrating the importance of the suprachiasmatic nucleus of the hypothalamus (SCN) in regulating circadian rhythmicity of behaviour and the endocrine system (Moore and Eichler, 1972, Stephan and Zucker, 1972). The SCN in mice is a collection of ~10000 cells either side of the third ventricle. The dominance of the SCN in propagating daily rhythms in behaviour and physiology was subsequently demonstrated *in vivo;* critically behavioural circadian rhythms in SCN-lesioned animals can be restored by SCN transplants (Ralph et al., 1990).

An extensive array of further studies has established the importance of the SCN as the master-synchroniser of circadian rhythms in mammals; however the SCN is not unique in its capability to oscillate with a circadian frequency. Most tissues and cell types in the body display circadian patterns of gene expression when isolated from SCN, including extra-SCN regions of the central nervous system (CNS, Tosini and Menaker, 1996, Yamazaki et al., 2000, Brown and Azzi, 2013). A significant question is how cellular clocks throughout the body are synchronised to one another and whether the SCN and its functional efferent pathways provide a coherent timekeeping signal to couple and synchronise peripheral clocks. The SCN are important for rhythmic locomotor activity and hormone secretion (Lehman et al., 1987). Light information is perceived by the SCN via intrinsically photosensitive retinal ganglion cells (ipRGCs) which express the photopigment, melanopsin (Fernandez et al., 2016). These cells form the retinohypothalamic tract which terminates in the SCN, onto neurons that express vasoactive intestinal polypeptide and arginine vasopressin. This projection is important for light-induced phase-resetting of the SCN clock (Antle et al., 2009, Golombek and Rosenstein, 2010). Coherent SCN activity which is entrained to environmental signals can then synchronise populations of weakly coupled or non-coupled cells throughout the periphery.

The circadian molecular clockwork

In cells of the SCN, other brain regions and peripheral tissues a conserved network of interlocked transcription-translation feedback loops (TTFL, Figure 1) are responsible for driving 24-hour rhythms in cellular physiology (Balsalobre et al., 2000, Panda et al., 2002a, Panda et al., 2002b, Buhr and Takahashi, 2013, Partch et al., 2014). The first evidence that suggested genetic oscillations may underlie measurable circadian rhythms originated from mutagenesis screening studies in Drosophila, which demonstrated the importance of *Period (Per)* in maintaining normal 24-hour rhythms in locomotor activity (Konopka and Benzer, 1971). Genetic lesioning experiments also led to the discovery of the *Circadian Locomotor Output Cycle Kaput* (*Clock*) in mammals; targeted ablation of *Clock* and the resulting severe arrhythmia, led to postulation that similar genetic timekeeping mechanisms are conserved in evolution (Vitaterna et al., 1994).

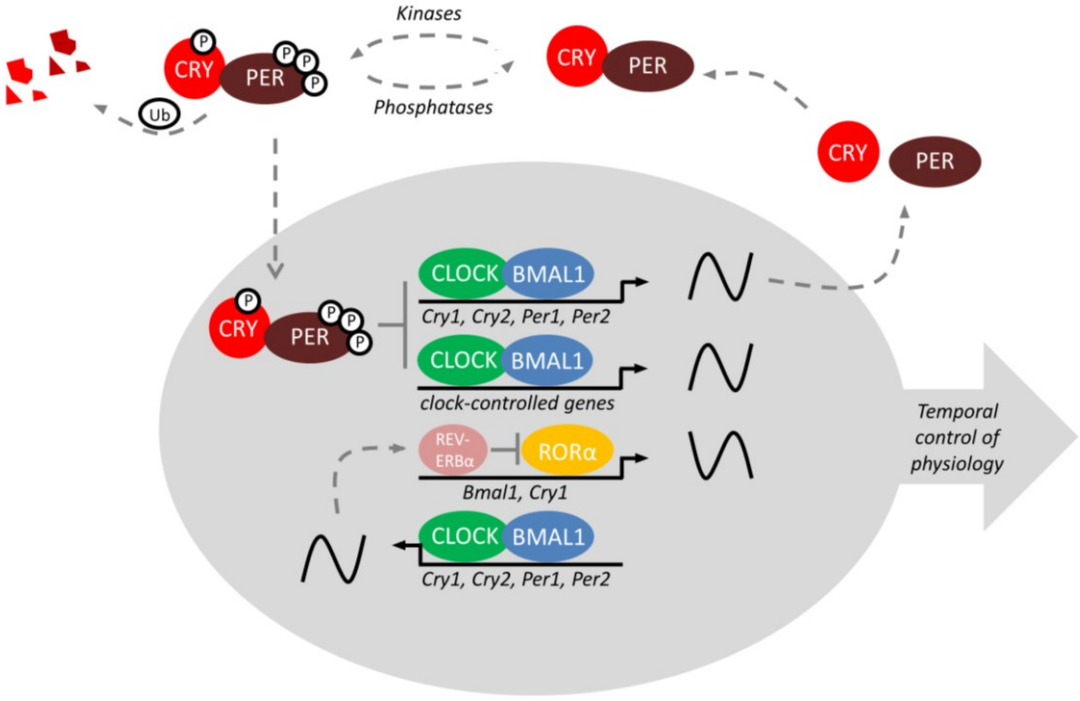

Figure 1: The cell-autonomous molecular clock in mammals is made up of two interlocking transcription-translation feedback loops (TTFLs). The core TTFL is generated by four key clock proteins. CLOCK and BMAL1 function as activators and PER and CRY as repressors of the core TTFL mechanism. CLOCK- BMAL1 heterodimers activate the transcription of *Per* and *Cry* genes as well as other clock-controlled genes involved in rhythmic physiological outputs. PER and CRY proteins dimerise in the cytoplasm, translocate to the nucleus, and then interact with CLOCK-BMAL1 inhibiting transcriptional activation. PER and CRY proteins are degraded through ubiquitin-dependent pathways (Ub). A second TTFL is formed through transcriptional activation by RORα, and repression by REV-ERBα. Kinases (for example CK1ε) and phosphatases regulate the localisation and stability of clock proteins. (Figure adapted from Partch et al. 2014).

Subsequently, a series of functional studies and genetic lesions led to the identification of clock genes that interact to form the basic TTFL mechanism. A functional analysis of CLOCK revealed its role as a positive transcription factor of the TTFL by forming a PAS-dependent heterodimer with BMAL1 (Bunger et al., 2000, Gekakis et al., 1998). The CLOCK-BMAL1 heterodimer complex then upregulates the expression of target genes through binding to Enhancer box (E-box) elements on target genes including the mammalian homologues *Per1,2,3* and *Cryptochrome 1* and *2* and other clock controlled genes (CCGs) (Bae et al., 2001, Ko and Takahashi, 2006, Yoo et al., 2005).

At the behavioural and molecular level, at least one member of *Per* and *Cry* are required for the maintenance of robust rhythms, as *Per1*$^{-/-}$*Per2*$^{-/-}$ mice and *Cry1*$^{-/-}$*Cry2*$^{-/-}$ mice do not have intrinsic circadian rhythmicity (Bae et al., 2001, Zheng et al., 1999). PER-CRY dimerise before translocation back into the nucleus and inhibit further transcriptional activity of CLOCK/BMAL1 (Sato et al., 2006, Griffin et al., 1999). Subsequently, the PER-CRY heterodimers drive further CCG expression while the CLOCK-BMAL1 complex is released to initiate the TFFL (Balsalobre et al., 2000).

The CLOCK-BMAL1 dimers also initiate E-box mediated transcription of a second feedback loop which runs in parallel with the loop described above. Orphan nuclear-receptors genes *Rev-erbα/β* and *Rorα/β* are major antagonistic elements of the TTFL that down-regulate and promote the expression of *Bmal1* respectively (Guillaumond et al., 2005, Preitner et al., 2002). This additional transcriptional loop is essential to circadian rhythm generation and does not simply modulate the phase of positive and negative component rhythms (Cho et al., 2012). Although the above auto-regulatory feedback loops are recognised as the principal oscillatory components, the stability and temporal precision of core clock genes is further enhanced by histone-dependent chromatin remodelling and enzymes involved in degradation of PER such as CK1delta/epsilon (Meng et al., 2008, Etchegaray et al., 2009).

Visualisation of clock gene expression

Reporters of TTFL component expression are powerful tools for investigating the state of the molecular clock. Traditional approaches such as immunohistochemistry and *in situ* hybridisation are often selected to quantify expression longitudinally, however they do

not allow real-time analysis of core clock component expression. The development of bioluminescence reporter mice has enabled accurate study of *Per1* oscillations in real-time (Yoo et al., 2004, Wilsbacher et al., 2002). *Per*-Luciferase reporters are commonly utilised *in vitro* to study SCN explants, but they are somewhat limited in distinguishing signal between individual neuronal oscillators.

Consequentially high-resolution imaging of fluorescent proteins, including green fluorescent protein (GFP), has been incorporated into circadian research to circumvent this issue. The *Per1*-GFP mouse initially described by Kuhlman *et al* has been used extensively to monitor circadian timing in single cells (LeSauter et al., 2003, Kuhlman et al., 2003). While the spatial resolution is vastly improved, only a short 3kb promoter fragment drives transgene expression, therefore the phase of endogenous *Per1* expression may not be accurately reported. Enhancements to the parent GFP gene in the *mPer1::*dsEGFP reporter mouse (LeSauter et al., 2003) and the introduction of other modified fluorescent reporter animals, including the *Per1*::Venus mouse, have optimised both temporal and spatial resolution while monitoring *Per* expression patterns (Cheng et al., 2009).

The *Per1*::Venus mouse constructed by Cheng et al. offers unprecedented fluorescence signal in individual neurons due to targeted genetic modifications of the native reporter gene (Cheng et al., 2009). In the Yellow fluorescent protein (YFP) derivative Venus, point mutations in the parent gene enhanced protein folding efficiency and also provided a 3-fold acceleration of chromophore oxidation, to ensure that peak Venus fluorescence follows the peak in *Per1* promoter activity with a short lag time (~1.5h). The fluorescence signal is highly concentrated to the nucleus, a characteristic that is highly favoured for targeted somatic whole-cell electrophysiological recordings.

Venus immunoreactivity (IR) in coronal SCN-containing brain slices exhibited a robust circadian rhythm with a short phase delay with respect to *Per1*, with expression peaking at ~CT11. To further verify the suitability of Venus as a circadian reporter, response to photic stimulation was tested in dark-adapted *Per1*::Venus by brief light pulses spanning the subjective day and night. Expression of Venus was induced by light and this effect was restricted to the subjective night period. Thus, two key features of dynamic *Per1*-

dependent transcription, rhythmic expression and time-dependent induction by light, are translated in the signal from Venus. Important to the studies performed for this thesis, the *Per1*::Venus reporter mouse also facilitates the dynamic monitoring of *Per1*-dependent transcription in single cells of extra-SCN brain regions.

The hypothalamus contains extra-SCN clocks

Located in the ventral diencephalon below the thalamus, the hypothalamus is a small but critically important CNS region that can be anatomically divided into distinct nuclei, which collectively function to regulate endocrine, autonomic and behavioural functions pertinent to an organisms survival (Dietrich and Horvath, 2013, Strange et al., 2014). The anterior hypothalamus contains the medial and lateral preoptic nuclei, the supraoptic (SON) nuclei, SCN and the paraventricular nuclei (PVN). The middle zone contains the lateral hypothalamus and a collection of nuclei commonly referred to as the mediobasal hypothalamus (MBH). Finally, the mammillary bodies and posterior hypothalamic nuclei are located in the posterior zone (Diez-Roux et al., 2011). Each hypothalamic nucleus contains its own complement of neuronal subtypes and plays a unique role in homeostatic regulation. Complex inter-nuclei neuronal and humoral signals allow the hypothalamus to function in concert as a network and project coherently to other regions in the CNS (Hardy, 2001, Zhu et al., 2006, Saper et al., 2001).

Recent studies have challenged the omnipotence of the SCN in governing all aspects of rhythmic physiology (Guilding and Piggins, 2007). Intriguingly, while immunohistochemistry and *in situ* hybridisation has demonstrated the presence of the *Per* transcript in multiple brain regions, bioluminescence studies monitoring *Per1*/PER2 expression in isolated explants have identified extra-SCN sites in the hypothalamus that contain an autonomous circadian clock (Yamamoto et al., 2001, Pezuk et al., 2010, Abe et al., 2002, Guilding et al., 2009, Guilding et al., 2010). Furthermore, extra-SCN hypothalamic clock sites play diverse and well-established roles in regulating a range of physiological processes.

Overt self-sustained circadian oscillations have been demonstrated in neural structures of the MBH, an area which modulates metabolic homeostasis (Abe et al., 2002, Guilding et al., 2009). The MBH comprises of the arcuate nuclei (ARC), dorsomedial hypothalamus

(DMH), ventromedial hypothalamus (VMH), median eminence (ME) and pars tuberalis (Flier and Maratos-Flier, 1998, Williams et al., 2009), all of which have been implemented in biological timekeeping (Bechtold and Loudon, 2013). Notably, the most robust circadian oscillations in the MBH have been demonstrated in the ARC and DMH which play well-established roles in energy homeostasis (Guilding et al., 2009, Abe et al., 2002).

Using semi-quantitative *in situ* hybridisation with 35S-riboprobes to evaluate mRNA levels, *Per1* and *Per2* mRNA exhibited diurnal rhythmicity in ARC. Peak levels of *Per1* and *Per2* mRNA expression in the ARC were detected at Zeitgeber Time (ZT) 12 and ZT12-16 respectively (Shieh et al., 2005). Under identical experimental conditions, peak expression of *Per1* and *Per2* mRNA in the SCN were ZT4 and ZT8 respectively. Therefore, the phase of ARC *Per* mRNA rhythmicity was delayed with respect to the SCN (Shearman et al., 1997, Shigeyoshi et al., 1997).

As previously mentioned, the development of transgenic luciferase reporter animals has made it possible to continuously measure the expression of the *Per* gene in tissue explants where the SCN input is removed. While lower in amplitude when compared to SCN, real-time *Per1*-luc rhythms detected by photomultiplier tube were sustained for 3 to 6 cycles in micro-dissected ARC explants (Abe et al., 2002). The period of oscillations in SCN and ARC were similar, however consistent with previous *in situ* hybridisation experiments, the expression of *Per1*-luc in the ARC was out of phase with the SCN, with levels peaking at approximately ZT14 (Shearman et al., 1997).

MBH containing brain slices from mice expressing a PER2::LUCIFERASE(LUC) reporter construct can be visualised using highly sensitive EM-CCD camera-equipped microscopy to investigate the clockwork in individual neurons *in vitro* (Guilding et al., 2009). PER2::LUC was robustly expressed in the ARC, with significant circadian rhythmicity in both dorsal (ARCD) and lateral (ARCL) sub-regions. Single neuron discrimination revealed a higher proportion of PER2::LUC expressing cells were rhythmic in the dorsal ARC (ARCD) when compared to the lateral ARC (ARCL) (Guilding et al., 2009). Within the ARCD, 129 PER2::LUC positive cells were discriminated, 89% of which were rhythmic, while of 97 cells identified in the ARCL, 67% displayed rhythmicity. As previously discussed, one defining characteristic of brain clocks is the ability of individual neurons to sustain

oscillation in the absence of external input. Albeit lower amplitude than SCN, PER2::LUC expression cycled for 3 days during continuous recordings made from 12 live slices maintained for up to 14 days.

In the SCN, cyclic expression of molecular clock components are accompanied by daily shifts in measurements of basic membrane excitability, including resting membrane potential, spontaneous firing rate and input resistance (Belle et al., 2009). Parallel to bioluminescence experiments, Guilding et al. performed extracellular recordings to assess whether rhythmic firing patterns observed in the SCN are conserved in the ARCD. Population and single cell extracellular electrophysiological activity was recorded for at least 48 hours *in vitro*. Clear circadian oscillations were detected in population discharge in 5 of 6 recordings with a mean period of 24.0 ± 0.7 h. From these five rhythmic recordings overt circadian firing profiles were identified in 10 of 12 (83%) neurons identified following single-unit discrimination (Guilding et al., 2009). However while multiunit analysis is a reliable indicator of rhythmic population discharge, extracellular recordings are unable to resolve whether *Per* containing cells of the ARC exhibit similar electrophysiological phenotypes compared to those observed in the SCN.

ARC nucleus neural circuitry

While the role of the local molecular clockwork is unknown, a vast array of literature supports ARC function in appetite and metabolism regulation. A complex network of humoral and neuronal signalling mechanisms inform the CNS of systemic metabolic status. In its simplest form, fluctuating levels of hormones such as leptin, insulin, ghrelin and Peptide YY_{3-36} are secreted in the periphery at quantities indicative of metabolic status, while neuronal information from the periphery is relayed back to the CNS via the vagal pathways through the brainstem (Broberger, 2005). Due to its anatomical location and prototypical chemical regulators of energy balance, early reports indicated that the MBH may play a critical role in interpreting this peripheral input and orchestrating the regulation of food intake, body weight, energy and glucose homeostasis (Meister et al., 1989).

The ARC is ideally suited to sense humoral factors due to its high density of receptors for circulating factors such as leptin, ghrelin, insulin and glucose (van den Top and Spanswick,

2006, Shuto et al., 2002, Willesen et al., 1999) and circumventricular location in a part of the brain with a compromised blood brain barrier (BBB, Norsted et al., 2008, Rethelyi, 1984, Figure 2). Major appetite regulating ARC neuronal populations send dendritic projections into the median eminence (ME, Horvath, 2005). In the ventromedial portion of ARC, a subpopulation of capillary endothelial cells (ECs) which form the BBB have fenestrations that allow a direct route for blood-borne signals of energy balance to access ARC neurons (Norsted et al., 2008, Ciofi, 2011). A specialised group of ependymal cells called tanycytes line the third ventricle (3V) and project into the brain parenchyma where they contact ARC neurons and ECs (Rodriguez et al., 2005). Tanycytes are thought to form a physical barrier that prevents molecules originating via fenestrated capillaries in the adjacent ME from diffusing dorsally into ARC (Rodriguez et al., 2005). However, recent studies suggest that tanycytes also have a degree of active control over the access of blood-borne signals, such as leptin and ghrelin, to ARC from the blood or cerebrospinal fluid (Collden et al., 2015, Balland et al., 2014, Rodriguez et al., 2005, Peruzzo et al., 2004).

Indeed, an intact ARC is critical for energy homeostasis. Systemic administration of neurotoxic gold thioglucose, or treatment of neonatal rats with high doses of monosodium glutamate, result in severe neuronal loss in the ARC which is associated with the development of obesity syndrome characterised by hyperphagia (Debons et al., 1982, Meister et al., 1989). Furthermore, genetic defects in the ARC are correlated to obesity and metabolic disturbances in humans (Barsh et al., 2000), which is likely to blockade of the anorexic effects of peripheral signals such as leptin.

The complexity of the ARC neuronal network controlling energy balance is reflected by the inputs, outputs, neuronal circuits and integrative properties of individual ARC neurons. In order to understand inner workings of the ARC, a greater appreciation of the functional organisation of these neurons and their circuits is important. Drop-seq analysis of ARC and ME revealed 50 transcriptionally unique ARC-ME cell populations, highlighting the complexity distinct cellular signatures play in regulating energy balance, growth and fertility (Campbell et al., 2017).

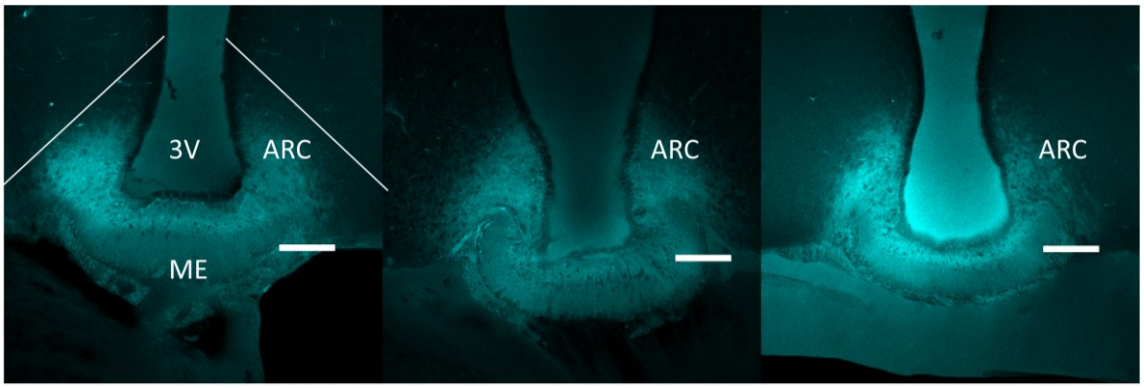

Figure 2: The ARC has a compromised blood-brain barrier (BBB) and is permeable to the blood-borne dye Evans blue. Mice were intravenously perfused with Evans blue dye (EB). EB binds to albumin, which cannot cross the normal BBB, therefore this method is a test for the permeability of blood-borne signals into the ARC brain parenchyma. Confocal images (20x) of ARC-containing coronal brain slices (30µm) display EB staining in ventromedial ARC. Blood-borne signals of energy status signal directly with ARC neurons by diffusing into the brain parenchyma via the compromised BBB. 3V, third ventricle, ME = median eminence. Scale bar represents 100µm.

The best characterised interoceptive sensory neurons residing in the ARC are the orexingenic Neuropeptide-Y and agouti-related peptide (NPY/AgRP) expressing neurons and the anorexigenic Proopiomelanocortin (POMC) neurons, which play parallel but antagonistic energy-balancing roles (Cowley et al., 1999, Garfield et al., 2015). Aside from NPY/AgRP and POMC, other energy balance-regulating neuropeptides originate in the ARC, including galanin-like peptide (GALP), neuromedin U and CART (cocaine and amphetamine regulated transcript) (Legradi and Lechan, 1999, DeFalco et al., 2001).

Dopaminergic neurons expressing tyrosine hydroxylase (TH) also reside in ARC and play an orexigenic role in energy homeostasis (Zhang and van den Pol, 2016, Zhang and van den Pol, 2015). Stimulation of mouse ARC TH neurons evokes increases in food intake by synaptic inhibition of POMC neurons and inhibition of paraventricular nucleus neurons by co-release of dopamine and GABA (Zhang and van den Pol, 2016).

Since the identification of these distinct neural populations, many studies have focused on dissecting the core ARC circuitry responsible for governing energy homeostasis, primarily NPY/AgRP and POMC neurons and their downstream targets. An intact NPY/AgRP microcircuitry within the ARC is critical for monitoring and positively regulating appetite in response to a short-term energy deficit (Atasoy et al., 2012, Marks et al., 1992, Fenselau et al., 2017). However, targeted removal of either GABA, NPY or AgRP release

from these neurons demonstrates that while either NPY or GABA are required for rapid stimulation of feeding, AgRP release evokes feeding over a delayed and prolonged period (Krashes et al., 2013). Direct optogenetic or pharmacogenetic activation of AgRP neurons potently upregulates acute food intake *in vivo* (Aponte et al., 2011, Atasoy et al., 2012, Krashes et al., 2011). Conversely, targeted inhibition or toxin-induced ablation of NPY/AgRP neurons in adult rodents profoundly decreases food intake (Wu and Palmiter, 2011, Krashes et al., 2011, Luquet et al., 2005). NPY/AgRP neurons project to the PVN where the co-release of NPY and AgRP act via the Y1 receptor and melanocortin receptors respectively on orexinergic downstream neurons respectively to increase appetite (Ollmann et al., 1997, Li et al., 1999, Fenselau et al., 2017). GABAergic collaterals from NPY/AgRP neurons also contact ARC POMC neurons to decrease their satiety-promoting activity (Cowley et al., 2001, Horvath et al., 1992).

Neurons that express processed peptides of POMC are by far the best described catabolic ARC neurons (Cone, 2005) and potently supress feeding, stimulate energy expenditure and enhance metabolism through the release of various melanocortin peptides such as α-melanocyte stimulating hormone (αMSH), adrenocorticotropic hormone (ACTH) and the opioid β-endorphin, (Meister, 2007, Elias et al., 1998). Following the identification of these neurons and localisation to the ARC (Dube et al., 1978), their importance in appetite regulation was highlighted by central injection of αMSH into the lateral ventricle, which resulted in decreased food intake (Poggioli et al., 1986). Molecular cloning experiments then identified 5 melanocortin receptors, of which type 3 and 4 (MC3R/MC4R) were localised to the brain (Mountjoy et al., 1992). The dominant role of αMSH interacting with MC4R was then determined when it was observed that MC4R deficiency in mice and humans led to obesity (Huszar et al., 1997, Vaisse et al., 1998, Yeo et al., 1998).

A key question is which downstream sites mediate the anorexigenic effects of POMC neuronal activity. PVN neurons abundantly express MC4Rs and receive strong innervation from ARC POMC neurons (Kishi et al., 2003, Mountjoy et al., 1994, Liu et al., 2003, Kim et al., 2015). However, MC4Rs are expressed in multiple brain regions and injection of MC3/4R agonists into additional sites other than the PVN also regulates feeding, therefore the specific role of the PVN was unclear (Skibicka and Grill, 2009). Manipulation

of MC4R expression in specific anatomical sites demonstrated that MC4Rs on PVN neurons are necessary and sufficient for regulating appetite/satiety, and that these cells are glutamatergic (Balthasar et al., 2005, Shah et al., 2014).

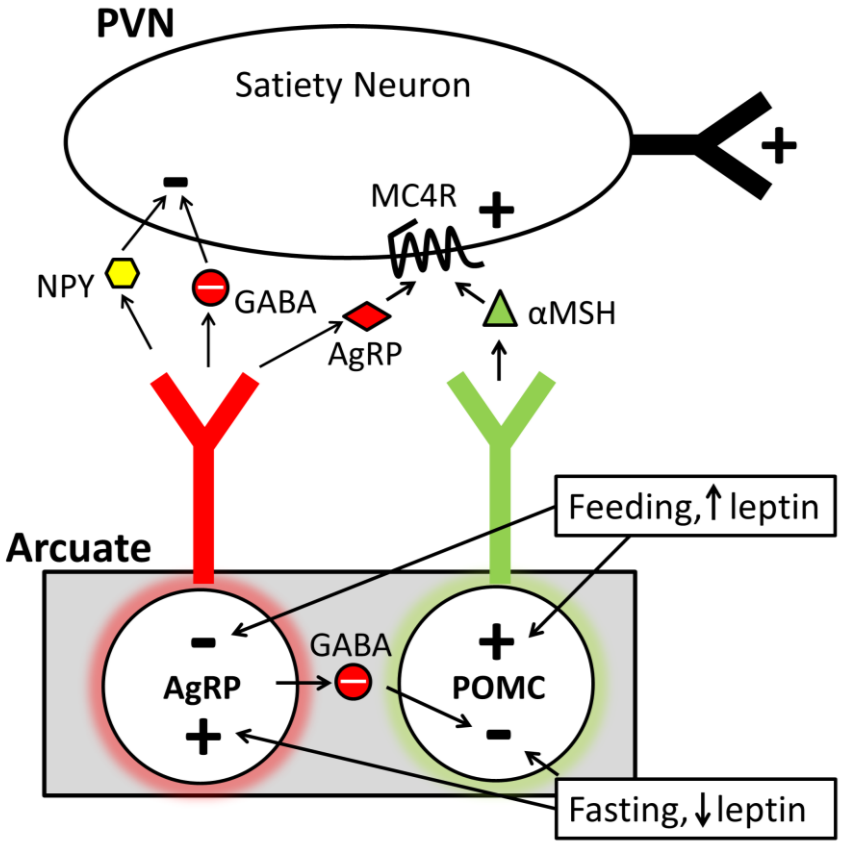

Figure 3: The ARC to PVN satiety circuit. A simplified diagram of the major pathways by which two main appetite-regulating populations residing in the ARC modulate satiety and appetite; those that co-release AgRP, NPY and GABA and a distinct population that release αMSH and other downstream products of POMC. Both AgRP neurons and POMC ARC neurons signal to downstream satiety-promoting PVN neurons. αMSH interacts with the MC4R to increase PVN neuron activity, whereas AgRP antagonises this action at the MC4R. AgRP-expressing neurons also send inhibitory GABAergic collaterals to inhibit POMC neuron activity under fasted conditions and when circulating levels of leptin are increased. (Figure adapted from Andermann et al. 2017).

Electrical silencing of POMC neurons has dramatic effects on food intake and eventually causes obesity (Plum et al., 2006). Interestingly, reports suggest the activity of ARC POMC circuitry is more involved in chronic regulation of energy homeostasis, as bilateral cre-dependent destruction of ARC POMC neurons does not acutely increase food intake but does strongly influence long-term food intake (Zhan et al., 2013). Optogenetic stimulation of POMC neurons reduces food intake over the course of many hours (Aponte et al., 2011). POMC neurons integrate major inputs from orexin-releasing lateral hypothalamic

neurons (de Lecea et al., 1998, Sakurai et al., 1998, Ma et al., 2007, Acuna-Goycolea and van den Pol, 2009) and peripheral humoral signals diffusing across the compromised blood-brain interface.

Further computational capability of the ARC is added through the presence of the fast neurotransmitter gamma-aminobutyric acid (GABA) both within and separate from neuropeptide circuits. GABAergic neurons play key internal roles in many of the functions of the ARC, including regulation of the endocrine system and energy homeostasis (Kelly and Grossman, 1979, Kalra et al., 1999, Cone et al., 2001). The GABA-synthesising enzyme glutamate decarboxylase (GAD) is found in 50 percent of the synaptic terminals in ARC and is sensitive to fasting diet conditions (Decavel and Van den Pol, 1990, Horvath et al., 1997). In vivo, the selective deletion of the GABAergic vesicular transporter (VGAT) alone from AgRP neurons results in a lean phenotype and mice that are resistant to DIO (Tong et al., 2008). GABAergic modulation of the classical ARC neuropeptide circuitry has become an important feature of the primary model of hypothalamic regulation of food intake; NPY/AgRP neurons appear to disinhibit POMC cells by reducing inhibitory tone from a neuronal population of GABAergic cells via activation of G-protein-linked inwardly rectifying potassium (GIRK) (Wang et al., 2002, Cowley et al., 2001, Vong et al., 2011, Acuna-Goycolea et al., 2005). Double-label *in situ* mRNA hybridization for POMC and GAD, revealed colocalisation of mRNAs in approximately one-third of POMC ARC neurons (Hentges et al., 2004). In addition to the more sustained actions elicited by POMC peptides (Zhan et al., 2013, Aponte et al., 2011), whole-cell electrophysiology suggests that these neurons can exert rapid inhibitory effects via the release of GABA (Hentges et al., 2004). However, GABA-dependent rapid inhibition may not play a major role within local ARC circuits, but rather is likely to be involved in more distant projection areas as indicated by the colocalisation of VGAT IR predominately in extra-hypothalamic POMC terminals (Mercer et al., 2013).

The physiological role of the ARC clock

Diffusible output signals are sufficient to restore locomotor activity cycles following transplantation of an embryonic SCN encased in a semipermeable membrane (LeSauter et al., 1996). However, transplants do not restore endocrine and other physiological

rhythms, demonstrating the importance of axonal projections to target areas (Meyer-Bernstein et al., 1999). Neural tracing studies show projections from the master clock to multiple other hypothalamic areas, including areas critical in the homeostatic regulation of metabolism (Kalsbeek et al., 2006). The subparaventricular zone (SPZ) is a major relay site for polysynaptic neuroendocrine and pre-autonomic projections (LeSauter and Silver, 1998). Arousal-promoting orexin neurons in the lateral hypothalamus (Kroemer et al.), circumventricular neurons of the ARC and integrative neurons of the dorsomedial hypothalamus (DMH) are all innervated by the SCN in this manner (Date et al., 1999, Abrahamson et al., 2001, Buijs et al., 1994). *In vivo* extracellular electrophysiological recordings in rats also reveal that SCN sends direct and indirect projections to ARC which consist of both excitatory and inhibitory components (Saeb-Parsy et al., 2000).

When food is made available to nocturnal rodents *ad libitum*, food intake is broadly partitioned to the dark phase of the light-dark cycle and is not a passive result of sleep-wake activity (Armstrong et al., 1980). Few attempts have been made to determine brain regions responsible for the circadian coordination of feeding, although multiple lines of experimental evidence suggest the MBH is critical in sculpting these rhythms in appetite and feeding behaviours. Although SCN projections to the MBH provide a means for gating feeding behaviour, the integration of physiological signals to derive rhythms compatible with homeostatic requirements is likely to occur outside the SCN, thus providing maximum flexibility for responding to varying challenges.

Indeed, MBH lesions result in hyperphagia and disruption (here they refer to MBH as ARC and VMH) in diurnal feeding patterns (Chou et al., 2003). In rats maintained on 12-12 light-dark conditions with lights on at 0600h, Akabayashi et al. reported diurnal rhythms in hypothalamic NPY mRNA peaking at 1400-1600h (Akabayashi et al., 1994). In agreement, Xu et al monitored NPY gene expression and showed daily rhythmic fluctuations with highest levels during the light phase (Xu et al., 1999). Expression of major ARC neuropeptide POMC rises significantly during the subjective day in conjunction with low serum leptin levels and feeding behaviour (Steiner et al., 1994).

Sleep-wake and feeding rhythms are distributed equally across the light-dark cycle following the targeted destruction of ARC neurons by bilateral injection of a NPY-

Saporin(SAP) conjugate (Wiater et al., 2011). As this ribosomal disaggregating agent specifically supresses NPY-expressing ARC neurons, they appear critically important for the integration of sleep-wake cycles and feeding rhythms. Furthermore, these physiological consequences are unlikely to be secondary to hyperphagia as they persistent when rats were no longer hyperphagic (Wiater et al., 2011). To further support this finding, deletion of NPY receptors (Y2 or Y4) causes abnormal daily patterns in locomotor activity and feeding (Edelsbrunner et al., 2009). The targeted toxin, SAP conjugated to leptin (Leptin-SAP), was also injected into the ARC, and resulting feeding rhythms and body-weight under light-dark (LD) and continuous darkness (DD) were evaluated (Li et al., 2012). Rats given Lep-SAP injections in the ARC fed arrhythmically when housed under 12:12hr LD and DD conditions with *ad libitum* access to food, and as a result of hyperphagia rapidly became obese. Furthermore, these toxin-induced lesions produced sustained metabolic deficits for up to 8 weeks after Leptin-SAP injection. These results reveal a critical role for leptin-receptive neurons in the ARC region in the emergence of feeding rhythms.

Recent studies also demonstrate that the temporal pattern of ARC neuronal excitability may be influenced to some degree by daily or circadian signals. NPY/AgRP neurons display a five-fold increase in firing in parallel to mounting caloric deficit in the afternoon compared to morning (Mandelblat-Cerf et al., 2015). Satiety-promoting POMC neurons exhibited antagonistic and opposite spiking to NPY/AgRP neuron. Further, whole-cell recordings suggest that ARC NPY/AgRP neurons may generate APs more frequently during the night compared to the day (Krashes et al., 2013). Over recent years, interest has mounted regarding the mechanisms by which the circadian system may influence the excitability of known ARC populations.

The finding that light-driven daily behaviour can easily be overcome by a restricted feeding schedule (RFS) suggests that a food entrainable oscillator (FEO) exists within the body (Mistlberger, 1994). Under RFS, physiological and metabolic circadian rhythms become entrained to the availability of food and not to the light-dark cycle. Despite many efforts the anatomical location of the FEO is unknown. Interestingly, this food-based entrainment is not dependent on the SCN, as lesions of the master clock do not affect food-anticipatory activity (FAA, Stephan et al., 1979). This implies that important feeding

centres in the brain may function as a network FEO which is capable of operating separately from the SCN when the timing and availability of food are altered. The location and exact mechanism of the FEO has been a topic of hot and controversial debate over the past decades. Targeted disruption of all major feeding areas does not seem to locate the anatomical location of the FEO, therefore the mechanism likely manifests itself through interaction of multiple brain regions. Although peripheral clocks entrain to meal timing (Hara et al., 2001, Damiola et al., 2000), evidence does not support a view that the FEO is located in the periphery (Mieda and Sakurai, 2011, Feillet et al., 2006).

Intriguingly, genetic targeting of canonical clock genes does not disrupt FAA. Two independent reports demonstrated that *Clock*$^{\Delta 19}$ mice had intact FAA during RFS (Pitts et al., 2003, Horikawa et al., 2005). Further, *Cry1*$^{-/-}$*Cry2*$^{-/-}$ mice with an ablated SCN still exhibited FAA during RFS and fasting (Iijima et al., 2005). Thus the location and genetic mechanisms remain unknown (Pendergast and Yamazaki, 2018). However, given the importance of the ARC in sensing fluctuations in metabolic signals and regulating SCN function, it is likely that ARC is involved in the workings of a FEO.

Linking rhythmic excitability to the molecular clockwork

A key question is how the autonomous molecular clockwork influences ARC neuronal activity. Electrical activity is essential for integrative processing in the ARC; the Intrinsic firing rates of ARC NPY/AgRP and POMC neurons directly correlate with nutritional status and consequentially drive the maintenance of homeostasis (Takahashi and Cone, 2005). The frequency of intrinsic action potentials (APs) of NPY neurons measured intra- and extracellularly becomes elevated (Dinno et al., 2011) in food-deprived mice compared to those that are satiated (Takahashi and Cone, 2005, Liu et al., 2012). Thus, any underlying clock-dependent changes in the temporal pattern of firing rate suggest that cell-autonomous clocks in ARC may play a function in appetite regulation.

The collective behaviour of a neural network depends on the physiological properties of individual neurons and the cellular mechanisms through which they integrate peripheral inputs (Bean, 2007, Atasoy et al., 2012). For ARC neurons, signal transduction pathways, the ion channel complement and biophysical architecture are critical for determining how leptin, ghrelin and other hormonal indicators of systemic energy status are encoded into

electrical activity and neuropeptide release (Gao and Horvath, 2007, Hill et al., 2008). Due to the complexity of neuronal sub-populations in ARC, the signal transduction mechanisms and biophysical properties responsible for the integration of peripheral humoral cues remain largely unknown. The patch-clamp method has revolutionised the study of individual components of neural networks. Precise information gained from whole-cell studies can be applied in the ARC to construct a model of whole-nucleus function (Qiu et al., 2014, Zhang and van den Pol, 2013, van den Pol et al., 2009).

In practice, the simplest way to report neuronal whole-cell electrical activity is to analyse parameters of basic membrane properties obtained from current clamp recordings, such as resting membrane potential (RMP), spontaneous firing rate (SFR) and input resistance (R_{input}), that reflect the intrinsic excitability of the patched cell. ARC neurons are spontaneously active within a broad electrophysiological range which is reflected in the typically reported RMP, SFR and R_{input} values (van den Pol et al., 2009, Ma et al., 2007, Acuna-Goycolea et al., 2005, Qiu et al., 2014). ARC neurons heterogeneously fire action-potentials within a wide dynamic range of SFR values from ~1 to 10Hz, or are silent at hyperpolarised resting states (Acuna-Goycolea et al., 2005, Burdakov and Ashcroft, 2002, Takahashi and Cone, 2005, Ghamari-Langroudi et al., 2005, Zhang and van den Pol, 2016). In addition, previously reported RMP values are highly variable in the ARC, ranging from approximately -40 to -75mV, which is perhaps unsurprising considering the need for adaptability when integrating rising and falling levels of peripheral signals (Baver et al., 2014, Cowley et al., 2001). Under basal conditions (normal aCSF and holding potential (V_{hold}) -70mV) ARC neurons have a relatively high R_{input}, which allows them to respond to input with a high sensitivity (Spanswick et al., 2000, van den Top et al., 2004). The majority of ARC neurons are not silent, generate APs, and do so with both an irregular and regular firing pattern. Heterogeneity has been reported between distinct neuropeptide-expressing populations regarding the proportion of hyperpolarised silent versus irregular/ regular firing neurons. For example, almost all tested NPY/AgRP neurons generate APs with either a regular or irregular pattern (van den Pol et al., 2009). However, approximately a quarter of Kisspeptin neurons tested by whole-cell recordings spontaneously generate APs with an almost exclusively irregular pattern that depends on A-type potassium (K+) and persistent sodium conductances (Mendonca et al., 2018).

Whole-cell recordings represent a unique opportunity to study how the molecular clockwork in ARC may influence neuronal excitability. Such experiments probe beyond firing rate and permit the investigation of how membrane parameters such as RMP and R_{input} may be modulated across the day-night.

Channel modulation, which contributes strongly to the integrative properties of ARC neurons, also shapes the activity of *Per1*-expressing neurons in the SCN. While many studies have demonstrated day-night differences in the firing rate of SCN neurons (Welsh et al., 1995, Green and Gillette, 1982, Aujard et al., 2001, Groos and Hendriks, 1982, Inouye and Kawamura, 1979), recent observations in the master clock have challenged our understanding of neuronal electrophysiological boundaries. During the day, *Per1*-expressing SCN neurons are driven towards depolarised RMP values and begin to enter depolarised low amplitude membrane oscillations (DLAMOs) states and depolarisation block (Belle et al., 2009). Interestingly, non-*Per1*-expressing SCN neurons do not transition into depolarised states during the morning-afternoon, suggesting that coupling to the molecular clockwork is imperative for the broad range of electrophysiological behaviours (Diekman et al., 2013).

It was originally hypothesised that electrophysiology oscillations in SCN neural activity are slave to the molecular clockwork in a unidirectional manner, however a number of studies began to suggest that a more dynamic interplay is required for precise circadian timekeeping (Quintero et al., 2003). Targeted genetic lesioning of the molecular clock components *Cry*1-2 abolish rhythmic electrical activity in the SCN (Albus et al., 2002). Aside from disruption to core clock function, the Hamster tau mutation in *CK1ε* shortens both wheel-running period and neural activity rhythms (Liu et al., 1997). The reciprocity between molecular and electrical arms of the circadian clock can be demonstrated by application of voltage-gated sodium channel blocker tetrodotoxin (TTX), which decreases the precision and amplitude of *Per1*-luciferase oscillations *in vitro* (Yamaguchi et al., 2003). Thus, recent evidence suggests that electrical activity and genetic oscillations sustain molecular clock loops in neurons expressing high relative levels of *Per1* during the day.

The link between the molecular clock and excitability is thought to be mediated by clock-mediated control of ion conductance. Interestingly, some K^+-permeable ion pores including the large conductance Ca^{2+}-dependent K^+ channel (BK) and 2-pore domain (K2P) channels are rhythmically expressed in the SCN (Pitts et al., 2006, Kuhlman and McMahon, 2004, Meredith et al., 2006, Whitt et al., 2016). Furthermore, in the fruit fly *Drosophila melanogaster* recent emerging evidence suggests that *Cry* is able to actively modulate K^+ conductance (Fogle et al., 2011). A number of other currents exhibit circadian variation within SCN neurons including fast-delayed rectifier conductance (FDR; *KCNC KCNC2*,(Kudo, 2011 #227), A-type conductance (*KCND1,KCND2*,((Granados-Fuentes, 2012 #174)(Itri et al., 2010), L-type Ca^+ channels (*CACNA1C, CACNA1S*) which peaks during the day (Pennartz et al., 2002), and an anonymous TEA-sensitive K^+ conductance (Kuhlman and McMahon, 2004). Thus, molecular clock components may drive the rhythmic expression of channels across the projected day, altering ionic conductance and resulting electrophysiological behaviours. Specifically, decreases in extracellular K^+ composition induce a chronic membrane hyperpolarisation, which supresses rhythmic expression of Per1/PER2, suggesting a more pivotal role of rhythmic K^+ conductance in mediating the molecular clockwork (Lundkvist and Block., 2005).

Considering the identification of individual cellular oscillators and diurnal patterns in electrical activity in ARC, one might postulate that the electrical states observed in the SCN are conserved in the ARC. While no studies have reported depolarised resting states in ARC neurons, one explanation for this could be that no studies have yet targeted *Per1*-containing neurons. Also, In the past SCN neurons entering depolarisation block during current clamp recordings have been interpreted as 'physiologically-unsound' due to leakage from the electrode seal, therefore they were excluded from analysis (Jackson et al., 2004). As previously mentioned, multiple extra-SCN brain sites contain their own autonomous circadian oscillator (Abe et al., 2002). Indeed, similar electrophysiological states to those observed in the SCN are found in the medial habenula (Sakhi et al., 2014). Given the fundamental importance of electrical properties in ARC function, an investigation into the characteristics of *Per1*-targeted neurons would prove valuable. Furthermore, depolarised states are within a physiologically achievable repertoire of electrical behaviours previously reported in ARC neurons. Treatment of NPY neurons with

bombesin or the related mammalian peptide neuromedin B evokes transient fluctuations in RMP (van den Pol et al., 2009); intriguingly cyclic shifts RMP enter states of depolarisation block before returning to basal levels. Moreover, in rat ARC neurons, local release of glutamate is sufficient to drive neurons to depolarised RMP values and exhibit a spiking behaviour reminiscent of DLAMOs in SCN (Belousov and van den Pol, 1997).

Leptin

Leptin is a hormone produced in white adipose tissue which serves as a peripheral signal to the central nervous system to convey information regarding nutrition (Flier and Maratos-Flier, 2010, Friedman, 2004, Friedman, 2010). It was discovered following the identification the *ob* gene by Jeffery Friedman's positional cloning experiments in 1994 (Friedman, 2010). They demonstrated that the *ob* transcript was expressed exclusively within adipose tissue (Friedman, 2010, Zhang et al., 1994). Rodents and Humans with mutations in the *ob* ($Lep^{ob/ob}$) or leptin's endogenous receptor ($Lep^{db/db}$) are hyperphagic and obese (Coleman and Hummel, 1973, Tartaglia et al., 1995, Berglund et al., 2012). The long isoform leptin receptor (lepRb) is highly expressed throughout the ARC (Chua et al., 1996, Mercer et al., 1996, Elmquist et al., 1998b). Furthermore, a large proportion of ARC neurons densely express c-Fos mRNA, a potent early marker of neuronal activity, after intravenous injection of leptin (Elmquist et al., 1998a).

Lesions of the ARC result in complete insensitivity to leptin *in vivo* suggesting that the metabolic deficiencies in global knockouts primarily result from loss-of-function in the ARC (Choi et al., 1999, Li et al., 2012). In addition, viral transfection of leptin receptor into ARC neurons alone is sufficient to reduce food intake in leptin receptor-deficient rats (Morton et al., 2003). Leptin binds directly to lepRb on at least 2 populations of ARC neurons (Schwartz et al., 1996, Baskin et al., 1999), inhibiting NPY/AgRP neurons and activating POMC neurons, accounting for its anti-obesity actions (Morton et al., 2006).

Recent studies have investigated the loss of expression of LepR in neuronal populations chemically identified by NPY/AgRP and POMC expression and determined that lepR in these various cell populations only modestly contribute to satiety effects (~10-20% effect in global leptin knockout) (Scott et al., 2009, Vong et al., 2011). Modern genetic ablation techniques have revolutionised experiments on circuitry mediating leptin effects, for

example dramatic effects are observed when lepRb are removed from GABAergic neurons alone (Vong et al., 2011). Vong et al. constructed VGAT-Cre and VGLUT2 (vesicular glutamate transporter 2)-Cre transgenic mice and crossed these with $LepR^{flox/flox}$ mice (Balthasar et al., 2004) to specifically knock-out LepR from GABAergic and glutamatergic ARC neurons. The resulting weight gain due to hyperphagia in the VGAT-Cre, $LepR^{flox/flox}$ mice was significantly higher than in the VGLUT2-Cre, $LepR^{flox/flox}$ mice, which showed minimal changes in body weight or feeding behaviour.

Leptin rapidly alters electrical activity of ARC neurons *in vitro* however little is known regarding the leptin-dependent modulation of ion channels. (Spanswick et al., 1997, Cowley et al., 2001, Mirshamsi et al., 2004, Yang et al., 2010). Whole-cell electrophysiological studies in the ARC have demonstrated that diazoxide-sensitive ATP-sensitive K+ channels (K_{ATP}) channels are expressed in the majority of cells including those expressing NPY/AgRP and POMC (Ibrahim et al., 2003, van den Top et al., 2007). Based on previous studies demonstrating K_{ATP} channels are well conserved humoral targets (Pocai et al., 2005, Obici et al., 2002), one potential route for leptin is the modulation of K_{ATP} channels. Indeed, single-channel recordings demonstrate that leptin activates a K_{ATP} channel (Spanswick et al., 2000). In the periphery, leptin shares a common pathway with insulin, activating phosphoinositide 3-kinase (PI3K), an enzyme which is necessary for anorectic responses (Niswender et al., 2003), and therefore may represent a route through which K_{ATP} channels are modulated. A second challenge is how parallel leptin-dependent inhibition of NPY/AgRP neurons and activation of POMC neurons occurs in tandem in the ARC. Although both NPY/AgRP neurons express functional K_{ATP} channels, recent evidence suggests that leptin's actions on ARC POMC neurons are attributable to activation of transient receptor potential (TRPC) channels (Qiu et al., 2010). The identification of TRPC activation by leptin built on previous work which identified a nonselective cation current that mediated the depolarising effects of leptin on POMC neurons (Cowley et al., 2001).

Baver et al. were able to completely abolish the long-duration hyperpolarising effects of leptin by 4-AP, suggesting its anorectic actions are due to modulation of voltage-gated K+ channels (Kv). Although poorly selective among Kv channels, 4-AP preferentially blocks Kv over non-voltage gated channels such as K_{ATP} (Lesage, 2003, Tamargo et al., 2004).

Following rough pharmacological isolation from $I_{A,}$ they postulate that leptin activity is partially mediated via a delayed rectifier channel, possibly Kv2.1 (Baver et al., 2014). Aside from K_{ATP} and K_v, the effects of leptin may also be attributable to modulation of calcium-dependent K+ channels such as big conductance (BK) channels (Mirshamsi et al., 2004, Yang et al., 2010).

When considering signal-transduction mechanisms responsible for the sense of other humoral signals in the ARC, K+ channels appear to be key components to peripheral integration in the CNS. Hypoglycaemia and increased circulating insulin inhibits ARC neurons through the opening of K_{ATP} channels (Spanswick et al., 1997). Cholecystokinin, a hormone and neurotransmitter long recognised for regulation of food intake, also regulates a Kv channel to potentiate I_A current in the ARC (Burdakov and Ashcroft, 2002).

Ghrelin

Of course, not all central responses to the periphery in the ARC NPY/AgRP POMC circuit are attributable to leptin. Other humoral indicators such as the gut-synthesised peptide ghrelin act in the brain to regulate food intake, body weight, glucose metabolism and adiposity (Tschop et al., 2000). Ghrelin is a multifaceted modulator of metabolism, released from the stomach, that was first discovered in 1999 as the endogenous ligand for the growth hormone secretagogue receptor (GHSR)1a (Kojima et al., 1999). The ghrelin receptor gene generates two isoforms, functional GHSR1a and a separate truncated form terms GHST1b. GHSR1a is a G-protein-coupled receptor that is able to form heterodimers with key components of energy homeostasis including the MC3R, which colocalise in ARC neurons (Rediger et al., 2011). This interaction stimulates MC3R signalling while simultaneously supressing GHSR1a signalling (Rediger et al., 2011). Knockout mice for the GHSR (*Ghsr*$^{-/-}$) display reduced body weight (Sun et al., 2004). Both ghrelin and GHSR1a are widely expressed in numerous brain regions (Cowley et al., 2003) and in peripheral tissues such as the kidney, intestine and heart (Palus et al., 2011, Ueberberg et al., 2009, Granata et al., 2011).

In humans, peripheral ghrelin robustly induces a physical feeling of hunger and increases food intake in individuals of varying body weight and adiposity (Wren et al., 2001). In healthy volunteers, intravenous administration of ghrelin increases hypothalamic brain

activity (Holsen et al., 2014, Kroemer et al., 2013). Ghrelin levels display a preprandial rise and decrease within the first hour of food intake (Cummings et al., 2001). The magnitude of this reduction is proportional to the caloric and macronutrient content of the ingested meal (Monteleone et al., 2003).

Ghrelin was found to modify systemic metabolism by stimulating orexigenic circuits in the brain (Cowley et al., 2003, Nakazato et al., 2001). Ghrelin mRNA is distributed throughout the brain (Kojima et al., 1999). In the hypothalamus, ghrelin stimulates endocannabinoid release which consequently leads to activation of the calcium/calmodulin-dependent protein kinase 2 (CaMKK2) and increases phosphorylation of AMP-activated protein kinase (AMPK) (Kola et al., 2008, Anderson et al., 2008, Lopez et al., 2008). Ghrelin-mediated activation of GHSR1a results in deacetylastion of p53, leading to increased phosphorylation of AMPK (Kola et al., 2005). Ghrelin in the hypothalamus also increases expression of prolyl carboxypeptidase (PRCP) which negatively regulates α- melanocyte stimulating hormone (αMSH) (Kwon Jeong et al., 2013). Also, ghrelin stimulates expression of the mechanistic target of rapamycin (mTOR) in the ARC (Kwon Jeong et al., 2013).

In the ARC, GHSR1a is expressed in neurons that express NPY/AgRP (Willesen et al., 1999, Guan et al., 1997). Genetic deletion of NPY and AgRP totally blunt ghrelin-induced feeding responses (Wang et al., 2014). By *in vivo* imaging, circulating fluorescent-labeled ghrelin was shown to diffuse into the hypothalamus through fenestrated capillaries on the ME, which project to the ventromedial portion of the ARC (Schaeffer et al., 2013). Ghrelin upregulates activity of NPY/AgRP neurons, thus opposing the inhibitory effects of leptin (Morton et al., 2006, Theander-Carrillo et al., 2006, Cowley et al., 2003). Ghrelin hyperpolarises ARC POMC neurons resulting in decreases firing rate, an effect which is likely mediated by GABAergic collaterals from NPY/AgRP neurons (Cowley et al., 2003). Indeed, ghrelin predominantly colocalised with NPY/AgRP neurons and not POMC neurons (Dickson and Luckman, 1997, Hewson and Dickson, 2000). When NPY/AgRP neurons are chemically or genetically inhibited, ghrelin fails to stimulate feeding (Nakazato et al., 2001, Chen et al., 2004, Luquet et al., 2005, Aponte et al., 2011, Andrews et al., 2008). Notably, NPY/AgRP neurons are not essential for ghrelin to induce food

intake with a palatable diet, demonstrating that ARC NPY/AgRP neurons are essential for homeostatic, but not hedonic feeding modulation by ghrelin (Denis et al., 2015).

Although ARC is an important target for ghrelin, administration to paraventricular nucleus (PVN, Olszewski et al., 2003) lateral hypothalamus (van der Lely et al., 2004) also has orexigenic effects on energy balance. Ghrelin also promotes positive energy when applied to hindbrain (Faulconbridge et al., 2005) and limbic regions including the amygdala (Alvarez-Crespo et al., 2012). Ghrelin also has a number of other central and peripheral effects including upregulation of gastric acid secretion and gut motility (Masuda et al., 2000), modulation of reward seeking behaviour and taste (Jerlhag et al., 2007) and modulation of sleep (Szentirmai et al., 2006).

Aims

This thesis represents an investigation into the role of local cellular clocks in the ARC in modulating neuronal activity and the function they may play in overall appetite homeostasis. The first two chapters focus on determining whether the presence of oscillating clock genes drives daily and circadian changes in ARC neuronal activation. Chapter one provides an in-depth characterisation of *Per1*-expressing ARC neurons using a Venus protein reporter mouse line. Further, we investigate whether daily rhythms in excitability are maintained at a cell population level and whether synaptic activity displays any ~24h temporal pattern. The content of this chapter is also structured to highlight how experiments in extra-SCN oscillators may add to studies in SCN to develop our understanding of how the core TTFL influences general neuronal excitability. The second chapter employs *in vitro* and *ex vivo* approaches to establish whether rhythmic changes in ARC excitability depend on a functioning molecular clock within ARC cells. We use *Cry*-deficient mice to assess the effect of global clock disruption of daily and circadian excitability in ARC. A more targeted approach is adopted by targeting ARC with viral vectors designed to knockout the core clock gene *Bmal1*. The final chapter focuses on a related aspect of circadian interactions with appetite regulation by investigating whether daily changes in excitability are maintained when performing recordings from NPY neurons in brain slices. This final chapter adopts a purely electrophysiological approach. The overarching aim of this thesis is to characterise how local molecular clock oscillations

regulate ARC neuronal excitability. Progress in this area may help elucidate how the ARC clock regulates behaviour and physiology under normal conditions with *ad libitum* food. This study also aims to shed light on how the ARC functions as part of a network of brain oscillators, and may shed light on how timekeeping processes in ARC regulate other aspects of behaviour and physiology such as reproduction and growth.

References

ABE, M., HERZOG, E. D., YAMAZAKI, S., STRAUME, M., TEI, H., SAKAKI, Y., MENAKER, M. & BLOCK, G. D. 2002. Circadian rhythms in isolated brain regions. *J Neurosci,* 22**,** 350-6.

ABRAHAMSON, E. E., LEAK, R. K. & MOORE, R. Y. 2001. The suprachiasmatic nucleus projects to posterior hypothalamic arousal systems. *Neuroreport,* 12**,** 435-40.

ACUNA-GOYCOLEA, C., TAMAMAKI, N., YANAGAWA, Y., OBATA, K. & VAN DEN POL, A. N. 2005. Mechanisms of neuropeptide Y, peptide YY, and pancreatic polypeptide inhibition of identified green fluorescent protein-expressing GABA neurons in the hypothalamic neuroendocrine arcuate nucleus. *J Neurosci,* 25**,** 7406-19.

ACUNA-GOYCOLEA, C. & VAN DEN POL, A. N. 2009. Neuroendocrine proopiomelanocortin neurons are excited by hypocretin/orexin. *J Neurosci,* 29**,** 1503-13.

AKABAYASHI, A., WAHLESTEDT, C., ALEXANDER, J. T. & LEIBOWITZ, S. F. 1994. Specific inhibition of endogenous neuropeptide Y synthesis in arcuate nucleus by antisense oligonucleotides suppresses feeding behavior and insulin secretion. *Brain Res Mol Brain Res,* 21**,** 55-61.

ALBUS, H., BONNEFONT, X., CHAVES, I., YASUI, A., DOCZY, J., VAN DER HORST, G. T. & MEIJER, J. H. 2002. Cryptochrome-deficient mice lack circadian electrical activity in the suprachiasmatic nuclei. *Curr Biol,* 12**,** 1130-3.

ALVAREZ-CRESPO, M., SKIBICKA, K. P., FARKAS, I., MOLNAR, C. S., EGECIOGLU, E., HRABOVSZKY, E., LIPOSITS, Z. & DICKSON, S. L. 2012. The amygdala as a neurobiological target for ghrelin in rats: neuroanatomical, electrophysiological and behavioral evidence. *PLoS One,* 7**,** e46321.

ANDERSON, K. A., RIBAR, T. J., LIN, F., NOELDNER, P. K., GREEN, M. F., MUEHLBAUER, M. J., WITTERS, L. A., KEMP, B. E. & MEANS, A. R. 2008. Hypothalamic CaMKK2 contributes to the regulation of energy balance. *Cell Metab,* 7**,** 377-88.

ANDREWS, Z. B., LIU, Z. W., WALLLINGFORD, N., ERION, D. M., BOROK, E., FRIEDMAN, J. M., TSCHOP, M. H., SHANABROUGH, M., CLINE, G., SHULMAN, G. I., COPPOLA, A., GAO, X. B., HORVATH, T. L. & DIANO, S. 2008. UCP2 mediates ghrelin's action on NPY/AgRP neurons by lowering free radicals. *Nature,* 454**,** 846-51.

ANTLE, M. C., SMITH, V. M., STERNICZUK, R., YAMAKAWA, G. R. & RAKAI, B. D. 2009. Physiological responses of the circadian clock to acute light exposure at night. *Rev Endocr Metab Disord,* 10**,** 279-91.

APONTE, Y., ATASOY, D. & STERNSON, S. M. 2011. AGRP neurons are sufficient to orchestrate feeding behavior rapidly and without training. *Nat Neurosci,* 14**,** 351-5.

ARMSTRONG, S., COLEMAN, G. & SINGER, G. 1980. Food and water deprivation: changes in rat feeding, drinking, activity and body weight. *Neurosci Biobehav Rev,* 4**,** 377-402.

ATASOY, D., BETLEY, J. N., SU, H. H. & STERNSON, S. M. 2012. Deconstruction of a neural circuit for hunger. *Nature,* 488**,** 172-7.

AUJARD, F., HERZOG, E. D. & BLOCK, G. D. 2001. Circadian rhythms in firing rate of individual suprachiasmatic nucleus neurons from adult and middle-aged mice. *Neuroscience,* 106**,** 255-61.

BAE, K., JIN, X., MAYWOOD, E. S., HASTINGS, M. H., REPPERT, S. M. & WEAVER, D. R. 2001. Differential functions of mPer1, mPer2, and mPer3 in the SCN circadian clock. *Neuron,* 30**,** 525-36.

BALLAND, E., DAM, J., LANGLET, F., CARON, E., STECULORUM, S., MESSINA, A., RASIKA, S., FALLUEL-MOREL, A., ANOUAR, Y., DEHOUCK, B., TRINQUET, E., JOCKERS, R., BOURET, S. G. & PREVOT, V. 2014. Hypothalamic tanycytes are an ERK-gated conduit for leptin into the brain. *Cell Metab,* 19**,** 293-301.

BALSALOBRE, A., MARCACCI, L. & SCHIBLER, U. 2000. Multiple signaling pathways elicit circadian gene expression in cultured Rat-1 fibroblasts. *Curr Biol,* 10**,** 1291-4.

BALTHASAR, N., DALGAARD, L. T., LEE, C. E., YU, J., FUNAHASHI, H., WILLIAMS, T., FERREIRA, M., TANG, V., MCGOVERN, R. A., KENNY, C. D., CHRISTIANSEN, L. M., EDELSTEIN, E., CHOI, B., BOSS, O., ASCHKENASI, C., ZHANG, C. Y., MOUNTJOY, K., KISHI, T., ELMQUIST, J. K. & LOWELL, B. B. 2005. Divergence of melanocortin pathways in the control of food intake and energy expenditure. *Cell,* 123**,** 493-505.

BARSH, G. S., FAROOQI, I. S. & O'RAHILLY, S. 2000. Genetics of body-weight regulation. *Nature,* 404**,** 644-51.

BASKIN, D. G., HAHN, T. M. & SCHWARTZ, M. W. 1999. Leptin sensitive neurons in the hypothalamus. *Horm Metab Res,* 31**,** 345-50.

BAVER, S. B., HOPE, K., GUYOT, S., BJORBAEK, C., KACZOROWSKI, C. & O'CONNELL, K. M. 2014. Leptin modulates the intrinsic excitability of AgRP/NPY neurons in the arcuate nucleus of the hypothalamus. *J Neurosci,* 34**,** 5486-96.

BEAN, B. P. 2007. The action potential in mammalian central neurons. *Nat Rev Neurosci,* 8**,** 451-65.

BECHTOLD, D. A. & LOUDON, A. S. 2013. Hypothalamic clocks and rhythms in feeding behaviour. *Trends Neurosci,* 36**,** 74-82.

BELL-PEDERSEN, D., CASSONE, V. M., EARNEST, D. J., GOLDEN, S. S., HARDIN, P. E., THOMAS, T. L. & ZORAN, M. J. 2005. Circadian rhythms from multiple oscillators: lessons from diverse organisms. *Nat Rev Genet,* 6**,** 544-56.

BELLE, M. D., DIEKMAN, C. O., FORGER, D. B. & PIGGINS, H. D. 2009. Daily electrical silencing in the mammalian circadian clock. *Science,* 326**,** 281-4.

BELOUSOV, A. B. & VAN DEN POL, A. N. 1997. Local synaptic release of glutamate from neurons in the rat hypothalamic arcuate nucleus. *J Physiol,* 499 (Pt 3)**,** 747-61.

BERGLUND, E. D., VIANNA, C. R., DONATO, J., JR., KIM, M. H., CHUANG, J. C., LEE, C. E., LAUZON, D. A., LIN, P., BRULE, L. J., SCOTT, M. M., COPPARI, R. & ELMQUIST, J. K. 2012. Direct leptin action on POMC neurons regulates glucose homeostasis and hepatic insulin sensitivity in mice. *J Clin Invest,* 122**,** 1000-9.

BROBERGER, C. 2005. Brain regulation of food intake and appetite: molecules and networks. *J Intern Med,* 258**,** 301-27.

BROWN, S. A. & AZZI, A. 2013. Peripheral circadian oscillators in mammals. *Handb Exp Pharmacol*, 45-66.

BUHR, E. D. & TAKAHASHI, J. S. 2013. Molecular components of the Mammalian circadian clock. *Handb Exp Pharmacol*, 3-27.

BUIJS, R. M., HOU, Y. X., SHINN, S. & RENAUD, L. P. 1994. Ultrastructural evidence for intra- and extranuclear projections of GABAergic neurons of the suprachiasmatic nucleus. *J Comp Neurol,* 340, 381-91.

BUNGER, M. K., WILSBACHER, L. D., MORAN, S. M., CLENDENIN, C., RADCLIFFE, L. A., HOGENESCH, J. B., SIMON, M. C., TAKAHASHI, J. S. & BRADFIELD, C. A. 2000. Mop3 is an essential component of the master circadian pacemaker in mammals. *Cell,* 103, 1009-17.

BURDAKOV, D. & ASHCROFT, F. M. 2002. Cholecystokinin tunes firing of an electrically distinct subset of arcuate nucleus neurons by activating A-Type potassium channels. *J Neurosci,* 22, 6380-7.

CAMERON, M. A., BARNARD, A. R. & LUCAS, R. J. 2008. The electroretinogram as a method for studying circadian rhythms in the mammalian retina. *J Genet,* 87, 459-66.

CAMPBELL, J. N., MACOSKO, E. Z., FENSELAU, H., PERS, T. H., LYUBETSKAYA, A., TENEN, D., GOLDMAN, M., VERSTEGEN, A. M., RESCH, J. M., MCCARROLL, S. A., ROSEN, E. D., LOWELL, B. B. & TSAI, L. T. 2017. A molecular census of arcuate hypothalamus and median eminence cell types. *Nat Neurosci,* 20, 484-496.

CHEN, H. Y., TRUMBAUER, M. E., CHEN, A. S., WEINGARTH, D. T., ADAMS, J. R., FRAZIER, E. G., SHEN, Z., MARSH, D. J., FEIGHNER, S. D., GUAN, X. M., YE, Z., NARGUND, R. P., SMITH, R. G., VAN DER PLOEG, L. H., HOWARD, A. D., MACNEIL, D. J. & QIAN, S. 2004. Orexigenic action of peripheral ghrelin is mediated by neuropeptide Y and agouti-related protein. *Endocrinology,* 145, 2607-12.

CHENG, H. Y., ALVAREZ-SAAVEDRA, M., DZIEMA, H., CHOI, Y. S., LI, A. & OBRIETAN, K. 2009. Segregation of expression of mPeriod gene homologs in neurons and glia: possible divergent roles of mPeriod1 and mPeriod2 in the brain. *Hum Mol Genet,* 18, 3110-24.

CHO, H., ZHAO, X., HATORI, M., YU, R. T., BARISH, G. D., LAM, M. T., CHONG, L. W., DITACCHIO, L., ATKINS, A. R., GLASS, C. K., LIDDLE, C., AUWERX, J., DOWNES, M., PANDA, S. & EVANS, R. M. 2012. Regulation of circadian behaviour and metabolism by REV-ERB-alpha and REV-ERB-beta. *Nature,* 485, 123-7.

CHOI, S., SPARKS, R., CLAY, M. & DALLMAN, M. F. 1999. Rats with hypothalamic obesity are insensitive to central leptin injections. *Endocrinology,* 140, 4426-33.

CHOU, T. C., SCAMMELL, T. E., GOOLEY, J. J., GAUS, S. E., SAPER, C. B. & LU, J. 2003. Critical role of dorsomedial hypothalamic nucleus in a wide range of behavioral circadian rhythms. *J Neurosci,* 23, 10691-702.

CHUA, S. C., JR., CHUNG, W. K., WU-PENG, X. S., ZHANG, Y., LIU, S. M., TARTAGLIA, L. & LEIBEL, R. L. 1996. Phenotypes of mouse diabetes and rat fatty due to mutations in the OB (leptin) receptor. *Science,* 271, 994-6.

CIOFI, P. 2011. The arcuate nucleus as a circumventricular organ in the mouse. *Neurosci Lett,* 487, 187-90.

CLARKSON, J. & HERBISON, A. E. 2006. Postnatal development of kisspeptin neurons in mouse hypothalamus; sexual dimorphism and projections to gonadotropin-releasing hormone neurons. *Endocrinology,* 147, 5817-25.

COLEMAN, D. L. & HUMMEL, K. P. 1973. The influence of genetic background on the expression of the obese (Ob) gene in the mouse. *Diabetologia,* 9**,** 287-93.

COLLDEN, G., BALLAND, E., PARKASH, J., CARON, E., LANGLET, F., PREVOT, V. & BOURET, S. G. 2015. Neonatal overnutrition causes early alterations in the central response to peripheral ghrelin. *Mol Metab,* 4**,** 15-24.

CONE, R. D. 2005. Anatomy and regulation of the central melanocortin system. *Nat Neurosci,* 8**,** 571-8.

CONE, R. D., COWLEY, M. A., BUTLER, A. A., FAN, W., MARKS, D. L. & LOW, M. J. 2001. The arcuate nucleus as a conduit for diverse signals relevant to energy homeostasis. *Int J Obes Relat Metab Disord,* 25 Suppl 5**,** S63-7.

COWLEY, M. A., PRONCHUK, N., FAN, W., DINULESCU, D. M., COLMERS, W. F. & CONE, R. D. 1999. Integration of NPY, AGRP, and melanocortin signals in the hypothalamic paraventricular nucleus: evidence of a cellular basis for the adipostat. *Neuron,* 24**,** 155-63.

COWLEY, M. A., SMART, J. L., RUBINSTEIN, M., CERDAN, M. G., DIANO, S., HORVATH, T. L., CONE, R. D. & LOW, M. J. 2001. Leptin activates anorexigenic POMC neurons through a neural network in the arcuate nucleus. *Nature,* 411**,** 480-4.

COWLEY, M. A., SMITH, R. G., DIANO, S., TSCHOP, M., PRONCHUK, N., GROVE, K. L., STRASBURGER, C. J., BIDLINGMAIER, M., ESTERMAN, M., HEIMAN, M. L., GARCIA-SEGURA, L. M., NILLNI, E. A., MENDEZ, P., LOW, M. J., SOTONYI, P., FRIEDMAN, J. M., LIU, H., PINTO, S., COLMERS, W. F., CONE, R. D. & HORVATH, T. L. 2003. The distribution and mechanism of action of ghrelin in the CNS demonstrates a novel hypothalamic circuit regulating energy homeostasis. *Neuron,* 37**,** 649-61.

CUMMINGS, D. E., PURNELL, J. Q., FRAYO, R. S., SCHMIDOVA, K., WISSE, B. E. & WEIGLE, D. S. 2001. A preprandial rise in plasma ghrelin levels suggests a role in meal initiation in humans. *Diabetes,* 50**,** 1714-9.

DAMIOLA, F., LE MINH, N., PREITNER, N., KORNMANN, B., FLEURY-OLELA, F. & SCHIBLER, U. 2000. Restricted feeding uncouples circadian oscillators in peripheral tissues from the central pacemaker in the suprachiasmatic nucleus. *Genes Dev,* 14**,** 2950-61.

DATE, Y., UETA, Y., YAMASHITA, H., YAMAGUCHI, H., MATSUKURA, S., KANGAWA, K., SAKURAI, T., YANAGISAWA, M. & NAKAZATO, M. 1999. Orexins, orexigenic hypothalamic peptides, interact with autonomic, neuroendocrine and neuroregulatory systems. *Proc Natl Acad Sci U S A,* 96**,** 748-53.

DE LECEA, L., KILDUFF, T. S., PEYRON, C., GAO, X., FOYE, P. E., DANIELSON, P. E., FUKUHARA, C., BATTENBERG, E. L., GAUTVIK, V. T., BARTLETT, F. S., 2ND, FRANKEL, W. N., VAN DEN POL, A. N., BLOOM, F. E., GAUTVIK, K. M. & SUTCLIFFE, J. G. 1998. The hypocretins: hypothalamus-specific peptides with neuroexcitatory activity. *Proc Natl Acad Sci U S A,* 95**,** 322-7.

DEBONS, A. F., SICLARI, E., DAS, K. C. & FUHR, B. 1982. Gold thioglucose-induced hypothalamic damage, hyperphagia, and obesity: dependence on the adrenal gland. *Endocrinology,* 110**,** 2024-9.

DECAVEL, C. & VAN DEN POL, A. N. 1990. GABA: a dominant neurotransmitter in the hypothalamus. *J Comp Neurol,* 302**,** 1019-37.

DEFALCO, J., TOMISHIMA, M., LIU, H., ZHAO, C., CAI, X., MARTH, J. D., ENQUIST, L. & FRIEDMAN, J. M. 2001. Virus-assisted mapping of neural inputs to a feeding center in the hypothalamus. *Science,* 291**,** 2608-13.

DENIS, R. G., JOLY-AMADO, A., WEBBER, E., LANGLET, F., SCHAEFFER, M., PADILLA, S. L., CANSELL, C., DEHOUCK, B., CASTEL, J., DELBES, A. S., MARTINEZ, S., LACOMBE, A., ROUCH, C., KASSIS, N., FEHRENTZ, J. A., MARTINEZ, J., VERDIE, P., HNASKO, T. S., PALMITER, R. D., KRASHES, M. J., GULER, A. D., MAGNAN, C. & LUQUET, S. 2015. Palatability Can Drive Feeding Independent of AgRP Neurons. *Cell Metab,* 22**,** 646-57.

DICKSON, S. L. & LUCKMAN, S. M. 1997. Induction of c-fos messenger ribonucleic acid in neuropeptide Y and growth hormone (GH)-releasing factor neurons in the rat arcuate nucleus following systemic injection of the GH secretagogue, GH-releasing peptide-6. *Endocrinology,* 138**,** 771-7.

DIEKMAN, C. O., BELLE, M. D., IRWIN, R. P., ALLEN, C. N., PIGGINS, H. D. & FORGER, D. B. 2013. Causes and consequences of hyperexcitation in central clock neurons. *PLoS Comput Biol,* 9**,** e1003196.

DIETRICH, M. O. & HORVATH, T. L. 2013. Hypothalamic control of energy balance: insights into the role of synaptic plasticity. *Trends Neurosci,* 36**,** 65-73.

DIEZ-ROUX, G., BANFI, S., SULTAN, M., GEFFERS, L., ANAND, S., ROZADO, D., MAGEN, A., CANIDIO, E., PAGANI, M., PELUSO, I., LIN-MARQ, N., KOCH, M., BILIO, M., CANTIELLO, I., VERDE, R., DE MASI, C., BIANCHI, S. A., CICCHINI, J., PERROUD, E., MEHMETI, S., DAGAND, E., SCHRINNER, S., NURNBERGER, A., SCHMIDT, K., METZ, K., ZWINGMANN, C., BRIESKE, N., SPRINGER, C., HERNANDEZ, A. M., HERZOG, S., GRABBE, F., SIEVERDING, C., FISCHER, B., SCHRADER, K., BROCKMEYER, M., DETTMER, S., HELBIG, C., ALUNNI, V., BATTAINI, M. A., MURA, C., HENRICHSEN, C. N., GARCIA-LOPEZ, R., ECHEVARRIA, D., PUELLES, E., GARCIA-CALERO, E., KRUSE, S., UHR, M., KAUCK, C., FENG, G., MILYAEV, N., ONG, C. K., KUMAR, L., LAM, M., SEMPLE, C. A., GYENESEI, A., MUNDLOS, S., RADELOF, U., LEHRACH, H., SARMIENTOS, P., REYMOND, A., DAVIDSON, D. R., DOLLE, P., ANTONARAKIS, S. E., YASPO, M. L., MARTINEZ, S., BALDOCK, R. A., EICHELE, G. & BALLABIO, A. 2011. A high-resolution anatomical atlas of the transcriptome in the mouse embryo. *PLoS Biol,* 9**,** e1000582.

DUBE, D., LISSITZKY, J. C., LECLERC, R. & PELLETIER, G. 1978. Localization of alpha-melanocyte-stimulating hormone in rat brain and pituitary. *Endocrinology,* 102**,** 1283-91.

DUNLAP, J. C. 1999. Molecular bases for circadian clocks. *Cell,* 96**,** 271-90.

ECKEL-MAHAN, K. & SASSONE-CORSI, P. 2009. Metabolism control by the circadian clock and vice versa. *Nat Struct Mol Biol,* 16**,** 462-7.

EDELSBRUNNER, M. E., PAINSIPP, E., HERZOG, H. & HOLZER, P. 2009. Evidence from knockout mice for distinct implications of neuropeptide-Y Y2 and Y4 receptors in the circadian control of locomotion, exploration, water and food intake. *Neuropeptides,* 43**,** 491-7.

ELIAS, C. F., LEE, C., KELLY, J., ASCHKENASI, C., AHIMA, R. S., COUCEYRO, P. R., KUHAR, M. J., SAPER, C. B. & ELMQUIST, J. K. 1998. Leptin activates hypothalamic CART neurons projecting to the spinal cord. *Neuron,* 21**,** 1375-85.

ELMQUIST, J. K., AHIMA, R. S., ELIAS, C. F., FLIER, J. S. & SAPER, C. B. 1998a. Leptin activates distinct projections from the dorsomedial and ventromedial hypothalamic nuclei. *Proc Natl Acad Sci U S A,* 95**,** 741-6.

ELMQUIST, J. K., BJORBAEK, C., AHIMA, R. S., FLIER, J. S. & SAPER, C. B. 1998b. Distributions of leptin receptor mRNA isoforms in the rat brain. *J Comp Neurol,* 395**,** 535-47.

ETCHEGARAY, J. P., MACHIDA, K. K., NOTON, E., CONSTANCE, C. M., DALLMANN, R., DI NAPOLI, M. N., DEBRUYNE, J. P., LAMBERT, C. M., YU, E. A., REPPERT, S. M. & WEAVER, D. R. 2009. Casein kinase 1 delta regulates the pace of the mammalian circadian clock. *Mol Cell Biol,* 29**,** 3853-66.

FAULCONBRIDGE, L. F., GRILL, H. J. & KAPLAN, J. M. 2005. Distinct forebrain and caudal brainstem contributions to the neuropeptide Y mediation of ghrelin hyperphagia. *Diabetes,* 54**,** 1985-93.

FEILLET, C. A., ALBRECHT, U. & CHALLET, E. 2006. "Feeding time" for the brain: a matter of clocks. *J Physiol Paris,* 100**,** 252-60.

FENSELAU, H., CAMPBELL, J. N., VERSTEGEN, A. M., MADARA, J. C., XU, J., SHAH, B. P., RESCH, J. M., YANG, Z., MANDELBLAT-CERF, Y., LIVNEH, Y. & LOWELL, B. B. 2017. A rapidly acting glutamatergic ARC-->PVH satiety circuit postsynaptically regulated by alpha-MSH. *Nat Neurosci,* 20**,** 42-51.

FERNANDEZ, D. C., CHANG, Y. T., HATTAR, S. & CHEN, S. K. 2016. Architecture of retinal projections to the central circadian pacemaker. *Proc Natl Acad Sci U S A,* 113**,** 6047-52.

FLIER, J. S. & MARATOS-FLIER, E. 1998. Obesity and the hypothalamus: novel peptides for new pathways. *Cell,* 92**,** 437-40.

FLIER, J. S. & MARATOS-FLIER, E. 2010. Lasker lauds leptin. *Cell Metab,* 12**,** 317-320.

FOGLE, K. J., PARSON, K. G., DAHM, N. A. & HOLMES, T. C. 2011. CRYPTOCHROME is a blue-light sensor that regulates neuronal firing rate. *Science,* 331**,** 1409-13.

FOSTER, R. G., PEIRSON, S. N., WULFF, K., WINNEBECK, E., VETTER, C. & ROENNEBERG, T. 2013. Sleep and circadian rhythm disruption in social jetlag and mental illness. *Prog Mol Biol Transl Sci,* 119**,** 325-46.

FRIEDMAN, J. M. 2004. Modern science versus the stigma of obesity. *Nat Med,* 10**,** 563-9.

FRIEDMAN, J. M. 2010. A tale of two hormones. *Nat Med,* 16**,** 1100-6.

FU, L. & LEE, C. C. 2003. The circadian clock: pacemaker and tumour suppressor. *Nat Rev Cancer,* 3**,** 350-61.

GACHON, F., NAGOSHI, E., BROWN, S. A., RIPPERGER, J. & SCHIBLER, U. 2004. The mammalian circadian timing system: from gene expression to physiology. *Chromosoma,* 113**,** 103-12.

GAO, Q. & HORVATH, T. L. 2007. Neurobiology of feeding and energy expenditure. *Annu Rev Neurosci,* 30**,** 367-98.

GARFIELD, A. S., LI, C., MADARA, J. C., SHAH, B. P., WEBBER, E., STEGER, J. S., CAMPBELL, J. N., GAVRILOVA, O., LEE, C. E., OLSON, D. P., ELMQUIST, J. K., TANNOUS, B. A., KRASHES, M. J. & LOWELL, B. B. 2015. A neural basis for melanocortin-4 receptor-regulated appetite. *Nat Neurosci,* 18**,** 863-71.

GEKAKIS, N., STAKNIS, D., NGUYEN, H. B., DAVIS, F. C., WILSBACHER, L. D., KING, D. P., TAKAHASHI, J. S. & WEITZ, C. J. 1998. Role of the CLOCK protein in the mammalian circadian mechanism. *Science,* 280**,** 1564-9.

GHAMARI-LANGROUDI, M., COLMERS, W. F. & CONE, R. D. 2005. PYY3-36 inhibits the action potential firing activity of POMC neurons of arcuate nucleus through postsynaptic Y2 receptors. *Cell Metab,* 2**,** 191-9.

GOLOMBEK, D. A. & ROSENSTEIN, R. E. 2010. Physiology of circadian entrainment. *Physiol Rev,* 90**,** 1063-102.

GRANATA, R., ISGAARD, J., ALLOATTI, G. & GHIGO, E. 2011. Cardiovascular actions of the ghrelin gene-derived peptides and growth hormone-releasing hormone. *Exp Biol Med (Maywood),* 236**,** 505-14.

GREEN, D. J. & GILLETTE, R. 1982. Circadian rhythm of firing rate recorded from single cells in the rat suprachiasmatic brain slice. *Brain Res,* 245**,** 198-200.

GRIFFIN, E. A., JR., STAKNIS, D. & WEITZ, C. J. 1999. Light-independent role of CRY1 and CRY2 in the mammalian circadian clock. *Science,* 286**,** 768-71.

GROOS, G. & HENDRIKS, J. 1982. Circadian rhythms in electrical discharge of rat suprachiasmatic neurones recorded in vitro. *Neurosci Lett,* 34**,** 283-8.

GUAN, X. M., YU, H., PALYHA, O. C., MCKEE, K. K., FEIGHNER, S. D., SIRINATHSINGHJI, D. J., SMITH, R. G., VAN DER PLOEG, L. H. & HOWARD, A. D. 1997. Distribution of mRNA encoding the growth hormone secretagogue receptor in brain and peripheral tissues. *Brain Res Mol Brain Res,* 48**,** 23-9.

GUILDING, C., HUGHES, A. T., BROWN, T. M., NAMVAR, S. & PIGGINS, H. D. 2009. A riot of rhythms: neuronal and glial circadian oscillators in the mediobasal hypothalamus. *Mol Brain,* 2**,** 28.

GUILDING, C., HUGHES, A. T. & PIGGINS, H. D. 2010. Circadian oscillators in the epithalamus. *Neuroscience,* 169**,** 1630-9.

GUILDING, C. & PIGGINS, H. D. 2007. Challenging the omnipotence of the suprachiasmatic timekeeper: are circadian oscillators present throughout the mammalian brain? *Eur J Neurosci,* 25**,** 3195-216.

GUILLAUMOND, F., DARDENTE, H., GIGUERE, V. & CERMAKIAN, N. 2005. Differential control of Bmal1 circadian transcription by REV-ERB and ROR nuclear receptors. *J Biol Rhythms,* 20**,** 391-403.

HAN, S. K., GOTTSCH, M. L., LEE, K. J., POPA, S. M., SMITH, J. T., JAKAWICH, S. K., CLIFTON, D. K., STEINER, R. A. & HERBISON, A. E. 2005. Activation of gonadotropin-releasing hormone neurons by kisspeptin as a neuroendocrine switch for the onset of puberty. *J Neurosci,* 25**,** 11349-56.

HAN, S. Y., MCLENNAN, T., CZIESELSKY, K. & HERBISON, A. E. 2015. Selective optogenetic activation of arcuate kisspeptin neurons generates pulsatile luteinizing hormone secretion. *Proc Natl Acad Sci U S A,* 112**,** 13109-14.

HARA, R., WAN, K., WAKAMATSU, H., AIDA, R., MORIYA, T., AKIYAMA, M. & SHIBATA, S. 2001. Restricted feeding entrains liver clock without participation of the suprachiasmatic nucleus. *Genes Cells,* 6**,** 269-78.

HARDY, S. G. 2001. Hypothalamic projections to cardiovascular centers of the medulla. *Brain Res,* 894**,** 233-40.

HASTINGS, M. H., MEAD, S. M., VINDLACHERUVU, R. R., EBLING, F. J., MAYWOOD, E. S. & GROSSE, J. 1992. Non-photic phase shifting of the circadian activity rhythm of Syrian hamsters: the relative potency of arousal and melatonin. *Brain Res,* 591**,** 20-6.

HENTGES, S. T., NISHIYAMA, M., OVERSTREET, L. S., STENZEL-POORE, M., WILLIAMS, J. T. & LOW, M. J. 2004. GABA release from proopiomelanocortin neurons. *J Neurosci,* 24**,** 1578-83.

HEWSON, A. K. & DICKSON, S. L. 2000. Systemic administration of ghrelin induces Fos and Egr-1 proteins in the hypothalamic arcuate nucleus of fasted and fed rats. *J Neuroendocrinol,* 12**,** 1047-9.

HILL, J. W., ELMQUIST, J. K. & ELIAS, C. F. 2008. Hypothalamic pathways linking energy balance and reproduction. *Am J Physiol Endocrinol Metab,* 294**,** E827-32.

HOLSEN, L. M., LAWSON, E. A., CHRISTENSEN, K., KLIBANSKI, A. & GOLDSTEIN, J. M. 2014. Abnormal relationships between the neural response to high- and low-calorie foods and endogenous acylated ghrelin in women with active and weight-recovered anorexia nervosa. *Psychiatry Res,* 223**,** 94-103.

HONMA, K., VON GOETZ, C. & ASCHOFF, J. 1983. Effects of restricted daily feeding on freerunning circadian rhythms in rats. *Physiol Behav,* 30**,** 905-13.

HORIKAWA, K., MINAMI, Y., IIJIMA, M., AKIYAMA, M. & SHIBATA, S. 2005. Rapid damping of food-entrained circadian rhythm of clock gene expression in clock-defective peripheral tissues under fasting conditions. *Neuroscience,* 134**,** 335-43.

HORVATH, T. L. 2005. The hardship of obesity: a soft-wired hypothalamus. *Nat Neurosci,* 8**,** 561-5.

HORVATH, T. L., BECHMANN, I., NAFTOLIN, F., KALRA, S. P. & LERANTH, C. 1997. Heterogeneity in the neuropeptide Y-containing neurons of the rat arcuate nucleus: GABAergic and non-GABAergic subpopulations. *Brain Res,* 756**,** 283-6.

HORVATH, T. L., NAFTOLIN, F., KALRA, S. P. & LERANTH, C. 1992. Neuropeptide-Y innervation of beta-endorphin-containing cells in the rat mediobasal hypothalamus: a light and electron microscopic double immunostaining analysis. *Endocrinology,* 131**,** 2461-7.

HUGHES, A. T. & PIGGINS, H. D. 2012. Feedback actions of locomotor activity to the circadian clock. *Prog Brain Res,* 199**,** 305-36.

HUSZAR, D., LYNCH, C. A., FAIRCHILD-HUNTRESS, V., DUNMORE, J. H., FANG, Q., BERKEMEIER, L. R., GU, W., KESTERSON, R. A., BOSTON, B. A., CONE, R. D., SMITH, F. J., CAMPFIELD, L. A., BURN, P. & LEE, F. 1997. Targeted disruption of the melanocortin-4 receptor results in obesity in mice. *Cell,* 88**,** 131-41.

IBRAHIM, N., BOSCH, M. A., SMART, J. L., QIU, J., RUBINSTEIN, M., RONNEKLEIV, O. K., LOW, M. J. & KELLY, M. J. 2003. Hypothalamic proopiomelanocortin neurons are glucose responsive and express K(ATP) channels. *Endocrinology,* 144**,** 1331-40.

IIJIMA, M., YAMAGUCHI, S., VAN DER HORST, G. T., BONNEFONT, X., OKAMURA, H. & SHIBATA, S. 2005. Altered food-anticipatory activity rhythm in Cryptochrome-deficient mice. *Neurosci Res,* 52**,** 166-73.

INOUYE, S. T. & KAWAMURA, H. 1979. Persistence of circadian rhythmicity in a mammalian hypothalamic "island" containing the suprachiasmatic nucleus. *Proc Natl Acad Sci U S A,* 76**,** 5962-6.

ITRI, J. N., VOSKO, A. M., SCHROEDER, A., DRAGICH, J. M., MICHEL, S. & COLWELL, C. S. 2010. Circadian regulation of a-type potassium currents in the suprachiasmatic nucleus. *J Neurophysiol,* 103**,** 632-40.

JACKSON, A. C., YAO, G. L. & BEAN, B. P. 2004. Mechanism of spontaneous firing in dorsomedial suprachiasmatic nucleus neurons. *J Neurosci,* 24**,** 7985-98.

JERLHAG, E., EGECIOGLU, E., DICKSON, S. L., DOUHAN, A., SVENSSON, L. & ENGEL, J. A. 2007. Ghrelin administration into tegmental areas stimulates locomotor activity and increases extracellular concentration of dopamine in the nucleus accumbens. *Addict Biol,* 12**,** 6-16.

JOHNSON, C. H., GOLDEN, S. S., ISHIURA, M. & KONDO, T. 1996. Circadian clocks in prokaryotes. *Mol Microbiol,* 21**,** 5-11.

KALRA, S. P., DUBE, M. G., PU, S., XU, B., HORVATH, T. L. & KALRA, P. S. 1999. Interacting appetite-regulating pathways in the hypothalamic regulation of body weight. *Endocr Rev,* 20**,** 68-100.

KALSBEEK, A., PALM, I. F., LA FLEUR, S. E., SCHEER, F. A., PERREAU-LENZ, S., RUITER, M., KREIER, F., CAILOTTO, C. & BUIJS, R. M. 2006. SCN outputs and the hypothalamic balance of life. *J Biol Rhythms,* 21**,** 458-69.

KELLY, J. & GROSSMAN, S. P. 1979. GABA and hypothalamic feeding systems. II. A comparison of GABA, glycine and actylcholine agonists and their antagonists. *Pharmacol Biochem Behav,* 11**,** 647-52.

KIM, E. R., WU, Z., SUN, H., XU, Y., MANGIERI, L. R., XU, Y. & TONG, Q. 2015. Hypothalamic Non-AgRP, Non-POMC GABAergic Neurons Are Required for Postweaning Feeding and NPY Hyperphagia. *J Neurosci,* 35**,** 10440-50.

KISHI, T., ASCHKENASI, C. J., LEE, C. E., MOUNTJOY, K. G., SAPER, C. B. & ELMQUIST, J. K. 2003. Expression of melanocortin 4 receptor mRNA in the central nervous system of the rat. *J Comp Neurol,* 457**,** 213-35.

KO, C. H. & TAKAHASHI, J. S. 2006. Molecular components of the mammalian circadian clock. *Hum Mol Genet,* 15 Spec No 2**,** R271-7.

KOJIMA, M., HOSODA, H., DATE, Y., NAKAZATO, M., MATSUO, H. & KANGAWA, K. 1999. Ghrelin is a growth-hormone-releasing acylated peptide from stomach. *Nature,* 402**,** 656-60.

KOLA, B., FARKAS, I., CHRIST-CRAIN, M., WITTMANN, G., LOLLI, F., AMIN, F., HARVEY-WHITE, J., LIPOSITS, Z., KUNOS, G., GROSSMAN, A. B., FEKETE, C. & KORBONITS, M. 2008. The orexigenic effect of ghrelin is mediated through central activation of the endogenous cannabinoid system. *PLoS One,* 3**,** e1797.

KOLA, B., HUBINA, E., TUCCI, S. A., KIRKHAM, T. C., GARCIA, E. A., MITCHELL, S. E., WILLIAMS, L. M., HAWLEY, S. A., HARDIE, D. G., GROSSMAN, A. B. & KORBONITS, M. 2005. Cannabinoids and ghrelin have both central and peripheral metabolic and cardiac effects via AMP-activated protein kinase. *J Biol Chem,* 280**,** 25196-201.

KONOPKA, R. J. & BENZER, S. 1971. Clock mutants of Drosophila melanogaster. *Proc Natl Acad Sci U S A,* 68**,** 2112-6.

KRASHES, M. J., KODA, S., YE, C., ROGAN, S. C., ADAMS, A. C., CUSHER, D. S., MARATOS-FLIER, E., ROTH, B. L. & LOWELL, B. B. 2011. Rapid, reversible activation of AgRP neurons drives feeding behavior in mice. *J Clin Invest,* 121**,** 1424-8.

KRASHES, M. J., SHAH, B. P., KODA, S. & LOWELL, B. B. 2013. Rapid versus delayed stimulation of feeding by the endogenously released AgRP neuron mediators GABA, NPY, and AgRP. *Cell Metab,* 18**,** 588-95.

KROEMER, N. B., KREBS, L., KOBIELLA, A., GRIMM, O., PILHATSCH, M., BIDLINGMAIER, M., ZIMMERMANN, U. S. & SMOLKA, M. N. 2013. Fasting levels of ghrelin covary with the brain response to food pictures. *Addict Biol,* 18**,** 855-62.

KUHLMAN, S. J. & MCMAHON, D. G. 2004. Rhythmic regulation of membrane potential and potassium current persists in SCN neurons in the absence of environmental input. *Eur J Neurosci,* 20**,** 1113-7.

KUHLMAN, S. J., SILVER, R., LE SAUTER, J., BULT-ITO, A. & MCMAHON, D. G. 2003. Phase resetting light pulses induce Per1 and persistent spike activity in a subpopulation of biological clock neurons. *J Neurosci,* 23**,** 1441-50.

KWON JEONG, J., DAE KIM, J. & DIANO, S. 2013. Ghrelin regulates hypothalamic prolyl carboxypeptidase expression in mice. *Mol Metab,* 2**,** 23-30.

LEGRADI, G. & LECHAN, R. M. 1999. Agouti-related protein containing nerve terminals innervate thyrotropin-releasing hormone neurons in the hypothalamic paraventricular nucleus. *Endocrinology,* 140**,** 3643-52.

LEHMAN, M. N., SILVER, R., GLADSTONE, W. R., KAHN, R. M., GIBSON, M. & BITTMAN, E. L. 1987. Circadian rhythmicity restored by neural transplant. Immunocytochemical characterization of the graft and its integration with the host brain. *J Neurosci,* 7**,** 1626-38.

LESAGE, F. 2003. Pharmacology of neuronal background potassium channels. *Neuropharmacology,* 44**,** 1-7.

LESAUTER, J., LEHMAN, M. N. & SILVER, R. 1996. Restoration of circadian rhythmicity by transplants of SCN "micropunches". *J Biol Rhythms,* 11**,** 163-71.

LESAUTER, J. & SILVER, R. 1998. Output signals of the SCN. *Chronobiol Int,* 15**,** 535-50.

LESAUTER, J., YAN, L., VISHNUBHOTLA, B., QUINTERO, J. E., KUHLMAN, S. J., MCMAHON, D. G. & SILVER, R. 2003. A short half-life GFP mouse model for analysis of suprachiasmatic nucleus organization. *Brain Res,* 964**,** 279-87.

LI, A. J., WIATER, M. F., OOSTROM, M. T., SMITH, B. R., WANG, Q., DINH, T. T., ROBERTS, B. L., JANSEN, H. T. & RITTER, S. 2012. Leptin-sensitive neurons in the arcuate nuclei contribute to endogenous feeding rhythms. *Am J Physiol Regul Integr Comp Physiol,* 302**,** R1313-26.

LI, C., CHEN, P. & SMITH, M. S. 1999. Morphological evidence for direct interaction between arcuate nucleus neuropeptide Y (NPY) neurons and gonadotropin-releasing hormone neurons and the possible involvement of NPY Y1 receptors. *Endocrinology,* 140**,** 5382-90.

LIU, C., WEAVER, D. R., STROGATZ, S. H. & REPPERT, S. M. 1997. Cellular construction of a circadian clock: period determination in the suprachiasmatic nuclei. *Cell,* 91**,** 855-60.

LIU, H., KISHI, T., ROSEBERRY, A. G., CAI, X., LEE, C. E., MONTEZ, J. M., FRIEDMAN, J. M. & ELMQUIST, J. K. 2003. Transgenic mice expressing green fluorescent protein under the control of the melanocortin-4 receptor promoter. *J Neurosci,* 23**,** 7143-54.

LIU, T., KONG, D., SHAH, B. P., YE, C., KODA, S., SAUNDERS, A., DING, J. B., YANG, Z., SABATINI, B. L. & LOWELL, B. B. 2012. Fasting activation of AgRP neurons requires NMDA receptors and involves spinogenesis and increased excitatory tone. *Neuron,* 73**,** 511-22.

LOPEZ, M., LAGE, R., SAHA, A. K., PEREZ-TILVE, D., VAZQUEZ, M. J., VARELA, L., SANGIAO-ALVARELLOS, S., TOVAR, S., RAGHAY, K., RODRIGUEZ-CUENCA, S., DEOLIVEIRA, R. M., CASTANEDA, T., DATTA, R., DONG, J. Z., CULLER, M., SLEEMAN, M. W., ALVAREZ, C. V., GALLEGO, R., LELLIOTT, C. J., CARLING, D., TSCHOP, M. H., DIEGUEZ, C. & VIDAL-PUIG, A. 2008. Hypothalamic fatty acid metabolism mediates the orexigenic action of ghrelin. *Cell Metab,* 7**,** 389-99.

LUQUET, S., PEREZ, F. A., HNASKO, T. S. & PALMITER, R. D. 2005. NPY/AgRP neurons are essential for feeding in adult mice but can be ablated in neonates. *Science,* 310**,** 683-5.

MA, X., ZUBCEVIC, L., BRUNING, J. C., ASHCROFT, F. M. & BURDAKOV, D. 2007. Electrical inhibition of identified anorexigenic POMC neurons by orexin/hypocretin. *J Neurosci,* 27**,** 1529-33.

MANDELBLAT-CERF, Y., RAMESH, R. N., BURGESS, C. R., PATELLA, P., YANG, Z., LOWELL, B. B. & ANDERMANN, M. L. 2015. Arcuate hypothalamic AgRP and putative POMC neurons show opposite changes in spiking across multiple timescales. *Elife,* 4.

MARKS, J. L., LI, M., SCHWARTZ, M., PORTE, D., JR. & BASKIN, D. G. 1992. Effect of fasting on regional levels of neuropeptide Y mRNA and insulin receptors in the rat hypothalamus: An autoradiographic study. *Mol Cell Neurosci,* 3**,** 199-205.

MASUDA, Y., TANAKA, T., INOMATA, N., OHNUMA, N., TANAKA, S., ITOH, Z., HOSODA, H., KOJIMA, M. & KANGAWA, K. 2000. Ghrelin stimulates gastric acid secretion and motility in rats. *Biochem Biophys Res Commun,* 276**,** 905-8.

MAYWOOD, E. S., SMITH, E., HALL, S. J. & HASTINGS, M. H. 1997. A thalamic contribution to arousal-induced, non-photic entrainment of the circadian clock of the Syrian hamster. *Eur J Neurosci,* 9**,** 1739-47.

MEISTER, B. 2007. Neurotransmitters in key neurons of the hypothalamus that regulate feeding behavior and body weight. *Physiol Behav,* 92**,** 263-71.

MEISTER, B., CECCATELLI, S., HOKFELT, T., ANDEN, N. E., ANDEN, M. & THEODORSSON, E. 1989. Neurotransmitters, neuropeptides and binding sites in the rat mediobasal hypothalamus: effects of monosodium glutamate (MSG) lesions. *Exp Brain Res,* 76**,** 343-68.

MENDONCA, P. R. F., KYLE, V., YEO, S. H., COLLEDGE, W. H. & ROBINSON, H. P. C. 2018. Kv4.2 channel activity controls intrinsic firing dynamics of arcuate kisspeptin neurons. *J Physiol,* 596**,** 885-899.

MENG, Q. J., LOGUNOVA, L., MAYWOOD, E. S., GALLEGO, M., LEBIECKI, J., BROWN, T. M., SLADEK, M., SEMIKHODSKII, A. S., GLOSSOP, N. R., PIGGINS, H. D., CHESHAM, J. E., BECHTOLD, D. A., YOO, S. H., TAKAHASHI, J. S., VIRSHUP, D. M., BOOT-HANDFORD, R. P., HASTINGS, M. H. & LOUDON, A. S. 2008. Setting clock speed in mammals: the CK1 epsilon tau mutation in mice accelerates circadian pacemakers by selectively destabilizing PERIOD proteins. *Neuron,* 58**,** 78-88.

MERCER, A. J., HENTGES, S. T., MESHUL, C. K. & LOW, M. J. 2013. Unraveling the central proopiomelanocortin neural circuits. *Front Neurosci,* 7**,** 19.

MERCER, J. G., HOGGARD, N., WILLIAMS, L. M., LAWRENCE, C. B., HANNAH, L. T. & TRAYHURN, P. 1996. Localization of leptin receptor mRNA and the long form splice variant (Ob-Rb) in mouse hypothalamus and adjacent brain regions by in situ hybridization. *FEBS Lett,* 387**,** 113-6.

MEREDITH, A. L., WILER, S. W., MILLER, B. H., TAKAHASHI, J. S., FODOR, A. A., RUBY, N. F. & ALDRICH, R. W. 2006. BK calcium-activated potassium channels regulate circadian behavioral rhythms and pacemaker output. *Nat Neurosci,* 9**,** 1041-9.

MEYER-BERNSTEIN, E. L., JETTON, A. E., MATSUMOTO, S. I., MARKUNS, J. F., LEHMAN, M. N. & BITTMAN, E. L. 1999. Effects of suprachiasmatic transplants on circadian rhythms of neuroendocrine function in golden hamsters. *Endocrinology,* 140**,** 207-18.

MIEDA, M. & SAKURAI, T. 2011. Bmal1 in the nervous system is essential for normal adaptation of circadian locomotor activity and food intake to periodic feeding. *J Neurosci,* 31**,** 15391-6.

MIRSHAMSI, S., LAIDLAW, H. A., NING, K., ANDERSON, E., BURGESS, L. A., GRAY, A., SUTHERLAND, C. & ASHFORD, M. L. 2004. Leptin and insulin stimulation of signalling pathways in arcuate nucleus neurones: PI3K dependent actin reorganization and KATP channel activation. *BMC Neurosci,* 5**,** 54.

MISTLBERGER, R. E. 1994. Circadian food-anticipatory activity: formal models and physiological mechanisms. *Neurosci Biobehav Rev,* 18**,** 171-95.

MOHAWK, J. A., GREEN, C. B. & TAKAHASHI, J. S. 2012. Central and peripheral circadian clocks in mammals. *Annu Rev Neurosci,* 35**,** 445-62.

MONTELEONE, P., BENCIVENGA, R., LONGOBARDI, N., SERRITELLA, C. & MAJ, M. 2003. Differential responses of circulating ghrelin to high-fat or high-carbohydrate meal in healthy women. *J Clin Endocrinol Metab,* 88**,** 5510-4.

MOORE, R. Y. & EICHLER, V. B. 1972. Loss of a circadian adrenal corticosterone rhythm following suprachiasmatic lesions in the rat. *Brain Res,* 42**,** 201-6.

MORTON, G. J., CUMMINGS, D. E., BASKIN, D. G., BARSH, G. S. & SCHWARTZ, M. W. 2006. Central nervous system control of food intake and body weight. *Nature,* 443**,** 289-95.

MORTON, G. J., NISWENDER, K. D., RHODES, C. J., MYERS, M. G., JR., BLEVINS, J. E., BASKIN, D. G. & SCHWARTZ, M. W. 2003. Arcuate nucleus-specific leptin receptor gene therapy attenuates the obesity phenotype of Koletsky (fa(k)/fa(k)) rats. *Endocrinology,* 144**,** 2016-24.

MOUNTJOY, K. G., MORTRUD, M. T., LOW, M. J., SIMERLY, R. B. & CONE, R. D. 1994. Localization of the melanocortin-4 receptor (MC4-R) in neuroendocrine and autonomic control circuits in the brain. *Mol Endocrinol,* 8**,** 1298-308.

MOUNTJOY, K. G., ROBBINS, L. S., MORTRUD, M. T. & CONE, R. D. 1992. The cloning of a family of genes that encode the melanocortin receptors. *Science,* 257**,** 1248-51.

MROSOVSKY, N. 1996. Locomotor activity and non-photic influences on circadian clocks. *Biol Rev Camb Philos Soc,* 71**,** 343-72.

MROSOVSKY, N., REEBS, S. G., HONRADO, G. I. & SALMON, P. A. 1989. Behavioural entrainment of circadian rhythms. *Experientia,* 45**,** 696-702.

NAKAZATO, M., MURAKAMI, N., DATE, Y., KOJIMA, M., MATSUO, H., KANGAWA, K. & MATSUKURA, S. 2001. A role for ghrelin in the central regulation of feeding. *Nature,* 409**,** 194-8.

NISWENDER, K. D., MORRISON, C. D., CLEGG, D. J., OLSON, R., BASKIN, D. G., MYERS, M. G., JR., SEELEY, R. J. & SCHWARTZ, M. W. 2003. Insulin activation of phosphatidylinositol 3-kinase in the hypothalamic arcuate nucleus: a key mediator of insulin-induced anorexia. *Diabetes,* 52**,** 227-31.

NORSTED, E., GOMUC, B. & MEISTER, B. 2008. Protein components of the blood-brain barrier (BBB) in the mediobasal hypothalamus. *J Chem Neuroanat,* 36**,** 107-21.

OBICI, S., WANG, J., CHOWDURY, R., FENG, Z., SIDDHANTA, U., MORGAN, K. & ROSSETTI, L. 2002. Identification of a biochemical link between energy intake and energy expenditure. *J Clin Invest,* 109**,** 1599-605.

OLLMANN, M. M., WILSON, B. D., YANG, Y. K., KERNS, J. A., CHEN, Y., GANTZ, I. & BARSH, G. S. 1997. Antagonism of central melanocortin receptors in vitro and in vivo by agouti-related protein. *Science,* 278**,** 135-8.

PALUS, S., SCHUR, R., AKASHI, Y. J., BOCKMEYER, B., DATTA, R., HALEM, H., DONG, J., CULLER, M. D., ADAMS, V., ANKER, S. D. & SPRINGER, J. 2011. Ghrelin and its analogues, BIM-28131 and BIM-28125, improve body weight and regulate the expression of MuRF-1 and MAFbx in a rat heart failure model. *PLoS One,* 6**,** e26865.

PANDA, S., ANTOCH, M. P., MILLER, B. H., SU, A. I., SCHOOK, A. B., STRAUME, M., SCHULTZ, P. G., KAY, S. A., TAKAHASHI, J. S. & HOGENESCH, J. B. 2002a.

Coordinated transcription of key pathways in the mouse by the circadian clock. *Cell,* 109**,** 307-20.

PANDA, S., HOGENESCH, J. B. & KAY, S. A. 2002b. Circadian rhythms from flies to human. *Nature,* 417**,** 329-35.

PARTCH, C. L., GREEN, C. B. & TAKAHASHI, J. S. 2014. Molecular architecture of the mammalian circadian clock. *Trends Cell Biol,* 24**,** 90-9.

PENDERGAST, J. S. & YAMAZAKI, S. 2018. The Mysterious Food-Entrainable Oscillator: Insights from Mutant and Engineered Mouse Models. *J Biol Rhythms***,** 748730418789043.

PENNARTZ, C. M., DE JEU, M. T., BOS, N. P., SCHAAP, J. & GEURTSEN, A. M. 2002. Diurnal modulation of pacemaker potentials and calcium current in the mammalian circadian clock. *Nature,* 416**,** 286-90.

PERUZZO, B., PASTOR, F. E., BLAZQUEZ, J. L., AMAT, P. & RODRIGUEZ, E. M. 2004. Polarized endocytosis and transcytosis in the hypothalamic tanycytes of the rat. *Cell Tissue Res,* 317**,** 147-64.

PEZUK, P., MOHAWK, J. A., YOSHIKAWA, T., SELLIX, M. T. & MENAKER, M. 2010. Circadian organization is governed by extra-SCN pacemakers. *J Biol Rhythms,* 25**,** 432-41.

PIET, R., DE CROFT, S., LIU, X. & HERBISON, A. E. 2015. Electrical properties of kisspeptin neurons and their regulation of GnRH neurons. *Front Neuroendocrinol,* 36**,** 15-27.

PITTS, G. R., OHTA, H. & MCMAHON, D. G. 2006. Daily rhythmicity of large-conductance Ca2+ -activated K+ currents in suprachiasmatic nucleus neurons. *Brain Res,* 1071**,** 54-62.

PITTS, S., PERONE, E. & SILVER, R. 2003. Food-entrained circadian rhythms are sustained in arrhythmic Clk/Clk mutant mice. *Am J Physiol Regul Integr Comp Physiol,* 285**,** R57-67.

PLUM, L., MA, X., HAMPEL, B., BALTHASAR, N., COPPARI, R., MUNZBERG, H., SHANABROUGH, M., BURDAKOV, D., ROTHER, E., JANOSCHEK, R., ALBER, J., BELGARDT, B. F., KOCH, L., SEIBLER, J., SCHWENK, F., FEKETE, C., SUZUKI, A., MAK, T. W., KRONE, W., HORVATH, T. L., ASHCROFT, F. M. & BRUNING, J. C. 2006. Enhanced PIP3 signaling in POMC neurons causes KATP channel activation and leads to diet-sensitive obesity. *J Clin Invest,* 116**,** 1886-901.

POCAI, A., LAM, T. K., GUTIERREZ-JUAREZ, R., OBICI, S., SCHWARTZ, G. J., BRYAN, J., AGUILAR-BRYAN, L. & ROSSETTI, L. 2005. Hypothalamic K(ATP) channels control hepatic glucose production. *Nature,* 434**,** 1026-31.

POGGIOLI, R., VERGONI, A. V. & BERTOLINI, A. 1986. ACTH-(1-24) and alpha-MSH antagonize feeding behavior stimulated by kappa opiate agonists. *Peptides,* 7**,** 843-8.

PREITNER, N., DAMIOLA, F., LOPEZ-MOLINA, L., ZAKANY, J., DUBOULE, D., ALBRECHT, U. & SCHIBLER, U. 2002. The orphan nuclear receptor REV-ERBalpha controls circadian transcription within the positive limb of the mammalian circadian oscillator. *Cell,* 110**,** 251-60.

QIU, J., FANG, Y., RONNEKLEIV, O. K. & KELLY, M. J. 2010. Leptin excites proopiomelanocortin neurons via activation of TRPC channels. *J Neurosci,* 30**,** 1560-5.

QIU, J., ZHANG, C., BORGQUIST, A., NESTOR, C. C., SMITH, A. W., BOSCH, M. A., KU, S., WAGNER, E. J., RONNEKLEIV, O. K. & KELLY, M. J. 2014. Insulin excites anorexigenic

proopiomelanocortin neurons via activation of canonical transient receptor potential channels. *Cell Metab,* 19**,** 682-93.

QUINTERO, J. E., KUHLMAN, S. J. & MCMAHON, D. G. 2003. The biological clock nucleus: a multiphasic oscillator network regulated by light. *J Neurosci,* 23**,** 8070-6.

RALPH, M. R., FOSTER, R. G., DAVIS, F. C. & MENAKER, M. 1990. Transplanted suprachiasmatic nucleus determines circadian period. *Science,* 247**,** 975-8.

RETHELYI, M. 1984. Diffusional barrier around the hypothalamic arcuate nucleus in the rat. *Brain Res,* 307**,** 355-8.

RODRIGUEZ, E. M., BLAZQUEZ, J. L., PASTOR, F. E., PELAEZ, B., PENA, P., PERUZZO, B. & AMAT, P. 2005. Hypothalamic tanycytes: a key component of brain-endocrine interaction. *Int Rev Cytol,* 247**,** 89-164.

SAEB-PARSY, K., LOMBARDELLI, S., KHAN, F. Z., MCDOWALL, K., AU-YONG, I. T. & DYBALL, R. E. 2000. Neural connections of hypothalamic neuroendocrine nuclei in the rat. *J Neuroendocrinol,* 12**,** 635-48.

SAKHI, K., BELLE, M. D., GOSSAN, N., DELAGRANGE, P. & PIGGINS, H. D. 2014. Daily variation in the electrophysiological activity of mouse medial habenula neurones. *J Physiol,* 592**,** 587-603.

SAKURAI, T., AMEMIYA, A., ISHII, M., MATSUZAKI, I., CHEMELLI, R. M., TANAKA, H., WILLIAMS, S. C., RICHARSON, J. A., KOZLOWSKI, G. P., WILSON, S., ARCH, J. R., BUCKINGHAM, R. E., HAYNES, A. C., CARR, S. A., ANNAN, R. S., MCNULTY, D. E., LIU, W. S., TERRETT, J. A., ELSHOURBAGY, N. A., BERGSMA, D. J. & YANAGISAWA, M. 1998. Orexins and orexin receptors: a family of hypothalamic neuropeptides and G protein-coupled receptors that regulate feeding behavior. *Cell,* 92**,** 1 page following 696.

SAPER, C. B., CHOU, T. C. & SCAMMELL, T. E. 2001. The sleep switch: hypothalamic control of sleep and wakefulness. *Trends Neurosci,* 24**,** 726-31.

SATO, T. K., YAMADA, R. G., UKAI, H., BAGGS, J. E., MIRAGLIA, L. J., KOBAYASHI, T. J., WELSH, D. K., KAY, S. A., UEDA, H. R. & HOGENESCH, J. B. 2006. Feedback repression is required for mammalian circadian clock function. *Nat Genet,* 38**,** 312-9.

SCHAEFFER, M., LANGLET, F., LAFONT, C., MOLINO, F., HODSON, D. J., ROUX, T., LAMARQUE, L., VERDIE, P., BOURRIER, E., DEHOUCK, B., BANERES, J. L., MARTINEZ, J., MERY, P. F., MARIE, J., TRINQUET, E., FEHRENTZ, J. A., PREVOT, V. & MOLLARD, P. 2013. Rapid sensing of circulating ghrelin by hypothalamic appetite-modifying neurons. *Proc Natl Acad Sci U S A,* 110**,** 1512-7.

SCHWARTZ, M. W., SEELEY, R. J., CAMPFIELD, L. A., BURN, P. & BASKIN, D. G. 1996. Identification of targets of leptin action in rat hypothalamus. *J Clin Invest,* 98**,** 1101-6.

SCOTT, M. M., LACHEY, J. L., STERNSON, S. M., LEE, C. E., ELIAS, C. F., FRIEDMAN, J. M. & ELMQUIST, J. K. 2009. Leptin targets in the mouse brain. *J Comp Neurol,* 514**,** 518-32.

SHAH, B. P., VONG, L., OLSON, D. P., KODA, S., KRASHES, M. J., YE, C., YANG, Z., FULLER, P. M., ELMQUIST, J. K. & LOWELL, B. B. 2014. MC4R-expressing glutamatergic neurons in the paraventricular hypothalamus regulate feeding and are synaptically connected to the parabrachial nucleus. *Proc Natl Acad Sci U S A,* 111**,** 13193-8.

SHEARMAN, L. P., ZYLKA, M. J., WEAVER, D. R., KOLAKOWSKI, L. F., JR. & REPPERT, S. M. 1997. Two period homologs: circadian expression and photic regulation in the suprachiasmatic nuclei. *Neuron,* 19**,** 1261-9.

SHIEH, K. R., YANG, S. C., LU, X. Y., AKIL, H. & WATSON, S. J. 2005. Diurnal rhythmic expression of the rhythm-related genes, rPeriod1, rPeriod2, and rClock, in the rat brain. *J Biomed Sci,* 12**,** 209-17.

SHIGEYOSHI, Y., TAGUCHI, K., YAMAMOTO, S., TAKEKIDA, S., YAN, L., TEI, H., MORIYA, T., SHIBATA, S., LOROS, J. J., DUNLAP, J. C. & OKAMURA, H. 1997. Light-induced resetting of a mammalian circadian clock is associated with rapid induction of the mPer1 transcript. *Cell,* 91**,** 1043-53.

SHUTO, Y., SHIBASAKI, T., OTAGIRI, A., KURIYAMA, H., OHATA, H., TAMURA, H., KAMEGAI, J., SUGIHARA, H., OIKAWA, S. & WAKABAYASHI, I. 2002. Hypothalamic growth hormone secretagogue receptor regulates growth hormone secretion, feeding, and adiposity. *J Clin Invest,* 109**,** 1429-36.

SKIBICKA, K. P. & GRILL, H. J. 2009. Hypothalamic and hindbrain melanocortin receptors contribute to the feeding, thermogenic, and cardiovascular action of melanocortins. *Endocrinology,* 150**,** 5351-61.

SPANSWICK, D., SMITH, M. A., GROPPI, V. E., LOGAN, S. D. & ASHFORD, M. L. 1997. Leptin inhibits hypothalamic neurons by activation of ATP-sensitive potassium channels. *Nature,* 390**,** 521-5.

SPANSWICK, D., SMITH, M. A., MIRSHAMSI, S., ROUTH, V. H. & ASHFORD, M. L. 2000. Insulin activates ATP-sensitive K+ channels in hypothalamic neurons of lean, but not obese rats. *Nat Neurosci,* 3**,** 757-8.

STEINER, R. A., KABIGTING, E., LENT, K. & CLIFTON, D. K. 1994. Diurnal rhythm in proopiomelanocortin mRNA in the arcuate nucleus of the male rat. *J Neuroendocrinol,* 6**,** 603-8.

STEPHAN, F. K., SWANN, J. M. & SISK, C. L. 1979. Entrainment of circadian rhythms by feeding schedules in rats with suprachiasmatic lesions. *Behav Neural Biol,* 25**,** 545-54.

STEPHAN, F. K. & ZUCKER, I. 1972. Circadian rhythms in drinking behavior and locomotor activity of rats are eliminated by hypothalamic lesions. *Proc Natl Acad Sci U S A,* 69**,** 1583-6.

STRANGE, B. A., WITTER, M. P., LEIN, E. S. & MOSER, E. I. 2014. Functional organization of the hippocampal longitudinal axis. *Nat Rev Neurosci,* 15**,** 655-69.

SUN, Y., WANG, P., ZHENG, H. & SMITH, R. G. 2004. Ghrelin stimulation of growth hormone release and appetite is mediated through the growth hormone secretagogue receptor. *Proc Natl Acad Sci U S A,* 101**,** 4679-84.

SZENTIRMAI, E., HAJDU, I., OBAL, F., JR. & KRUEGER, J. M. 2006. Ghrelin-induced sleep responses in ad libitum fed and food-restricted rats. *Brain Res,* 1088**,** 131-40.

TAKAHASHI, K. A. & CONE, R. D. 2005. Fasting induces a large, leptin-dependent increase in the intrinsic action potential frequency of orexigenic arcuate nucleus neuropeptide Y/Agouti-related protein neurons. *Endocrinology,* 146**,** 1043-7.

TAMARGO, J., CABALLERO, R., GOMEZ, R., VALENZUELA, C. & DELPON, E. 2004. Pharmacology of cardiac potassium channels. *Cardiovasc Res,* 62**,** 9-33.

TARTAGLIA, L. A., DEMBSKI, M., WENG, X., DENG, N., CULPEPPER, J., DEVOS, R., RICHARDS, G. J., CAMPFIELD, L. A., CLARK, F. T., DEEDS, J., MUIR, C., SANKER, S., MORIARTY, A., MOORE, K. J., SMUTKO, J. S., MAYS, G. G., WOOL, E. A., MONROE,

C. A. & TEPPER, R. I. 1995. Identification and expression cloning of a leptin receptor, OB-R. *Cell,* 83**,** 1263-71.

THEANDER-CARRILLO, C., WIEDMER, P., CETTOUR-ROSE, P., NOGUEIRAS, R., PEREZ-TILVE, D., PFLUGER, P., CASTANEDA, T. R., MUZZIN, P., SCHURMANN, A., SZANTO, I., TSCHOP, M. H. & ROHNER-JEANRENAUD, F. 2006. Ghrelin action in the brain controls adipocyte metabolism. *J Clin Invest,* 116**,** 1983-93.

TONG, Q., YE, C. P., JONES, J. E., ELMQUIST, J. K. & LOWELL, B. B. 2008. Synaptic release of GABA by AgRP neurons is required for normal regulation of energy balance. *Nat Neurosci,* 11**,** 998-1000.

TOSINI, G. & MENAKER, M. 1996. Circadian rhythms in cultured mammalian retina. *Science,* 272**,** 419-21.

TUREK, F. W., JOSHU, C., KOHSAKA, A., LIN, E., IVANOVA, G., MCDEARMON, E., LAPOSKY, A., LOSEE-OLSON, S., EASTON, A., JENSEN, D. R., ECKEL, R. H., TAKAHASHI, J. S. & BASS, J. 2005. Obesity and metabolic syndrome in circadian Clock mutant mice. *Science,* 308**,** 1043-5.

UEBERBERG, B., UNGER, N., SAEGER, W., MANN, K. & PETERSENN, S. 2009. Expression of ghrelin and its receptor in human tissues. *Horm Metab Res,* 41**,** 814-21.

VAISSE, C., CLEMENT, K., GUY-GRAND, B. & FROGUEL, P. 1998. A frameshift mutation in human MC4R is associated with a dominant form of obesity. *Nat Genet,* 20**,** 113-4.

VAN DEN POL, A. N., YAO, Y., FU, L. Y., FOO, K., HUANG, H., COPPARI, R., LOWELL, B. B. & BROBERGER, C. 2009. Neuromedin B and gastrin-releasing peptide excite arcuate nucleus neuropeptide Y neurons in a novel transgenic mouse expressing strong Renilla green fluorescent protein in NPY neurons. *J Neurosci,* 29**,** 4622-39.

VAN DEN TOP, M., LEE, K., WHYMENT, A. D., BLANKS, A. M. & SPANSWICK, D. 2004. Orexigen-sensitive NPY/AgRP pacemaker neurons in the hypothalamic arcuate nucleus. *Nat Neurosci,* 7**,** 493-4.

VAN DEN TOP, M., LYONS, D. J., LEE, K., CODERRE, E., RENAUD, L. P. & SPANSWICK, D. 2007. Pharmacological and molecular characterization of ATP-sensitive K(+) conductances in CART and NPY/AgRP expressing neurons of the hypothalamic arcuate nucleus. *Neuroscience,* 144**,** 815-24.

VAN DEN TOP, M. & SPANSWICK, D. 2006. Integration of metabolic stimuli in the hypothalamic arcuate nucleus. *Prog Brain Res,* 153**,** 141-54.

VAN DER LELY, A. J., TSCHOP, M., HEIMAN, M. L. & GHIGO, E. 2004. Biological, physiological, pathophysiological, and pharmacological aspects of ghrelin. *Endocr Rev,* 25**,** 426-57.

VITATERNA, M. H., KING, D. P., CHANG, A. M., KORNHAUSER, J. M., LOWREY, P. L., MCDONALD, J. D., DOVE, W. F., PINTO, L. H., TUREK, F. W. & TAKAHASHI, J. S. 1994. Mutagenesis and mapping of a mouse gene, Clock, essential for circadian behavior. *Science,* 264**,** 719-25.

VONG, L., YE, C., YANG, Z., CHOI, B., CHUA, S., JR. & LOWELL, B. B. 2011. Leptin action on GABAergic neurons prevents obesity and reduces inhibitory tone to POMC neurons. *Neuron,* 71**,** 142-54.

WANG, H., STORLIEN, L. H. & HUANG, X. F. 2002. Effects of dietary fat types on body fatness, leptin, and ARC leptin receptor, NPY, and AgRP mRNA expression. *Am J Physiol Endocrinol Metab,* 282**,** E1352-9.

WANG, Q., LIU, C., UCHIDA, A., CHUANG, J. C., WALKER, A., LIU, T., OSBORNE-LAWRENCE, S., MASON, B. L., MOSHER, C., BERGLUND, E. D., ELMQUIST, J. K. & ZIGMAN, J. M.

2014. Arcuate AgRP neurons mediate orexigenic and glucoregulatory actions of ghrelin. *Mol Metab,* 3**,** 64-72.

WELSH, D. K., LOGOTHETIS, D. E., MEISTER, M. & REPPERT, S. M. 1995. Individual neurons dissociated from rat suprachiasmatic nucleus express independently phased circadian firing rhythms. *Neuron,* 14**,** 697-706.

WHITT, J. P., MONTGOMERY, J. R. & MEREDITH, A. L. 2016. BK channel inactivation gates daytime excitability in the circadian clock. *Nat Commun,* 7**,** 10837.

WIATER, M. F., MUKHERJEE, S., LI, A. J., DINH, T. T., ROONEY, E. M., SIMASKO, S. M. & RITTER, S. 2011. Circadian integration of sleep-wake and feeding requires NPY receptor-expressing neurons in the mediobasal hypothalamus. *Am J Physiol Regul Integr Comp Physiol,* 301**,** R1569-83.

WILLESEN, M. G., KRISTENSEN, P. & ROMER, J. 1999. Co-localization of growth hormone secretagogue receptor and NPY mRNA in the arcuate nucleus of the rat. *Neuroendocrinology,* 70**,** 306-16.

WILLIAMS, K. W., SCOTT, M. M. & ELMQUIST, J. K. 2009. From observation to experimentation: leptin action in the mediobasal hypothalamus. *Am J Clin Nutr,* 89**,** 985S-990S.

WILSBACHER, L. D., YAMAZAKI, S., HERZOG, E. D., SONG, E. J., RADCLIFFE, L. A., ABE, M., BLOCK, G., SPITZNAGEL, E., MENAKER, M. & TAKAHASHI, J. S. 2002. Photic and circadian expression of luciferase in mPeriod1-luc transgenic mice invivo. *Proc Natl Acad Sci U S A,* 99**,** 489-94.

WREN, A. M., SEAL, L. J., COHEN, M. A., BRYNES, A. E., FROST, G. S., MURPHY, K. G., DHILLO, W. S., GHATEI, M. A. & BLOOM, S. R. 2001. Ghrelin enhances appetite and increases food intake in humans. *J Clin Endocrinol Metab,* 86**,** 5992.

WU, Q. & PALMITER, R. D. 2011. GABAergic signaling by AgRP neurons prevents anorexia via a melanocortin-independent mechanism. *Eur J Pharmacol,* 660**,** 21-7.

XU, B., KALRA, P. S., FARMERIE, W. G. & KALRA, S. P. 1999. Daily changes in hypothalamic gene expression of neuropeptide Y, galanin, proopiomelanocortin, and adipocyte leptin gene expression and secretion: effects of food restriction. *Endocrinology,* 140**,** 2868-75.

YAMAMOTO, S., SHIGEYOSHI, Y., ISHIDA, Y., FUKUYAMA, T., YAMAGUCHI, S., YAGITA, K., MORIYA, T., SHIBATA, S., TAKASHIMA, N. & OKAMURA, H. 2001. Expression of the Per1 gene in the hamster: brain atlas and circadian characteristics in the suprachiasmatic nucleus. *J Comp Neurol,* 430**,** 518-32.

YAMAZAKI, S., NUMANO, R., ABE, M., HIDA, A., TAKAHASHI, R., UEDA, M., BLOCK, G. D., SAKAKI, Y., MENAKER, M. & TEI, H. 2000. Resetting central and peripheral circadian oscillators in transgenic rats. *Science,* 288**,** 682-5.

YANG, M. J., WANG, F., WANG, J. H., WU, W. N., HU, Z. L., CHENG, J., YU, D. F., LONG, L. H., FU, H., XIE, N. & CHEN, J. G. 2010. PI3K integrates the effects of insulin and leptin on large-conductance Ca2+-activated K+ channels in neuropeptide Y neurons of the hypothalamic arcuate nucleus. *Am J Physiol Endocrinol Metab,* 298**,** E193-201.

YEO, G. S., FAROOQI, I. S., AMINIAN, S., HALSALL, D. J., STANHOPE, R. G. & O'RAHILLY, S. 1998. A frameshift mutation in MC4R associated with dominantly inherited human obesity. *Nat Genet,* 20**,** 111-2.

YIP, S. H., BOEHM, U., HERBISON, A. E. & CAMPBELL, R. E. 2015. Conditional Viral Tract Tracing Delineates the Projections of the Distinct Kisspeptin Neuron Populations

to Gonadotropin-Releasing Hormone (GnRH) Neurons in the Mouse. *Endocrinology,* 156**,** 2582-94.

YOO, S. H., KO, C. H., LOWREY, P. L., BUHR, E. D., SONG, E. J., CHANG, S., YOO, O. J., YAMAZAKI, S., LEE, C. & TAKAHASHI, J. S. 2005. A noncanonical E-box enhancer drives mouse Period2 circadian oscillations in vivo. *Proc Natl Acad Sci U S A,* 102**,** 2608-13.

YOO, S. H., YAMAZAKI, S., LOWREY, P. L., SHIMOMURA, K., KO, C. H., BUHR, E. D., SIEPKA, S. M., HONG, H. K., OH, W. J., YOO, O. J., MENAKER, M. & TAKAHASHI, J. S. 2004. PERIOD2::LUCIFERASE real-time reporting of circadian dynamics reveals persistent circadian oscillations in mouse peripheral tissues. *Proc Natl Acad Sci U S A,* 101**,** 5339-46.

ZHAN, C., ZHOU, J., FENG, Q., ZHANG, J. E., LIN, S., BAO, J., WU, P. & LUO, M. 2013. Acute and long-term suppression of feeding behavior by POMC neurons in the brainstem and hypothalamus, respectively. *J Neurosci,* 33**,** 3624-32.

ZHANG, X. & VAN DEN POL, A. N. 2013. Direct inhibition of arcuate proopiomelanocortin neurons: a potential mechanism for the orexigenic actions of dynorphin. *J Physiol,* 591**,** 1731-47.

ZHANG, X. & VAN DEN POL, A. N. 2015. Dopamine/Tyrosine Hydroxylase Neurons of the Hypothalamic Arcuate Nucleus Release GABA, Communicate with Dopaminergic and Other Arcuate Neurons, and Respond to Dynorphin, Met-Enkephalin, and Oxytocin. *J Neurosci,* 35**,** 14966-82.

ZHANG, X. & VAN DEN POL, A. N. 2016. Hypothalamic arcuate nucleus tyrosine hydroxylase neurons play orexigenic role in energy homeostasis. *Nat Neurosci,* 19**,** 1341-7.

ZHANG, Y., PROENCA, R., MAFFEI, M., BARONE, M., LEOPOLD, L. & FRIEDMAN, J. M. 1994. Positional cloning of the mouse obese gene and its human homologue. *Nature,* 372**,** 425-32.

ZHENG, B., LARKIN, D. W., ALBRECHT, U., SUN, Z. S., SAGE, M., EICHELE, G., LEE, C. C. & BRADLEY, A. 1999. The mPer2 gene encodes a functional component of the mammalian circadian clock. *Nature,* 400**,** 169-73.

ZHU, J. N., YUNG, W. H., KWOK-CHONG CHOW, B., CHAN, Y. S. & WANG, J. J. 2006. The cerebellar-hypothalamic circuits: potential pathways underlying cerebellar involvement in somatic-visceral integration. *Brain Res Rev,* 52**,** 93-106.

General Methods

General Methods

Experimental approach

A range of experimental techniques were used to collect the data presented in this thesis. Broadly, the methods can be split into *in vitro* and *in vivo* experimental techniques. These two elements were used in combination to investigate the physiological function of the local clock housed within the ARC.

The first and last chapters focus primarily on *in vitro* electrophysiological techniques. The middle chapter adopts a multi-disciplinary approach, utilising a wide range of electrophysiological and in vivo methodologies to investigate the role of the local ARC clock in regulating food and drink consumption. This chapter also builds on findings presented in the first, and focuses on identifying whether changes to ARC neuronal excitability depend on the presence of intact local molecular clockwork components.

Electrophysiology

CNS tissues maintain their circadian properties *in vitro*. For example, hypothalamic SCN slices exhibit rhythms in excitability in culture that are observed *in vivo* (Belle et al., 2009, Wang et al., 2012, Kuhlman and McMahon, 2004, Groos and Hendriks, 1982). Electrophysiological rhythms in the SCN are accompanied by daily and circadian rhythms in gene expression as assessed using bioluminescent reporters of core molecular clock components (Evans et al., 2013, Guilding et al., 2013, Yamaguchi et al., 2003). Sustained genetic oscillations are also detectable in individual cells of the MBH, including the DMH and ARC (Guilding et al., 2009). These properties make *in vitro* recordings a suitable model for studying the molecular and electrophysiological mechanisms of circadian timekeeping in a given brain region. Moreover, recordings from slices enable study of extra-SCN regions in isolation.

Animals

All procedures were carried out in accordance with the UK Animals (Scientific Procedures) Act of 1986 using procedures approved by The University of Manchester Review Ethics

Panel. All animals were group housed under a 12/12h light/dark (LD) cycle. In these LD conditions, lights on was defined as Zeitgeber Time 0 (ZT0) and lights off as ZT12. Animals had *ad libitum* access to food and water, temperature was maintained at 20 ± 2 °C and humidity at ~40%. Experiments were conducted on male mice (8-14 week old) expressing a Venus fluorescent protein reporter for the *Per1* gene (Cheng et al., 2009), hence called *Per1*::Venus (generated from breeding pairs kindly provided by Prof. K. Obrietan, The Ohio State University, Columbus, Oh, USA). Bodyweight was recorded prior to all electrophysiology experiments on *Per1*::Venus mice, and only data from animals in the 22-28g range were included for analysis.

For some electrophysiology experiments, 10-18 week old male *Cryptochrome1(Cry1)* and *Cry2* gene knockout mice ($Cry1^{-/-}Cry2^{-/-}$) which lack functional molecular circadian clocks and their congenic wild-type littermates ($Cry1^{+/+}Cry2^{+/+}$, molecular circadian clock intact) were used (van der Horst et al., 1999). These were bred from $Cry1^{+/-}Cry2^{+/-}$ mice kindly provided by Prof. B. van der Horst, Erasmus Medical Center, Rotterdam, NL. Animals were housed in the same conditions as stated above or transferred from LD to constant dark (DD) 72h days prior to recording. Animals with bodyweight of 22-28g were used for electrophysiological recordings. Male mice (7-10 weeks old) in which the Brain and Muscle ARNT-Like1 (*Bmal1)* loci is flanked by *lox-p* sites (Storch et al., 2007) were housed under LD conditions prior to and following viral microinjections. $Bmal1^{fl/fl}$ mice were generated from breeding pairs initially provided by Prof. C. Weitz, Harvard Medical School, Boston, Ma, USA.

The third results chapter of this thesis utilises mice expressing a humanised *Renilla* green fluorescent protein (hrGFP) in neuropeptide-Y(NPY)-expressing cells of the brain (van den Pol et al., 2009). These NPY-hrGFP mice were kindly provided as a gift from Prof. S. Luckman, The University of Manchester, UK. The high relative brightness of this reporter mouse makes it ideal for targeted neurons in slices during whole-cell recordings. 5-7 week old male NPY-hrGFP mice were group housed under an LD cycle before brains were extracted for electrophysiology.

Slice preparation

For whole-cell electrophysiology and pMEA recordings, brains were harvested at ZT1 for daytime recordings (ZT4-10) or ZT11 for the night epoch (ZT14-20). For recordings performed from mice that have been housed in constant darkness, the subjective day or night was defined based on Circadian Time. The onset of wheel-running activity was defined as CT12. Cull time (CT1 or CT11) and recording epochs (CT4-10 or CT14-20, respective to cull time) were calculated based on the average free-running period of the genotype from which slices were collected.

Mice were deeply anaesthetised with isoflurane and decapitated. Brains were quickly extracted and immersed in ice-cold high-sucrose cutting solution containing (in mM): 0.5 NaCl, 1.8 KCl, 1.2 KH_2PO_4, 7 $MgSO_4$, 26 $NaHCO_3$, 15 Glucose and 50 Sucrose (300-310 $mosmol^{-1}$; pregassed with 95% O_2/ 5% CO_2). The composition of this solution, with high magnesium, low calcium and sodium, was formulated to protect the tissue from excitotoxic neuronal death while maintaining sufficient energy levels.

The forebrain and cerebellum were removed and coronal brain slices (300μm) containing the MBH were prepared using a vibratome (Campden Instruments, Loughborough, UK) and transferred into an incubation chamber filled with cutting solution to rest at room temperature. After 30min recovery period, slices were transferred into artificial cerebrospinal solution (aCSF) solution, composed of the following constituents (in mM): 127 NaCl, 1.8 KCl, 1.2 KH_2PO_4, 1.3 $MgSO_4$, 26 $NaHCO_3$, 15 Glucose and 2.4 $CaCl_2$. For experiments performed on slices harvested from NPY-hrGFP mice, the glucose concentration was lowered to 5mM, and sucrose concentration was increased to maintain an appropriate osmolality value. After a further 1h recovery period, slices were transferred to a recording chamber for whole-cell experiments or onto pMEAs and continuously perfused with aCSF.

Slices for all electrophysiology recordings were selected based on rostrocaudal position using Paxinos and Franklin's 4^{th} edition mouse brain atlas (Paxinos and Franklin, 2012). Here, slices containing ARC, DMH and VMH at the level of -1.7 to -1.9mm bregma were used. The recording surface for both whole-cell and pMEA experiments was typically -1.8mm from bregma.

Current clamp recordings

Whole-cell current clamp recordings were performed on a rig mounted on a vibration-free air table to ensure stability during the experiment (TMC 63-500 series, Ma, USA). Slices were placed in a bespoke tissue chamber which permits a continuous and even supply of oxygenated aCSF to the tissue. Slices were secured with a platinum tissue harp, ensuring that the fine strings did not rest on or occlude the ARC. An Olympus BX51W1 upright microscope (Olympus Corporation, Tokyo, Japan) combined with a Hamamatsu Orca R^2 camera system (Hamamatsu Photonics, Tohoku, Japan) in conjunction with a Hitachi monitor (Hitachi ltd., Tokyo, Japan) was used during visually-guided whole-cell recordings. The rig optics could be switched between infrared-differential interference contrast (IR-DIC) optics and epifluorescence. Targeted recordings were performed on *Per1*::Venus neurons using an epifluorescence filter set for GFP/Venus.

Slices were imaged through a 40-fold and 10-fold magnification water-immersion objective lens (Olympus Corporation, Tokyo, Japan). Images were recorded live using micromanager 1.4 (μManager, Cal, USA) and still photos were taken to assess whether cells, which were clearly visible by IR-DIC, displayed a strong Venus signal localised to the soma. The same optical setup and imaging software were used to visualise NPY-hrGFP-positive neurons. For recordings on neurons from *Cry1*$^{+/+}$*Cry2*$^{+/+}$ and *Cry1*$^{-/-}$*Cry2*$^{-/-}$ mice recordings were visually-guided using the same setup, however no fluorescent targeting was performed. Cells in medial or lateral areas of ARC (mARC/latARC) were visually targeted and the location was later confirmed by biocytin immunostaining (see *immunohistochemistry*). Those designated as latARC were at least 200μm from the wall of the 3V. All whole-cell recordings were performed at room temperature which was typically 20-22°C.

A gravity assisted vertical PC-10 puller (Narishige, Tokyo, Japan) was used to prepare pipettes from thick-walled borosilicate glass capillaries (Harvard Apparatus Ltd, Ma, USA). A two stage pull with different heating filament temperatures was used to make 7-10MΩ pipettes for current clamp recordings. Pipettes of this resistance ensure tight-seal patch-clamp recordings with low access resistance. Prior to head stage mounting, pipettes were backfilled with a specially designed anti-dilution intracellular solution containing (in mM):

130 K-gluconate, 10 KCl, 2mM $MgCl_2$, 10 Hepes, 0.5 EGTA, 2 K_2ATP and 0.5 NaGTP (Belle et al., 2009). The presence of ATP and GTP in this solution prevents rundown of the cell by providing energy for cellular phosphorylation reactions and G-protein-dependent cascades. The intracellular solution also contained biocytin (Tocris Bioscience, Bristol, UK) for cell filling and subsequent post hoc localisation by immunohistochemistry. Intracellular solution was made as a frozen stock solution. A benchmark osmolarity of 295-300 mosmol kg^{-1} was tested for before the solution was aliquoted into 2ml microcentrifuge tubes and frozen ready for use. For the duration of the recording session, intracellular solution was stored on ice and microfiltered during backfilling to increase sterility and improve the recording quality and longevity.

The recording apparatus used here was designed specifically for optimal whole-cell recordings in the current clamp configuration. An npi BA-03X amplifier in bridge configuration (npi electronics, Tamm, Germany), compensating for the transient capacitance of the pipette, and a CED 1401 mark II A/D data acquisition interface (Cambridge Electronic Design, Cambridge, UK) were used to record current clamp data. All recording signals were sampled at a frequency of 30 kHz in Spike 2 Version 7 (Cambridge Electronic Design) and saved on a PC for future extraction and analysis.

The silver-chloride recording and reference electrodes were regularly immersed in bleach to reduce the solid-liquid junction potential that occurs after days of patch-clamp recordings. Using the amplifiers' bridge balance, any visible junction potential (typically ~6-10mV) between the intracellular solution and extracellular aCSF was corrected. Offline correction of liquid junction potential was not performed for the experimental data presented in this thesis.

During the recording procedure, the recording pipette was first lowered to the surface of the slice using the 10x objective lens, and the recording location was selected (mARC or latARC). Once the pipette was above the surface of the slice, neurons were approached at 40x resolution, using IR-DIC to carefully navigate through the slice to avoid disrupting the tissue architecture. Positive pressure was applied using a syringe prior to entry into the bath to reduce the chance of blockage. Cells were selected based upon visual inspection of both the morphology and integrity of the membrane.

A gigaohm seal was established by releasing the positive pressure and creating suction when the pipette aperture was close to the membrane. 110pA positive current pulses were applied to electrically distinguish when the gigaseal had been formed. The positive current pulse was then removed and manual suction was applied while maintaining the cell membrane at ~45mV by injecting negative current. Whole-cell configuration was confirmed by the presence of action-potentials and/or increased variability in the voltage trace. The holding current was then removed and the cell was allowed to reach its intrinsic behaviour. A series of current steps and pulses were then applied to assess a range of membrane properties including input resistance.

Drugs were bath applied using a gravity driven system which shares the flow of drug-free aCSF. The majority of drugs were stored in aliquots at -20°C and frozen on the day of use. All frozen drugs were tested on pMEA prior to use for whole-cell experiments. A detailed description of the drug application procedure including the duration and concentration, as well as the analysis of effect protocol is provided within the methods section of each results chapter.

Data Analysis

The data collected by whole-cell recording provides a rich understanding of a given cells electrophysiological characteristics that cannot be obtained by extracellular recording, such that intricate details about electrical behaviours and ion channel function can be determined (Sakmann and Neher, 1984, Cahalan and Neher, 1992). The following parameters were measured for each neuron:

Resting membrane potential (RMP, mV): Calculated by using a Spike2 script that functions to quantify mean potential difference across all points at which the derivative of the phase-plane plot (ΔdV/dT) is <4% maximum – this function excludes APs from the calculation.

Spontaneous Firing Rate (SFR, Hz): A 60s epoch of the raw data file was extracted and APs were processed as time-stamped waveforms with an exclusion threshold of -5mV (spike must exceed from baseline ~ -40mV). The waveform data was then plotted as an instantaneous frequency plot from which time values were extracted to calculate firing

rate and interspike interval (ISI). Firing regularity was determined by calculating the coefficient of variance (ISI/ mean ISI) of the ISIs in a given recording window. A standard cut-off coefficient of variance value of <0.35 was used to define a cell as regular firing. Irregular firing cells had coefficient of variances of ≥0.35 (Pristera et al., 2015, Young et al., 1988).

Input resistance (R_{input}, GΩ): Calculated from baseline RMP and response to 20pA current pulses in accordance with Ohm's law (ΔV/I) where ΔV = RMP/Peak of -20pA deflection. Care was taken to ensure that postsynaptic potentials did not influence voltage responses to current pulses.

Waveform average: Spike's waveform average tool was used to generate representative average waveform from all spikes within a 1min time window from the baseline of a current clamp recording. From this waveform, a number of parameters were measured, including amplitude, afterhyperpolarisation, half AP duration (ADP50) and AP threshold.

To maintain objective analysis while determining the intrinsic behaviour of the cell, a set of criteria were used, in agreement with published methods from our group (Sakhi et al., 2014a, Sakhi et al., 2014b, Belle et al., 2009, Timothy et al., 2017).

1. A stable RMP must be achieved within 30 seconds of when intracellular access of the pipette has occurred (demarcated by emergence of APs).
2. A stable RMP must be maintained for at least 1 minute. RMP must not fluctuate by more than 1mV. This period is used to calculate the parameters used for analysis.
3. If a cell then reaches a second stable RMP then the cell is rejected from the pool of recordings used for calculation of mean values (unless drug has been applied).
4. The SFR must also be consistent across this 1 minute baseline period.
5. Cells which are defined as depolarised silent must exhibit all electrical states when manually hyperpolarised or be induced to fire by application of hyperpolarising drugs.
6. Hyperpolarised silent cells must fire AP trains in response to positive current pulses.

All Current clamp data was recorded and analysed using Spike2 software v7 (Cambridge Electronic Design, Cambridge, United Kingdom). Data was exported from Excel 2010

(Microsoft Corporation, Wa, USA) into Origin version 9.0 (OriginLab Corporation, Ma, USA) for statistical analysis and constructing figures.

Voltage clamp Electrophysiology

Coordinated timekeeping by cellular oscillators in the SCN depends largely on GABA, the release of which displays circadian rhythmicity (Itri et al., 2004, Evans et al., 2013). Fast neurotransmitters also play an important role in the neuronal circuitry of ARC. Glutamate decarboxylase, a marker of GABAergic cells can be stained for in ARC (Decavel and Van den Pol, 1990). Furthermore, both NPY/AgRP and POMC neurons receive glutamatergic and GABAergic inputs (Pinto et al., 2004).

To investigate synaptic events we employed voltage clamp electrophysiology, in gap-free mode, to measure postsynaptic currents (PSCs) evoked by neurotransmitter fusion with the postsynaptic membrane. Brain slices were prepared and loaded into the same rig which was used to perform the current clamp experiments presented in this thesis. However, a dedicated recording setup was used to record synaptic events during visually guided whole-cell recordings.

Synaptic input activity was measured using an Axopatch 200b amplifier (Molecular Devices, Cal, USA). Signals were acquired using pClamp 10.2 (Clampex and Clampfit) in conjunction with a Digidata 1440A interface (Molecular Devices). Miniature and spontaneous PSCs (mPSCs and sPSCs respectively) were recorded with larger aperture 4-6MΩ patch pipettes using an internal solution that was identical to the one used in current clamp recordings, except for 120mM K-gluconate and 20KCl mM (Belle et al., 2014). In ARC neurons, this concentration of Cl^- causes inhibitory PSCs (IPSCs) to reverse at approximately -45mV. Therefore, this positive shift in Cl- reversal potential causes both GABAergic and glutamatergic excitatory (EPSCs) to appear as inward currents when the membrane is clamped at a holding potential of -70mV.

To discriminate the origin of these inward currents, a cocktail of receptor antagonists (D-2-amino-5-phosphonopentanoic acid, AP5; 6-cyano-7-nitroquinoxaline-2,3-dione, CNQX) for the glutamate receptors and/or for the $GABA_A$ receptor (Gabazine) were bath applied during recording. To determine the contribution of AP-dependent synaptic

communication to ARC network activity, we applied TTX (1µM) to block Na^+ channels, and recorded mPSCs which occur due to spontaneous and quantal release of neurotransmitter. This type of neurotransmitter release was first identified in frog neuromuscular junctions, however has been demonstrated by voltage clamp recordings in ARC (Fatt and Katz, 1952, Pinto et al., 2004, Baquero et al., 2015, Qiu et al., 2014). The recording procedure including break in was similar to current clamp experiments, except for differences in amplifier settings and transient compensation. Three separate modes in the Clampex software were used, which are equivalent to the bridge-mode setting in current clamp. In bath mode voltage steps of 5mV at 100kHz were applied with no holding current. During sealing, the amplifier was switched to patch mode and the membrane was held at -60mV while the amplifier simultaneously applied positive voltage steps of 10mV. Following membrane rupture by mouth suction, pulses were removed, and ARC neurons were held at a resting potential of -70mV in cell mode.

Pipette and whole-cell capacitance transients were compensated in patch and cell mode respectively. Cell capacitance (C_m) and series resistance (R_{series}) was compensated 70-80%. Throughout the recording of an individual neuron, C_m and R_{series} were continuously monitored for consistency, with a change of ≥15% resulting in rejection of that cell from future analysis. R_{series} was typically ~20 MΩ and recordings with an access resistance of ≤30 MΩ were considered viable. These values ensure that good pipette-cell access is maintained during the recording procedure. Like current clamp recordings, a strong seal must form between the pipette and cell membrane. In voltage clamp mode seal resistance was ≥5 GΩ.

Data Analysis

Raw traces generated in Clampex were exported into Clampfit, the analysis package that comes with pClamp 10.2 (Molecular Devices, Cal, USA). The template search function built into Clampfit was used to discriminate PSCs exceeding an amplitude threshold of 5pA from the baseline current. This function creates an average waveform and then extracts recognised single waveforms and their timestamps over the recording window. Here, baseline PSC frequency was determined over a minimum baseline time period of

100s. Baseline leak current was adjusted to zero throughout the 100s recording to ensure accurate analysis of event amplitudes.

PSC frequency was then analysed after the addition of glutamatergic or GABAergic blockers to determine the relative contribution of each fast neurotransmitter system. After the drug cocktail 1 (either glutamatergic or GABAergic blockade) was bath applied for 3min, 100s was recorded drug-free, then cocktail 2 was added. 30s of data was analysed at baseline, 30s at the end of the 100s drug-free period, and 30s after cocktail 2 application. The frequency of glutamatergic or GABAergic events was calculated by subtracting the event frequency after cocktail 1 from the baseline frequency, ensuring that after the addition of all antagonists, no events were present. Similarly, PSC frequency was determined after the addition of TTX to the bath to investigate the contribution of AP-dependent versus quantal events. Clampfit automatically calculates a large range of parameters from the template search function, including event amplitude and interevent interval.

Multielectrode array recordings

The development of planar multielectrode array to record network activity of neuronal circuits represents a powerful advance in neuroscience methods (Shaban et al., 2017). This is especially applicable in circadian biology as these tools can determine changes in network activity of a large population of neurons with high spatial and temporal resolution (Walmsley et al., 2015). However, conventional multielectrode arrays present numerous challenges and limitations. For example it may be difficult to maintain good contact between the surface of the tissue and the electrode contacts. Conventional multielectrode arrays may also restrict oxygenation and nutrient supply to the recording surface. These issues have been resolved by the development of dual-perfusion perforated multielectrode array (pMEA) systems. These systems enable recording of neuronal activity in slices with excellent signal-to-noise ratio due to close contact with the pMEA electrodes. Furthermore, the continuous flow of aCSF deep into the parenchyma of the slice ensures oxygenation and nutrient supply to the tissue.

Brain slices were harvested using identical methods to those outlined above (see *slice preparation*). Following cutting and incubation in high-Mg2+/low-Ca2+ solution slices

were transferred into aCSF at room temperature. A 2L bottle of aCSF was warmed to 33°C in a water bath and gassed with 95% O_2 before addition of calcium chloride. Meanwhile, the pMEA system was set up to run water through all of the tubing to allow easy switch to aCSF prior to recording and maintain cleanliness of the system. Slices were then transferred to a reservoir of 33°C aCSF for a further 30min to reduce the effects of sharp changes in temperature on neuronal activity. The pMEA system was then switched to aCSF and slices were then loaded. Typically two opposing faces (approx. -1.8mm from bregma) of adjacent slices were selected as the recording surface. Consistent placement of the slice was essential for the reliability of this experiment in which comparisons were drawn between neighbouring electrodes and brain areas. Photos were taken of the slice *in situ* to confirm that slice placement was indeed consistent between experiments.

A dual-MEA2100-HS2x60 head-stage system (Multichannel Systems, Reutlingen, Germany) was used to record extracellular spiking activity. The duality of this pMEA system allows simultaneous recording of two ARC-containing brain slices. This device integrates data from 120 pMEA recording electrodes (60 per chamber) embedded in a perforated polyimide foil and communicates with the PC via a MEA2100 interface board. The pMEAs used for these experiments consist of an 8x8 grid of titanium nitride electrodes (30µm diameter, 200µm spacing) which allows sufficient coverage of ARC and adjacent MBH subnuclei (DMH/VMH, 60pMEA200/30iR-Ti-gr, Multichannel Systems).

For each of the pMEA chambers there are two perfusion systems; and “upper” and “lower” perfusion chamber. Importantly, perforations in the polyimidine foil allow aCSF exchange above and below the pMEA electrodes. This permits the formation of negative pressure/suction underneath the brain slice in the under perfusion chamber and ensures that the tissue remains in the same location on the electrodes throughout recording. Negative pressure in the under perfusion chamber was created using a vacuum pump which enabled very accurate feed-back control of pressure. As many air bubbles as possible were removed from the under perfusion chamber during setup in water to minimise the possibility of bubbles disrupting the suction and compromising the experiment. Gravity-driven flow of aCSF directly into the under perfusion chamber maintained the volume and stabilised negative pressure formation.

The upper perfusion system comprises of inflow tubing, removal tubing and a slice chamber, at the bottom of which sits the 8x8 grid of electrodes. The inflow of aCSF into the slice chamber (above the polyimide foil) and outflow of aCSF to a waste bottle were regulated by two separate pumps. A variety of drugs were diluted in aCSF and bath-applied via the same route. An inward flow of ~2ml/min was selected to ensure continuous supply of oxygenated aCSF while the slice was fully immersed. The temperature of the aCSF was boosted on transit from the water bath to the slice chamber by two cannula temperature units set to heat the aCSF to 33°C controlled by a TC02 temperature controller (Multichannel systems, Reutlingen, Germany).

To ensure we kept a suitable spike detection threshold, we bath applied tetrodotoxin (TTX) at the end of each recording session (Tocris Bioscience, Bristol, UK). TTX was stored in frozen aliquots at -20°C and was thawed and diluted to working concentration in aCSF. 5minute bath application of 1µM TTX was sufficient to block all spiking activity in all cases.

Data Analysis

Raw data signals were acquired at 25kHz using MC rack software (Multichannel systems) and saved as 10min files due to the large individual file size (1.5gigabytes per 10min). Files were then merged chronologically and a 300Hz high-pass filter was applied to the raw data signals. Spikes were then discriminated from the raw data using a thresholding tool in MC rack. Based on the typical noise of the recordings after the application of TTX, a threshold of -15.5µV was used to discriminate spikes for all recordings.

The processed file containing just the spikes (not raw data signal) was then imported into Neuroexplorer (Nex technologies, CO, USA) to extract the baseline spiking frequency. Spike waveforms and timestamps can be analysed in Neuroexplorer in great detail with a number of outputs. Here, multiunit spike frequency analysis was performed. Histograms can be constructed with a set bin time (e.g. 1min bins), that can be manually adjusted to calculate multiunit spike frequency. Bin size used for analysis and the duration of baseline activity within each time epoch varies between each results chapter - these are stated in the respective results chapter method sections.

One advantage of recording multiunit activity is that individual neurons can be analysed separately by extracting single-unit waveforms from a recording which potentially represents the firing frequency of many. This provides insights to how a single neuron may be contributing to overall network activity, and is a useful comparator to data collected from whole-cell experiments.

A 1min section of the raw data file within the initial baseline was imported into offline sorter v4 (Plexon Inc., TX, USA). Using this software, principal component-based sorting was used to discriminate single units, identifiable as an isolated cluster of spikes in principal component space. Data from each electrode channel was sorted manually to ensure that all single-unit signals were accurately discriminated. The spike sorted data was then exported to Neuroexplorer for analysis.

Post-recording Immunofluorescence

Brain slices used for whole-cell electrophysiological recording were immediately post-fixed in ice-cold 4% paraformaldehyde in 0.1M PBS (pH 7.4). After 24h the slices were transferred to 0.1M PBS alone, and stored for a maximum for 3 days. The slices were then washed with PBS and incubated in Triton-X 100 (0.6% in PBS;10% normal donkey serum) for 3h at room temperature and transferred to a solution containing Cy3-conjugated Extravidin (1:250 in PBS, Sigma-Aldrich, MO, USA) and rabbit anti-GFP primary antibody (1:1000, Abcam, Cambridge, UK) in PBS, 2% NDS and 0.3% Triton-X 100. Slices were incubated in the primary antibody/Extravidin solution for 1-3 days in darkness at 4°C.

Subsequently, slices were transferred to a secondary antibody solution containing a fluorescein conjugated anti-rabbit antibody (Jackson ImmunoResearch, USA) diluted 1:800 in PBS and incubated at 4°C overnight. The next day, slices were washed in PBS and mounted onto gelatine-coated slides for visualisation. Image stacks were captured using a Leica SP5 Upright confocal microscope using a 20x objective with 3x confocal zoom (Leica systems, Wetzlar, Germany).

A select number of *Per1*::Venus slices were also stained against glial fibrillary acidic protein (Primary antibody anti-GFAP, 1:400, Sigma-Aldrich), Vimentin (1:1000, Abcam) and GFP (1:1000, *Results* Fig1). Secondary antibodies for GFAP (anti-mouse CY3, 1:800,

Jackson ImmunoResearch), Vimentin (anti-chicken alexa488, 1:800, Jackson) and GFP (anti-rabbit CY5, Jackson ImmunoResearch) were used following an identical wash/mounting protocol to that outlined above.

Slices recorded on pMEAs from rAAV2-Cre-GFP injected animals were screened for reconstruction of the site of virus microinjection using the same protocol as above except Cy3-conjugated Extravidin was not added to the primary antibody solution. Images from these slices were captured on a Olympus BX51 microscope equipped with a DP71 camera in conjunction with an U-RFLT light source (Olympus Corporation, Tokyo, Japan) due to the large number of slices collected from experiments.

In vivo assessment of wheel-running, feeding and drinking behaviour

When singly-housed and presented with a running-wheel, mice and other rodents exhibit rhythmic bouts of activity that can be used to assess the output of the circadian system (Pittendrigh and Daan, 1976). Despite consideration regarding concerns that wheel behaviour occurs only in captivity (Mason et al., 2007) and that exercise feedback directly to the SCN may affect the animals natural behaviour (Hughes and Piggins, 2012, van Oosterhout et al., 2012), wheel-running is a well-established model to study in vivo circadian rhythms (Novak et al., 2012). Importantly for this study, observing wheel-running is consistently able to highlight circadian behavioural deficits following lesion of clock genes (Vitaterna et al., 1994).

Here, the assessment of wheel-running, feeding and drinking behaviour was primarily performed to support the findings made from electrophysiological experiments. The daily and circadian profile of activity was assessed in $Cry1^{+/+}Cry2^{+/+}$ and $Cry1^{-/-}Cry2^{-/-}$ mice to ensure that whole-cell recordings were performed during an appropriate period of the subjective day and night under constant dark conditions. We also assessed whether targeted cre-dependent deletion of *Bmal1* by nanoinjection of viral vectors into ARC altered the circadian profile of feeding and drinking activity.

$Cry1^{+/+}Cry2^{+/+}$ and $Cry1^{-/-}Cry2^{-/-}$ mice were singly-housed in running wheel-equipped cages with a drinking bottle and food hopper hanging from a precision balance to monitor activity (TSE systems, Bad Homburg, Germany). Wheel-running, drinking and feeding

activities were recorded using Phenomaster in 10min bins (TSE systems). The precision balances of this system were sensitive to very small negative changes in water volume (0.01ml) and food weight (0.01g) ensuring accurate and high resolution measurement of intake. Mice were fed and watered *ad libitum* with a standard lab chow diet: 5/20/75% calories from fat, protein and carbohydrates respectively. Cages were environmentally enriched with a variety of bedding material and a cardboard tube. Light and temperature conditions were continuously monitored prior to and when animals were housed in the cages using a HOBO data logger (Tempcon Ltd., Sussex, UK). Consistent temperature was particularly important for these experiments as maintenance of appropriate body weight was critical to ensure mice were within a comparable range.

Mice were initially allowed to entrain in LD conditions for at least 8 days followed by free-running in constant darkness (DD) for 10 days. Period was calculated by chi-squared periodogram to give a quantitative measure of the dominant periodic component (Sokolove and Bushell, 1978). Circadian behavioural phenotypes were analysed and actograms and chi-squared periodograms were constructed using the ClockLab plugin (Actimetrics, IL, USA) for Matlab 2014 (MathWorks, MA, USA). Images obtained were analysed in ImageJ. After DD the room was returned to LD.

An identical cage setup and lighting paradigm to that described above was used to screen injected *Bmal1*$^{fl/fl}$ mice for changes in food and drink intake following knockout of *Bmal1* in the ARC. However, whilst feeding and drinking were assessed in an identical manner to *Cry1*$^{+/+}$*Cry2*$^{+/+}$ and *Cry1*$^{-/-}$*Cry2*$^{-/-}$ mice cages were not equipped with running wheels. Instead, some cages were fitted with a roof mounted infrared monitoring system that was centrally placed to measure locomotor activity (Inframot, TSE Systems). Infrared data was used purely to monitor animals throughout the experiment and was not used in the analysis - the system only measures locomotor activity in a crude and space-restricted manner.

Food and water intake were recorded using Phenomaster (TSE systems). Data was exported as a table from Phenomaster into Microsoft Excel 2010 (Microsoft Corporation, Wa, USA). Average food and water intake during the light and dark phase were statistically compared by repeated measures ANOVA performed in Origin version 9

(OriginLab Corporation, Ma, USA). The same analysis was performed on subjective day and night data when animals were in DD. Food and water intake in 1h bins was also analysed to examine temporal patterns in food and water intake across the LD cycle. All data was adjusted to each animal's body weight to account for fluctuations due to differences in individual energy demands. Meal frequency and size was calculated from 10min bins in which food consumption exceeded >0.05g.

Viral injections

7-10 week old male *Bmal1*$^{fl/fl}$ mice were group housed under LD conditions prior to viral injection experiments to ensure mice were entrained to a robust and controlled light schedule. For surgery mice were temporarily relocated to a specially equipped theatre for the duration of the procedure. All procedures were carried out in accordance with the UK Animals (Scientific Procedures) Act of 1986 using procedures approved by The University of Manchester Review Ethics Panel. Animal care and comfort was dealt with extreme care and consideration. A qualified veterinary surgeon was available throughout the surgery and all procedures were performed by a personal license holder with ample experience and training.

To ensure precise and replicable viral injections we used a Neurostar drill and injection robot (Neurostar, Tubingen, Germany). The robot allows motorised, computer controlled positioning of a drill bit and injection needle in the X,Y and Z axis. These two arms of the robot system work together to ensure accurate drilling and manipulation of the needle to the injection site. Prior to each surgery session, a series of calibration steps were performed to ensure that the correct distances measured by the motorised frame were programmed into the StereoDrive software package (Neurostar).

For knockout of *Bmal1* we made 70nl injections of premade recombinant (r)AAV2-CMV-Cre-GFP (rAAV2-Cre-GFP) which was diluted in 0.1M PBS to a concentration of ~1E+12 VG/mL (SL100814, SignaGen Laboratories, MD, USA). rAAV2-Cre-GFP is a pre-packaged rAAV2 with serotype-2 capsid and 2x inverted terminal repeat sequences which over-expresses Cre recombinase and EGFP under control of CMV promoters in two separate expression cassettes. Pre-packaged rAAV2-GFP vectors, which over-express EGFP and lack

Cre recombinase were injected as a control (SL100812, SignaGen Laboratories). All rAAVs were diluted immediately in sterile 0.1M PBS and stored at -80°C.

Injection needles were pulled from borosilicate glass capillaries, back-filled with mineral oil and then an excess of either rAAV2-Cre-GFP or rAAV2-GFP and loaded into the injection device, which was controlled by Injectomate software (Neurostar).

Animals were initially anaesthetised deeply with isoflurane to ease handling and placement into a stereotaxic frame apparatus. Mice were positioned using a bite-bar and ear bars while under continuous deep anaesthesia with isoflurane through a nose cone. At this stage, tilt and angle was corrected for as best possible by eye.

All surgical procedures were performed with full aseptic technique. All instruments, tools and drapes were autoclaved the morning of surgery. Whilst a trained partner positioned the animal in the stereotaxic frame, the individual performing the surgery scrubbed up with iodine wash and a surgical gown and gloves were worn in order to reduce the risk of the animals developing an infection during the recovery period.

A sterile scalpel was then used to make an incision in a rostrocaudal direction to expose the animal's skull. A series of references points are given by touching the injection needle or drill bit to bregma and lambda to align the position of the mouse skull with a virtual brain atlas within the StereoDrive software package (Neurostar). This software corrects for head tilt and can then be used to select multiple targets for injection.

After aligning the drill and injection needle with the exposed mouse skull landmarks, and completing a series of tilt and scaling correction steps, a small but sufficiently sized hole (~1mm diameter) was drilled in the skull at the calculated entry point for the injection needle. One hole was sufficient for all bilateral injections performed.

To maximise the likelihood of successful bilateral virus injection into the ARC, we made 2 injections either side of the 3rd ventricle at bregma -1.7mm followed by 2 more at bregma -1.9mm. Firstly, the injection needle was tested before entry into the brain. Then the needle was lowered towards the injection site slowly to prevent blocking of the needle aperture. By visually guiding the needle using the virtual brain atlas, the tip was approached to the injection site. The needle was then lowered and raised (~50µm) to

create a pocket for the viral vector solution. This step reduced the pressure at the tip of the needle ensuring full and smooth delivery to the injection site. The needle was then left in position for 5min to ensure full diffusion of the viral vector away from the tip and reduce leakage on withdrawal into brain areas along the injection tract. The process above was repeated for the remaining 3 injection sites.

Following the injection procedure, the head opening was closed with reverse cutting 6-0 grade Merksilk sutures (Ethicon, NJ, USA). Mice were given an intramuscular injection of the analgesic, buprenorphine (1mg/kg; Animalcare ltd, York, UK), and 5% lidocaine (Aspen pharmacare, KwaZulu-Natal, South Africa) was topically applied to the animals head. Mice were then placed in a fresh home cage in a warm cabinet maintained at 30°C. Typically mice made a full recovering 30min after cessation of isoflurane. Following recovery, all mice were returned to group-housing in controlled LD cycle.

After a minimum of 2 weeks recovery, mice were then single-housed and behaviour was screened using the TSE system. Following behavioural profiling, mice were culled at ZT1 and brains were used for pMEA recordings to assess firing activity. Injection location was confirmed by imaging post-fixed slices after anti-GFP immunostaining. Slices with rAAV2 expression outside ARC or in the injection tract were excluded from analysis.

References

BAQUERO, A. F., KIRIGITI, M. A., BAQUERO, K. C., LEE, S. J., SMITH, M. S. & GROVE, K. L. 2015. Developmental changes in synaptic distribution in arcuate nucleus neurons. *J Neurosci,* 35**,** 8558-69.

BELLE, M. D., DIEKMAN, C. O., FORGER, D. B. & PIGGINS, H. D. 2009. Daily electrical silencing in the mammalian circadian clock. *Science,* 326**,** 281-4.

BELLE, M. D., HUGHES, A. T., BECHTOLD, D. A., CUNNINGHAM, P., PIERUCCI, M., BURDAKOV, D. & PIGGINS, H. D. 2014. Acute suppressive and long-term phase modulation actions of orexin on the mammalian circadian clock. *J Neurosci,* 34**,** 3607-21.

CAHALAN, M. & NEHER, E. 1992. Patch clamp techniques: an overview. *Methods Enzymol,* 207**,** 3-14.

CHENG, H. Y., ALVAREZ-SAAVEDRA, M., DZIEMA, H., CHOI, Y. S., LI, A. & OBRIETAN, K. 2009. Segregation of expression of mPeriod gene homologs in neurons and glia:

possible divergent roles of mPeriod1 and mPeriod2 in the brain. *Hum Mol Genet,* 18**,** 3110-24.

DECAVEL, C. & VAN DEN POL, A. N. 1990. GABA: a dominant neurotransmitter in the hypothalamus. *J Comp Neurol,* 302**,** 1019-37.

EVANS, J. A., LEISE, T. L., CASTANON-CERVANTES, O. & DAVIDSON, A. J. 2013. Dynamic interactions mediated by nonredundant signaling mechanisms couple circadian clock neurons. *Neuron,* 80**,** 973-83.

FATT, P. & KATZ, B. 1952. Spontaneous subthreshold activity at motor nerve endings. *J Physiol,* 117**,** 109-28.

GROOS, G. & HENDRIKS, J. 1982. Circadian rhythms in electrical discharge of rat suprachiasmatic neurones recorded in vitro. *Neurosci Lett,* 34**,** 283-8.

GUILDING, C., HUGHES, A. T., BROWN, T. M., NAMVAR, S. & PIGGINS, H. D. 2009. A riot of rhythms: neuronal and glial circadian oscillators in the mediobasal hypothalamus. *Mol Brain,* 2**,** 28.

HUGHES, A. T. & PIGGINS, H. D. 2012. Feedback actions of locomotor activity to the circadian clock. *Prog Brain Res,* 199**,** 305-36.

ITRI, J., MICHEL, S., WASCHEK, J. A. & COLWELL, C. S. 2004. Circadian rhythm in inhibitory synaptic transmission in the mouse suprachiasmatic nucleus. *J Neurophysiol,* 92**,** 311-9.

KUHLMAN, S. J. & MCMAHON, D. G. 2004. Rhythmic regulation of membrane potential and potassium current persists in SCN neurons in the absence of environmental input. *Eur J Neurosci,* 20**,** 1113-7.

NOVAK, C. M., BURGHARDT, P. R. & LEVINE, J. A. 2012. The use of a running wheel to measure activity in rodents: relationship to energy balance, general activity, and reward. *Neurosci Biobehav Rev,* 36**,** 1001-1014.

PINTO, S., ROSEBERRY, A. G., LIU, H., DIANO, S., SHANABROUGH, M., CAI, X., FRIEDMAN, J. M. & HORVATH, T. L. 2004. Rapid rewiring of arcuate nucleus feeding circuits by leptin. *Science,* 304**,** 110-5.

PRISTERA, A., LIN, W., KAUFMANN, A. K., BRIMBLECOMBE, K. R., THRELFELL, S., DODSON, P. D., MAGILL, P. J., FERNANDES, C., CRAGG, S. J. & ANG, S. L. 2015. Transcription factors FOXA1 and FOXA2 maintain dopaminergic neuronal properties and control feeding behavior in adult mice. *Proc Natl Acad Sci U S A,* 112**,** E4929-38.

QIU, J., ZHANG, C., BORGQUIST, A., NESTOR, C. C., SMITH, A. W., BOSCH, M. A., KU, S., WAGNER, E. J., RONNEKLEIV, O. K. & KELLY, M. J. 2014. Insulin excites anorexigenic proopiomelanocortin neurons via activation of canonical transient receptor potential channels. *Cell Metab,* 19**,** 682-93.

SAKHI, K., BELLE, M. D., GOSSAN, N., DELAGRANGE, P. & PIGGINS, H. D. 2014a. Daily variation in the electrophysiological activity of mouse medial habenula neurones. *J Physiol,* 592**,** 587-603.

SAKHI, K., WEGNER, S., BELLE, M. D., HOWARTH, M., DELAGRANGE, P., BROWN, T. M. & PIGGINS, H. D. 2014b. Intrinsic and extrinsic cues regulate the daily profile of mouse lateral habenula neuronal activity. *J Physiol,* 592**,** 5025-45.

SAKMANN, B. & NEHER, E. 1984. Patch clamp techniques for studying ionic channels in excitable membranes. *Annu Rev Physiol,* 46**,** 455-72.

SHABAN, H., O'CONNOR, R., OVSEPIAN, S. V., DINAN, T. G., CRYAN, J. F. & SCHELLEKENS, H. 2017. Electrophysiological approaches to unravel the neurobiological basis of

appetite and satiety: use of the multielectrode array as a screening strategy. *Drug Discov Today,* 22**,** 31-42.

SOKOLOVE, P. G. & BUSHELL, W. N. 1978. The chi square periodogram: its utility for analysis of circadian rhythms. *J Theor Biol,* 72**,** 131-60.

STORCH, K. F., PAZ, C., SIGNOROVITCH, J., RAVIOLA, E., PAWLYK, B., LI, T. & WEITZ, C. J. 2007. Physiological importance of a circadian clock outside the suprachiasmatic nucleus. *Cold Spring Harb Symp Quant Biol,* 72**,** 307-18.

TIMOTHY, J. W. S., KLAS, N., SANGHANI, H. R., AL-MANSOURI, T., HUGHES, A. T. L., KIRSHENBAUM, G. S., BRIENZA, V., BELLE, M. D. C., RALPH, M. R., CLAPCOTE, S. J. & PIGGINS, H. D. 2017. Circadian Disruptions in the Myshkin Mouse Model of Mania Are Independent of Deficits in Suprachiasmatic Molecular Clock Function. *Biol Psychiatry*.

VAN DEN POL, A. N., YAO, Y., FU, L. Y., FOO, K., HUANG, H., COPPARI, R., LOWELL, B. B. & BROBERGER, C. 2009. Neuromedin B and gastrin-releasing peptide excite arcuate nucleus neuropeptide Y neurons in a novel transgenic mouse expressing strong Renilla green fluorescent protein in NPY neurons. *J Neurosci,* 29**,** 4622-39.

VAN OOSTERHOUT, F., LUCASSEN, E. A., HOUBEN, T., VANDERLEEST, H. T., ANTLE, M. C. & MEIJER, J. H. 2012. Amplitude of the SCN clock enhanced by the behavioral activity rhythm. *PLoS One,* 7**,** e39693.

VITATERNA, M. H., KING, D. P., CHANG, A. M., KORNHAUSER, J. M., LOWREY, P. L., MCDONALD, J. D., DOVE, W. F., PINTO, L. H., TUREK, F. W. & TAKAHASHI, J. S. 1994. Mutagenesis and mapping of a mouse gene, Clock, essential for circadian behavior. *Science,* 264**,** 719-25.

WALMSLEY, L., HANNA, L., MOULAND, J., MARTIAL, F., WEST, A., SMEDLEY, A. R., BECHTOLD, D. A., WEBB, A. R., LUCAS, R. J. & BROWN, T. M. 2015. Colour as a signal for entraining the mammalian circadian clock. *PLoS Biol,* 13**,** e1002127.

WANG, T. A., YU, Y. V., GOVINDAIAH, G., YE, X., ARTINIAN, L., COLEMAN, T. P., SWEEDLER, J. V., COX, C. L. & GILLETTE, M. U. 2012. Circadian rhythm of redox state regulates excitability in suprachiasmatic nucleus neurons. *Science,* 337**,** 839-42.

YOUNG, E. D., ROBERT, J. M. & SHOFNER, W. P. 1988. Regularity and latency of units in ventral cochlear nucleus: implications for unit classification and generation of response properties. *J Neurophysiol,* 60**,** 1-29.

Chapter 1

Period1-expressing neurons in the arcuate nucleus of the hypothalamus exhibit daily rhythms in excitability

Period1-expressing neurons in the arcuate nucleus of the hypothalamus exhibit daily rhythms in excitability

Introduction

Since the first mammalian clock gene, *Circadian Locomotor Output Cycle Kaput* (*CLOCK*) was described in 1994, a number of other genes have been revealed as instrumental components of the core molecular clockwork (Vitaterna et al., 1994). Coherent function of the molecular clockwork depends on interlocking autoregulatory transcription-translation feedback loops (TTFL) involving an array of core clock genes including *Period1,2,3 (Per1,2,3)*, *Cryptochrome1* and *2* (*Cry1/2*), and *Bmal1* (Bunger et al., 2000, Gekakis et al., 1998, Partch et al., 2014).

In addition to molecular rhythms SCN neurons exhibit daily variation in spontaneous electrical activity (Welsh et al., 1995). At the level of both single neurons and the SCN population, electrical activity increases during the day, peaking during the afternoon and becomes most quiescent during the night (Belle et al., 2009, Groos and Hendriks, 1982, Kuhlman and McMahon, 2004). This daily pattern in cellular excitability was first demonstrated by multiunit recordings performed *in vivo* in rats, which showed that electrical rhythms persisted after the SCN was isolated from synaptic inputs (Inouye and Kawamura, 1979).

While multiunit recordings *in vivo* reveal that electrical output in the mouse SCN follows a smooth increase and decrease in firing across the daily cycle (van Oosterhout et al., 2012), whole-cell recordings reveal that *Per1*-expressing neurons in the SCN actually become depolarised and silent during the afternoon (Scott et al., 2010, Belle et al., 2009). Targeted recordings from non-*Per1*-expressing neurons (*Per1*::GFP-negative) show that SCN neurons that do not putatively contain the molecular clockwork generate APs with a high frequency during the day compared to the night (Belle et al., 2009). This complexity in electrophysiological states of the SCN suggests that the molecular clock directly modulates cellular excitability. Indeed, the mechanism that underpins the generation of

electrical rhythms in SCN neurons is thought to be a combination of circadian and non-circadian ion conductances (Colwell, 2011). These summate to increase resting membrane potential (RMP) and spontaneous firing rate (SFR) during the day and reduce RMP and SFR at night (Belle et al., 2009, Kuhlman and McMahon, 2004, Wang et al., 2012).

An intact neuronal network reinforces electrical rhythms in the SCN

At the whole tissue level, coherent electrical output of SCN depends on an intact network of cells which function as a collective unit. This becomes evident when individual SCN neurons are isolated from their neighbours, which results in highly variable molecular and electrical rhythms (Webb et al., 2009). The necessity of an intact network for coordinated SCN activity is further demonstrated when increasing the density of SCN neurons, which increases the strength of cellular and population-level rhythms in the SCN network (Freeman et al., 2013). This property is also evident from studies in which key clock components have been disrupted by genetic lesioning. In knockout strains such as *Cry1*$^{-/-}$ or *ClockΔ19,* dissociated SCN neurons do not express molecular or electrical rhythms. However, tissue-level rhythms emerge when whole SCN explants from the same genotype are cultured (Herzog et al., 1998, Liu et al., 2007, Nakamura et al., 2002). These studies demonstrate the SCN networks' powerful capacity to facilitate rhythmicity even in cases when cellular oscillators are of a poor quality.

Studies into cell to cell communication in the SCN have revealed a prominent role for both neuropeptides and fast neurotransmitters in regulating synchronised spatiotemporal SCN activity. The neuropeptide vasoactive intestinal polypeptide (VIP) interacting with its receptor VPAC2 is essential for maintaining appropriate behavioural rhythmicity (Aton et al., 2005, Hughes and Piggins, 2008). Tissues from *Vip* knockout mice have impaired electrical rhythms and a decrease in the proportion of rhythmically firing neurons *in vitro* (Brown et al., 2007). In addition to neuropeptide signalling, nearly all SCN neurons express GABA (Moore and Speh, 1993) the release of which follows a circadian pattern (Itri et al., 2004). GABA release and activation of the $GABA_A$ receptor evokes a fast inhibitory action in postsynaptic cells which is important for setting SFR and RMP in spontaneously active SCN neurons (Jackson et al., 2004, Kononenko and Dudek, 2004).

The rhythm augmenting properties of the SCN network are further emphasised by comparing long-term rhythm generation in the master clock to extra-SCN brain oscillators (Guilding and Piggins, 2007). A variety of brain regions outside the SCN express clock genes and possess the ability for autonomous molecular oscillations in culture, including the dorsomedial hypothalamus (DMH), arcuate nucleus (ARC) and the Habenula (Hb) (Abe et al., 2002, Guilding et al., 2009, Guilding et al., 2010). Like the SCN, each of these extra-SCN oscillators appears to possess the same capacity for intercellular synaptic communication, however rhythms in DMH, ARC and Hb diminish at a greater rate in culture compared to SCN. The reason for this disparity between SCN and extra-SCN oscillators is yet to be understood.

The arcuate nucleus of the hypothalamus plays well established roles in physiology and behaviour and contains a local molecular clock

When considering the function of the SCN as the master circadian pacemaker, it is perhaps not surprising that the network has evolved to reinforce its own rhythmic output. Signals from the SCN synchronise other central and peripheral clocks throughout the body maintain phase-alignment across the daily cycle (Buhr and Takahashi, 2013). Therefore, it is perhaps not surprising that the ensemble activity of the SCN must be robust enough to support its role as a master synchroniser. Research conducted over the past decade has challenged the omnipotence of the SCN in organising rhythms in sleep-wake cycle, temperature and metabolism as well as a myriad of other physiological parameters (Guilding et al., 2010).

A number of brain regions outside the SCN exhibit oscillatory properties albeit with a lower rhythm strength than SCN. One such region is the arcuate nucleus of the hypothalamus (ARC) which houses a local autonomous circadian clock (Abe et al., 2002). MBH containing brain slices from mice expressing a PER2::LUCIFERASE(LUC) fusion protein reporter construct can be visualised using highly sensitive EM-CCD camera-equipped microscopy to investigate the clockwork in individual neurons *in vitro* (Guilding et al., 2009). PER2::LUC is robustly expressed throughout the ARC which was further divided into dorsal and lateral areas in this study (dARC and latARC). Single cells exhibit significant circadian rhythmicity in both dARC and latARC. The rhythms in the cells are

lower in amplitude compared to SCN cultures from the same reporter line, however ARC was able to sustain rhythmicity for 3 days during continuous recordings made from ARC slices. In situ hybridisation also reveals rhythmic expression of *Per* in the rat which peaks during the night in antiphase to the SCN (Shieh et al., 2005). This phase difference suggests that local clockwork in ARC may function to regulate temporal aspects of physiology that are distinct from SCN output.

Importantly, the ARC plays a number of well-established roles in physiology and behavioural processing including regulation of feeding behaviour, reproduction and feedback to the SCN (Buijs et al., 2017, Mendonca et al., 2018, Andermann and Lowell, 2017). The ARC is ideally suited to sense circulating humoral factors due to its high density of receptors for factors such as leptin and ghrelin (van den Top and Spanswick, 2006, Shuto et al., 2002, Willesen et al., 1999) and circumventricular location in a part of the brain with a weakened blood-brain barrier (Norsted et al., 2008, Rethelyi, 1984). Early studies demonstrated that an intact ARC is essential for appropriate energy regulation and metabolism. Systemic administration of the neurotoxic gold thioglucose, or treatment of neonatal rats with high doses of monosodium glutamate, result in severe neuronal loss in the ARC and hyperphagia leading to obesity (Debons et al., 1982, Meister et al., 1989). In humans, genetic defects in the ARC are correlated to obesity and metabolic disturbances (Barsh et al., 2000).

GABAergic ARC neurons play an integral role in regulation of the endocrine system and energy homeostasis (Kelly and Grossman, 1979, Kalra et al., 1999, Cone et al., 2001). Glutamate decarboxylase (GAD) is found in half of all ARC neurons and is sensitive to fasting (Decavel and Van den Pol, 1990, Horvath et al., 1997). Recent studies show that GABA release from ARC neurons plays a role in promoting food intake (Vong et al., 2011). Like the SCN, GABA is expressed both in neurons belonging to well researched neuropeptide subtypes and separately in otherwise unidentified neurons (Hentges et al., 2004, Vong et al., 2011, Cowley et al., 2001, Campbell et al., 2017).

Modulation of ARC electrical output is critical for both integrative processing of peripheral energy cues and output to downstream feeding centres. The Intrinsic firing rates of ARC

neurons directly correlate with nutritional status under food-deprived conditions (Takahashi and Cone, 2005). Profound diet-induced changes in firing rate are also accompanied by changes in action potential geometry (Baver et al., 2014). Forced activation of ARC neurons by opto- or chemogenetic methods enables rapid and robust modulation of feeding behaviour and appetite *in vivo* (Krashes et al., 2011, Atasoy et al., 2012, Aponte et al., 2011).

Targeting the ARC clockwork using the *Per1*::Venus reporter mouse

In order to study the temporal patterns of ARC electrical activity in neurons expressing the molecular clockwork a suitable clock controlled reporter mouse line is required to target individual cells for electrophysiological investigation. The *Per1*::Venus mouse, constructed by Cheng et al., offers unprecedented clock-coupled fluorescence tracking in individual neurons due to targeted genetic modifications of the native reporter gene (Cheng et al., 2009). In the Yellow fluorescent protein (YFP) derivative Venus, point mutations in the parent gene enhanced protein folding efficiency and also provided a 3-fold acceleration of chromophore oxidation, the rate-limiting step in maturation. Further improvements to the kinetic properties of Venus were made through in-frame cloning of a nuclear localisation sequence (NLS) and proline (P), glutamic acid (E), serine (S), and threonine (T) (PEST) rich domain. In transfected cells expressing the Venus-NLS-PEST construct the fluorescence signal is highly concentrated to the nucleus, a characteristic that is highly advantageous during optical targeting of cellular Venus signal.

Venus immunoreactivity in coronal SCN-containing brain slices exhibited a robust circadian rhythm with a short phase delay with respect to *Per1*, with expression peaking at ~CT11. To further verify the suitability of Venus as a circadian reporter, response to photic stimulation was tested in dark-adapted *Per1*::Venus by brief light pulses spanning the subjective day and night. Expression of Venus was induced by light restricted to the subjective night period, thus two key features of *Per1*-dependent transcription, rhythmic expression and time-dependent induction by light, are translated in the expression of Venus in the SCN. Indeed, the *Per1*::Venus reporter mouse also facilitates the dynamic monitoring of *Per1*-dependent transcription in single cells of extra-SCN brain regions.

Venus immunoreactivity was co-localised with a post-mitotic neuron-specific antigen, neuronal nuclei, in multiple brain areas, including the MBH, striatum, and cortex.

Aims

The experiments performed for this chapter aim to address a number of key questions introduced above. Firstly, as the molecular clockwork in the SCN drives daily rhythms in membrane excitability and firing frequency, this prompts a full investigation into whether the molecular clockwork in ARC drives similar electrical rhythms. The general mechanisms linking molecular clock oscillations with parallel changes in firing frequency are not well understood. These studies may add to our understanding from experiments conducted in the SCN. Second, the functional role of the extra-SCN clock in ARC is not clear. As ARC neuronal excitability is a key integration point for metabolic signals any potential temporal modulation may highlight a physiological role for the local clock. To address this we performed whole-cell electrophysiological recordings and pMEA experiments in brain slices harvested from *Per1*::Venus mice, specifically targeting *Per1*-expressing neurons that putatively contain the molecular clockwork. A brief description of the methodologies employed throughout this chapter is outlined below.

Methods

Animal housing

Experiments for this chapter were conducted on male *Per1*::Venus mice (8-14 week old) expressing a Venus fluorescent protein reporter for the *Per1* gene (Cheng et al., 2009). All procedures were carried out in accordance with the UK Animals (Scientific Procedures) Act of 1986 using procedures approved by The University of Manchester Review Ethics Panel. Animals were group housed under a 12/12h light/dark (LD) cycle. Animals had *ad libitum* access to food and water and temperature in the housing area was maintained at 20 ± 2 °C and humidity at ~40%.

Whole-cell Electrophysiology

Slices were harvested from *Per1*::Venus brains at ZT1 for daytime recordings (ZT4-10) or ZT11 for night recordings (ZT14-20). Initially, brains were placed in cutting solution containing (in mM): 0.5 NaCl, 1.8 KCl, 1.2 KH_2PO_4, 7 $MgSO_4$, 26 $NaHCO_3$, 15 Glucose and 50 Sucrose (300-310 $mosmol^{-1}$, pregassed with 95% O_2/ 5% CO_2). 300µm slices containing ARC were prepared using a vibroslicer (Campden Instruments, Loughborough, UK) and transferred into an incubation chamber filled with cutting solution to rest at room temperature. Slices were then transferred to artificial cerebrospinal fluid (aCSF) comprised of (in mM): 127 NaCl, 1.8 KCl, 1.2 KH_2PO_4, 1.3 $MgSO_4$, 26 $NaHCO_3$, 15 Glucose and 2.4 $CaCl_2$. Slices containing ARC, DMH and VMH at the level of -1.7 to -1.9mm bregma were used. 300 µm thick SCN-containing slices were also harvested during the same times for comparison.

Pipettes (7-10MΩ) were backfilled with intracellular solution containing (in mM): 130 K-gluconate, 10 KCl, 2mM $MgCl_2$, 10 Hepes, 0.5 EGTA, 2 K_2ATP and 0.5 NaGTP (Belle et al., 2009). Visually guided whole-cell recordings were performed while targeting *Per1*::Venus neurons by epifluorescence. Location was recorded by capturing live images with a Hamamatsu Orca R^2 camera system (Hamamatsu Photonics, Tohoku, Japan) during recordings and by filling cells with biocytin for post-recording immunohistochemistry. An npi BA-03X amplifier in bridge configuration (npi electronics, Tamm, Germany), compensating for the transient capacitance of the pipette, and a CED 1401 mark II A/D data acquisition interface (Cambridge Electronic Design, Cambridge, United Kingdom) were used to record current clamp data.

All recording signals were sampled at a frequency of 30 kHz in Spike 2 Version 7 (Cambridge Electronic Design, Cambridge, United Kingdom). Spike 2 was also used to analyse raw data signals and statistical analysis (two-sample t-test) were performed on population day-night excitability data (RMP, SFR, R_{input}, ISI, ADP50 etc.) in Origin version 9.0 (OriginLab Corporation, Ma, USA). Representative traces displayed in figures were exported directly from Spike 2 as image files.

Electrical behaviour was defined as either depolarised silent, firing or hyperpolarised silent. Firing cells generate APs whereas depolarised silent and hyperpolarised silent cells

rest above and below (respectively) the threshold for fast sodium conductance responsible for initiating APs. Glutamate receptor antagonists (AP5 at 50µM/CNQX at 10µM, Tocris bioscience, Bristol, UK) were bath applied for 1min to investigate the mechanism responsible for driving *Per1*::Venus ARC neurons into the depolarised silent state. Variation in the proportion of electrical states or firing regularity (coefficient of variance (C.V.) <0.35 for regular firing, (Pristera et al., 2015, Young et al., 1988) were analysed by Fisher's exact-test ($p<0.05$).

Leptin and Ghrelin (Tocris Bioscience, Bristol, UK) were diluted from stock solutions and stored as frozen aliquots. On the day of recording, aliquots were thawed and further diluted in aCSF. Leptin (10nM) and Orexin (100nM) were gravity-applied for 4min into the recording chamber. Responses were defined as a ±2mV change in RMP between a 10s window of baseline prior to drugs and 10s of stable activity after application. Individual responses to metabolic cues were quantified in Spike 2 and compiled to calculate average responses in Origin 9.

Synaptic event frequency was measured using an Axopatch 200b amplifier (Molecular Devices, Cal, USA). The internal solution was identical to the one used in current clamp recordings, except for 120mM K-gluconate and 20KCl mM. This concentration of Cl- causes IPSCs to reverse at approximately -45mV. Therefore, this positive shift in Cl- reversal potential causes both GABAergic and glutamatergic postsynaptic currents (PSCs) to appear as inward currents when the membrane is clamped at -70mV. To discriminate the origin of these inward currents, receptor antagonists (AP5 at 50µM/CNQX at 10µM, Tocris bioscience, Bristol, UK) for the glutamate receptors and $GABA_A$ receptor (Gabazine, Tocris) were bath applied in series. Synaptic event (PSC) frequency was determined at baseline initially for a minimum of 100s. Then, after each application of antagonist(s) a 100s drug-free window was recorded. A 30s data period at baseline, 30s at the end of the 100s drug-free period, and 30s after all antagonists were compared to assess event frequency and amplitude in the absence of either glutamatergic or GABAergic signalling. Statistical comparison (two-sample t-test) and analysis was performed in Origin 9.

Recordings were excluded when series resistance (typically <20 MΩ) changed by >15% during the protocol. TTX (1µM) was applied to discriminate between PSCs arising from

AP-dependent synaptic communication and spontaneous quantal release of neurotransmitter (miniature PSCs). Signals were acquired using pClamp 10.2 (Clampex and Clampfit) in conjunction with a Digidata 1440A interface (Molecular Devices).

Multielectrode array Electrophysiology

To evaluate whether network activity displays daily rhythmicity, perforated multielectrode array (pMEA) recordings were performed during the day (ZT4-10) and night (ZT14-20). 300 µm thick brain slices were prepared from *Per1*::Venus mice in an identical manner and at the same ZTs as those used for whole-cell experiments. The cutting solution and aCSF composition used for pMEA experiments was identical to that outlined above except aCSF was heated to 33°C for the final stage of slice incubation.

Extracellular measurement of multiunit activity (MUA) was performed using a dual-MEA2100-HS2x60 head-stage system in conjunction with a MEA2100 interface board (Multichannel systems, Reutlingen, Germany). Raw data was integrated across 120 pMEA recording electrodes (60 per chamber, 30µm diameter, 200µm spacing) arranged in an 8x8 grid (60pMEA200/30iR-Ti-gr, Multichannel systems, Reutlingen, Germany). Consistent slice placement was verified between slices using photographs taken before and after recording. The recording surface for pMEA experiments was typically -1.8mm from bregma. Negative pressure was created to hold the slice in close contact with the recording electrodes.

ACSF was maintained at 33°C in a water bath and boosted on transit to the pMEA slice chamber with a TC02 temperature controller (Multichannel systems). Bath application of tetrodotoxin (TTX) at the end of each recording session was performed to ensure a suitable spike detection threshold was used (Tocris Bioscience, Bristol, UK).

Raw data signals were acquired at 25kHz using MC rack software (Multichannel systems) and saved as 10min files due to the large individual file size (>1.5gb per 10min). Subsequently files were merged chronologically and a 300Hz high-pass filter was applied to the raw data signals. Spikes were then discriminated from the raw data using a thresholding tool. A TTX-based threshold of -15.5µV was used to discriminate spikes for all recordings. MC rack data files containing spikes only were then imported into were

exported to Neuroexplorer (Nex technologies, CO, USA). MUA was extracted from the spiking data using a set time bin. For the analysis of data presented in this chapter, spikes were averaged across 1h bins for a minimum of 3h baseline recording within either the day or night time epoch. Mean spike frequency data was then exported into Origin 9 for statistical comparison (two-sample t-test) and construction of histograms and contour plots.

Immunohistochemistry

Brain slices used for whole-cell electrophysiological recording were post-fixed in ice-cold 4% paraformaldehyde in 0.1M PBS (pH 7.4). After 24h the slices were transferred to 0.1M PBS alone, and stored for a maximum for 3 days. The slices were then washed with PBS and incubated in Triton-X 100 (0.6% in PBS, 10% normal donkey serum) for 3h at room temperature. Slices were then transferred to a solution containing Cy3-conjugated Extravidin (1:250 in PBS, Sigma-Aldrich, MO, USA) and rabbit anti-GFP primary antibody (1:1000, Abcam, Cambridge, UK) in PBS, 2% NDS and 0.3% Triton-X 100 and incubated at 4°C in darkness for 1-3 days. Slices were then transferred to a secondary antibody solution containing a fluorescein conjugated anti-rabbit antibody (Jackson ImmunoResearch, USA) diluted 1:800 in PBS and incubated at 4°C overnight. The next day, slices were washed in PBS and mounted onto gelatine-coated slides for visualisation. Images were captured using a Leica SP5 Upright confocal microscope using a 20x objective with 3x confocal zoom (Leica systems, Wetzlar, Germany).

A select number of *Per1*::Venus slices were also stained against glial fibrillary acidic protein (Primary antibody anti-GFAP, 1:400, Sigma-Aldrich), Vimentin (1:1000, Abcam) and GFP (1:1000, *Results* Fig1). Secondary antibodies for GFAP (anti-mouse CY3, 1:800, Jackson ImmunoResearch), Vimentin (anti-chicken alexa488, 1:800, Jackson) and GFP (anti-rabbit CY5, Jackson) were used following an identical wash/mounting protocol to that outlined above.

Results

Declaration: The pMEA data collection and analysis for the results presented in Figure 7 was performed in collaboration by Dr. Mino Belle, The University of Manchester.

Per1::Venus neurons can be visualised during whole-cell recordings and exhibit three distinct electrophysiological behaviours

Per1::Venus was observed throughout neurons of the ARC and also in other adjacent regions including the DMH and VMH, although the apparent intensity of anti-GFP staining was highest in ARC (Fig1A). The lateral boundaries of ARC were also characterised by staining for vimentin and glial fibrillary active protein (GFAP, Fig1A). To determine whether ARC neurons that express the core molecular clock component *Per1* display daily rhythms in excitability, *Per1*::Venus mice were bred and acute brain slices were collected for recording during the day (ZT4-10) and night (ZT14-20). *Per1*::Venus neurons are distributed throughout the ARC and can be readily targeted for whole-cell electrophysiology recording (Fig1C). The day and night recording windows were selected to ensure recordings coincided with the times when mice would either be active and consuming the majority of their food (night) or during relative inactivity (day). Furthermore, these epochs correspond to time period when *Per1* expression is at its peak and lowest levels in ARC (Shieh et al., 2005, Abe et al., 2002). Based on this information, a series of preliminary whole-cell experiments were conducted to guide future experiments, which suggested the daily variation in ARC excitability outlined in this chapter occurred between the middle of the day and night and not at times spanning the transition between light and dark conditions in the animals housing area (data not shown).

We sampled a total of 130 *Per1*::Venus neurons in ARC and found that they rest at three distinct electrophysiological states (Fig3A): 1) Firing and spontaneously generating action potentials (APs), 2) depolarised silent and 3) hyperpolarised silent. The majority of *Per1*::Venus neurons were firing (-40.8 ± 0.34mV, 0.1-9Hz, 3.25 ± 0.29Hz, 92/130 cells, 70.1%) with either a regular or irregular pattern. Depolarised silent (-27.9 ± 1.1mV, 17/130 cells, 13.01%) and hyperpolarised silent (-53.2 ± 2.2mV, 21/130 cells, 16.89%) cells

are unable to fire APs. When taken as the whole ARC population, the proportion of cells in these states did not vary from day to night (Chi square test, $p>0.05$).

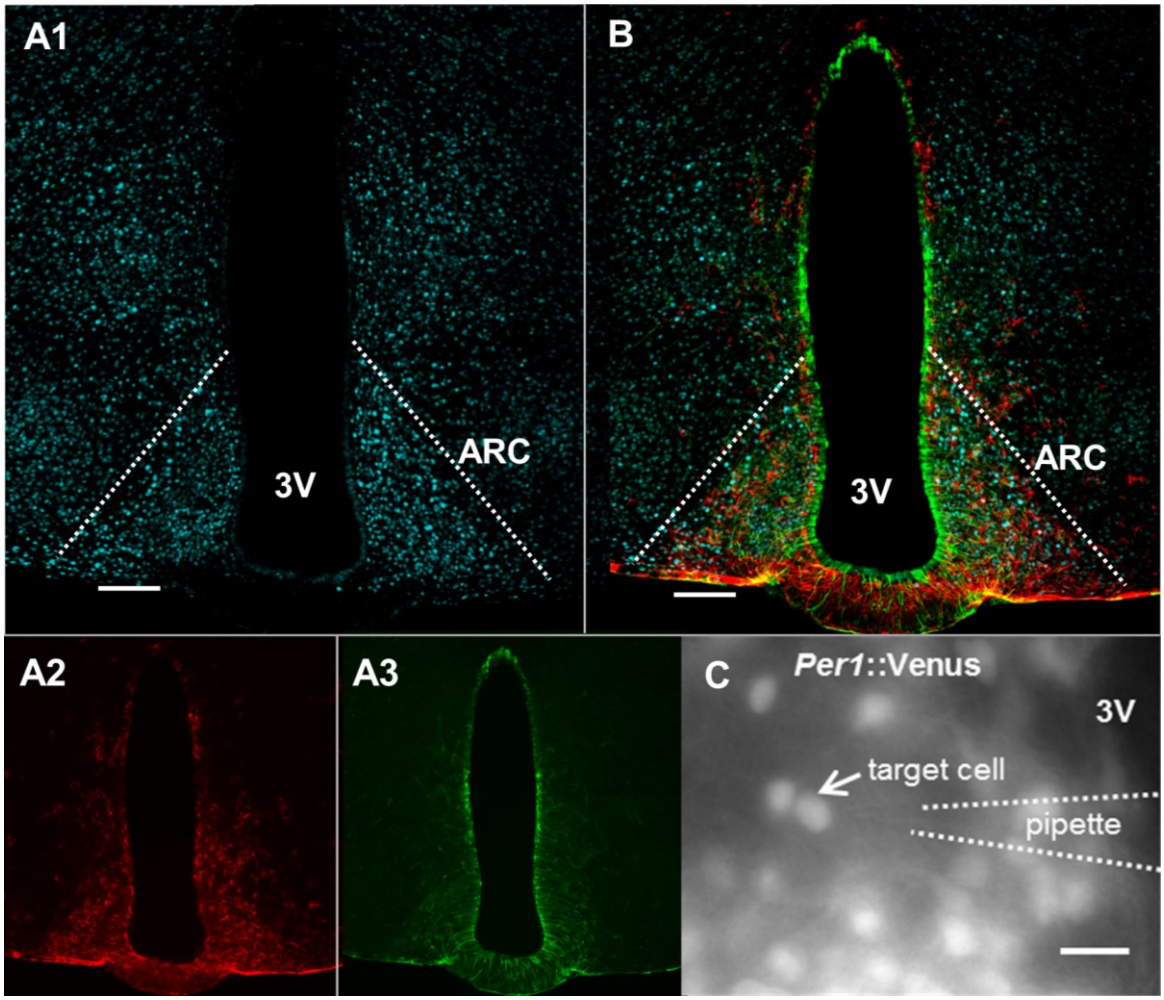

Figure 1: *Per1*::Venus is widely expressed throughout the ARC and can be visualised during whole-cell recording: Representative confocal images of the MBH, including ARC, DMH and VMH in a 300µm thick brain slice harvested from the *Per1*::Venus mouse. **A1:** Anti-GFP immunohistochemistry against Venus shows *Per1*::Venus (Cyan) throughout the MBH including the ARC. Dots correspond to single cells which are densely distributed throughout ARC. Staining is less intense in adjacent areas. The borders of ARC are depicted by the white dotted lines. third ventricle (3V). Confocal image stacks captured at 20x. Scale bar 200µm. **A2,3:** Immunostaining for glial fibrillary acidic protein (GFAP) and intermediate filament protein Vimentin depicts borders of ARC which overlap with intense anti-GFP staining. **B:** Merged confocal image showing overlay of *Per1*::Venus neurons, supporting glia and cytoskeletal elements in ARC. **C:** Epifluorescence imaging of *Per1*::Venus during approach of pipette to target cell for whole-cell recording. Individual neurons were clearly distinguishable. Photos were captured for each cell to ensure *Per1*::Venus overlapped with cell targeted visually with bright-field optics. Scale bar 30µm.

In addition to capturing images of each recording site, *Per1*::Venus ARC neurons were filled with biocytin and postrecording immunohistochemistry was performed using extravidin conjugated to CY3. This allowed precise localisation of cells, which were

assigned to latARC if >200µm from the wall of the third ventricle (Fig2). *Per1*::Venus neurons in close proximity to the third ventricle were designated as mARC neurons. This subregion localisation provides more information regarding the potential overlap of well-known ARC neuronal subtypes and *Per1* expression. During the daytime, the majority of *Per1*::Venus in mARC and latARC fired APs (23/36, 64% and 19/23, 86% respectively, Fig3B). Depolarised silent *Per1*::Venus neurons were present in both latARC and mARC during both the day (mARC, 6/36, -29.9mV, latARC, 2/19, -23.7mV) and night (5/36, -29.5mV: 4/35, -28.5mV). Similar to analysis compiling all cells throughout the ARC, the proportion of these states did not vary significantly from day to night in either subregion (Fisher's exact-test, p>0.08).

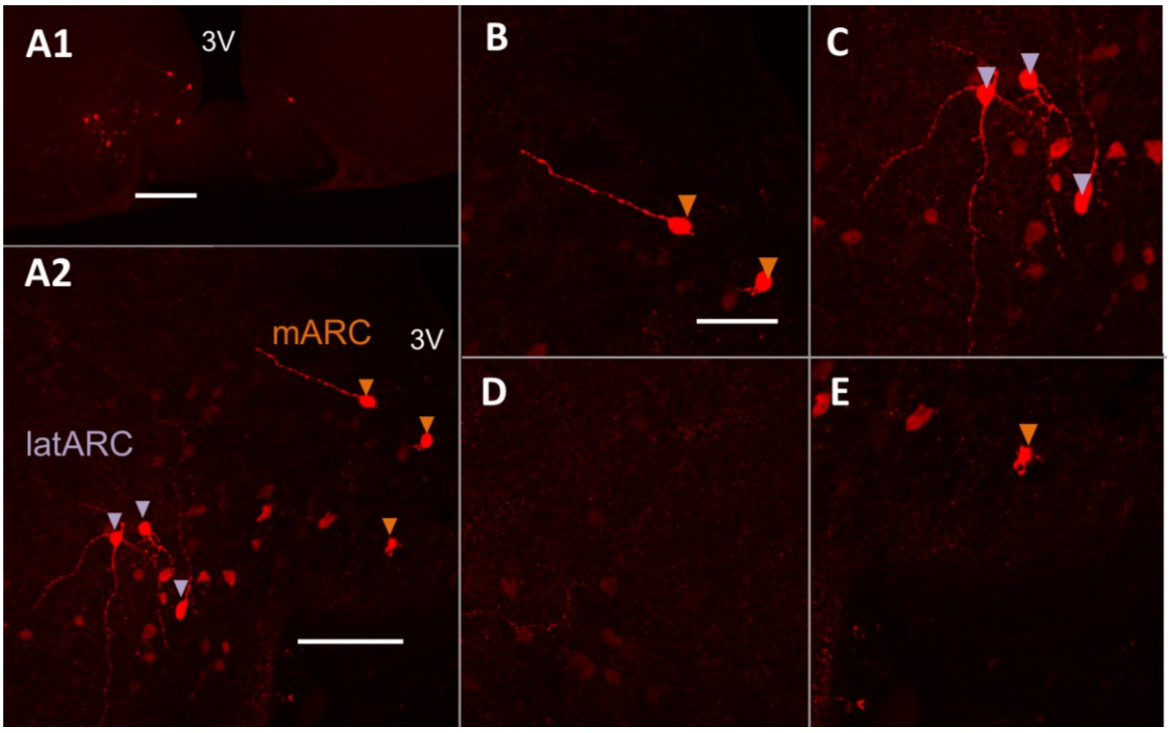

Figure 2: ARC neurons were filled with biocytin during recording to confirm location in either mARC or latARC. After recording slices were stored in 4% PFA in PBS and stained for biocytin with conjugated extravidin-CY3 (1:250) to localise recorded *Per1*::Venus neurons. **A1,2:** Representative confocal images of *Per1*::Venus neuronal somas and proximal processes filled with biocytin during electrophysiological recording. Confocal images of ARC taken at 20x and 63x. Cells in close proximity to the third ventricle (3V) were located in mARC. Those identified as being >200µm from the wall of the 3V were assigned to latARC. Scale bars 200µm for (A1) and for 100µm (A2). **B:** Confocal image of biocytin filled mARC *Per1*::Venus neuron showing processes extending dorsolaterally. 63x with digital zoom. Scale bar 50µm. **C:** Biocytin filled latARC neurons (n=3) are closely opposed by faintly stained cells, likely the result of through diffusion of biocytin via functional gap junctions. **D,E:** faintly stained cells in mARC and latARC are present >50µm from recorded cells. Confocal Images with 63x and digital zoom of two.

Depolarised silent *Per1*::Venus neurons were characterised by fast ~5mV membrane oscillations at depolarised RMP values (Fig3A). Similar states have previously been demonstrated during the afternoon in *Per1*-expressing neurons in the SCN master circadian clock (Belle et al., 2009). Interestingly, similar depolarised states to those we observe here have been reported in rat ARC, however unlike in SCN, these states in ARC are driven by local glutamatergic inputs and not by intrinsic regulation of ion conductances (Belousov and van den Pol, 1997).

Manual injection of depolarising current was sufficient to artificially induce depolarised silent electrical state in cells which were otherwise too hyperpolarised to fire APs (Fig3D). Slow ramped positive current progressed hyperpolarised silent cells through firing states to sustained hyperexcited RMPs. Furthermore, in all depolarised silent *Per1*::Venus cells tested, injection of negative current evoked firing behaviour demonstrating that these neurons were not hyperexcited due to damage or poor access to the cell during whole-cell recording.

To investigate the mechanism responsible for driving *Per1*::Venus neurons into depolarised silent states, the glutamate receptor blockers CNQX (10µM) and AP5 (50µM) were bath applied during recording to antagonise AMPA and NMDA receptors respectively. Application of CNQX/AP5 hyperpolarised 8 of 10 depolarised silent neurons *Per1*::Venus neurons tested (mean ΔRMP, -23.1mV, n=8). Glutamatergic receptor blockade evoked paradoxical excitation of 4 of 8 responsive depolarised silent cells, such that an inhibitory response resulted in the emergence of APs. In the remaining cells CNQX/AP5 resulted in hyperpolarisation below the threshold for AP firing (n=4). Following blockade of NMDA/AMPA receptor-dependent communication, one cell displayed complex bursting activity, characterised by periodic increased and decreased excitability over a 10s time course (Fig3C). These findings suggest that glutamatergic activity may play an important role *in vitro* in determining whether ARC neurons fire APs. Indeed, the presence of depolarised silent states may result in paradoxical effects of inhibitory metabolic cues.

Per1::Venus ARC neurons respond to central and peripheral metabolic cues

Leptin and orexin have important roles in regulating long-term energy balance by rapidly modulating neuronal activity (Ghamari-Langroudi et al., 2011). In the ARC, leptin increases the frequency of APs in anorexigenic POMC neurons and decreases frequency of APs in NPY/AgRP neurons (Cowley et al., 2001, Takahashi and Cone, 2005, Baver et al., 2014). Orexin inhibits POMC neurons and excites NPY/GABAergic neurons of the ARC (Ma et al., 2007, Burdakov et al., 2003, van den Top et al., 2004). To test whether *Per1*::Venus neurons are also able to respond to metabolic cues, leptin (10nM) and orexin (100nM) were bath-applied to ARC slices throughout the day-night cycle during current clamp recordings.

All *Per1*::Venus neurons tested were sensitive to orexin (100nM), which evoked increases (4 of 8, ΔRMP 8.3 ± 3.2 mV, ΔSFR 2.6 ± 1.5 Hz) and decreases (4 of 8, ΔRMP -16.9 ± 5.9 mV, ΔSFR -3.7 ± 2.2 Hz) in excitability (Fig4). The effects of orexin were long lasting (>20 min), with maximum amplitude in the response occurring 5-6 min after the onset of application.

The majority of *Per1*::Venus neurons also responded to leptin (10nM) during the day and night with changes in neuronal activity (6 of 8, Fig4C,D). In the 83% of responsive *Per1*::Venus cells (5 of 6), leptin evoked inhibitory effects (ΔRMP -4.6 ± 2.1 mV). Frequency of AP discharge was also significantly reduced (ΔSFR -1.7 ± 0.3 Hz). 2 of 5 Venus +ve neurons entered quiescent hyperpolarised states following leptin application. A small remaining proportion were excited by leptin (1 of 6, ΔRMP 5.1 mV; ΔSFR -2.8 Hz).

ARC *Per1*::Venus neurons exhibit localised daily variations in excitability

To investigate whether ARC *Per1*::Venus neurons varied in their excitability from day to night, we used epifluorescence to visualise these neurons in the slice preparation and then made targeted current clamp recordings to assess their basic electrophysiological properties (RMP, R_{input} and spontaneous firing rate; SFR) during the day (ZT4-10, n=59 cells) and night (ZT14-20, n=71 cells). To compare electrical properties, we also made current clamp recordings from *Per1*::Venus SCN neurons in more rostral hypothalamic slices during the day (ZT4-10, n=32 cells) and night (ZT14-20, n=22).

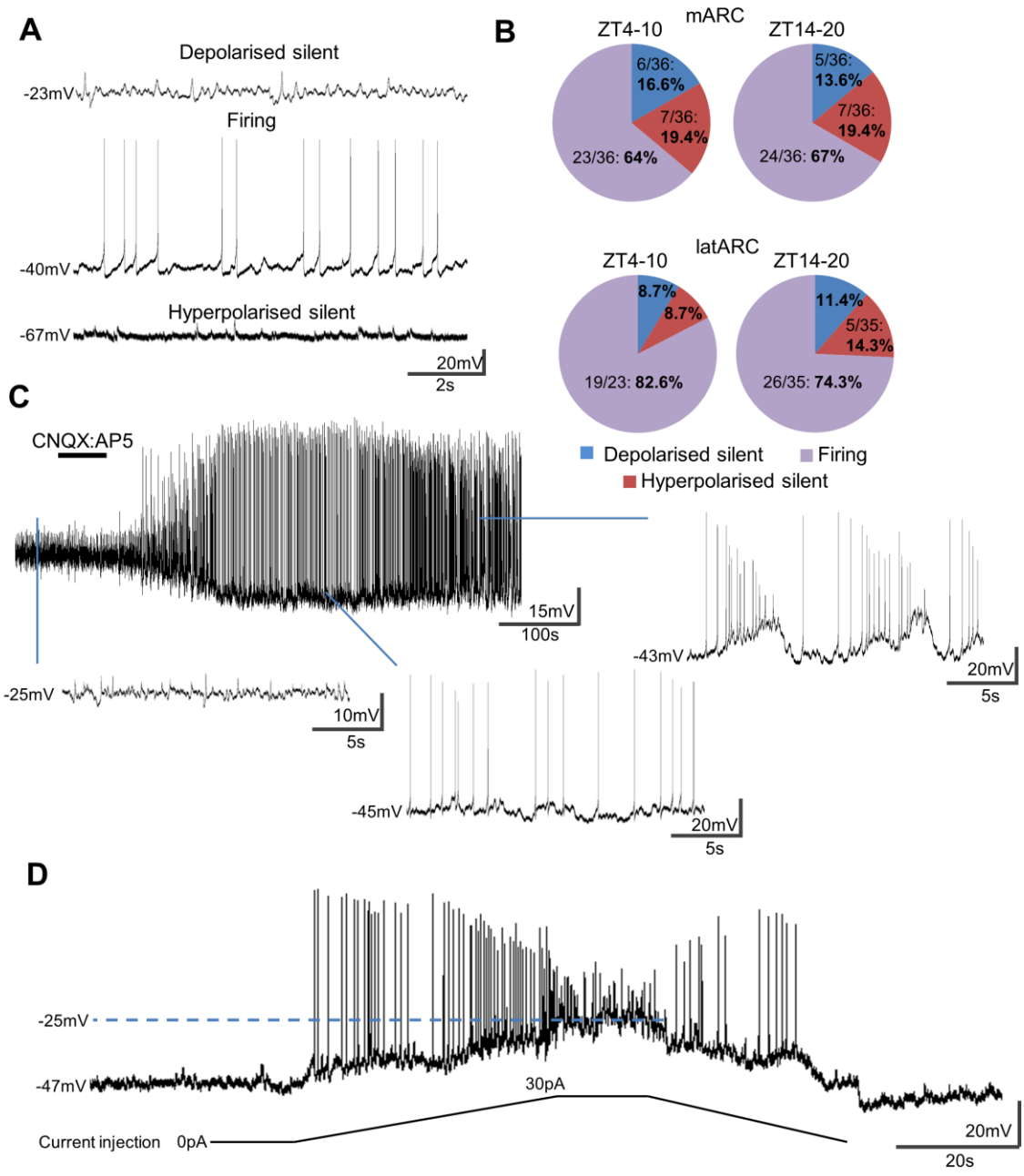

Figure 3: *Per1*::Venus ARC neurons exhibit three distinct electrophysiological states A: Representative 10s current clamp traces showing example depolarised silent, firing (~1Hz) and hyperpolarised silent neuronal behaviours. Electrical state depends on individual neuron RMP value e.g. depolarised silent neurons typically rest above -30mV. **B:** The proportion of states during the day(ZT4-10)-night(ZT14-20) did not significantly vary in the mARC or latARC *(*$\chi 2$, p=0.09*).* **C:** CNQX (10µM) /AP5 (50µM) hyperpolarised 8/10 *Per1*::Venus neurons tested (mean ΔRMP, -23.1mV). Glutamatergic blockade evoked firing behaviour or suppressed cells to hyperpolarised silent states. In 1/8, complex bursting behaviour was evoked (right-hand inset). **D:** Example trace showing manual injection of positive current which drives (all tested) hyperpolarised *Per1*::Venus neurons to display firing and subsequent depolarised silent states.

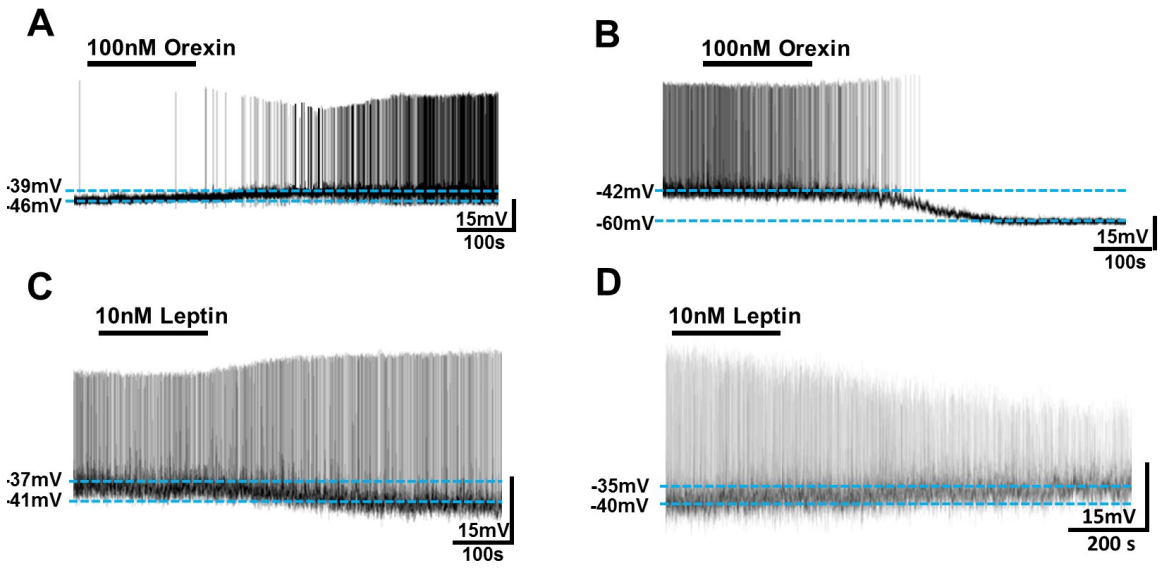

Figure 4: *Per1*::Venus ARC neurons respond to central and peripheral metabolic cues. A,B: Representative whole-cell recordings made from *Per1*::Venus neurones in the presence of orexin (100nM). Bath-application (4min) induced both excitation and suppression of electrical activity. 4 of 8 *Per1*::Venus neurones responded with sustained increases in RMP and SFR. The remaining 4 of 8 *Per1*::Venus neurones tested with orexin were hyperpolarised by application. APs were abolished as cells were supressed beyond the threshold for AP firing. **C,D:** Typical whole-cell recordings from *Per1*::Venus ARC neurones under bath-application of leptin (10nM). Leptin causes long term membrane hyperpolarisation and suppression of *Per1*::Venus neuronal activity in 5 of 6 neurones tested. 1 of 6 cells was depolarised following leptin administration.

In SCN, *Per1*::Venus neurons were significantly more depolarised during the day (-34.7 ± 1.27mV, n=32) compared to the night (-42.88 ± 0.79mV, n=22, two-sample t-test p=0.000009, Fig5A). RMP of ARC *Per1*::Venus neurons did not vary from day to night when data from both areas were combined (Day, -42.04 ± 1.24mV, n=59; Night, -40.90 ± 0.94mV, n= 71, p=0.45). Indeed, no variation in RMP was detected between day and night in either the mARC (Day, -41.88 ± 1.6mV, n=36; Night, -41.18 ± 1.18mV, n=36, p=0.73) or latARC (Day, -42.3 ± 1.98mV, n=23; Night, -40.61 ± 1.45mV, n=35, p=0.5, Fig5C).

In SCN, R_{input} did not change from day (2.37 ± 0.15GΩ, n=32) to night (2.2 ± 0.13 GΩ, n=22, two-sample t-test, p=0.42). Similarly, time of day did not have a significant effect on R_{input} in ARC (Day, 1.83 ± 0.09GΩ, n=58; Night, 1.64 ± 0.1GΩ, n=58) when all cells were compiled included in the analysis (p=0.18, Fig5B). When the test group was divided into latARC and mARC cells no day-night differences in R_{input} were observed (p>0.29, Fig5D).

Although R_{input} did not show any daily variation in ARC or SCN, the contrast in the temporal pattern of RMP values observed between these two brain regions suggests that the molecular clock may have different effects on cellular excitability outside the master clock. Interestingly, whole-cell current clamp recordings revealed that ARC *Per1*::Venus neurons generated APs more frequently during the night (3.45 ± 0.27Hz, n=50) compared to the day (2.31 ± 0.30Hz, n=42 cells, two-sample t-test, p=0.0075, Fig6B). However, such variation was only observed in *Per1*::Venus neurons located in the latARC (Day, 2.52 ± 0.42Hz, n=19; Night, 3.93 ± 0.43Hz, n=26, p=0.025) and not the mARC (Day, 2.19 ± 0.47Hz, n=23; Night, 2.89 ± 0.39Hz, n=24, p=0.25, Fig6C). LatARC neurons generated APs more frequently in antiphase to *Per1*::Venus SCN neurons which fired APs at higher frequency during the day (3.8 ± 0.32Hz, n=18) than the night (2.70 ± 0.27Hz, n=21, p=0.013). This indicates that peak firing of *Per1*-expressing neurons in the latARC is delayed with respect to the SCN. Interspike interval (ISI), the time between subsequent APs of a neuron, varied significantly between day and night in latARC (0.73s, n=19 and 0.31s, n=26 respectively, two-sample t-test, p=0.0012) but not in mARC (0.78s, n=23 and 0.60s, n=24, p=0.25, Fig6D). A two-fold reduction in ISI during the night-time corresponds with increased firing frequency.

AP half-width is influenced by changes in diet and fasting conditions (Baver et al., 2014). To assess whether daily changes in firing frequency are accompanied by changes in AP geometry we analysed the half-duration of the cumulative average waveform of APs for each neuron (ADP50, Fig6E). Time of day did not influence ADP50 in mARC (Day, 4.36ms, n=23 ; Night, 4.15ms, n=24 , p=0.66) or latARC (Day, 5.26ms, n=19 ; Night, 4.33ms, n=26 , p=0.11, Fig6F). This suggests that ion conductances that broaden the repolarising phase of the AP are not overtly influenced by time of day.

Interestingly in latARC, the pattern of AP firing of *Per1*::Venus neurons was significantly weighted towards regular firing during the night compared to the day. During the day, 5/19 neurons were regularly firing, while at night, 16/26 fired regularly (Fisher's exact-test, p=0.035). No variation in AP firing pattern was observed in mARC (Fisher's exact, p=0.5). Overall *Per1*::Venus neurons in latARC exhibit daily changes in SFR, ISI and the regularity of firing without changes in AP duration. Therefore, it is hypothesised that during the day either ion conductances responsible for reducing *Per1*::Venus neuron firing

regularity are upregulated or network activity disrupts firing activity during that day and not at night.

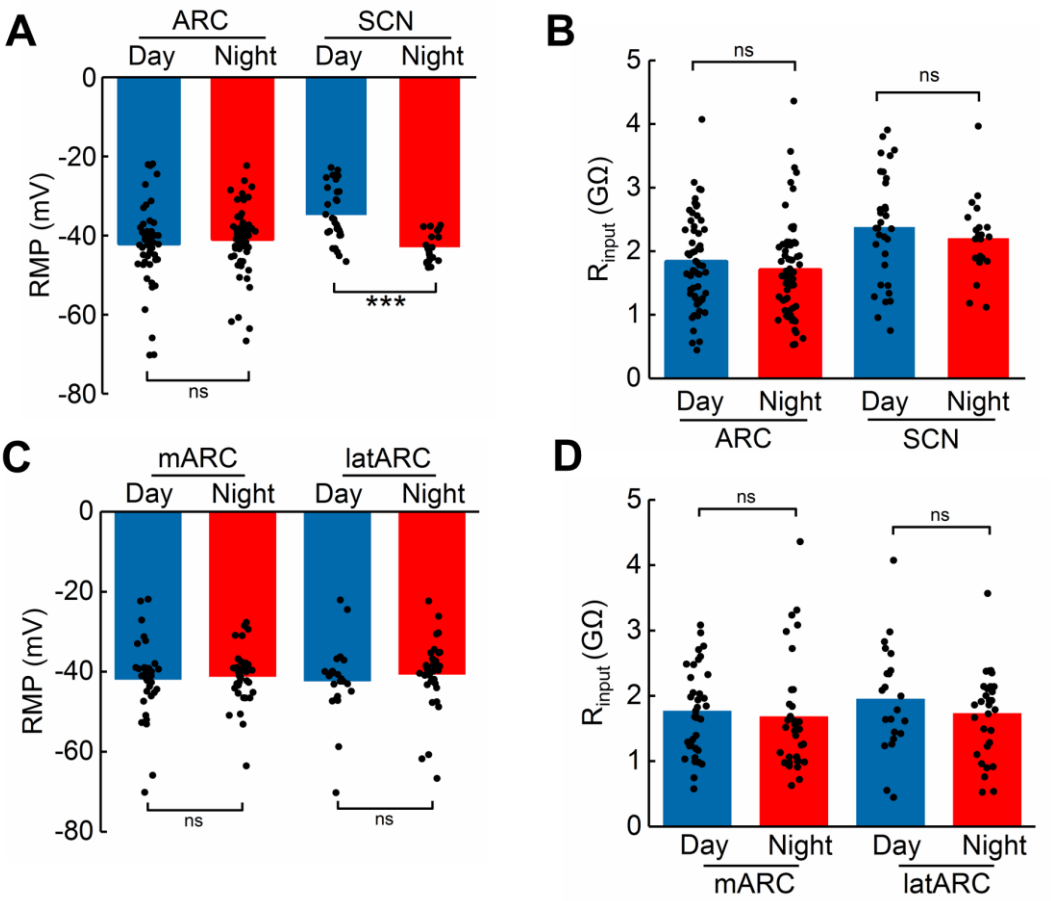

Figure 5: Membrane excitability of *Per1*::Venus neurons in ARC does not vary across the day-night cycle. A: RMP of all neurons recorded in ARC and SCN *Per1*::Venus neurons during the day (ZT4-10) and night (ZT14-20). Circles represent individual cells (ARC, n=130, SCN, n=54). Mean RMP did not vary in ARC (two-sample t test, p=0.45). SCN *Per1*::Venus neurons were significantly depolarised during the day compared to the night (p=0.000009). **B:** R_{input} was determined by current pulses during whole-cell recordings and calculated in accordance with Ohms law. No time of day effect on R_{input} was observed in SCN or ARC (p>0.18). **C:** Cells were filled with biocytin localise them to either mARC or latARC subregions. Analysis of the same data set in subregions revealed that RMP did not significantly vary from day to night in mARC or latARC (p>0.5). **D:** Similarly, time of day did not influence R_{input} in either mARC (p=0.65) or latARC (p=0.29).

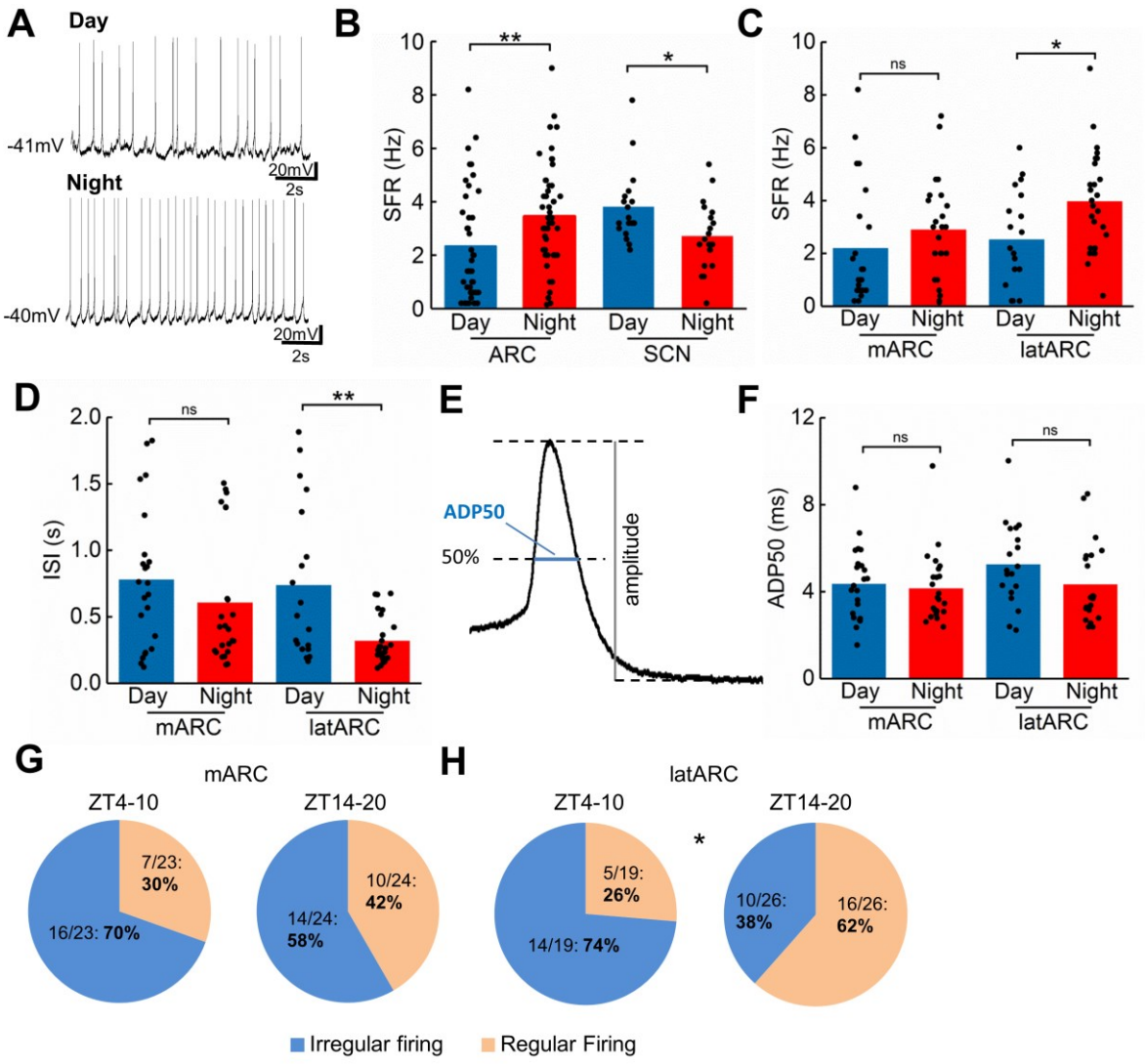

Figure 6: Spontaneous firing rate is elevated in *Per1*::Venus ARC neurons during the night compared to the day. **A:** Representative 10s whole-cell recording traces of latARC *Per1*::Venus neuron activity during the day (ZT4-10) and night (ZT14-20). Firing frequency is elevated in the cell recorded at night but RMP is of a similar level. **B:** Quantification of mean SFR in ARC and SCN slices. Circles represent single *Per1*::Venus neurons. SFR is elevated during the night compared to the day in ARC (two-sample t test, p=0.0075), however in SCN the opposite relationship is observed with higher firing during the day (p=0.013). **C:** When analysed by subregion, neurons in the latARC generated APs more frequently during the night (p=0.025) whereas those situated in mARC did not (p=0.25). **D:** Interspike interval displayed corresponding shortening associated with increased SFR in latARC (p=0.0012) but in not mARC p=0.25) **E:** AP half-duration (ADP50) was used to assess whether AP geometry changes across the daily cycle. Analysis was performed on average AP waveforms. **F:** ADP50 did not vary day to night in either subregion (p>0.11). **G,H:** C.V of ISI was used to distinguish between irregular and regular firing (C.V <0.35) *Per1*::Venus ARC neurons. The proportion of regular vs irregular firing neurons was significantly altered by time of day in latARC, with more cells generating APs with a regular firing pattern (Fisher's exact test, p=0.035). No such variation was observed in mARC (two-sample t test, p=0.5).

ARC network activity is elevated during the night compared to the day

Brain regions adjacent to ARC which also possess the molecular clock machinery are intact in the slices used here for electrophysiological experiments (Guilding et al., 2009). Therefore, to determine whether the ARC and the adjacent VMH and DMH nuclei exhibit daily changes in electrical output, we recorded extracellular MUA during the day (ZT4-10) and night (ZT14-20) in slices harvested from *Per1*::Venus mice. The pMEA recordings performed for this chapter were designed to simultaneously investigate two questions: 1) Is daily variation in single neuron firing frequency is maintained at the network level, and 2) do all extra-SCN MBH regions showing molecular clock oscillations exhibit parallel changes in electrical output.

A minimum of 3h continuous baseline data (analysed in 1h bins) was recorded within either the 6h day or night epoch. Electrodes designated to ARC, DMH and VMH (Fig7) all showed spontaneous extracellular spiking activity on pMEAs. In all cases, application of TTX (1μM) abolished spiking activity across all electrodes and allowed us to determine our threshold for spike detection during analysis (Fig7B). MUA showed significant daily variation in the ARC, but not the VMH or DMH (Fig7C). Similar to whole-cell recordings, MUA averaged across designated electrodes in ARC was significantly elevated during the night (4.68 ± 0.58Hz, n=15 slices, Fig7C) compared to the day (3.10 ± 0.51Hz; n=15, two-sample t-test, p=0.048). No daily variation in MUA was observed in these slices from the VMH (Day, 4.31 ± 1.16Hz; Night, 5.56 ± 1.13Hz, p=0.33) or DMH (Day, 2.63 ± 0.53Hz; Night, 2.96 ± 0.50Hz, p=0.43).

Night elevation in MUA was most evident in electrodes in more lateral area of ARC (Fig7D). Collectively these results demonstrate that the electrical output of the ARC network is elevated at night compared to day, particularly in lateral areas of ARC. This data validates the whole-cell approach as a method for studying both the mechanism responsible for generating daily changes in firing frequency and also variation in ARC network electrical output.

Per1::Venus neurons in latARC receive more frequent GABAergic inputs during the day compared to the night

The absence of temporal changes in membrane properties such as RMP and R_{input} suggests that network changes in synaptic activity, rather than intrinsic factors, may shape firing of *Per1*::Venus neurons situated in the latARC. To address this, voltage clamp synaptic event recordings were performed to measure the frequency of excitatory or inhibitory postsynaptic currents (EPSCs/IPSCs) in these cells during the day and night. With the intracellular recording conditions used in these experiments (20mM KCl- filled pipettes) Cl- currents have a reversal potential of approximately -43mV therefore both $GABA_A$ and AMPA/NMDA currents appear as inward currents at a holding potential of -70mV (Belle et al., 2014). A cocktail of receptor antagonists was used to reveal whether glutamatergic (EPSC) or GABAergic (IPSC) events differ in frequency across the day-night cycle.

Sequential application of antagonists and subtraction of PSC frequency from baseline were used to determine relative frequency of glutamatergic (EPSC) and GABAergic events (IPSC, Fig8A,B). In all latARC *Per1*::Venus neurons tested, bath application of the glutamatergic receptor antagonists, CNQX (10µM)/AP5 (50µM), and the $GABA_A$ receptor antagonist, Gabazine (20µM), abolished all PSCs.

Although the frequency of glutamatergic EPSCs did not significantly change from day to night (2.35 ± 0.58 Hz, n=11; 3.74 ± 1.42 Hz, n=11 respectively, two-sample t-test, p=0.38, Fig8C), *Per1*::Venus latARC neurons received more frequent GABAergic inputs during the day (4.23 ± 1.11 Hz; n=11) compared to the night (1.4 ± 0.35 Hz; n=11; p=0.025). The mean amplitude of glutamatergic EPSCs was unchanged from day (36.2 ± 2.52pA, n=11) to night (38.1 ± 3.54pA, n=11, p=0.43, Fig8D). In addition, the amplitude of GABAergic IPSCs did not differ from day (27.4 ± 1.1pA, n=11) to night (30.1 ± 0.98pA, n=11, p=0.23). This experiment highlights the potential mechanism responsible for reducing daytime firing rate and disrupting regular firing in latARC.

Next, TTX (1µM) was applied to determine the relative contribution of mini-postsynaptic currents (mPSCs arising from spontaneous vesicle fusion) to the total number of PSCs. TTX is conventionally used to block all AP-driven synaptic communication, however previous reports demonstrate that TTX has little effect on PSC frequency in ARC (Pinto et al., 2004, Baquero et al., 2015). Consistent with this, the vast majority of PSCs onto *Per1*::Venus neurons appear to arise from spontaneous release as bath application of TTX had no effect on average PSC frequency (Fig8E).

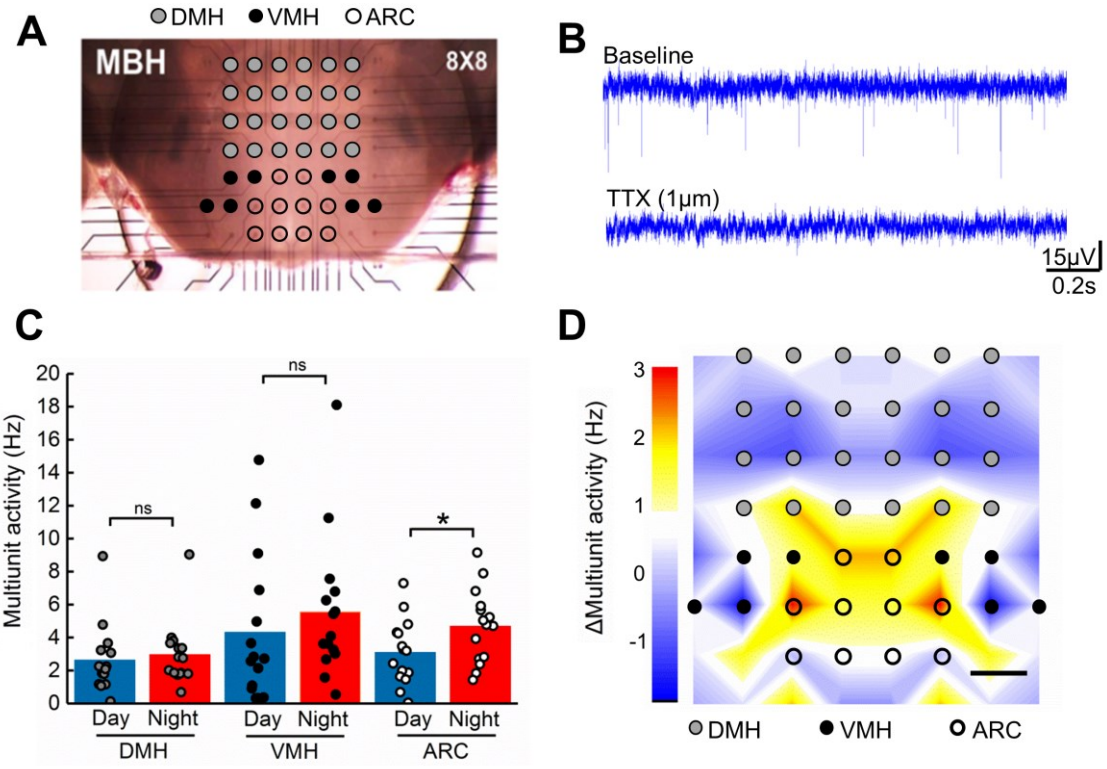

Figure 7: ARC network activity measured by pMEAs exhibits daily variation similar to whole-cell firing frequency. A: Coronal brain slices containing the ARC, DMH and VMH were harvested and MUA was measured using pMEAs. Recordings were made during the day and night (ZT4-10 and ZT14-20 respectively). **B:** At the end of each recording session TTX (1µM) was applied to validate the threshold used for spike detection. Typically spikes exceeding a threshold of -15µV were taken for frequency analysis**. C:** MUA is lower during the day (n=15 slices) compared to the night (n=15) in ARC (p=0.048), but not in other adjacent nuclei, DMH (p=0.43) or VMH (p=0.33). Two-sample t test, ns, not significant, *p<0.05. **D:** Contour plot displaying change in MUA between the night and the daytime. Red/yellow electrode areas represent areas of higher night electrical output versus day. Scale bar represents 200µm.

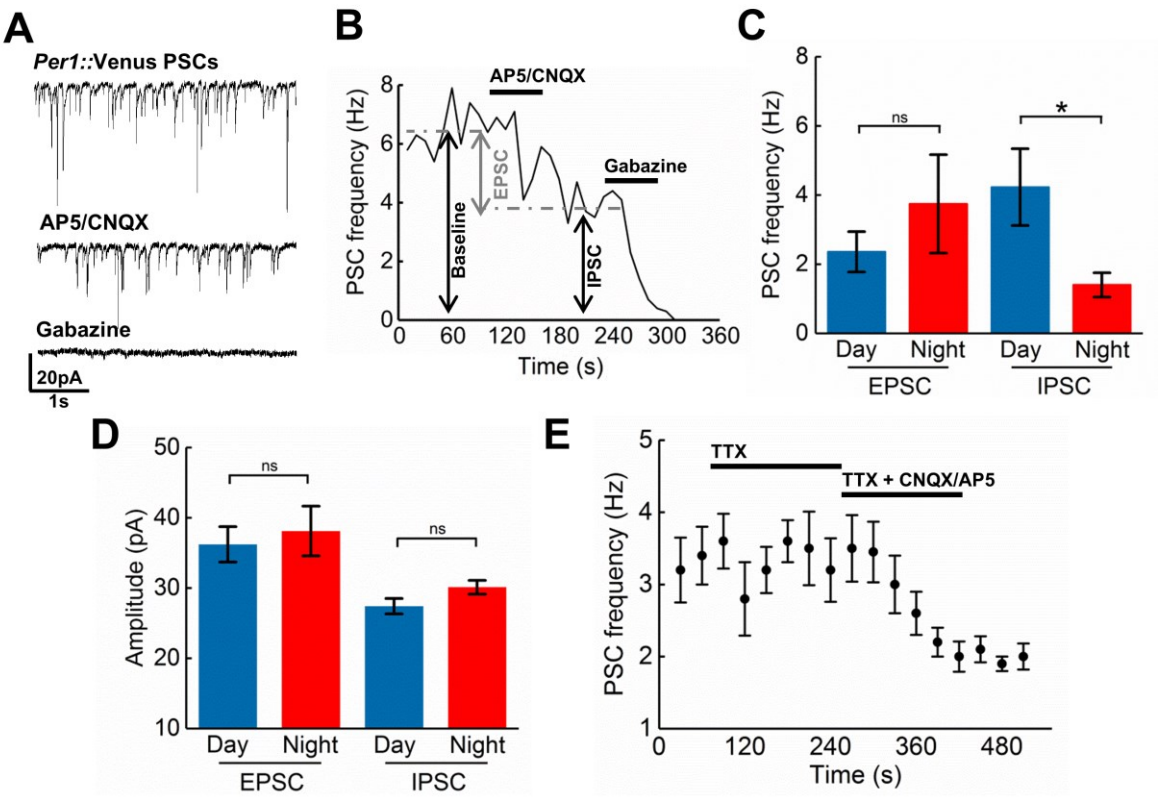

Figure 8: GABAergic synaptic event frequency is higher in latARC during the day compared to the night. A: Postsynaptic currents (PSCs) of a latARC *Per1*::Venus cell during baseline and after application of AP5 (50µM)/CNQX(10µM) or Gabazine (20µM) recorded at a holding potential of -70mV**.** Application of all antagonists was sufficient to abolish all PSCs (>5pA only for analysis). **B:** Antagonists were bath-applied in series to isolate glutamatergic EPSCs and GABAergic IPSCs in latARC *Per1*::Venus neurons. **C:** Mean EPSC frequency did not change between the day (ZT4-10, n=11) and night epoch (ZT14-20, n=11, two-sample t test, p=0.38). Neurons received significantly more frequent IPSCs during the day compared to the night (p=0.025). **D:** Mean amplitude of EPSCs and IPSCs remained consistent across the day-night (p>0.23). **E:** TTX (1µM) did not affect PSC frequency demonstrating that synaptic events were not dependent on the generation of APs. Error bars indicate SEM.

Discussion

The results presented in this chapter provide novel insights into how the intrinsic properties of mouse ARC neurons are influenced by the possession of an intracellular timekeeping mechanism. Initially we assessed the suitability of the *Per1*::Venus reporter mouse line in studying temporal rhythms in ARC. *Per1*::Venus is expressed throughout the ARC and anti-GFP immunostaining for the Venus protein can also be resolved to single cells. We found that *Per1*::Venus cells are densely clustered in medial areas of the ARC

close to the third ventricle and sparsely populate the lateral region between the mARC and VMH (latARC). This area is bordered by a cell sparse zone between the ARC and neighbouring VMH (Chronwall, 1985). *Per1*::Venus cells are situated in close apposition to GFAP+ve cells and processes which are generally distributed over the same area of the slice. These initial imaging studies suggested that the core molecular clock component *Per1* is ubiquitously expressed throughout the ARC. This was confirmed by epifluorescence monitoring during whole-cell targeting of *Per1*::Venus neurons which revealed that almost all cells tested were positive for bright epifluorescence signal.

On the basis that SCN *Per1*-expressing neurons exhibit unique electrical behaviours the baseline electrophysiological states of *Per1*::Venus neurons in ARC were investigated. In addition to previously described firing, hyperpolarised silent and bursting neurons a subset of ARC neurons rest at hyperexcited RMPs and did not generate APs – thus called depolarised silent (Burdakov et al., 2003, van den Pol et al., 2009). We found that *Per1*::Venus neurons that exhibited this depolarised silent behaviour (~13%) were observed during both the day and night recording epochs therefore. This finding is unlike the temporal distribution of depolarised silent states in SCN, which are confined to the afternoon (Belle et al., 2009). Similar behaviours have been previously reported in the rat ARC which were shown to be evoked as a result of local glutamatergic synaptic transmission (Belousov and van den Pol, 1997). Notably, blockade of glutamatergic transmission by CNQX/AP5 caused depolarised silent *Per1*::Venus neurons in both the mARC and latARC to hyperpolarise and fire APs. Glutamatergic transmission in ARC has been shown to be important for appetite control and response to fasting (Liu et al., 2012, Horvath et al., 1997).

Depolarised silent states exist in the SCN and in extra-SCN sites implicated in circadian timekeeping such as the medial and lateral habenula (MHb/LHb) and cerebellum (Belle et al., 2009, Sakhi et al., 2014b, Sakhi et al., 2014a, Raman et al., 2000). In SCN depolarised silent states have been linked to a postsynaptic L-type calcium current (Belle et al., 2009, Diekman et al., 2013). In the Hb depolarised states generally emerge during a time period when *Per* expression is broadly near peak levels (Bano-Otalora and Piggins, 2017). However, in ARC *Per1*::Venus neurons the proportion of depolarised states did not significantly vary across the day-night cycle which together with ours and previous

findings in rats regarding the importance of glutamatergic drive, supports that these states may be driven by mechanisms distinct to those at play in SCN neurons.

This study is the first to describe this novel behaviour in the ARC, but the physiological relevance is unknown. Furthermore, it is unclear whether such hyperexcited neurons occur *in vivo.* Here, depolarised silent neurons were carefully scrutinised to ensure that recordings were viable and that these states were not artificially induced as the result of poor cell access or damage. It is also possible that such states do not regularly occur in well-studied neuronal populations such as those expressing neuropeptide-Y and agouti-related protein (NPY/AgRP). However, the occurrence of these behaviours may function to increase the range of potential responses to metabolic cues such as leptin and ghrelin. For example inhibitory metabolic signals such as leptin (Spanswick et al., 1997, Spanswick et al., 2000, Takahashi and Cone, 2005, Cowley et al., 2001) which ordinarily decrease firing rate may induce paradoxical AP generation in depolarised ARC neurons. Depolarised states could also function to mask complex electrical behaviours such as bursting activity which is associated with neuropeptide release in the hypothalamus (van den Top et al., 2004). Indeed, CNQX/AP5 evoked firing and bursting activity with a similar temporal pattern to that previously reported in ARC tyrosine hydroxylase-expressing neurons (Zhang and van den Pol, 2016).

The majority of *Per1*::Venus ARC neurons spontaneously generated APs with a regular or irregular pattern with a firing rate of 0.1-9Hz. Broadly, this range agrees with previous whole-cell electrophysiology experiments in ARC, which typically report a firing rate of 0.5Hz-4Hz and regular and irregular firing (van den Pol et al., 2009, Cowley et al., 2001, Burdakov et al., 2003, Acuna-Goycolea and van den Pol, 2009, Qiu et al., 2014). Neuronal activity indirectly reported by c-fos staining is higher during the night compared to the day in α-melanocyte stimulating hormone expressing cells (Guzman-Ruiz et al., 2014). Here we show with whole-cell electrophysiology a night-time activation of *Per1*::Venus in the latARC which generate APs more frequently during the night (~4Hz) compared to the day (~2.5Hz). These changes are associated with changes in ISI and occur in the absence of temporal changes in action potential geometry. We also found that a higher proportion of latARC *Per1*::Venus neurons fire APs with a regular pattern during the night than the day.

Therefore, like SCN neurons, high firing in latARC is associated with a regular firing pattern (Pennartz et al., 1998, Kim and Dudek, 1993).

MBH nuclei exhibit a continuum of temporal profiles in firing frequency; multiunit and single-unit electrical activity display robust rhythms in the ARC (Guilding et al., 2009). Recently neurons that are sensitive to the potent ARC-targeting adipokine leptin have been demonstrated to contribute to generating endogenous feeding rhythms in mice (Li et al., 2012). We found that *Per1*::Venus ARC neurons were able to sense both leptin and orexin. Orexinergic neurons of the lateral hypothalamus represent a major feeding orientated input to the ARC (Horvath et al., 1999, Guan et al., 2001). Interestingly, *Per1*::Venus neurons responded to both leptin and orexin, either with reductions or increases in excitability. In the ARC, the bipolar effects of leptin are thought to occur due to direct membrane and indirect network effects (Burdakov et al., 2003). The majority of cells that responded to leptin did so with reductions in excitability. Leptin is known to induce effects of different polarity in ARC (Spanswick et al., 1997, Cowley et al., 2001, Qiu et al., 2010). However, typically NPY/AgRP neurons respond with decreased firing in response to leptin (Baver et al., 2014). Collectively these results suggest that *Per1*::Venus neurons may form a key integration point between timekeeping and metabolic sensing.

This study is the first to demonstrate that ARC electrical activity peaks during the night in neurons express *Per1*, a core marker of the molecular clock. The ARC has a well-established role in energy homeostasis and intense research has begun to unravel the neural circuitry and outputs responsible for regulating the physical manifestation of hunger and satiety (Andermann and Lowell, 2017). However, meal initiation has many drivers including caloric deficiency, sight and smell of food, social interaction and of course, time of day (Begg and Woods, 2013, Woods et al., 1998, Schwartz et al., 2000). Signals relating to systemic energy levels reach the brain via a number of different pathways. The gut signals information related to ingested food to the Nucleus Tractus Solitarius (NTS) via the vagus nerve (Chambers et al., 2013, Berthoud and Neuhuber, 2000, Brookes et al., 2013). In addition to short-term feedback from the gut, energy stores transmit information to primary neurons in the hypothalamus through the controlled release of hormonal signals (Morton et al., 2006). NPY/AgRP and POMC-expressing neurons residing in the ARC are of great importance in regulating the

physiological and behaviour responses to circulating hormonal signals primarily through activation or inactivation of the melanocortin 4 receptor (MC4R) in downstream sites such as the paraventricular nucleus (Poggioli et al., 1986, Graham et al., 1997, Rossi et al., 1998, Luquet et al., 2005).

When AgRP neurons are opto- or chemo-genetically activated and neuronal firing is evoked, profound eating occurs (Aponte et al., 2011, Krashes et al., 2011). Stimulation of POMC neurons in ARC and NTS supresses feeding (Aponte et al., 2011, Zhan et al., 2013). While this 'forced' activation elicits downstream behaviours the mechanisms that regulate the initiation and appropriate timing of feeding are complex. Therefore the framework of feedforward input from predictive circadian oscillators to first-order neurons in ARC requires further investigation. Here, we demonstrate that when isolated from SCN, *Per1*-expressing ARC neurons are nocturnally active when mice would be awake and actively engaging in food-seeking behaviour. The physiological relevance of rhythmic firing rate recorded in single-cells was validated by studying network activity during the day and night with pMEAs. Network activity displayed significant daily variation particularly in electrodes in latARC. Such variation is not found in the adjacent ventromedial (VMH) or dorsomedial (DMH) nuclei. A previous report implicated VMH *Bmal1* expression in the circadian regulation of energy expenditure. Here, we found that VMH neuronal activity does not exhibit daily variation, therefore we suggest that physiological regulation occurs without associated daily changes in electrical output (Orozco-Solis et al., 2016).

When food is made available to nocturnal rodents *ad libitum*, food intake is broadly partitioned to the dark phase of the light-dark cycle and is not a passive result of sleep-wake activity (Armstrong et al., 1980). Few attempts have been made to determine brain regions responsible for the circadian coordination of feeding, although multiple lines of experimental evidence suggest the MBH is critical in sculpting these rhythms in appetite and feeding behaviours. Although SCN projections to the MBH provide a means for gating feeding behaviour, the Integration of physiological signals to derive rhythms compatible with homeostatic requirements is likely to occur outside the SCN, thus providing maximum flexibility for responding to varying challenges. Indeed, MBH (ARC and VMH) lesions result in hyperphagia and disruption in diurnal feeding patterns (Chou et al.,

2003). Sleep-wake and feeding rhythms are distributed equally across the light-dark cycle following the targeted destruction of ARC neurons by bilateral injection of a NPY-Saporin conjugate (Wiater et al., 2011). SAP conjugated to leptin (Leptin-SAP), was also injected into the ARC, and resulting feeding rhythms and body-weight under light-dark (LD) and continuous darkness (DD) were evaluated (Li et al., 2012). Rats given Lep-SAP injections in the ARC fed arrhythmically when housed under 12:12hr LD and DD conditions with *ad libitum* access to food, and as a result of hyperphagia rapidly became obese.

A recent study demonstrates that this night-active phase-relationship is maintained *in vivo* with multiunit recordings in freely-moving rats (Fifel et al., 2018). Based on the neuroanatomical position of latARC *Per1*::Venus neurons it is unlikely that the molecular clock drives high nocturnal firing rates in AgRP neurons, which form a dense plexus of cells close to the third ventricle (van den Pol et al., 2009). Given the ubiquitous expression of *Per1*::Venus through cells in latARC, this population is likely to overlap with a number of different neuropeptide-expressing populations with established orexigenic or anorexigenic properties including POMC-expressing neurons and tyrosine hydroxylase neurons that are distributed throughout more lateral areas of ARC (Zhang and van den Pol, 2015, Qiu et al., 2010). Further investigation is required to assess whether *Per1*::Venus neurons influence temporal patterns in feeding.

This study provides a unique insight into the role of the ARC in circadian rhythmicity as the brain slices used for electrophysiology do not contain SCN. The SCN sends direct and indirect neural projections to ARC which consists of both excitatory and inhibitory components (Saeb-Parsy et al., 2000). Reciprocal interaction of ARC with SCN, can regulate the sleep-wake cycle (Buijs et al., 2017). In the SCN, expression of *Per1* levels are higher during the day than the night and this correlates with the elevated excitability of SCN neurons at this time. Components of the core molecular clock are present in the ARC, with *Per1* expression peaking during the night, in antiphase to the rhythm in SCN (Shieh et al., 2005, Abe et al., 2002). Our recordings also revealed that ARC *Per1*::Venus neurons fire APs with a higher frequency at night, and indicate that this activity is in delayed with respect to that of *Per1*::Venus neurons in the SCN.

In SCN neurons firing rates are reported between 3 and 6Hz during daytime peaks and decrease to <2Hz at night although most reports suggest frequencies as low as 1Hz (Belle et al., 2009, Kuhlman and McMahon, 2004, Kudo et al., 2011). In this study *Per1*::Venus neurons displayed a similar range of firing rates (0.8-4Hz). In SCN, membrane potential displays a daily rhythm, by which neurons depolarise by ~6-10mV during the day compared to the night (Belle et al., 2009). This change is primarily mediated by a tetraethylammonium-sensitive hyperpolarising K^+-dependent conductance that inactivates during the day (Kuhlman and McMahon, 2004).

In agreement with previous studies, we found that *Per1*::Venus neurons in SCN exhibited significant daily variation in membrane excitability. We found that SCN neurons did not display variation in R_{input} while previous work from our lab using a *Per1*::GFP reporter line did demonstrate daily change in R_{input} (Belle et al., 2009). We postulate that this difference is likely due to differences between the cell populations that each reporter represent. Rhythmic AP firing in latARC was not accompanied by corresponding changes in RMP or R_{input} as is the case in the master clock. This finding is similar to LHb, in which *Per1*-expressing neurons exhibit diurnal rhythms in firing rate without changes in RMP (Sakhi et al., 2014b). These findings raise the possibility that the link between molecular clock and membrane dynamics is distinct in extra-SCN oscillators compared to SCN.

Simultaneous quantification of molecular clock status and firing rate in SCN neurons reveals a stable, phased relationship between E-box-regulated clock gene expression and firing rate, and that this relationship is independent of light input or $GABA_A$ mediated synaptic activity (Jones and McMahon, 2016). The link between the molecular clock and excitability in the SCN is thought to be mediated by clock-mediated control of ion conductance. A number of currents exhibit circadian variation within SCN neurons including A-type conductance (*KCND1,KCND2*, Itri et al., 2010, Granados-Fuentes et al., 2012), fast-delayed rectifier conductance (FDR; *KCNC KCNC2*, Kudo et al., 2011), the large conductance Ca^{2+}-dependent K^+ channels (BK, *KCNMA1*, Pitts et al., 2006, Whitt et al., 2016), L-type Ca^+ channels (*CACNA1C, CACNA1S*) which peaks during the day in rats (Pennartz et al., 2002), and an anonymous TEA-sensitive K^+ conductance (Kuhlman and McMahon, 2004).

In vitro studies reveal that metabolic signals target specific ion channels. For example, the satiety-promoting adipokine leptin modulates the activity of potassium channels including Kv2.1 and K_{ATP} channels that are critical for the control of neuronal firing (Baver et al., 2014, Spanswick et al., 1997). A range of ionic currents are responsible for setting the firing rate and pattern in mammalian neurons (Colwell, 2011). Prior studies demonstrate that under fasting conditions the firing rate of ARC AgRP neurons is elevated without significant changes in RMP, an effect which is mediated by small-conductance potassium channels (SK, (He et al., 2016). Moreover, a recent study in ARC showed that irregular firing can be induced by activation of A-type K^+ conductances (Mendonca et al., 2018).

Although no specific investigations were performed in this study, clock control of ARC firing rate could potentially act at the level of individual ion channels. However, here we found that *Per1*::Venus in the latARC receive more frequent GABAergic IPSCs during the day compared to the night, with no daily change in glutamatergic EPSC frequency. Therefore our data suggests that increased inhibitory synaptic tone during the daytime suppresses firing rate and regular firing patterns in the latARC. Histological staining for glutamate decarboxylase, a marker of GABAergic cells, reveal that ARC is also highly GABAergic (Decavel and Van den Pol, 1990). A GABAergic network in ARC plays an integral role in the function of neural circuits involved in the control of metabolism and feeding (Vong et al., 2011, Cowley et al., 2001, Horvath et al., 1992). Peptidergic cells in the ARC also corelease GABA which signals to other neurons in the ARC (Cravo et al., 2011, Zhang and van den Pol, 2016). In line with previous studies, no discernible effect on EPSC or IPSC frequency was detected following bath application of TTX (Pinto et al., 2004, Baquero et al., 2015). Therefore synaptic communication to *Per1*::Venus neurons *in vitro* is not largely dependent on AP-driven PSCs but via spontaneous vesicle fusion. This may account for the daily changes in event frequency but not amplitude as quantal neurotransmitter release is generally stochastic and coordinated release resulting from APs is likely required to evoke high amplitude EPSCs at the postsynaptic membrane (Otsu and Murphy, 2003, Popescu et al., 2010).

Bioluminescent reporters of the core molecular clock show clear ~24h rhythms which are distinguishable in individual cells throughout the ARC (Abe et al., 2002, Guilding et al., 2009). Single neuron discrimination revealed a higher proportion of PER2::LUC expressing

cells were rhythmic (89%) in close proximity to the third ventricle when compared to those broadly localised to lateral ARC (67%, Guilding et al., 2009). We found that *Per1*::Venus neurons in mARC do not express rhythmic daily variation in AP frequency. pMEA recordings reveal that the disparity between electrical rhythms in mARC and latARC is also evident in adjacent regions in the MBH during pMEA recordings. Synaptic communication and network activity is essential for coherent output of the SCN (Webb et al., 2009, Freeman et al., 2013). Intriguingly, the ARC may operate in a similar fashion to the SCN network to regulate timekeeping. We found that GABAergic communication to neurons in the latARC displays diurnal rhythmicity. However, the source of this GABAergic input is unknown. Indeed, GABAergic collateral projections from AgRP neurons which are primarily clustered close to the third ventricle provide a means by which pro-opiomelanocortin (POMC) neurons can be inhibited (Cowley et al., 2001, Horvath et al., 1992). Therefore, it is plausible that mARC, which contains a high proportion of rhythmic PER2::LUC cells during imaging studies, may impart a rhythmic inhibitory signal during the day onto latARC neurons. Further latARC clock neurons could communication with each other to regulate the temporal aspects of their own electrical output.

References

ABE, M., HERZOG, E. D., YAMAZAKI, S., STRAUME, M., TEI, H., SAKAKI, Y., MENAKER, M. & BLOCK, G. D. 2002. Circadian rhythms in isolated brain regions. *J Neurosci,* 22**,** 350-6.

ACUNA-GOYCOLEA, C. & VAN DEN POL, A. N. 2009. Neuroendocrine proopiomelanocortin neurons are excited by hypocretin/orexin. *J Neurosci,* 29**,** 1503-13.

ANDERMANN, M. L. & LOWELL, B. B. 2017. Toward a Wiring Diagram Understanding of Appetite Control. *Neuron,* 95**,** 757-778.

APONTE, Y., ATASOY, D. & STERNSON, S. M. 2011. AGRP neurons are sufficient to orchestrate feeding behavior rapidly and without training. *Nat Neurosci,* 14**,** 351-5.

ARMSTRONG, S., COLEMAN, G. & SINGER, G. 1980. Food and water deprivation: changes in rat feeding, drinking, activity and body weight. *Neurosci Biobehav Rev,* 4**,** 377-402.

ATASOY, D., BETLEY, J. N., SU, H. H. & STERNSON, S. M. 2012. Deconstruction of a neural circuit for hunger. *Nature,* 488**,** 172-7.

ATON, S. J., COLWELL, C. S., HARMAR, A. J., WASCHEK, J. & HERZOG, E. D. 2005. Vasoactive intestinal polypeptide mediates circadian rhythmicity and synchrony in mammalian clock neurons. *Nat Neurosci,* 8**,** 476-83.

BANO-OTALORA, B. & PIGGINS, H. D. 2017. Contributions of the lateral habenula to circadian timekeeping. *Pharmacol Biochem Behav,* 162**,** 46-54.

BAQUERO, A. F., KIRIGITI, M. A., BAQUERO, K. C., LEE, S. J., SMITH, M. S. & GROVE, K. L. 2015. Developmental changes in synaptic distribution in arcuate nucleus neurons. *J Neurosci,* 35**,** 8558-69.

BARSH, G. S., FAROOQI, I. S. & O'RAHILLY, S. 2000. Genetics of body-weight regulation. *Nature,* 404**,** 644-51.

BAVER, S. B., HOPE, K., GUYOT, S., BJORBAEK, C., KACZOROWSKI, C. & O'CONNELL, K. M. 2014. Leptin modulates the intrinsic excitability of AgRP/NPY neurons in the arcuate nucleus of the hypothalamus. *J Neurosci,* 34**,** 5486-96.

BEGG, D. P. & WOODS, S. C. 2013. The endocrinology of food intake. *Nat Rev Endocrinol,* 9**,** 584-97.

BELLE, M. D., DIEKMAN, C. O., FORGER, D. B. & PIGGINS, H. D. 2009. Daily electrical silencing in the mammalian circadian clock. *Science,* 326**,** 281-4.

BELLE, M. D., HUGHES, A. T., BECHTOLD, D. A., CUNNINGHAM, P., PIERUCCI, M., BURDAKOV, D. & PIGGINS, H. D. 2014. Acute suppressive and long-term phase modulation actions of orexin on the mammalian circadian clock. *J Neurosci,* 34**,** 3607-21.

BELOUSOV, A. B. & VAN DEN POL, A. N. 1997. Local synaptic release of glutamate from neurons in the rat hypothalamic arcuate nucleus. *J Physiol,* 499 (Pt 3)**,** 747-61.

BERTHOUD, H. R. & NEUHUBER, W. L. 2000. Functional and chemical anatomy of the afferent vagal system. *Auton Neurosci,* 85**,** 1-17.

BROOKES, S. J., SPENCER, N. J., COSTA, M. & ZAGORODNYUK, V. P. 2013. Extrinsic primary afferent signalling in the gut. *Nat Rev Gastroenterol Hepatol,* 10**,** 286-96.

BROWN, T. M., COLWELL, C. S., WASCHEK, J. A. & PIGGINS, H. D. 2007. Disrupted neuronal activity rhythms in the suprachiasmatic nuclei of vasoactive intestinal polypeptide-deficient mice. *J Neurophysiol,* 97**,** 2553-8.

BUHR, E. D. & TAKAHASHI, J. S. 2013. Molecular components of the Mammalian circadian clock. *Handb Exp Pharmacol***,** 3-27.

BUIJS, F. N., GUZMAN-RUIZ, M., LEON-MERCADO, L., BASUALDO, M. C., ESCOBAR, C., KALSBEEK, A. & BUIJS, R. M. 2017. Suprachiasmatic Nucleus Interaction with the Arcuate Nucleus; Essential for Organizing Physiological Rhythms. *eNeuro,* 4.

BUNGER, M. K., WILSBACHER, L. D., MORAN, S. M., CLENDENIN, C., RADCLIFFE, L. A., HOGENESCH, J. B., SIMON, M. C., TAKAHASHI, J. S. & BRADFIELD, C. A. 2000. Mop3 is an essential component of the master circadian pacemaker in mammals. *Cell,* 103**,** 1009-17.

BURDAKOV, D., LISS, B. & ASHCROFT, F. M. 2003. Orexin excites GABAergic neurons of the arcuate nucleus by activating the sodium--calcium exchanger. *J Neurosci,* 23**,** 4951-7.

CAMPBELL, J. N., MACOSKO, E. Z., FENSELAU, H., PERS, T. H., LYUBETSKAYA, A., TENEN, D., GOLDMAN, M., VERSTEGEN, A. M., RESCH, J. M., MCCARROLL, S. A., ROSEN, E. D., LOWELL, B. B. & TSAI, L. T. 2017. A molecular census of arcuate hypothalamus and median eminence cell types. *Nat Neurosci,* 20**,** 484-496.

CHAMBERS, A. P., SANDOVAL, D. A. & SEELEY, R. J. 2013. Integration of satiety signals by the central nervous system. *Curr Biol,* 23**,** R379-88.

CHENG, H. Y., ALVAREZ-SAAVEDRA, M., DZIEMA, H., CHOI, Y. S., LI, A. & OBRIETAN, K. 2009. Segregation of expression of mPeriod gene homologs in neurons and glia:

possible divergent roles of mPeriod1 and mPeriod2 in the brain. *Hum Mol Genet,* 18**,** 3110-24.

CHOU, T. C., SCAMMELL, T. E., GOOLEY, J. J., GAUS, S. E., SAPER, C. B. & LU, J. 2003. Critical role of dorsomedial hypothalamic nucleus in a wide range of behavioral circadian rhythms. *J Neurosci,* 23**,** 10691-702.

CHRONWALL, B. M. 1985. Anatomy and physiology of the neuroendocrine arcuate nucleus. *Peptides,* 6 Suppl 2**,** 1-11.

COLWELL, C. S. 2011. Linking neural activity and molecular oscillations in the SCN. *Nat Rev Neurosci,* 12**,** 553-69.

CONE, R. D., COWLEY, M. A., BUTLER, A. A., FAN, W., MARKS, D. L. & LOW, M. J. 2001. The arcuate nucleus as a conduit for diverse signals relevant to energy homeostasis. *Int J Obes Relat Metab Disord,* 25 Suppl 5**,** S63-7.

COWLEY, M. A., SMART, J. L., RUBINSTEIN, M., CERDAN, M. G., DIANO, S., HORVATH, T. L., CONE, R. D. & LOW, M. J. 2001. Leptin activates anorexigenic POMC neurons through a neural network in the arcuate nucleus. *Nature,* 411**,** 480-4.

CRAVO, R. M., MARGATHO, L. O., OSBORNE-LAWRENCE, S., DONATO, J., JR., ATKIN, S., BOOKOUT, A. L., ROVINSKY, S., FRAZAO, R., LEE, C. E., GAUTRON, L., ZIGMAN, J. M. & ELIAS, C. F. 2011. Characterization of Kiss1 neurons using transgenic mouse models. *Neuroscience,* 173**,** 37-56.

DEBONS, A. F., SICLARI, E., DAS, K. C. & FUHR, B. 1982. Gold thioglucose-induced hypothalamic damage, hyperphagia, and obesity: dependence on the adrenal gland. *Endocrinology,* 110**,** 2024-9.

DECAVEL, C. & VAN DEN POL, A. N. 1990. GABA: a dominant neurotransmitter in the hypothalamus. *J Comp Neurol,* 302**,** 1019-37.

DIEKMAN, C. O., BELLE, M. D., IRWIN, R. P., ALLEN, C. N., PIGGINS, H. D. & FORGER, D. B. 2013. Causes and consequences of hyperexcitation in central clock neurons. *PLoS Comput Biol,* 9**,** e1003196.

FIFEL, K., MEIJER, J. H. & DEBOER, T. 2018. Long-term effects of sleep deprivation on neuronal activity in four hypothalamic areas. *Neurobiol Dis,* 109**,** 54-63.

FREEMAN, G. M., JR., KROCK, R. M., ATON, S. J., THABEN, P. & HERZOG, E. D. 2013. GABA networks destabilize genetic oscillations in the circadian pacemaker. *Neuron,* 78**,** 799-806.

GEKAKIS, N., STAKNIS, D., NGUYEN, H. B., DAVIS, F. C., WILSBACHER, L. D., KING, D. P., TAKAHASHI, J. S. & WEITZ, C. J. 1998. Role of the CLOCK protein in the mammalian circadian mechanism. *Science,* 280**,** 1564-9.

GHAMARI-LANGROUDI, M., SRISAI, D. & CONE, R. D. 2011. Multinodal regulation of the arcuate/paraventricular nucleus circuit by leptin. *Proc Natl Acad Sci U S A,* 108**,** 355-60.

GRAHAM, M., SHUTTER, J. R., SARMIENTO, U., SAROSI, I. & STARK, K. L. 1997. Overexpression of Agrt leads to obesity in transgenic mice. *Nat Genet,* 17**,** 273-4.

GROOS, G. & HENDRIKS, J. 1982. Circadian rhythms in electrical discharge of rat suprachiasmatic neurones recorded in vitro. *Neurosci Lett,* 34**,** 283-8.

GUAN, J. L., SAOTOME, T., WANG, Q. P., FUNAHASHI, H., HORI, T., TANAKA, S. & SHIODA, S. 2001. Orexinergic innervation of POMC-containing neurons in the rat arcuate nucleus. *Neuroreport,* 12**,** 547-51.

GUILDING, C., HUGHES, A. T., BROWN, T. M., NAMVAR, S. & PIGGINS, H. D. 2009. A riot of rhythms: neuronal and glial circadian oscillators in the mediobasal hypothalamus. *Mol Brain,* 2**,** 28.

GUILDING, C., HUGHES, A. T. & PIGGINS, H. D. 2010. Circadian oscillators in the epithalamus. *Neuroscience,* 169**,** 1630-9.

GUILDING, C. & PIGGINS, H. D. 2007. Challenging the omnipotence of the suprachiasmatic timekeeper: are circadian oscillators present throughout the mammalian brain? *Eur J Neurosci,* 25**,** 3195-216.

GUZMAN-RUIZ, M., SADERI, N., CAZAREZ-MARQUEZ, F., GUERRERO-VARGAS, N. N., BASUALDO, M. C., ACOSTA-GALVAN, G. & BUIJS, R. M. 2014. The suprachiasmatic nucleus changes the daily activity of the arcuate nucleus alpha-MSH neurons in male rats. *Endocrinology,* 155**,** 525-35.

HENTGES, S. T., NISHIYAMA, M., OVERSTREET, L. S., STENZEL-POORE, M., WILLIAMS, J. T. & LOW, M. J. 2004. GABA release from proopiomelanocortin neurons. *J Neurosci,* 24**,** 1578-83.

HERZOG, E. D., TAKAHASHI, J. S. & BLOCK, G. D. 1998. Clock controls circadian period in isolated suprachiasmatic nucleus neurons. *Nat Neurosci,* 1**,** 708-13.

HORVATH, T. L., BECHMANN, I., NAFTOLIN, F., KALRA, S. P. & LERANTH, C. 1997. Heterogeneity in the neuropeptide Y-containing neurons of the rat arcuate nucleus: GABAergic and non-GABAergic subpopulations. *Brain Res,* 756**,** 283-6.

HORVATH, T. L., DIANO, S. & VAN DEN POL, A. N. 1999. Synaptic interaction between hypocretin (orexin) and neuropeptide Y cells in the rodent and primate hypothalamus: a novel circuit implicated in metabolic and endocrine regulations. *J Neurosci,* 19**,** 1072-87.

HORVATH, T. L., NAFTOLIN, F., KALRA, S. P. & LERANTH, C. 1992. Neuropeptide-Y innervation of beta-endorphin-containing cells in the rat mediobasal hypothalamus: a light and electron microscopic double immunostaining analysis. *Endocrinology,* 131**,** 2461-7.

HUGHES, A. T. & PIGGINS, H. D. 2008. Behavioral responses of Vipr2-/- mice to light. *J Biol Rhythms,* 23**,** 211-9.

INOUYE, S. T. & KAWAMURA, H. 1979. Persistence of circadian rhythmicity in a mammalian hypothalamic "island" containing the suprachiasmatic nucleus. *Proc Natl Acad Sci U S A,* 76**,** 5962-6.

ITRI, J., MICHEL, S., WASCHEK, J. A. & COLWELL, C. S. 2004. Circadian rhythm in inhibitory synaptic transmission in the mouse suprachiasmatic nucleus. *J Neurophysiol,* 92**,** 311-9.

ITRI, J. N., VOSKO, A. M., SCHROEDER, A., DRAGICH, J. M., MICHEL, S. & COLWELL, C. S. 2010. Circadian regulation of a-type potassium currents in the suprachiasmatic nucleus. *J Neurophysiol,* 103**,** 632-40.

JACKSON, A. C., YAO, G. L. & BEAN, B. P. 2004. Mechanism of spontaneous firing in dorsomedial suprachiasmatic nucleus neurons. *J Neurosci,* 24**,** 7985-98.

JONES, J. R. & MCMAHON, D. G. 2016. The core clock gene Per1 phases molecular and electrical circadian rhythms in SCN neurons. *PeerJ,* 4**,** e2297.

KALRA, S. P., DUBE, M. G., PU, S., XU, B., HORVATH, T. L. & KALRA, P. S. 1999. Interacting appetite-regulating pathways in the hypothalamic regulation of body weight. *Endocr Rev,* 20**,** 68-100.

KELLY, J. & GROSSMAN, S. P. 1979. GABA and hypothalamic feeding systems. II. A comparison of GABA, glycine and actylcholine agonists and their antagonists. *Pharmacol Biochem Behav,* 11**,** 647-52.

KIM, Y. I. & DUDEK, F. E. 1993. Membrane properties of rat suprachiasmatic nucleus neurons receiving optic nerve input. *J Physiol,* 464**,** 229-43.

KONONENKO, N. I. & DUDEK, F. E. 2004. Mechanism of irregular firing of suprachiasmatic nucleus neurons in rat hypothalamic slices. *J Neurophysiol,* 91**,** 267-73.

KRASHES, M. J., KODA, S., YE, C., ROGAN, S. C., ADAMS, A. C., CUSHER, D. S., MARATOS-FLIER, E., ROTH, B. L. & LOWELL, B. B. 2011. Rapid, reversible activation of AgRP neurons drives feeding behavior in mice. *J Clin Invest,* 121**,** 1424-8.

KUDO, T., LOH, D. H., KULJIS, D., CONSTANCE, C. & COLWELL, C. S. 2011. Fast delayed rectifier potassium current: critical for input and output of the circadian system. *J Neurosci,* 31**,** 2746-55.

KUHLMAN, S. J. & MCMAHON, D. G. 2004. Rhythmic regulation of membrane potential and potassium current persists in SCN neurons in the absence of environmental input. *Eur J Neurosci,* 20**,** 1113-7.

LI, A. J., WIATER, M. F., OOSTROM, M. T., SMITH, B. R., WANG, Q., DINH, T. T., ROBERTS, B. L., JANSEN, H. T. & RITTER, S. 2012. Leptin-sensitive neurons in the arcuate nuclei contribute to endogenous feeding rhythms. *Am J Physiol Regul Integr Comp Physiol,* 302**,** R1313-26.

LIU, A. C., WELSH, D. K., KO, C. H., TRAN, H. G., ZHANG, E. E., PRIEST, A. A., BUHR, E. D., SINGER, O., MEEKER, K., VERMA, I. M., DOYLE, F. J., 3RD, TAKAHASHI, J. S. & KAY, S. A. 2007. Intercellular coupling confers robustness against mutations in the SCN circadian clock network. *Cell,* 129**,** 605-16.

LIU, T., KONG, D., SHAH, B. P., YE, C., KODA, S., SAUNDERS, A., DING, J. B., YANG, Z., SABATINI, B. L. & LOWELL, B. B. 2012. Fasting activation of AgRP neurons requires NMDA receptors and involves spinogenesis and increased excitatory tone. *Neuron,* 73**,** 511-22.

LUQUET, S., PEREZ, F. A., HNASKO, T. S. & PALMITER, R. D. 2005. NPY/AgRP neurons are essential for feeding in adult mice but can be ablated in neonates. *Science,* 310**,** 683-5.

MA, X., ZUBCEVIC, L., BRUNING, J. C., ASHCROFT, F. M. & BURDAKOV, D. 2007. Electrical inhibition of identified anorexigenic POMC neurons by orexin/hypocretin. *J Neurosci,* 27**,** 1529-33.

MEISTER, B., CECCATELLI, S., HOKFELT, T., ANDEN, N. E., ANDEN, M. & THEODORSSON, E. 1989. Neurotransmitters, neuropeptides and binding sites in the rat mediobasal hypothalamus: effects of monosodium glutamate (MSG) lesions. *Exp Brain Res,* 76**,** 343-68.

MENDONCA, P. R. F., KYLE, V., YEO, S. H., COLLEDGE, W. H. & ROBINSON, H. P. C. 2018. Kv4.2 channel activity controls intrinsic firing dynamics of arcuate kisspeptin neurons. *J Physiol,* 596**,** 885-899.

MOORE, R. Y. & SPEH, J. C. 1993. GABA is the principal neurotransmitter of the circadian system. *Neurosci Lett,* 150**,** 112-6.

MORTON, G. J., CUMMINGS, D. E., BASKIN, D. G., BARSH, G. S. & SCHWARTZ, M. W. 2006. Central nervous system control of food intake and body weight. *Nature,* 443**,** 289-95.

NAKAMURA, W., HONMA, S., SHIRAKAWA, T. & HONMA, K. 2002. Clock mutation lengthens the circadian period without damping rhythms in individual SCN neurons. *Nat Neurosci,* 5**,** 399-400.

NORSTED, E., GOMUC, B. & MEISTER, B. 2008. Protein components of the blood-brain barrier (BBB) in the mediobasal hypothalamus. *J Chem Neuroanat,* 36**,** 107-21.

OROZCO-SOLIS, R., AGUILAR-ARNAL, L., MURAKAMI, M., PERUQUETTI, R., RAMADORI, G., COPPARI, R. & SASSONE-CORSI, P. 2016. The Circadian Clock in the Ventromedial Hypothalamus Controls Cyclic Energy Expenditure. *Cell Metab,* 23**,** 467-78.

OTSU, Y. & MURPHY, T. H. 2003. Mind-altering miniature neurotransmitter release? *Proc Natl Acad Sci U S A,* 100**,** 5589-90.

PARTCH, C. L., GREEN, C. B. & TAKAHASHI, J. S. 2014. Molecular architecture of the mammalian circadian clock. *Trends Cell Biol,* 24**,** 90-9.

PENNARTZ, C. M., DE JEU, M. T., BOS, N. P., SCHAAP, J. & GEURTSEN, A. M. 2002. Diurnal modulation of pacemaker potentials and calcium current in the mammalian circadian clock. *Nature,* 416**,** 286-90.

PENNARTZ, C. M., DE JEU, M. T., GEURTSEN, A. M., SLUITER, A. A. & HERMES, M. L. 1998. Electrophysiological and morphological heterogeneity of neurons in slices of rat suprachiasmatic nucleus. *J Physiol,* 506 (Pt 3)**,** 775-93.

PINTO, S., ROSEBERRY, A. G., LIU, H., DIANO, S., SHANABROUGH, M., CAI, X., FRIEDMAN, J. M. & HORVATH, T. L. 2004. Rapid rewiring of arcuate nucleus feeding circuits by leptin. *Science,* 304**,** 110-5.

POGGIOLI, R., VERGONI, A. V. & BERTOLINI, A. 1986. ACTH-(1-24) and alpha-MSH antagonize feeding behavior stimulated by kappa opiate agonists. *Peptides,* 7**,** 843-8.

POPESCU, I. R., MORTON, L. A., FRANCO, A., DI, S., UETA, Y. & TASKER, J. G. 2010. Synchronized bursts of miniature inhibitory postsynaptic currents. *J Physiol,* 588**,** 939-51.

PRISTERA, A., LIN, W., KAUFMANN, A. K., BRIMBLECOMBE, K. R., THRELFELL, S., DODSON, P. D., MAGILL, P. J., FERNANDES, C., CRAGG, S. J. & ANG, S. L. 2015. Transcription factors FOXA1 and FOXA2 maintain dopaminergic neuronal properties and control feeding behavior in adult mice. *Proc Natl Acad Sci U S A,* 112**,** E4929-38.

QIU, J., FANG, Y., RONNEKLEIV, O. K. & KELLY, M. J. 2010. Leptin excites proopiomelanocortin neurons via activation of TRPC channels. *J Neurosci,* 30**,** 1560-5.

QIU, J., ZHANG, C., BORGQUIST, A., NESTOR, C. C., SMITH, A. W., BOSCH, M. A., KU, S., WAGNER, E. J., RONNEKLEIV, O. K. & KELLY, M. J. 2014. Insulin excites anorexigenic proopiomelanocortin neurons via activation of canonical transient receptor potential channels. *Cell Metab,* 19**,** 682-93.

RAMAN, I. M., GUSTAFSON, A. E. & PADGETT, D. 2000. Ionic currents and spontaneous firing in neurons isolated from the cerebellar nuclei. *J Neurosci,* 20**,** 9004-16.

RETHELYI, M. 1984. Diffusional barrier around the hypothalamic arcuate nucleus in the rat. *Brain Res,* 307**,** 355-8.

ROSSI, M., KIM, M. S., MORGAN, D. G., SMALL, C. J., EDWARDS, C. M., SUNTER, D., ABUSNANA, S., GOLDSTONE, A. P., RUSSELL, S. H., STANLEY, S. A., SMITH, D. M., YAGALOFF, K., GHATEI, M. A. & BLOOM, S. R. 1998. A C-terminal fragment of Agouti-related protein increases feeding and antagonizes the effect of alpha-melanocyte stimulating hormone in vivo. *Endocrinology,* 139**,** 4428-31.

SAEB-PARSY, K., LOMBARDELLI, S., KHAN, F. Z., MCDOWALL, K., AU-YONG, I. T. & DYBALL, R. E. 2000. Neural connections of hypothalamic neuroendocrine nuclei in the rat. *J Neuroendocrinol,* 12**,** 635-48.

SAKHI, K., BELLE, M. D., GOSSAN, N., DELAGRANGE, P. & PIGGINS, H. D. 2014a. Daily variation in the electrophysiological activity of mouse medial habenula neurones. *J Physiol,* 592**,** 587-603.

SAKHI, K., WEGNER, S., BELLE, M. D., HOWARTH, M., DELAGRANGE, P., BROWN, T. M. & PIGGINS, H. D. 2014b. Intrinsic and extrinsic cues regulate the daily profile of mouse lateral habenula neuronal activity. *J Physiol,* 592**,** 5025-45.

SCHWARTZ, M. W., WOODS, S. C., PORTE, D., JR., SEELEY, R. J. & BASKIN, D. G. 2000. Central nervous system control of food intake. *Nature,* 404**,** 661-71.

SCOTT, F. F., BELLE, M. D., DELAGRANGE, P. & PIGGINS, H. D. 2010. Electrophysiological effects of melatonin on mouse Per1 and non-Per1 suprachiasmatic nuclei neurones in vitro. *J Neuroendocrinol,* 22**,** 1148-56.

SHIEH, K. R., YANG, S. C., LU, X. Y., AKIL, H. & WATSON, S. J. 2005. Diurnal rhythmic expression of the rhythm-related genes, rPeriod1, rPeriod2, and rClock, in the rat brain. *J Biomed Sci,* 12**,** 209-17.

SHUTO, Y., SHIBASAKI, T., OTAGIRI, A., KURIYAMA, H., OHATA, H., TAMURA, H., KAMEGAI, J., SUGIHARA, H., OIKAWA, S. & WAKABAYASHI, I. 2002. Hypothalamic growth hormone secretagogue receptor regulates growth hormone secretion, feeding, and adiposity. *J Clin Invest,* 109**,** 1429-36.

SPANSWICK, D., SMITH, M. A., GROPPI, V. E., LOGAN, S. D. & ASHFORD, M. L. 1997. Leptin inhibits hypothalamic neurons by activation of ATP-sensitive potassium channels. *Nature,* 390**,** 521-5.

SPANSWICK, D., SMITH, M. A., MIRSHAMSI, S., ROUTH, V. H. & ASHFORD, M. L. 2000. Insulin activates ATP-sensitive K+ channels in hypothalamic neurons of lean, but not obese rats. *Nat Neurosci,* 3**,** 757-8.

TAKAHASHI, K. A. & CONE, R. D. 2005. Fasting induces a large, leptin-dependent increase in the intrinsic action potential frequency of orexigenic arcuate nucleus neuropeptide Y/Agouti-related protein neurons. *Endocrinology,* 146**,** 1043-7.

VAN DEN POL, A. N., YAO, Y., FU, L. Y., FOO, K., HUANG, H., COPPARI, R., LOWELL, B. B. & BROBERGER, C. 2009. Neuromedin B and gastrin-releasing peptide excite arcuate nucleus neuropeptide Y neurons in a novel transgenic mouse expressing strong Renilla green fluorescent protein in NPY neurons. *J Neurosci,* 29**,** 4622-39.

VAN DEN TOP, M., LEE, K., WHYMENT, A. D., BLANKS, A. M. & SPANSWICK, D. 2004. Orexigen-sensitive NPY/AgRP pacemaker neurons in the hypothalamic arcuate nucleus. *Nat Neurosci,* 7**,** 493-4.

VAN DEN TOP, M. & SPANSWICK, D. 2006. Integration of metabolic stimuli in the hypothalamic arcuate nucleus. *Prog Brain Res,* 153**,** 141-54.

VAN OOSTERHOUT, F., LUCASSEN, E. A., HOUBEN, T., VANDERLEEST, H. T., ANTLE, M. C. & MEIJER, J. H. 2012. Amplitude of the SCN clock enhanced by the behavioral activity rhythm. *PLoS One,* 7**,** e39693.

VITATERNA, M. H., KING, D. P., CHANG, A. M., KORNHAUSER, J. M., LOWREY, P. L., MCDONALD, J. D., DOVE, W. F., PINTO, L. H., TUREK, F. W. & TAKAHASHI, J. S. 1994. Mutagenesis and mapping of a mouse gene, Clock, essential for circadian behavior. *Science,* 264**,** 719-25.

VONG, L., YE, C., YANG, Z., CHOI, B., CHUA, S., JR. & LOWELL, B. B. 2011. Leptin action on GABAergic neurons prevents obesity and reduces inhibitory tone to POMC neurons. *Neuron,* 71**,** 142-54.

WANG, T. A., YU, Y. V., GOVINDAIAH, G., YE, X., ARTINIAN, L., COLEMAN, T. P., SWEEDLER, J. V., COX, C. L. & GILLETTE, M. U. 2012. Circadian rhythm of redox state regulates excitability in suprachiasmatic nucleus neurons. *Science,* 337**,** 839-42.

WEBB, A. B., ANGELO, N., HUETTNER, J. E. & HERZOG, E. D. 2009. Intrinsic, nondeterministic circadian rhythm generation in identified mammalian neurons. *Proc Natl Acad Sci U S A,* 106**,** 16493-8.

WELSH, D. K., LOGOTHETIS, D. E., MEISTER, M. & REPPERT, S. M. 1995. Individual neurons dissociated from rat suprachiasmatic nucleus express independently phased circadian firing rhythms. *Neuron,* 14**,** 697-706.

WIATER, M. F., MUKHERJEE, S., LI, A. J., DINH, T. T., ROONEY, E. M., SIMASKO, S. M. & RITTER, S. 2011. Circadian integration of sleep-wake and feeding requires NPY receptor-expressing neurons in the mediobasal hypothalamus. *Am J Physiol Regul Integr Comp Physiol,* 301**,** R1569-83.

WILLESEN, M. G., KRISTENSEN, P. & ROMER, J. 1999. Co-localization of growth hormone secretagogue receptor and NPY mRNA in the arcuate nucleus of the rat. *Neuroendocrinology,* 70**,** 306-16.

WOODS, S. C., SEELEY, R. J., PORTE, D., JR. & SCHWARTZ, M. W. 1998. Signals that regulate food intake and energy homeostasis. *Science,* 280**,** 1378-83.

YOUNG, E. D., ROBERT, J. M. & SHOFNER, W. P. 1988. Regularity and latency of units in ventral cochlear nucleus: implications for unit classification and generation of response properties. *J Neurophysiol,* 60**,** 1-29.

ZHAN, C., ZHOU, J., FENG, Q., ZHANG, J. E., LIN, S., BAO, J., WU, P. & LUO, M. 2013. Acute and long-term suppression of feeding behavior by POMC neurons in the brainstem and hypothalamus, respectively. *J Neurosci,* 33**,** 3624-32.

ZHANG, X. & VAN DEN POL, A. N. 2015. Dopamine/Tyrosine Hydroxylase Neurons of the Hypothalamic Arcuate Nucleus Release GABA, Communicate with Dopaminergic and Other Arcuate Neurons, and Respond to Dynorphin, Met-Enkephalin, and Oxytocin. *J Neurosci,* 35**,** 14966-82.

ZHANG, X. & VAN DEN POL, A. N. 2016. Hypothalamic arcuate nucleus tyrosine hydroxylase neurons play orexigenic role in energy homeostasis. *Nat Neurosci,* 19**,** 1341-7.

Chapter 2

A local clockwork in ARC neurons drives daily changes in excitability

A local clockwork in ARC neurons drives daily changes in excitability

Introduction

The circadian system is an organised hierarchy in which complex rhythms in behaviour and physiology arise from coordinated network activity, and at its most simple denomination, single cell molecular rhythms (Ko and Takahashi, 2006, Balsalobre et al., 2000, Buhr and Takahashi, 2013, Freeman et al., 2013). The circadian molecular clockwork is found ubiquitously throughout cells in the mouse and is made up of genes which form a transcription-translation feedback loop (TTFL, Panda et al., 2002). Following the discovery of *Period* in drosophila (Konopka and Benzer, 1971), the first mammalian core clock gene, *Circadian Locomotor Output Cycle Kaput* (*Clock)* was isolated (Vitaterna et al., 1994). The discovery of *Clock* led to the isolation of a *Bmal1,* the protein form of which forms a heterodimer with CLOCK (Bunger et al., 2000, Gekakis et al., 1998). The CLOCK-BMAL1 complex, also referred to as the positive element of the primary TTFL loop, upregulates mammalian homologues *Per1,2,3* and *Cryptochrome 1* and *2* (*Cry1*/*Cry2*) as well as a number of other clock-controlled genes (Bae et al., 2001, Ko and Takahashi, 2006, Yoo et al., 2005).

At least one form of the primary loop negative elements *Per* and *Cry* are essential for robust behavioural and molecular rhythms (Bae et al., 2001, Zheng et al., 1999). The transcriptional activity of CLOCK/BMAL1 is inhibited by the PER-CRY complex before it reinitiates the TTFL (Sato et al., 2006, Griffin et al., 1999, Balsalobre et al., 2000). CLOCK-BMAL1 dimers also bind to E-box elements to mediate a secondary loop comprising *Rev-erbα/β* and *Rorα/β,* which down-regulate and promote the expression of *Bmal1* respectively (Guillaumond et al., 2005, Preitner et al., 2002, Cho et al., 2012). The autoregulatory cycling of the above components takes ~24h to complete and constitute a circadian molecular clock which imparts a timekeeping signal to cells and tissues by regulating a myriad of downstream clock-controlled genes.

The role of cryptochromes in circadian rhythm generation

Cryptochromes were first discovered in *Arabidopsis* where a mutation resulting in a deficiency in blue light signalling was shown to be located in a gene encoding a photolyase-like protein (Ahmad and Cashmore, 1993). Cryptochromes perform a range of functions in plants including entrainment of circadian rhythms (Cashmore, 2003). In drosophila and mammals, cryptochromes also function as an essential component of the molecular clock (Reppert and Weaver, 2002, van der Horst et al., 1999). However, loss of *Cry1* and *Cry2* in double null-mutant mice does not interfere with normal development and overall health (van der Horst et al., 1999, Kettner et al., 2015). Circadian wheel-running behaviour of *Cry*-knockout mice under a normal light/dark (LD) cycle resembles that of wild-type mice. These mice display a 24h rhythm under LD conditions, suggesting that even without CRY1 and CRY2, light input is sufficient to drive daily rhythms in locomotor activity (van der Horst et al., 1999).

Masking behaviour under LD conditions also occurs when shifted to a different regime for example a short-day lighting paradigm (6h:18h LD). $Cry1^{-/-}Cry2^{-/-}$ rapidly adapt to the new schedule and immediately become active in the dark period and extend fragmented activity across its entirety. Notably, the suppression of locomotor activity by light is a distinct process from the effect of light on phase-shifting of circadian rhythms. The lack of internal timekeeping mechanism becomes clear when $Cry1^{-/-}Cry2^{-/-}$ are presented with a period of constant darkness (DD), in which they exhibit arrhythmic behaviour which is distributed across the projected day and night cycle (van der Horst et al., 1999).

Tissue-specific differences in the molecular clockwork

Several studies have determined that the circadian clock is cell-autonomous and self-sufficient not only in the SCN but also in a number of other brain regions and peripheral tissues (Yoo et al., 2004, Balsalobre et al., 2000, Nagoshi et al., 2004, Brown et al., 2005, Guilding and Piggins, 2007, Mukherji et al., 2015). Peripheral tissue clocks can sustain rhythmicity when isolated from the SCN, although the phase of molecular clock rhythms are coordinated by SCN-derived output signals (Yoo et al., 2004). This finding has led to increasing interest in understanding the circadian mechanisms in independent central and

peripheral oscillators. What is clear is that the specific contribution of each core clock gene varies in a tissue-specific manner. For example, *Clock* mRNA is constitutively expressed in the SCN, but cycles in peripheral tissues (Lowrey and Takahashi, 2004). Further, *Rorα* and *β* exhibit strong rhythmicity in the SCN but only exhibit a weak oscillation in peripheral tissues (Sato et al., 2004, Akashi and Takumi, 2005, Guillaumond et al., 2005).

Genetic or physiological circadian disruption is associated with obesity and metabolic disorders in both rodents and humans, implicating the circadian system in maintaining appropriate body weight (Evans and Davidson, 2013, Zhang et al., 2013, Foster et al., 2013). However, no single mutant mouse model is able to recapitulate circadian disruption in Humans. Under 24h LD conditions, *Per1/2* mutants are significantly heavier, but *Cry1*$^{-/-}$*Cry2*$^{-/-}$ display a dramatically reduced body weight compared to wild-type animals (Kettner et al., 2015). The body weight of transgenic *Bmal1*$^{-/-}$ mice is similar to wild-type controls until 12weeks age then gradually decreases (Kettner et al., 2015, Bunger et al., 2005, Kondratov et al., 2006). Therefore clock gene mutants display divergence in energy homeostasis phenotypes. These studies suggest that tissues responsible for regulating appetite and energy expenditure homeostasis may differentially express core clock genes.

A number of brain regions display rhythms in *Per* when isolated explants are assessed with a bioluminescent reporter of clock activity (Abe et al., 2002). For example, autonomous and self-sustained rhythms in PERIOD2::LUCIFERASE are observed in the arcuate nucleus of the hypothalamus (ARC). These rhythms can be resolved to single cells and continue for 3-4 days in culture (Guilding et al., 2009). Such rhythms are also evident in the lateral and medial habenula (LHb/MHb) and are accompanied by rhythmic changes in neuronal excitability (Sakhi et al., 2014a, Sakhi et al., 2014b). It is well established that clock neurons in the SCN display rhythmic membrane excitability and firing rate, however while the link between genetic and electrophysiological rhythms likely result from regulation of many ion conductances, the exact mechanisms are unclear (Kuhlman and McMahon, 2004, Wang et al., 2012, Colwell, 2011). Given that molecular clock components operate in a tissue-specific manner, it is likely that the relationship between clock gene and neuronal excitability differs depending on the brain region.

Using Cre-Lox recombination for location-specific molecular clock disruption

Extra-SCN clocks oscillate within areas of the brain that play well-established roles in physiology and behaviour for example in ARC, an area which plays an critical function in appetite homeostasis (Meister et al., 1989, Dailey and Bartness, 2010, Bugarith et al., 2005). The influence of the molecular clock in ARC on the excitability of ARC neurons and on feeding and appetite regulation is currently unknown. *Cry1*$^{-/-}$*Cry2*$^{-/-}$ mice are useful tools for determining how the absence of a functional molecular clockwork influences physiological processes under a number of different light conditions (Van der Zee et al., 2008, Oishi et al., 2003, Kettner et al., 2015). However, the development of tools to target molecular clock components in a constrained physical area of the brain is a powerful advance in circadian biology. Such tools are particularly useful for determining the functional relevance of a local circadian clock in a single brain region, which is not possible by use of a global knockout model.

The Cre-Lox recombination-mediated neurogenetics has emerged as one of the most versatile and powerful technologies for cell-specific gene knockout as well as an array of other applications including neural pathway tracing, optogenetics and monitoring of neuronal activity (McHugh et al., 1996, Tsien et al., 1996, Madisen et al., 2010, Rogan and Roth, 2011, Tian et al., 2009, Beier et al., 2015). In ARC, Cre-Lox technology combined with optogenetic and chemogenetic tools have been instrumental in unravelling the neural circuitry mediating food intake (Kong et al., 2012, Aponte et al., 2011, Atasoy et al., 2012, Krashes et al., 2011). This technology can also be implemented to study the inner workings of the circadian system by modulating the speed of the molecular clock or by deleting clock components in a tissue-specific manner (Smyllie et al., 2016, Mieda and Sakurai, 2011, Lamia et al., 2008, Storch et al., 2007). Thus this approach represents a powerful and important method for probing the ARC local molecular clockwork to investigate potential function related to appetite and feeding regulation.

Aims and objectives

The primary aim of this chapter is to determine whether daily changes in ARC neuronal excitability are driven by the circadian clock and not by external environmental factors. To address this question we adopted an electrophysiological approach and performed whole-cell recordings from *Cry*-deficient mice. We investigated whether this global disruption of the molecular clock in all cells and tissues altered electrophysiological rhythms observed in wild-type ARC neurons. We also investigated whether rhythms were generated intrinsically to ARC or externally from another rhythmic brain region in the slice. To assess this we adopted a targeted approach. Injections of Cre-dependent recombinant adeno-associated virus (rAAV)2 were made into the ARC of *Bmal1*$^{fl/fl}$ mice to evaluate whether targeted ablation of the core molecular clock component influenced the temporal aspects of ARC neuronal excitability. Further, rAAV2-Cre injected mice were screened for alterations in food and water intake compared to controls. We also investigated the effect of the light schedule on rhythms in ARC excitability by performed recordings during the subjective day and night. We hypothesised that rhythms persist in constant dark (DD) due to being driven by an internal clockwork.

Methods

Animal housing

Male *Cry1*$^{+/+}$*Cry2*$^{+/+}$ and *Cry1*$^{-/-}$*Cry2*$^{-/-}$ mice were group-housed prior to experiments under a 12/12h LD cycle. The housing area was maintained at a constant temperature (20 ± 2 °C) and humidity (~40%), and animals had *ad libitum* access to food and water. These mice were bred from *Cry1*$^{+/-}$*Cry2*$^{+/-}$ mice kindly provided by Prof. Bert van der Horst, Erasmus Medical Center, Rotterdam, NL. Double knockout *Cry1*$^{-/-}$*Cry2*$^{-/-}$ mice lack the capacity to generate autonomous cellular rhythms therefore can be used to screen whether daily variations in physiology depend on an intact molecular clockwork (van der Horst et al., 1999). All *Cry1*$^{+/+}$*Cry2*$^{+/+}$ or *Cry1*$^{-/-}$*Cry2*$^{-/-}$ mice used for electrophysiological experiments were 10-18 weeks old and were weighed prior to brain extraction (22-28g).

Male *Bmal1*$^{fl/fl}$ mice (7-10 weeks old, 23-28g body weight) were group-housed in controlled light cabinets under a 12/12 LD cycle before surgical procedures were performed. These mice were generated from breeding pairs initially provided by Prof. C. Weitz, Harvard Medical School, Boston, Ma, USA.

Whole-cell Electrophysiology

Brains were harvested at ZT1 for daytime recordings (ZT4-10) or ZT11 for night recordings (ZT14-20). A subgroup of *Cry1*$^{+/+}$*Cry2*$^{+/+}$ and *Cry1*$^{-/-}$*Cry2*$^{-/-}$ mice were transferred to constant darkness (DD) for 72h to assess the effect of the light-dark cycle on electrophysiological rhythms in the ARC. For recordings performed on mice from DD during the subjective day or night, CT12 was defined as the onset of wheel-running activity. Cull and recording epochs were aligned based on the average free-running period of *Cry1*$^{+/+}$*Cry2*$^{+/+}$ mice.

After decapitation, brains were extracted and placed in cutting solution containing (in mM): 0.5 NaCl, 1.8 KCl, 1.2 KH_2PO_4, 7 $MgSO_4$, 26 $NaHCO_3$, 15 Glucose and 50 Sucrose (300-310 mosmol^{-1}; pregassed with 95% O_2/ 5% CO_2). 300μm thick coronal slices containing ARC were prepared using a vibroslicer (Campden Instruments, Loughborough, UK) and transferred into an incubation chamber filled with cutting solution to rest at room temperature. Slices were then transferred to aCSF, comprising of (in mM): 127 NaCl, 1.8 KCl, 1.2 KH_2PO_4, 1.3 $MgSO_4$, 26 $NaHCO_3$, 15 Glucose and 2.4 $CaCl_2$. Slices for all electrophysiology recordings were selected based on rostrocaudal position using Paxinos and Franklin's mouse brain atlas. Hypothalamic slices containing ARC, DMH and VMH at the level of -1.7 to -1.9mm bregma were used for whole-cell recording.

Pipettes (7-10MΩ) were backfilled with intracellular solution containing (in mM): 130 K-gluconate, 10 KCl, 2mM $MgCl_2$, 10 Hepes, 0.5 EGTA, 2 K_2ATP and 0.5 NaGTP (Belle et al., 2009). Visually-guided whole-cell recordings were performed in slices from *Cry1*$^{+/+}$*Cry2*$^{+/+}$ and *Cry1*$^{-/-}$*Cry2*$^{-/-}$ mice. Cells in medial or lateral areas of ARC were visually targeted and later confirmed by biocytin immunostaining.

An npi BA-03X amplifier in bridge configuration (npi electronics, Tamm, Germany), compensating for the transient capacitance of the pipette, and a CED 1401 mark II A/D

data acquisition interface (Cambridge Electronic Design, Cambridge, United Kingdom) were used to record current clamp data. All recording signals were sampled at a frequency of 30 kHz in Spike 2 Version 7 (Cambridge Electronic Design). Membrane parameters (RMP, R_{input} and SFR) were extracted from a 60s baseline file segment (and current pulses) and stored in Excel 2010 (Microsoft, Wa, USA). Genotype and time of day effects and possible interactions were evaluated by two-way ANOVA with planned single degree of freedom contrasts in JMP v11 (SAS, NC, USA). Fisher's exact-tests were used to analyse electrical state proportionality.

Locomotor, feeding and drinking behavioural characterisation

To assess circadian patterns of locomotor activity, *Cry1*$^{+/+}$*Cry2*$^{+/+}$ and *Cry1*$^{-/-}$*Cry2*$^{-/-}$ mice were singly-housed in cages equipped with a running wheel and drinking bottle and food hopper which hung from precision balances to monitor activity and food and drink consumption (TSE systems, Bad Homburg, Germany). Data was collected at 10min bin intervals and with a high sensitivity to small negative changes in food (0.01g) and water (0.01ml) intake. When housed in these cages mice had *ad libitum* access to a standard lab chow diet: 5/20/75% calories from fat, protein and carbohydrates. A 2-day acclimatisation period was used before test data was collected to ensure that the mice had learnt how to use the drinking bottles.

Wheel-running activity, feeding and drinking was monitored for a minimum of 8days in entrained LD conditions before the lights were switched off and free-running behaviour was monitored in constant darkness for a further 10days. Lights were then returned to LD. All activities were recorded using Phenomaster (TSE systems). Circadian behavioural phenotypes were analysed and actograms and chi-squared periodograms were constructed using the ClockLab plugin (Actimetrics, IL, USA) for Matlab 2014 (MathWorks, MA, USA). Images obtained were analysed in ImageJ.

An identical cage configuration and lighting paradigm to that described above was used to assess behavioural patterns of *Bmal1*$^{fl/fl}$ mice following viral targeting of the core molecular clockwork in ARC. For these experiments, running wheels were not fitted to the cages. Drinking and feeding activities were recorded using Phenomaster (TSE systems).

Average food and water intake during the light and dark phase (or subjective day versus subjective night in DD) were statistically compared by repeated measures ANOVA performed in Origin version 9 (OriginLab Corporation, Ma, USA). Food and water intake in 1h bins was also analysed to examine temporal patterns in feeding and drinking across the LD cycle. All data was adjusted to each animal's body weight to account for fluctuations due to differences in individual energy demands. Meal frequency was calculated from 10min bins in which food consumption exceeded >0.05g. All data for comparisons was averaged over a minimum of 5days from LD or DD.

Viral vector injections

Male *Bmal1*$^{fl/fl}$ mice (7-10 weeks old) were group housed under LD conditions prior to surgical procedures. All procedures were carried out in accordance with the UK Animals (Scientific Procedures) Act of 1986 using procedures approved by The University of Manchester Review Ethics Panel. Mice were anaesthetised with isoflurane and placed into a stereotaxic frame apparatus integrated into a Neurostar drill and injection robot (Neurostar, Tubingen, Germany). The animals incisors were placed over a bite bat and ear bars were used to ensure that the head remained in a fixed position throughout the procedure. Anaesthesia was maintained by isoflurane through a nose cone.

The Neurostar robot allows motorised, computer controlled positioning of a drill bit and injection needle in the X,Y and Z axis ensuring precise and replicable viral injections. We made injections of premade recombinant rAAV2-Cre-GFP or control rAAV2-GFP (~1E+12 VG/mL; SignaGen Laboratories, MD, USA). Injection needles back-filled with mineral oil and then an excess of rAAV2-Cre-GFP or rAAV2-GFP were loaded into the injection device, which was controlled by Injectomate software (Neurostar).

A sterile scalpel blade was used to make an incision along the rostrocaudal axis to expose bregma and lambda skull landmarks. The robot drill and injection needle were then given reference to these landmarks and a series of tilt and scaling steps were performed. To maximise the likelihood of successful bilateral virus injection into the ARC, we made 2 injections of 70nl either side of the 3rd ventricle at bregma -1.7mm followed by 2 more at bregma -1.9mm. After a 2-week recovery period, mice were then single-housed and behaviour was screened using the TSE system.

Multielectrode array Electrophysiology

Perforated multielectrode array (pMEA) recordings were performed during the day (ZT5-8) on slices harvested at ZT1 from viral vector injected *Bmal1*$^{fl/fl}$ mice following behavioural assessments (~30 days). Slice preparation procedure and cutting solution/aCSF composition used for pMEA experiments was identical to that outlined previously except aCSF was heated to 33°C for the final stage of slice incubation.

A dual-MEA2100-HS2x60 head-stage system in conjunction with a MEA2100 interface board (Multichannel systems, Reutlingen, Germany) was used to record extracellular multiunit spiking activity (MUA). This device integrates data from 120 pMEA recording electrodes (60 per chamber). pMEAs with titanium nitride electrodes (30µm diameter, 200µm spacing) arranged in an 8x8 grid (60pMEA200/30iR-Ti-gr, Multichannel systems). Slices were placed with care and photos were taken throughout the course of the experiment to ensure that the electrodes were consistently placed anatomically between slices. The recording surface for pMEA experiments was typically -1.8mm from bregma. Negative pressure was created by a vacuum pump connected to a lower perfusion chamber to hold the slice in close contact with the recording electrodes.

ACSF was maintained at 33°C in a water bath and boosted on transit to the pMEA slice chamber with a TC02 temperature controller (Multichannel systems). Bath application of tetrodotoxin (TTX) at the end of each recording session was performed to ensure a suitable spike detection threshold was used (Tocris Bioscience, Bristol, UK).

Raw data signals were acquired at 25kHz using MC rack software (Multichannel systems) and saved as 10min files due to the large individual file size (>1.5gb per 10min). Subsequently files were merged chronologically and a 300Hz high-pass filter was applied to the raw data signals. Spikes were then discriminated from the raw data using a thresholding tool. Based on the typical noise of the recordings after the application of TTX, a threshold of -15.5µV was used to discriminate spikes for all recordings.

Spikes were imported into Neuroexplorer and binned into 30min segments for further analysis. A minimum of an hour within the 3h day epoch (ZT5-8) was used for analysis of average MUA. Two-sample t-tests were performed on pMEA MUA data in Origin 9.0

(OriginLab Corporation, Ma, USA). A 1min section of the raw MC rack data was imported into offline sorter v4 (Plexon Inc., TX, USA). Using this software, principal component-based sorting was used to discriminate single units, identifiable as an isolated cluster of spikes in principal component space. Data from each electrode channel was sorted manually to ensure that all single-unit signals were accurately discriminated. The spike sorted data was then exported to Neuroexplorer for further analysis and Origin 9.0 for statistical comparisons.

Immunohistochemistry

Brain slices used for whole-cell electrophysiological recording were post-fixed in ice-cold 4% paraformaldehyde in 0.1M PBS (pH 7.4). After 24h the slices were transferred to 0.1M PBS alone. Within 3 days, the slices were then washed with PBS and incubated in Triton-X 100 (0.6% in PBS;10% normal donkey serum) for 3h at room temperature. Slices were then transferred to a solution containing Cy3-conjugated Extravidin (1:250 in PBS, Sigma-Aldrich, MO, USA) and rabbit anti-GFP primary antibody (1:1000, Abcam, Cambridge, UK) in PBS, 2% NDS and 0.3% Triton-X 100 and incubated at 4°C in darkness for 1-3 days.

Slices were then transferred to a secondary antibody solution containing a fluorescein conjugated anti-rabbit antibody (Jackson ImmunoResearch, USA) diluted 1:800 in PBS and incubated at 4°C overnight. Slices recorded on pMEAs from rAAV2-Cre-GFP injected animals were screened for reconstruction of the site of virus microinjection using the same protocol as above except Cy3-conjugated Extravidin was not added to the primary antibody solution. Images from all slices in this chapter were captured on an Olympus BX51 microscope equipped with a DP71 camera in conjunction with a U-RFLT light source (Olympus Corporation, Tokyo, Japan). Confocal imaging was not used in this chapter due to the large number of slices collected from electrophysiological experiments.

Results

Cry1$^{-/-}$*Cry2*$^{-/-}$ animals are active during the dark phase under a 12:12h LD cycle and arrhythmic in DD

To characterise the *Cry1*$^{+/+}$*Cry2*$^{+/+}$ and *Cry1*$^{-/-}$*Cry2*$^{-/-}$ circadian behavioural phenotype, mice were singly-housed in specialised cages equipped with running wheels, food and drink hoppers for a minimum of 8days under LD conditions. All *Cry1*$^{+/+}$*Cry2*$^{+/+}$ animals (n=3) entrained to the lighting schedule and initiated locomotor activity at the onset of the dark phase (Fig1A,C). When the lights in the animal housing area were switched to constant darkness (DD), *Cry1*$^{+/+}$*Cry2*$^{+/+}$ mice free-ran with a period of 28.3h (Fig1A,D). On return to LD conditions, *Cry1*$^{+/+}$*Cry2*$^{+/+}$ mice re-entrained for the remainder of the experiment. In mice lacking *Cry1* and *Cry1 (Cry1*$^{-/-}$*Cry2*$^{-/-}$*),* which as a result have a dysfunctional molecular clockwork*,* wheel running activity follows a similar pattern to their wild-type counterparts with activity being almost exclusively retained within the dark phase (Period of 24h, Fig1B,E). However, in DD *Cry1*$^{-/-}$*Cry2*$^{-/-}$ mice (n=4) became immediately circadianly arrhythmic, displaying disorganised wheel-running activity across the subjective day-night (Fig1F).

In LD conditions *Cry1*$^{+/+}$*Cry2*$^{+/+}$ mice consumed most of their food and water during the dark phase (78.6% and 83.7% respectively, Fig2A,C). Feeding and drinking data recorded under DD conditions was aligned respective to the free-running tau of each individual *Cry1*$^{+/+}$*Cry2*$^{+/+}$ animal. *Cry1*$^{+/+}$*Cry2*$^{+/+}$ mice consumed 71.8% and 79.4% (total average) of their food and water intake during the subjective night respectively (defined as CT12-24, CT12 onset of wheel-running). Thus, feeding and drinking activity broadly follows the pattern of wheel-running activity in *Cry1*$^{+/+}$*Cry2*$^{+/+}$ mice which restrict most of their activity to the night and subjective night compared to the day or subjective day.

Light has a dominant effect on the pattern of feeding and drinking in *Cry1*$^{-/-}$*Cry2*$^{-/-}$ mice which display rhythmically partitioned feeding and drinking behaviour despite possessing a dysfunctional molecular clock. This masking behaviour is characterised by higher food intake during the dark (66.1%) compared to the light phase in *Cry1*$^{-/-}$*Cry2*$^{-/-}$ mice (Fig2B,D). Similarly, drinking behaviour by *Cry1*$^{-/-}$*Cry2*$^{-/-}$ mice occurs more frequently during the night

(68.3%) than day. However, unlike their wild-type counterparts, when placed under DD conditions the temporal pattern of food and drink intake becomes arrhythmic. Feeding and drinking behaviour was circadianly arrhythmic in all *Cry1*$^{-/-}$*Cry2*$^{-/-}$ mice tested (n=4), therefore CT was aligned based on a period of 23.8h.

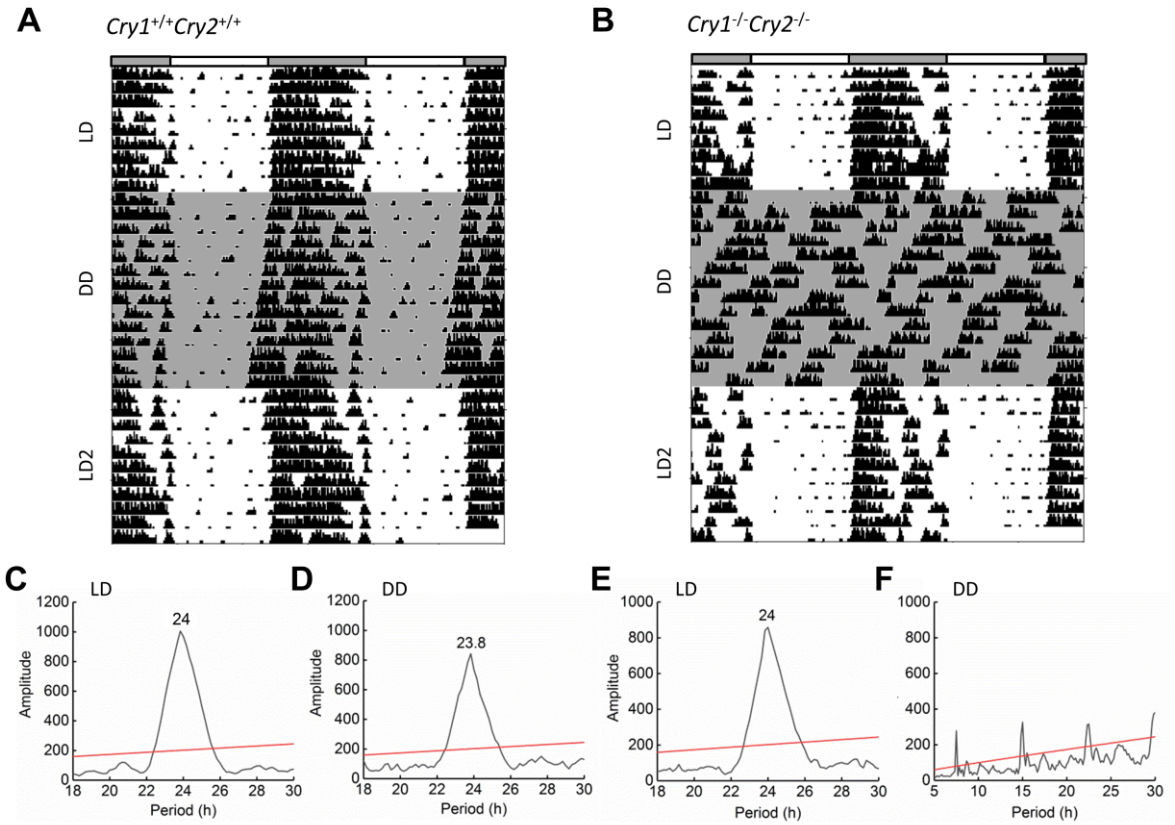

Figure 1: Light masks the defective biological clock in *Cry1*$^{-/-}$*Cry2*$^{-/-}$ mice: A: Representative double-plotted actogram of wheel-running activity (percentile) from a *Cry1*$^{+/+}$*Cry2*$^{+/+}$ animal across a 12/12h Light/Dark (LD) cycle. *Cry1*$^{+/+}$*Cry2*$^{+/+}$ animals entrained to the LD cycle and exhibited wheel-running behaviour almost exclusively within the dark phase. In constant darkness *Cry1*$^{+/+}$*Cry2*$^{+/+}$ mice continued to display rhythmic free-running locomotor activity. **B:** Under the same LD schedule *Cryptochrome* double knockout mice (*Cry1*$^{-/-}$*Cry2*$^{-/-}$) also display a ~24h circadian rhythm in wheel-running activity. However, in DD *Cry1*$^{-/-}$*Cry2*$^{-/-}$ mice immediately become strikingly circadianly arrhythmic. **C,D:** Chi-squared periodogram showing the period of the main rhythmic component of *Cry1*$^{+/+}$*Cry2*$^{+/+}$ wheel-running activity in LD and DD conditions. Mice exhibited a rhythm with a 24h period which shortened to ~23.8h in DD. **E,F:** *Cry1*$^{-/-}$*Cry2*$^{-/-}$ mice displayed rhythmic wheel-running in LD (24h period) but under DD conditions became arrhythmic.

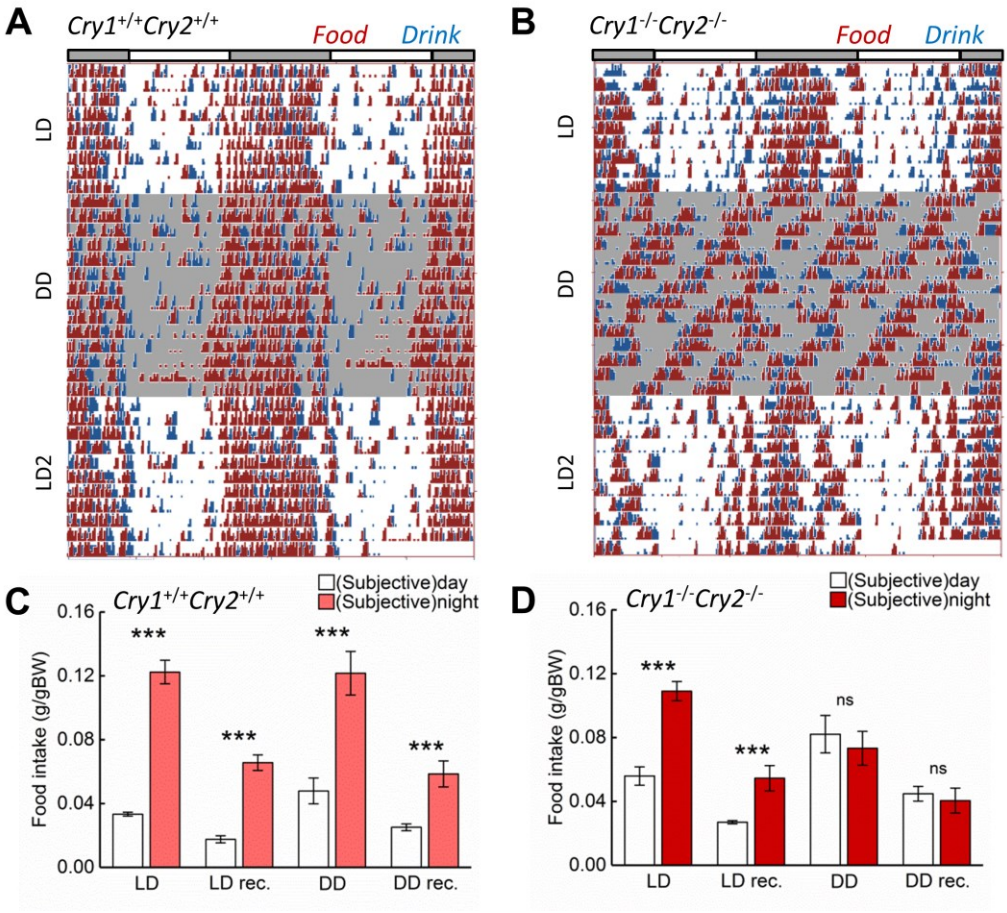

Figure 2: *Cry1*$^{+/+}$*Cry2*$^{+/+}$ and *Cry1*$^{-/-}$*Cry2*$^{-/-}$ mice display daily rhythms in food and water intake. A: Representative actogram from a *Cry1*$^{+/+}$*Cry2*$^{+/+}$ animal showing that both food and water intake is mostly constrained to the dark phase (~75%). Feeding and drinking behaviour exhibited a free-running pattern (period 23.8h) in DD, during which the majority of food/water intake occurred during the subjective night. **B:** In LD, *Cry1*$^{-/-}$*Cry2*$^{-/-}$ animals also exhibit rhythmic food and water intake (~24h period) with the majority of consumption occurring during the dark phase (~65%). In DD, the pattern of food and water intake becomes circadianly arrhythmic. **C:** Quantification of food intake (adjusted to body weight, BW; g/gBW) during the LD cycle and within the recording epochs (LD rec.) used for day and night whole-cell recordings (ZT4-10 and ZT14-20). Food intake was also compared during the subjective night and subjective day, and CT4-10 and CT14-20 (DD rec.). For *Cry1*$^{+/+}$*Cry2*$^{+/+}$ mice, food intake was higher during the (subjective)night phase compared to (subjective)day of all conditions analysed (t-test $p<0.001$). **D:** Food intake was equally distributed in DD conditions in *Cry1*$^{-/-}$*Cry2*$^{-/-}$ animals when aligned to a 23.8h cycle.

ARC neurons recorded from *Cry1*$^{+/+}$*Cry2*$^{+/+}$ and *Cry1*$^{-/-}$*Cry2*$^{-/-}$ slices rest at three distinct electrophysiological states

We performed whole-cell recordings during 6h epochs of the day (ZT4-10) or night (ZT14-20). These epochs did not capture all feeding and drinking activity across the light-dark cycle, however they did overlap with times of low and high food and drink intake (Fig2C) in experiments performed on brain slices from *Cry1*$^{+/+}$*Cry2*$^{+/+}$ mice. Approximately ~50% of all feeding activity during the light or dark phase was captured during ZT4-10 or ZT14-20 respectively for both *Cry1*$^{+/+}$*Cry2*$^{+/+}$ and *Cry1*$^{-/-}$*Cry2*$^{-/-}$ mice (Fig2C).

Cellular oscillators in the SCN exhibit daily changes in electrical behaviour and membrane properties that are observable during whole-cell recording (Belle et al., 2009). We found that untargeted ARC neurons from both *Cry1*$^{+/+}$*Cry2*$^{+/+}$ and *Cry1*$^{-/-}$*Cry2*$^{-/-}$ display three characteristic electrical behaviours similar to those reported in the SCN and in *Per1*-expressing neurons in ARC (see *Results chapter 1*). These behaviours include regular and irregular firing neurons, depolarised silent cells which rest at hyperexcited RMP values and hyperpolarised silent neurons (Fig3). The majority of ARC neurons recorded from either genotype or time period generated APs (~70%).

To investigate whether the proportion of each state is significantly affected by time of day or genotype, we carried out Fisher's exact-tests on pooled data from both mARC and latARC. Whole-cell recordings during the day-night revealed that the proportion of *Cry1*$^{+/+}$*Cry2*$^{+/+}$ or *Cry1*$^{-/-}$*Cry2*$^{-/-}$ neurons in each state (depolarised silent, firing and hyperpolarised silent) did not change between the two epochs (Fisher's, $p>0.5$ for all comparisons, Fig3C,D). No effects of genotype was observed during either time period under LD conditions ($p>0.32$). Similarly, time of day or ablation of the core clock (*Cry1*$^{-/-}$ *Cry2*$^{-/-}$) was not significantly associated with changes in electrical state during the subjective day(CT4-10) or subjective night (CT14-20; $p>0.3$ for all comparisons; Fig3E,F).

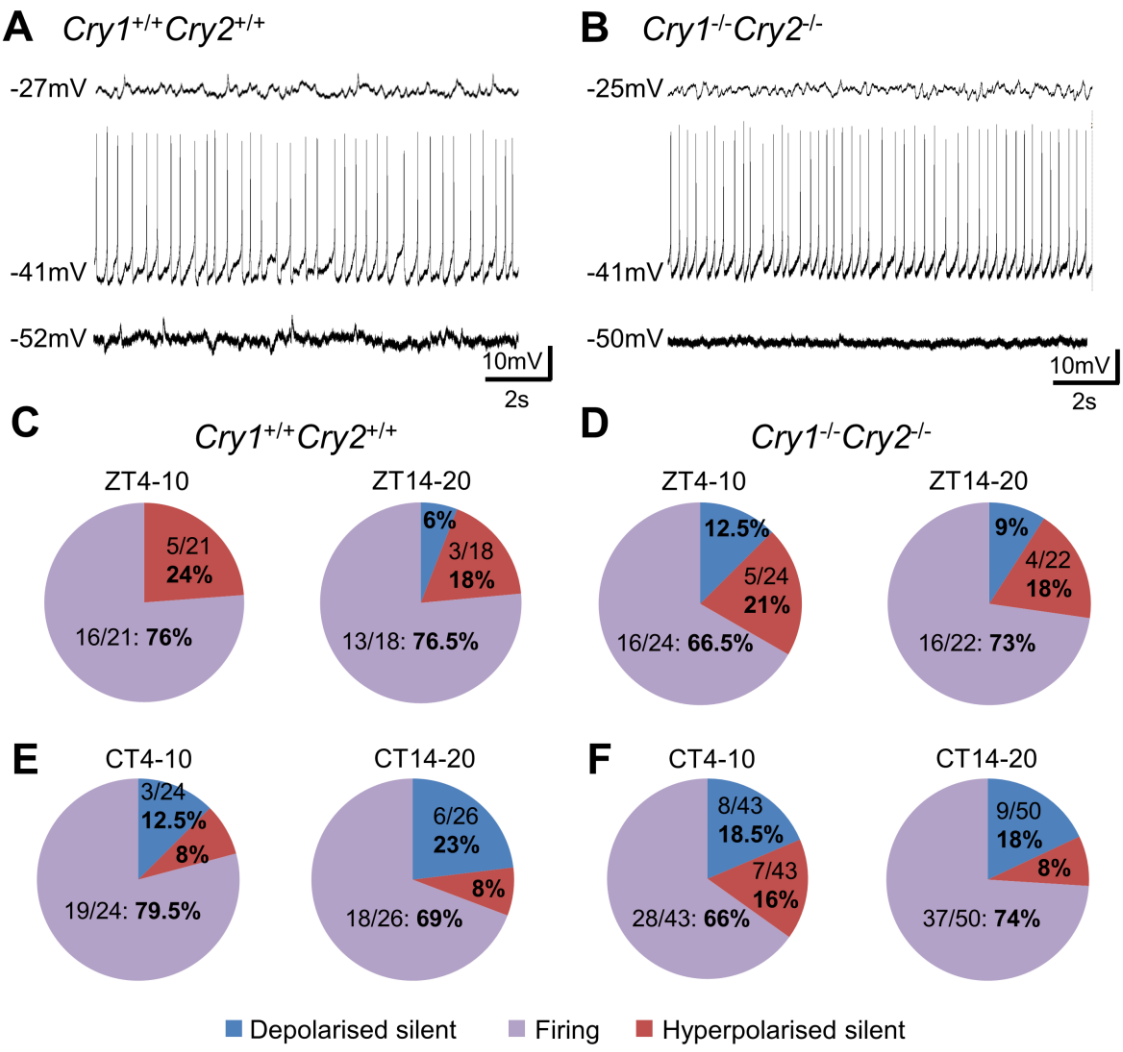

Figure 3: ARC neurons recorded from *Cry1*$^{+/+}$*Cry2*$^{+/+}$ and *Cry1*$^{-/-}$*Cry2*$^{-/-}$slices rest at three distinct electrophysiological states: *Cry1*$^{+/+}$*Cry2*$^{+/+}$ and *Cry1*$^{-/-}$*Cry2*$^{-/-}$ neurons exhibited similar electrical states. **A:** Example traces recorded from depolarised silent, firing (~2Hz) and hyperpolarised silent neurons. **B:** Similar states were observed in *Cry1*$^{-/-}$*Cry2*$^{-/-}$ neurons which displayed depolarised silent, firing (~3.5Hz) and hyperpolarised silent electrical behaviours. **C,D:** The proportion of states during the day(ZT4-10) and night(ZT14-20) did not significantly vary for *Cry1*$^{+/+}$*Cry2*$^{+/+}$ or *Cry1*$^{-/-}$ *Cry2*$^{-/-}$ neurons ($p>0.5$). No effect of genotype was reported under LD conditions ($p>0.32$). **E,F:** Under DD conditions, time (subjective day, CT4-10; subjective night, CT14-20) or genotype did not have a significant effect on the proportion of electrical states displayed by ($p>0.3$).

ARC neurons immediately resumed firing after hyperpolarising current injections or briefly increased firing frequency after the pulse (Fig4A,B). Current pulses can also be used to calculate R_{input} in accordance with Ohms law which generally correspond to relative K+ membrane conductance for a given cell (van den Top et al., 2007). Next we assessed whether the *Cry1*$^{-/-}$*Cry2*$^{-/-}$ mutation influenced the daily temporal expression of

RMP and R_{input}. The data collected during the day(ZT4-10) and night(ZT14-20) was further subdivided to investigate subregion specific effects on RMP and R_{Input} (*Cry1*$^{+/+}$*Cry2*$^{+/+}$ mARC, n=18; *Cry1*$^{-/-}$*Cry2*$^{-/-}$ mARC, n=21). Particular interest was taken in latARC cells (*Cry1*$^{+/+}$*Cry2*$^{+/+}$ mARC, n=21; *Cry1*$^{-/-}$*Cry2*$^{-/-}$ mARC, n=25) as we previously observed that *Per1*-expressing neurons in this area exhibit daily rhythms in SFR (see *Results chapter 1*).

For RMP in latARC neurons under LD conditions, two-way ANOVA revealed a significant effect of genotype ($F_{(1,42)}$ =4.92, p=0.035). A priori single degree of freedom contrasts indicated significant day to night differences in the RMP of latARC *Cry1*$^{+/+}$*Cry2*$^{+/+}$ neurons under LD conditions ($F_{(1,42)}$ =4.24, p=0.046; Fig4C). Such time of day differences in RMP were not detected by single degree of freedom analysis in latARC neurons from *Cry1*$^{-/-}$ *Cry2*$^{-/-}$ slices ($F_{(1,42)}$ =0.24, p=0.12). No significant time of day effect was observed for R_{input} in latARC between the day and night (p=0.28, Fig4D). In mARC no genotype, time or interaction effects on RMP or R_{input} were observed across the day (all p values >0.28, FigE,F).

To establish whether rhythms in RMP depend upon an internal timing mechanism and are not superimposed by external signals, temporal differences in RMP and R_{Input} between the subjective day (CT4-10) and subjective night (CT14-20) were analysed in brain slices prepared from mice in constant dark (DD, Fig4C,F). The total number of neurons recorded from each genotype and ARC subregion are as follows: *Cry1*$^{+/+}$*Cry2*$^{+/+}$ mARC, n=28; *Cry1*$^{-/-}$ *Cry2*$^{-/-}$ mARC, n=60; *Cry1*$^{+/+}$*Cry2*$^{+/+}$ latARC, n=22; *Cry1*$^{-/-}$*Cry2*$^{-/-}$ latARC, n=33. During the subjective day and subjective night, no genotype or time effects on RMP or R_{input} in mARC or latARC were observed (all p>0.17).

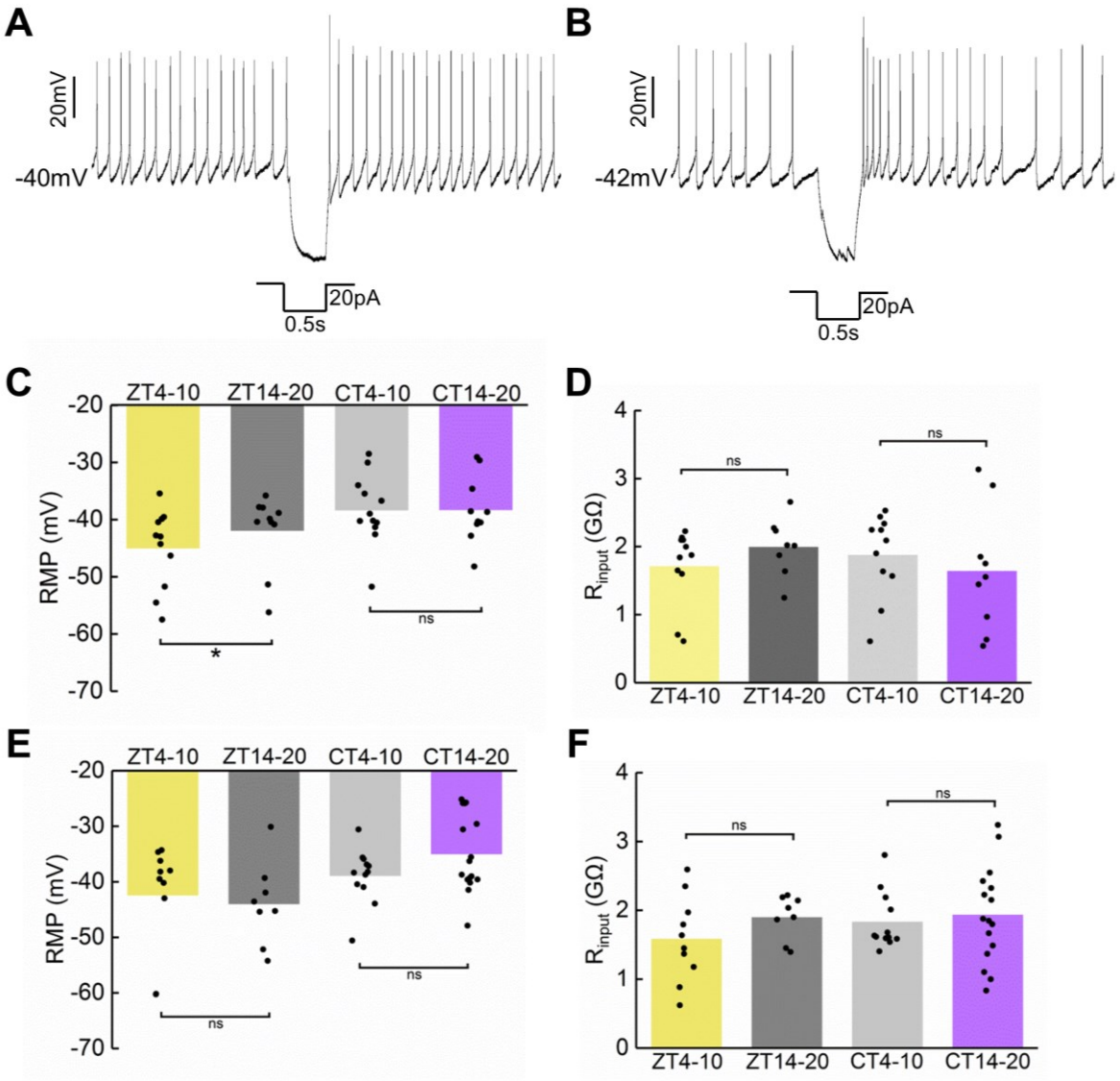

Figure 4: RMP of ARC *Cry1*$^{+/+}$*Cry2*$^{+/+}$ neurons exhibits significant daily variation only in latARC under LD conditions: Temporal changes in key membrane excitability parameters RMP and R_{input} were evaluated by whole-cell recording in latARC and mARC under LD and DD conditions. Individual dots on jitter plots correspond to single neurons **A:** Negative current injection in whole-cell configuration evoked rebound potentials in ARC cells which immediately resumed firing. **B:** Some ARC neurons displayed increased firing during rebound before returning to baseline firing rate. **C:** Interestingly, RMP of *Cry1*$^{+/+}$*Cry2*$^{+/+}$ cells in latARC exhibits a significant day(ZT4-10; -45.03mV, n=11)- night(ZT14-20; -41.95mV, n=10) variation (ANOVA, single degree of freedom contrast; p=0.046). No such variation was detected under DD conditions between CT4-10 (-38.36mV, n=12) and CT14-20 (-38.32mV, n=10, p=0.69). **D:** R_{input} of *Cry1*$^{+/+}$*Cry2*$^{+/+}$ cells in latARC, a measure corresponding to membrane K+ conductance, did not show significant day(1.69GΩ, n=11)- night(1.99GΩ, n=8) variation (p=0.28). Similar to RMP, this measure of intrinsically-regulated neuronal excitability showed no circadian variation between CT4-10 (1.88GΩ, n=11) and CT14-20 (1.64GΩ, n=9, p=0.17). **E:** RMP of *Cry1*$^{+/+}$*Cry2*$^{+/+}$ cells in mARC did not exhibit a significant day(-42.45mV, n=10)- night(-44mV, n=8) variation. Indeed, no such variation was detected between CT4-10 (-38.95mV, n=12) and CT14-20 (-35.03mV, n=16). **F:** R_{input} of *Cry1*$^{+/+}$*Cry2*$^{+/+}$ cells in mARC showed no day(1.58GΩ, n=10)- night(1.90GΩ, n=8) variation. No such variation was detected between CT4-10 (1.83GΩ, n=12) and CT14-20 (1.94GΩ, n=16).

Daily and circadian variation in the firing frequency of ARC neurons depends on an intact molecular clockwork

For analysis of the spontaneous firing activity of ARC neurons, those that displayed depolarised and hyperpolarised silent electrical states were excluded from the analysis as they do not discharge APs. To assess whether daily variations in SFR differ between ARC subregions, we recorded cells in the mARC (*Cry1*$^{+/+}$*Cry2*$^{+/+}$, n=13; *Cry1*$^{-/-}$*Cry2*$^{-/-}$, n=11) and latARC (*Cry1*$^{+/+}$*Cry2*$^{+/+}$, n=16; *Cry1*$^{-/-}$*Cry2*$^{-/-}$, n=21) in brain slices harvested from animals group-housed in a 12/12h LD cycle. Under these conditions in latARC, we detected a significant effect of genotype ($F_{(1,33)}$= 5.78, p=0.023) and genotype X time of day interaction ($F_{(1,38)}$ = 4.76, p=0.037). Planned single degree of freedom contrasts indicated that SFR in the latARC was significantly elevated at night compared to day in *Cry1*$^{+/+}$*Cry2*$^{+/+}$ slices ($F_{(1,33)}$ = 10.31, p=0.003, Fig5A,C). Furthermore, daytime SFR in latARC was significantly different between *Cry1*$^{+/+}$*Cry2*$^{+/+}$ and *Cry1*$^{-/-}$*Cry2*$^{-/-}$ cells ($F_{(1,33)}$= 6.17, p=0.02, Fig5C) and no daily variation was detected in *Cry1*$^{-/-}$*Cry2*$^{-/-}$ cells (p=0.1, Fig5B). This result indicates that an intact and functioning molecular clockwork supresses daytime firing rate in the neurons residing in the latARC.

In mARC, two-way ANOVA indicated a significant time of day effect ($F_{(1,57)}$= 6.9, p=0.012) and genotype X time of day interaction ($F_{(1,57)}$= 5.2, p=0.028). Unlike in latARC, no day-night variation in SFR was detected in mARC *Cry1*$^{+/+}$*Cry2*$^{+/+}$ cells ($F_{(1,57)}$= 3.69, p=0.06, Fig5E). However, daytime SFR was significantly different between *Cry1*$^{+/+}$*Cry2*$^{+/+}$ and *Cry1*$^{-/-}$*Cry2*$^{-/-}$ cells ($F_{(1,57)}$= 9.31, P=0.004, Fig5E).

To investigate the effect of the light-dark cycle on variation of SFR, we recorded cells in mARC (*Cry1*$^{+/+}$*Cry2*$^{+/+}$, n=20; *Cry1*$^{-/-}$*Cry2*$^{-/-}$, n=40) and latARC (*Cry1*$^{+/+}$*Cry2*$^{+/+}$, n=17; *Cry1*$^{-/-}$*Cry2*$^{-/-}$, n=25) in animals which were housed under DD conditions for 72h prior to experimentation. Recordings in the absence on a light-dark cycle reveal whether daily variations in SFR persist by an internal timing mechanism. In slices harvested from animals in DD, two-way ANOVA revealed a significant genotype effect in latARC ($F_{(1,38)}$= 6.19, p=0.017). No such genotype X time interaction was detected under DD conditions ($F_{(1,38)}$= 2.99, p=0.092). Single degree of freedom analysis indicated a significant circadian variation in *Cry1*$^{+/+}$*Cry2*$^{+/+}$ cells of latARC ($F_{(1,38)}$= 9.06, p=0.005, Fig5D). Similar to LD

conditions daytime SFR was significantly different between genotypes in DD ($F_{(1,38)}$= 4.47, p=0.041).

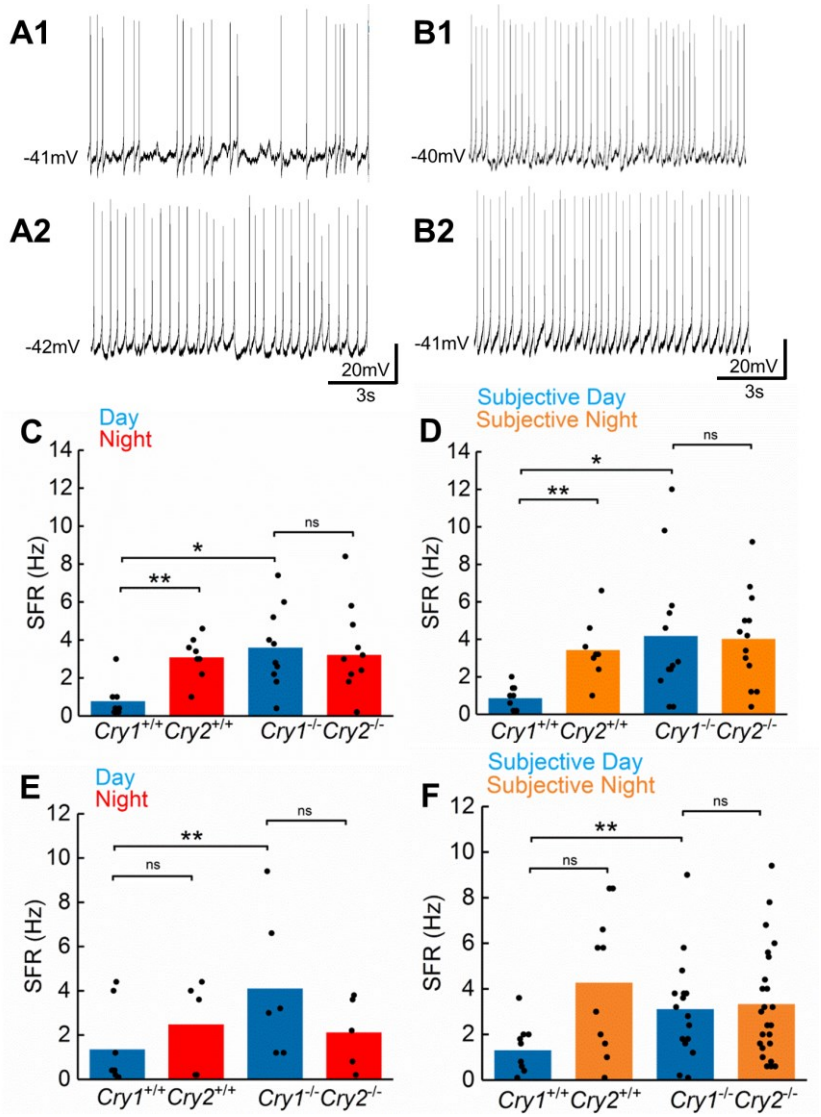

Figure 5: SFR varies in *Cry1*$^{+/+}$*Cry2*$^{+/+}$ but not in *Cry1*$^{-/-}$*Cry2*$^{-/-}$ cells: Under LD and DD conditions *Cry1*$^{-/-}$*Cry2*$^{-/-}$ cells do not exhibit variation in mean SFR where as those in latARC with an intact molecular clock do. **A:** Representative current clamp traces of *Cry1*$^{+/+}$*Cry2*$^{+/+}$ neurons in latARC during the day (ZT4-10, 0.8Hz) and night (ZT14-20, 3.6Hz). **B:** There is no clear day-night difference in the firing activity of *Cry1*$^{-/-}$*Cry2*$^{-/-}$ latARC neurons (both ~4Hz). **C:** Analysis of mean SFR revealed that *Cry1*$^{+/+}$*Cry2*$^{+/+}$ cells in latARC exhibit a significant day(0.8Hz, n=8) to night(3.1Hz, n=8) increase in SFR (Two-way ANOVA, single degree of freedom contrast; p=0.003). No such daily variation was detected for *Cry1*$^{-/-}$*Cry2*$^{-/-}$ neurons (3.62Hz, n=10 to 3.24Hz, n=11, p=0.1) and daytime SFR was significantly higher compared to *Cry1*$^{+/+}$*Cry2*$^{+/+}$ neurons (p=0.02). **D:** Current clamp recordings performed on cells in slices harvested under DD conditions revealed that variation in SFR persists in the absence of an LD cycle. LatARC neurons were more active during CT14-20 (0.88Hz, n=9) compared to CT4-10 (3.45Hz, n=8, p=0.005). **E:** SFR did not vary significantly across the day-night in mARC neurons, however *Cry1*$^{-/-}$*Cry2*$^{-/-}$ neurons did generate APs more frequently during the day (4.1Hz, n=6) compared to *Cry1*$^{+/+}$*Cry2*$^{+/+}$ neurons (1.35Hz, n=8, p=0.004). **F:** A similar effect of genotype was observed in mARC during the subjective day (p=0.007). These results suggest that the molecular clockwork in ARC functions to supress daytime electrical output.

We observed a significant time effect in mARC under DD conditions ($F_{(1,56)}$= 6.08, P=0.017) and a genotype X time interaction ($F_{(1,56)}$= 4.52, p=0.039). Planned single degree of freedom analysis indicated that unlike latARC, circadian variation was not significantly detected in *Cry1*$^{+/+}$*Cry2*$^{+/+}$ cells under DD conditions ($F_{(1,56)}$= 3.65, p=0.06, Fig5F). However, a significant subjective difference was detected between genotypes during the subjective day ($F_{(1,56)}$= 8.02, p=0.007). Interestingly, these whole-cell electrophysiology experiments demonstrate that this under all conditions tested and in both mARC and latARC, daytime or subjective daytime SFR is elevated in *Cry1*$^{-/-}$*Cry2*$^{-/-}$ compared to *Cry1*$^{+/+}$*Cry2*$^{+/+}$ cells.

Interestingly, none of the *Cry1*$^{+/+}$*Cry2*$^{+/+}$ cells recorded during the day in either mARC (mean ISI coefficient of variance (C.V)=0.57) or latARC (C.V=0.64) fired APs with a regular pattern (C.V<0.35). However, during the night the majority of latARC cells fired with a regular pattern and this shift in distribution compared to the day was significant (night C.V=0.36, 6 regular/8 total cells, Fisher's exact-test p=0.007). This temporal variation appeared dependent on a functional molecular clock. During the daytime regular firing states were observed in *Cry1*$^{-/-}$*Cry2*$^{-/-}$ cells in both latARC (CV=0.36, 4 regular/10) and mARC (CV=0.35, 4/6). Statistical analysis revealed that genotype had a significant effect on the proportion of regular versus irregular firing cells in mARC during the day (p=0.021), however no effect was shown in latARC cells (p=0.091). This finding suggests that intact molecular clockwork in ARC may supress AP frequency by disrupting high frequency, regular firing - however the effect of ablating the molecular clock is subtle in latARC.

Daytime multiunit activity in ARC is elevated by targeted deletion of *Bmal1*

A number of mammalian brain regions outside the SCN including the amygdala, habenula, olfactory bulb and multiple areas of the MBH, express circadian rhythms in core clock gene expression (Guilding and Piggins, 2007, Guilding et al., 2009). To investigate whether expression of a local molecular clock in the ARC drives daily changes in neuronal activity, we performed targeted bilateral injections of rAAV2-Cre-GFP or control rAAV2-GFP into the ARC of *Bmal1*$^{fl/fl}$ mice (Fig6). Successful transfection of the viral vectors *Bmal1* was confirmed by immunohistochemistry after a range of behavioural and electrophysiological experiments. Successful bilateral rAAV2-Cre-GFP or control rAAV2-GFP transduction within the ARC was observed in 6 and 8 *Bmal1*$^{fl/fl}$ mice respectively.

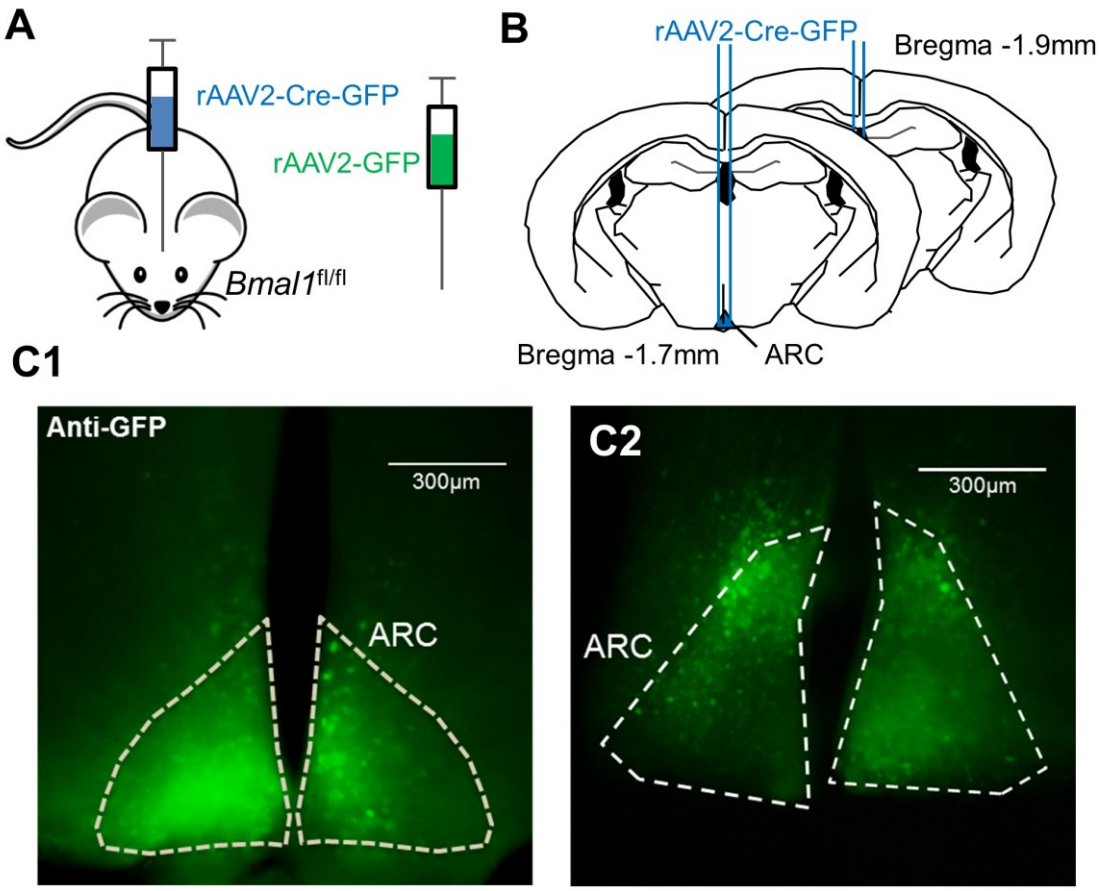

Figure 6: *In vivo* targeting of the core molecular clock in the ARC of *Bmal1*$^{fl/fl}$ mice: A: Bilateral Injections of rAAV2-Cre-GFP or control rAAV2-GFP were performed during stereotaxic surgery into the ARC of 7-10 week old male *Bmal1*$^{fl/fl}$ mice. After 2-weeks recovery post-surgery, animals were subject to behavioural assessment and brains were harvested for electrophysiological experimentation. **B:** 4x70nl injections were performed into the ARC at -1.7mm (2x) and -1.9mm (2x) from bregma to ensure sufficient rostrocaudal and mediolateral diffusion of the viral vectors. **C:** After electrophysiological experiments, brain slices were post-fixed in 4% PFA in 0.1M PBS and stained against GFP to confirm successful transfection. A hit was defined as all 4 injections being on target without extensive anti-GFP staining outside the ARC or along the injection tract. Both C1 and C2 were classed as hits.

Feeding and drinking behaviour of ARC-injected *Bmal1*$^{fl/fl}$ mice was assessed in cages (singly-housed) with a drinking bottle and food hopper hanging from a precision balance to monitor activity (TSE systems, Bad Homburg, Germany). Small incremental changes in water (0.01ml) and food (0.01g) intake (*ad libitum*) were measured in 10min bins and analysis was performed on data from LD and DD conditions. DD data was aligned to each animals free-running period as determined from feeding and drinking profiles (Fig7A,B).

To determine whether *Bmal1* knockout in the ARC affected total food and water intake during the light and dark phase, we performed analysis on the sum of food and water

consumed from ZT0-12 and ZT12-24 across multiple days. Intake was calculated by taking into account individual body weight (ml/gram bodyweight(gBW); g/gBW). Both rAAV2-GFP and rAAV2-Cre-GFP ARC-injected mice consumed the majority of their food during the dark phase (72% and 71% respectively, Fig7E). Similarly, water consumption was mostly partitioned to the dark phase (rAAV2-GFP, 83.3%, n=8; rAAV2-Cre-GFP, 84.3%, n=6). Targeted deletion of *Bmal1* in ARC had no effect on food or water intake in either the light or dark phase compared to control injected animals (two-sample t-test, $p>0.9$, Fig7E,H).

After 10days under LD conditions, the lights were switched off (DD) to investigate the free-running behaviour of injected *Bmal1*$^{fl/fl}$. As these cages were not equipped with running wheels, CT12 was defined as the onset of drinking activity. Food and drink intake was assessed during the subjective day (CT0-12) and subjective night (CT12-24) which were aligned to the animals' free-running period (typically ~23.8h). Again, consumption was averaged across multiple circadian cycles in DD. Mice consumed the majority of their food during the subjective night (rAAV2-GFP, 75.3%; rAAV2-Cre-GFP, 70.4%). Water intake was also higher during the subjective night in both rAAV2-GFP (83.4%) and rAAV2-Cre-GFP (82.8%) injected animals. However, similar to LD conditions, targeted deletion of *Bmal1* in ARC did not affect food or water intake during the subjective day or subjective night phase (two-sample t-test, $p>0.6$, Fig7F,I).

Loss of *Bmal1* in the ventral forebrain, which includes the ARC, results in disrupted temporal patterns of circadian feeding behaviour (Mieda et al., 2017). To investigate the potential effects of *Bmal1* deletion specifically in ARC on characteristic peaks and troughs in the pattern of feeding, data was organised into 1hr bins across the day-night and subjective day-night. Meal frequency (bouts of feeding >0.05g) and food intake were analysed by ANOVA to compare rAAV2-GFP versus rAAV2-Cre-GFP. Cre-dependent knockout of *Bmal1* in ARC did not affect meal frequency or food intake at any of the 1h bins across the day-night or subjective day-night cycle (repeated measures ANOVA, Holm-Sidak test, $p>0.1$). Similarly, no effects were observed on water intake (Holm-Sidak, $p>0.2$). From this data we can conclude that under the conditions tested here, viral targeting of the ARC molecular clock did not influence characteristic temporal patterns of feeding or drinking behaviour.

The coronal brain slices used for the electrophysiological recordings performed in this study permit investigation of the intrinsic rhythmicity of ARC without input from the SCN. However, there remains the potential for other brain regions within the slice to impart a timekeeping signal on the ARC. In animals with a global disruption of the molecular clockwork (*Cry1*$^{-/-}$*Cry2*$^{-/-}$), we found that daytime firing rate was not supressed with respect to night levels (Fig5). As adjacent regions of the MBH such as the DMH exhibit autonomous rhythms of molecular clock components (Guilding et al., 2009), it is possible that global clock disruption has an indirect effect on the temporal dynamics of ARC electrical output.

The experiments performed on *Cry1*$^{-/-}$*Cry2*$^{-/-}$ mice demonstrate that the intact clock supresses daytime electrical activity, therefore we hypothesised that knockout of *Bmal1* by rAAV2-Cre-GFP elevates MUA in ARC during the daytime (ZT5-8) compared to controls. Intriguingly the daytime MUA recorded by electrodes positioned within the ARC was elevated in rAAV2-Cre-GFP targeted slices (3.89 ± 0.79Hz, n=6) compared to those targeted with the control rAAV2-GFP virus (1.86 ± 0.50Hz, n=8, two-sample t-test, p=0.043, Fig8A).

No significant variation in MUA between slices targeted with rAAV2-Cre-GFP (2.6 ± 0.38Hz, n=6) or rAAV2-GFP (2.14± 0.0.52Hz, n=8, p=0.51) was recorded in DMH. Unexpectedly, MUA recorded by electrodes in the VMH was significantly elevated following rAAV2-Cre-GFP injection (4.37 ± 0.22Hz, n=6) compared with activity recorded in mice injected with rAAV2-GFP (2.69 ± 0.62Hz, n=8; p=0.045). Single-electrode analysis revealed that these large positive changes in daytime MUA were mostly confined to electrodes positioned within the ARC (Fig8B).

While extracellular recordings with pMEAs are useful for investigating the ensemble activity from a network of cells in close proximity to each electrode, one disadvantage is that one is unable to distinguish whether a higher number of silent cells are evoked to fire by injection of rAAV2-Cre-GFP or the firing rate of individual units is upregulated. Therefore, single-unit discrimination and analysis was performed on the same data to reveal whether daytime changes in electrical output induced by knockout of *Bmal1* are due to increased firing of individual cells. All units contributing to the multiunit activity

data were analysed by subregion for rAAV2-Cre-GFP or control rAAV2-GFP injected animals.

In ARC, rAAV2-Cre-GFP evoked a significant increase in daytime single-unit activity (2.02 ± 0.25Hz, n=67, Fig8C) compared to rAAV2-GFP injected animals (0.72 ± 0.14Hz, n=27, p=0.0018). Thus, not only was the firing rate of individual ARC cells upregulated, but the pMEA electrodes recorded a higher number of neurons that generated APs. Intriguingly, while we detected no change in multiunit activity in the DMH, single-unit activity was significantly lower in the rAAV2-Cre-GFP injected mice (1.1 ± 0.14Hz, n=94) compared to the rAAV2-GFP injected animals (1.93 ± 0.29Hz, n=58, p=0.005).

In the VMH, no significant effect of the Cre-containing virus on single-unit activity was detected (rAAV2-Cre-GFP, 1.35 ± 1.25Hz, n=39; rAAV2-GFP, 1.64 ± 0.46Hz, n=16, p=0.49). The disparity between the multiunit and single-unit is evident when considering the average activity per electrode (Fig8D). This data demonstrates that both multi- and single-unit analysis may field different results, and that a comparison of both is useful when interpreting the potential mechanisms behind alterations in recorded network activity.

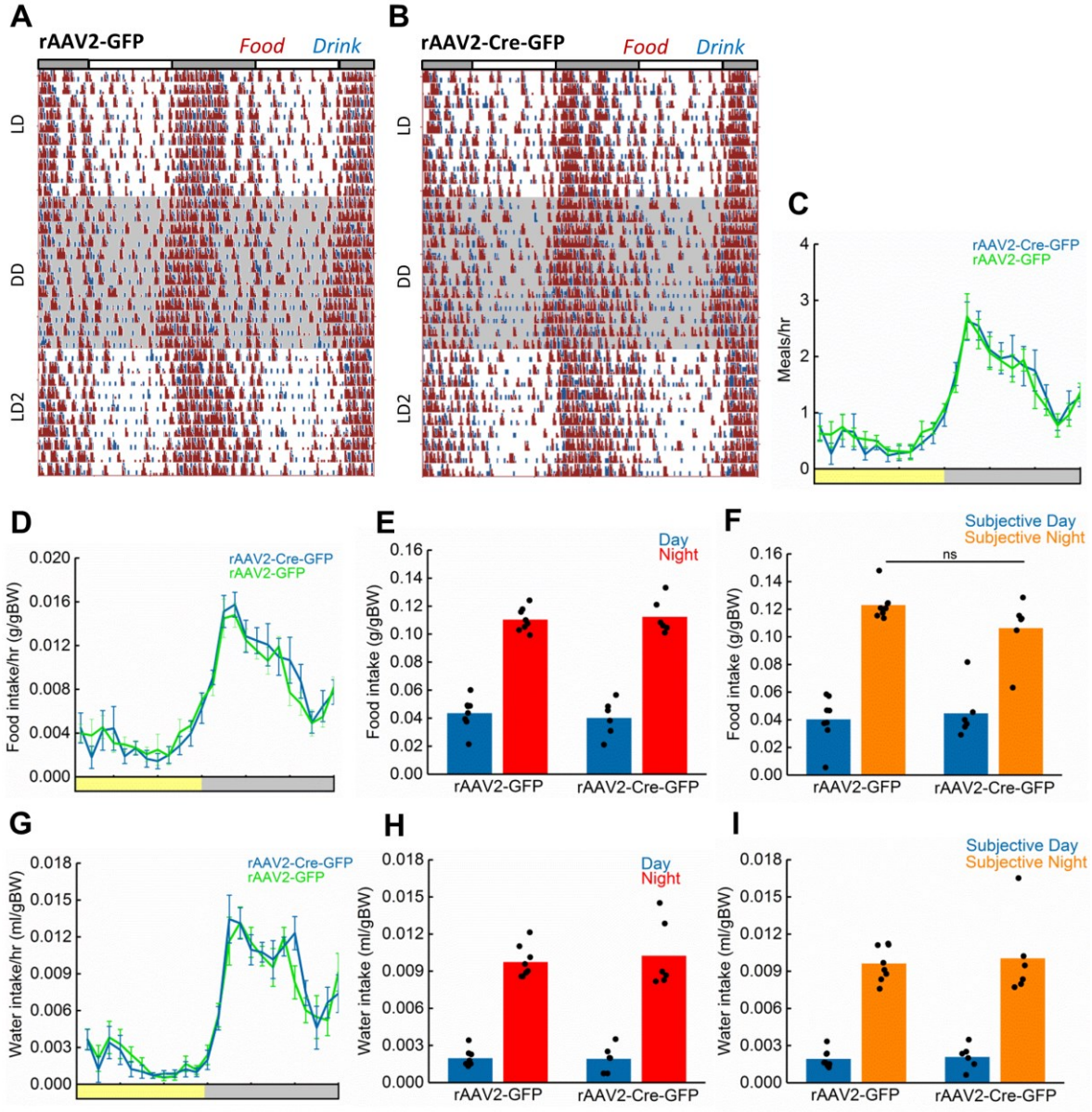

Figure 7: Targeted deletion of *Bmal1* in ARC did not influence food and water intake under LD or DD conditions: rAAV2-Cre-GFP and rAAV2-GFP injected *Bmal1*$^{fl/fl}$ mice were singly-housed with *ad libitum* access to food and water in specialised cages which measure food and water intake in small increments (0.01g/0.01ml). All data was adjusted based on individual body weight. **A,B:** Representative actograms displaying feeding and drinking activity profiles in LD and DD**. C:** Injection of rAAV2-Cre-GFP did not affect meal frequency (meals/hr) at any of the time points assessed under LD conditions (repeated measures ANOVA, Holm-Sidak test p>0.1). **D-F:** Targeted disruption of the ARC molecular clockwork had no effect on mean food intake assessed in 1h bins or when data across 24h was divided into light-dark phases (Holm-Sidak, p>0.1). **G-I:** Similarly, rAAV2-Cre-GFP injection did not influence water intake/hr or during light-dark/ subjective day-night (two-sample t test, p>0.2). Collectively these results suggest that the local molecular clockwork in ARC is not critical for regulating the temporal patterns of nutrient consumption when access to food and water is unrestricted.

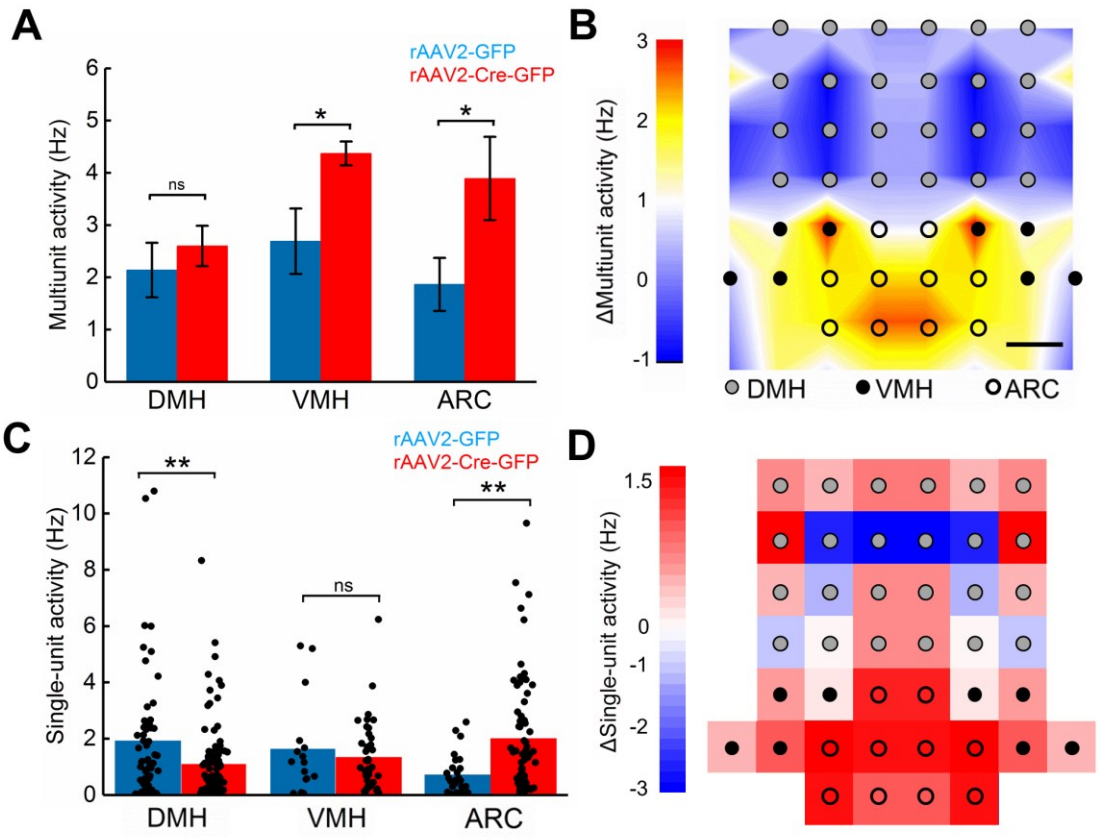

Figure 8: Specific targeting of the ARC molecular clock by deletion of *Bmal1* results in elevated daytime electrical output: *Bmal1*$^{fl/fl}$ mice received bilateral nanoinjections of either rAAV2-Cre-GFP or control rAAV2-GFP into the ARC. Bilateral hits were confirmed by immunohistochemistry after completion of pMEA experiments. **A:** Analysis of ARC multiunit activity (MUA) from ZT5-8 revealed that injection of rAAV2-Cre-GFP (successful bilateral hits) and subsequent deletion of *Bmal1* resulted in significantly elevated spike frequency (3.89 ± 0.79Hz, n=6 slices) compared to brain slices from rAAV2-GFP injected animals (1.86 ± 0.50Hz, n=8, two-sample t test, p=0.043). Interestingly, this effect was also detected in VMH (p=0.045), but not in the adjacent DMH (p=0.51). **B:** Contour plot displaying mean change in MUA from rAAV2-Cre-GFP to control rAAV2-GFP. Red and yellow areas represent areas with a higher increase in MUA with rAAV2-Cre-GFP vs .control. **C:** In agreement with the multiunit analysis, discrimination of single-units revealed that individual neurons in ARC generated spikes more frequently following rAAV2-Cre-GFP (2.02 ± 0.25Hz; n=67) compared to control injections of rAAV2-GFP (0.72 ± 0.14Hz; n=27; p=0.0018). However, opposing effects were revealed in DMH. Single-unit activity was significantly lower in rAAV2-Cre-GFP injected animals (1.1 ± 0.14Hz; n=94) compared to control vector injection (1.93 ± 0.29Hz; n=58; p=0.005). Unlike multiunit activity, no effect was observed in VMH (p=0.49). **D:** Heatmap showing average change in single-unit activity per electrode. Note that AAV2-Cre-GFP injection does not influence single-unit activity as strongly it influences MUA in the VMH (B).

Discussion

Collectively, the results presented in this chapter demonstrate that intact molecular clockwork is necessary for generating a daily rhythm in ARC electrical activity by supressing firing rate during the day. We reached this conclusion using 2 models of molecular clock disruption: *Cry1*$^{-/-}$*Cry2*$^{-/-}$ mice and targeted viral knockout of *Bmal1*. *Cry1*$^{-/-}$ *Cry2*$^{-/-}$ mice immediately exhibit arrhythmic locomotor activity when placed into DD conditions (van der Horst et al., 1999). However, in LD, the pattern of wheel-running activity displayed by *Cry1*$^{-/-}$*Cry2*$^{-/-}$ animals closely resembled that of *Cry1*$^{+/+}$*Cry2*$^{+/+}$ mice which have an intact molecular clockwork (van der Horst et al., 1999). Food and drink intake followed a similar pattern to wheel-running, and the majority was consumed (~65%) during the dark phase in LD conditions.

We found that whole-cell recordings performed on ARC neurons during the day and night revealed a significant daily variation in AP frequency in slices harvested from *Cry1*$^{+/+}$*Cry2*$^{+/+}$. Indeed, like *Per1*-expressing neurons this daily variation was also specific to neurons in latARC. To test whether rhythmic changes in AP firing are due to extrinsic factors or an intrinsic molecular clock we performed recordings on slices from *Cry1*$^{-/-}$*Cry2*$^{-/-}$ animals, which lack a functioning molecular clock. While AP frequency in latARC was significantly higher during the night compared to the daytime in *Cry1*$^{+/+}$*Cry2*$^{+/+}$ neurons, but no variation was observed in *Cry*-deficient slices despite both genotypes displaying similar daily patterns in wheel-running activity, food and water intake. Therefore daily variation of firing rate in latARC *Cry1*$^{+/+}$*Cry2*$^{+/+}$ neurons depends on a functioning molecular clockwork and not on the temporal pattern of feeding and drinking behaviour, which are potential feedback signals to ARC which could in theory superimpose rhythms in neuronal excitability (Wei et al., 2015, Baver et al., 2014).

We found three distinct electrical states, depolarised silent, firing and hyperpolarised silent, in *Cry1*$^{+/+}$*Cry2*$^{+/+}$ and *Cry1*$^{-/-}$*Cry2*$^{-/-}$ neurons indicating that the fundamental properties of ARC neurons are not influenced by the absence of Cryptochrome genes (Kuhlman and McMahon, 2004, Belle et al., 2009). Interestingly, neurons of the lateral habenula (LHb), a region which also displays self-sustained oscillations in *Per1*-luciferase, also display depolarised silent electrical states similar to those we recorded in ARC (Sakhi

et al., 2014b). Moreover, such states were recorded in LHb from *Cry1*$^{-/-}$*Cry2*$^{-/-}$ slices. Therefore, in oscillators that are weaker than SCN, depolarised states appear to manifest even when the molecular clockwork is aberrant.

RMP was significantly depolarised during the night compared to the day in latARC *Cry1*$^{+/+}$*Cry2*$^{+/+}$ neurons. We previously found that *Per1*-expressing neurons in latARC did not exhibit daily variation in RMP or R_{input} (*Results chapter 1*). Therefore, the molecular clock in *Cry1*$^{+/+}$*Cry2*$^{+/+}$ neurons may evoke a small semi-detectable variation in RMP which in turn leads to large changes in AP frequency. This difference may also be attributed to differences populations of neurons studied when targeting *Per1*.

We also performed whole-cell recordings on neurons in *Cry1*$^{+/+}$*Cry2*$^{+/+}$ and *Cry1*$^{-/-}$*Cry2*$^{-/-}$ slices during the subjective day (CT4-10) and subjective night (CT14-20) under DD conditions. No variation in RMP was observed from the subjective day epoch to the subjective night epoch, however SFR was elevated during the subjective night compared to the subjective day in latARC *Cry1*$^{+/+}$*Cry2*$^{+/+}$ neurons. This finding further demonstrates that circadian variation in latARC electrical output depends on the clock and is not as result of the light-dark cycle.

This study is the first to demonstrate that ARC electrical activity displays daily and circadian rhythmicity that depends on intact molecular clockwork. Consistent with this, these rhythms were found to depend on a functional local ARC molecular clock. ARC neurons receive projections from other rhythmic areas such as the SCN (Saeb-Parsy et al., 2000), therefore we targeted the core clock gene *Bmal1* by viral injection and then harvested brain slices to screen for changes in excitability on pMEAs. Bilateral injection of rAAV2-Cre-GFP into ARC of *Bmal1*$^{fl/fl}$ mice resulted in increased daytime multiunit activity (MUA) compared to control rAAV2-GFP injections.

In the DMH we found that MUA remained consistent between rAAV2-Cre-GFP and rAAV2-GFP injections in ARC. However, singleunit activity was significantly decreased by Cre-mediated knockout of *Bmal1* in ARC versus control virus. Due to the targeted nature of viral injections this change in DMH with ARC rAAV2-Cre-GFP is likely secondary to increases in ARC activity via projections to DMH neurons (Bouret et al., 2004). Spiking activity in the VMH was significantly increased following ARC injection of rAAV2-Cre-GFP

compared to control injections however single-unit activity did not change. These differences are likely due to variation in the number of single-units per electrode that contribute to the multiunit activity of that given electrode. This experiment raises the importance of discriminating between the activity of single units in addition to population/multiunit activity when interpreting the results for multielectrode array experiments.

The finding that viral knockout of *Bmal1(*ARC *Bmal1*$^{-/-}$*)* in ARC elevates low daytime firing rate is consistent with our whole-cell experiments on *Cry*-deficient mice. The daytime spike frequency of single unit activity in ARC (0.7Hz) closely matched the mean SFR (0.8Hz) recorded in *Cry1*$^{+/+}$*Cry2*$^{+/+}$ neurons by current clamp recording. Global or targeted ablation of the molecular clock by *Cry1*$^{-/-}$*Cry2*$^{-/-}$ or ARC *Bmal1*$^{-/-}$ respectively resulted in a 3-fold increase in firing rate during the day compared to control conditions. *Cry1*$^{-/-}$*Cry2*$^{-/-}$ neurons lack daily rhythmicity in firing rate which is evident in *Cry1*$^{+/+}$*Cry2*$^{+/+}$ neurons. Furthermore, without the influence of an intact molecular clock, the default resting firing rate of ARC neurons appears to be ~3Hz firing, which is similar to night-time levels.

Cry1$^{-/-}$*Cry2*$^{-/-}$ neurons in mARC also had elevated firing rate during the day compared to *Cry1*$^{+/+}$*Cry2*$^{+/+}$ neurons. Thus, the molecular clock in ARC functions to supress activity across the whole ARC and not just the latARC, where daily rhythms in firing rate are evident. Indeed, sustained rhythms in PER2::LUC are observed throughout the whole ARC (Guilding et al., 2009). *Bmal1*$^{-/-}$ also increased firing across all ARC electrodes, therefore the molecular clock may play a weak role on setting the daily excitability of mARC neurons. Notably, the firing activity of *Cry1*$^{-/-}$*Cry2*$^{-/-}$ neurons in the LHb remains constitutively low compared to *Cry1*$^{+/+}$*Cry2*$^{+/+}$ neurons (Sakhi et al., 2014b). However, similar to ARC, *Cry1*$^{-/-}$*Cry2*$^{-/-}$ neurons in the medial Hb fire APs at a constitutively high rate (Sakhi et al., 2014a). This indicates that the molecular clock may be either an excitatory or inhibitory driving factor on firing activity depending on the extra-SCN clock in question.

The inhibitory nature of the signal from the molecular clockwork is consistent with our previous finding that GABAergic tone, to *Per1*::Venus latARC neurons is higher during the day compared to the night. GABA is highly expressed in ARC, is conventionally inhibitory and is an important neurotransmitter for appetite regulation (Krashes et al., 2013,

Decavel and Van den Pol, 1990, Vong et al., 2011, Kong et al., 2012). All *Cry1*$^{+/+}$*Cry2*$^{+/+}$ neurons fired with an irregular firing pattern during the day, however at night the majority of cells generated APs with a regular pattern. Spiking irregularity in ARC neurons is also correlated with the presence of Kv4 conductance (Mendonca et al., 2018), which may display rhythmicity similar to SCN (Granados-Fuentes et al., 2012, Itri et al., 2010), although this was not-tested in this study. Regular firing in ARC is not abolished by blockade of synaptic transmission (Rauch et al., 2000). However, tonic, GABA-mediated inhibition may disrupt regular firing during the day and reduce firing rate.

Genetic or physiological circadian disruption is associated with obesity and metabolic disorders in both rodents and humans, implicating the circadian system in maintaining appropriate body weight (Evans and Davidson, 2013, Zhang et al., 2013, Foster et al., 2013, Bass and Takahashi, 2010). Global models of clock disruption, for example the *Cry1*$^{-/-}$*Cry2*$^{-/-}$ mouse, have played a key role in developing our understanding of the function of circadian clocks throughout the brain and periphery (Oishi et al., 2003, Van der Zee et al., 2008, Sujino et al., 2003, Sakhi et al., 2014b). For example, knockout of *Bmal1* in the ventral forebrain, which includes ARC as well as other MBH nuclei, results in a shift in the distribution of food intake from the early night to the late night (Mieda et al., 2017). Given the importance of the ARC neurons in regulating food intake and the timing of feeding behaviour (Li et al., 2012), we investigated whether specific knockout of *Bmal1* in ARC influenced the temporal pattern of food and water intake. As mentioned previously, rAAV2-Cre-GFP injection into ARC resulted in elevation of daytime firing rate which is normally suppressed by the intact molecular clockwork in ARC. *Bmal1*$^{-/-}$ in ARC did not have any effects on total food or water intake during either the day/night or subjective day/night. The distribution of food intake and meal frequency was also unchanged across the daily cycle in ARC *Bmal1*$^{-/-}$.

Current theories around the functions of extra-SCN clocks are based around fine-tuning of rhythmic physiology (Guilding et al., 2009, Guilding and Piggins, 2007). Further, the function of the molecular clock in ARC may only become clear under conditions of metabolic duress or when the SCN is dysfunctional; not when food and water are available *ad libitum*. Recent evidence suggests that reciprocal connections between ARC and SCN are essential for organising physiological rhythms (Buijs et al., 2017), therefore

feedback from extra-SCN clocks may subtly modulate SCN-driven physiology. Clock-mediated oscillations in ARC excitability may also function to modulate responses to metabolic cues across the day-night cycle.

References

ABE, M., HERZOG, E. D., YAMAZAKI, S., STRAUME, M., TEI, H., SAKAKI, Y., MENAKER, M. & BLOCK, G. D. 2002. Circadian rhythms in isolated brain regions. *J Neurosci,* 22**,** 350-6.

AHMAD, M. & CASHMORE, A. R. 1993. HY4 gene of A. thaliana encodes a protein with characteristics of a blue-light photoreceptor. *Nature,* 366**,** 162-6.

AKASHI, M. & TAKUMI, T. 2005. The orphan nuclear receptor RORalpha regulates circadian transcription of the mammalian core-clock Bmal1. *Nat Struct Mol Biol,* 12**,** 441-8.

APONTE, Y., ATASOY, D. & STERNSON, S. M. 2011. AGRP neurons are sufficient to orchestrate feeding behavior rapidly and without training. *Nat Neurosci,* 14**,** 351-5.

ATASOY, D., BETLEY, J. N., SU, H. H. & STERNSON, S. M. 2012. Deconstruction of a neural circuit for hunger. *Nature,* 488**,** 172-7.

BAE, K., JIN, X., MAYWOOD, E. S., HASTINGS, M. H., REPPERT, S. M. & WEAVER, D. R. 2001. Differential functions of mPer1, mPer2, and mPer3 in the SCN circadian clock. *Neuron,* 30**,** 525-36.

BALSALOBRE, A., MARCACCI, L. & SCHIBLER, U. 2000. Multiple signaling pathways elicit circadian gene expression in cultured Rat-1 fibroblasts. *Curr Biol,* 10**,** 1291-4.

BASS, J. & TAKAHASHI, J. S. 2010. Circadian integration of metabolism and energetics. *Science,* 330**,** 1349-54.

BAVER, S. B., HOPE, K., GUYOT, S., BJORBAEK, C., KACZOROWSKI, C. & O'CONNELL, K. M. 2014. Leptin modulates the intrinsic excitability of AgRP/NPY neurons in the arcuate nucleus of the hypothalamus. *J Neurosci,* 34**,** 5486-96.

BEIER, K. T., STEINBERG, E. E., DELOACH, K. E., XIE, S., MIYAMICHI, K., SCHWARZ, L., GAO, X. J., KREMER, E. J., MALENKA, R. C. & LUO, L. 2015. Circuit Architecture of VTA Dopamine Neurons Revealed by Systematic Input-Output Mapping. *Cell,* 162**,** 622-34.

BELLE, M. D., DIEKMAN, C. O., FORGER, D. B. & PIGGINS, H. D. 2009. Daily electrical silencing in the mammalian circadian clock. *Science,* 326**,** 281-4.

BOURET, S. G., DRAPER, S. J. & SIMERLY, R. B. 2004. Formation of projection pathways from the arcuate nucleus of the hypothalamus to hypothalamic regions implicated in the neural control of feeding behavior in mice. *J Neurosci,* 24**,** 2797-805.

BROWN, S. A., FLEURY-OLELA, F., NAGOSHI, E., HAUSER, C., JUGE, C., MEIER, C. A., CHICHEPORTICHE, R., DAYER, J. M., ALBRECHT, U. & SCHIBLER, U. 2005. The period length of fibroblast circadian gene expression varies widely among human individuals. *PLoS Biol,* 3**,** e338.

BUGARITH, K., DINH, T. T., LI, A. J., SPETH, R. C. & RITTER, S. 2005. Basomedial hypothalamic injections of neuropeptide Y conjugated to saporin selectively disrupt hypothalamic controls of food intake. *Endocrinology,* 146**,** 1179-91.

BUHR, E. D. & TAKAHASHI, J. S. 2013. Molecular components of the Mammalian circadian clock. *Handb Exp Pharmacol*, 3-27.

BUIJS, F. N., GUZMAN-RUIZ, M., LEON-MERCADO, L., BASUALDO, M. C., ESCOBAR, C., KALSBEEK, A. & BUIJS, R. M. 2017. Suprachiasmatic Nucleus Interaction with the Arcuate Nucleus; Essential for Organizing Physiological Rhythms. *eNeuro,* 4.

BUNGER, M. K., WALISSER, J. A., SULLIVAN, R., MANLEY, P. A., MORAN, S. M., KALSCHEUR, V. L., COLMAN, R. J. & BRADFIELD, C. A. 2005. Progressive arthropathy in mice with a targeted disruption of the Mop3/Bmal-1 locus. *Genesis,* 41**,** 122-32.

BUNGER, M. K., WILSBACHER, L. D., MORAN, S. M., CLENDENIN, C., RADCLIFFE, L. A., HOGENESCH, J. B., SIMON, M. C., TAKAHASHI, J. S. & BRADFIELD, C. A. 2000. Mop3 is an essential component of the master circadian pacemaker in mammals. *Cell,* 103**,** 1009-17.

CASHMORE, A. R. 2003. Cryptochromes: enabling plants and animals to determine circadian time. *Cell,* 114**,** 537-43.

CHO, H., ZHAO, X., HATORI, M., YU, R. T., BARISH, G. D., LAM, M. T., CHONG, L. W., DITACCHIO, L., ATKINS, A. R., GLASS, C. K., LIDDLE, C., AUWERX, J., DOWNES, M., PANDA, S. & EVANS, R. M. 2012. Regulation of circadian behaviour and metabolism by REV-ERB-alpha and REV-ERB-beta. *Nature,* 485**,** 123-7.

COLWELL, C. S. 2011. Linking neural activity and molecular oscillations in the SCN. *Nat Rev Neurosci,* 12**,** 553-69.

DAILEY, M. J. & BARTNESS, T. J. 2010. Arcuate nucleus destruction does not block food deprivation-induced increases in food foraging and hoarding. *Brain Res,* 1323**,** 94-108.

DECAVEL, C. & VAN DEN POL, A. N. 1990. GABA: a dominant neurotransmitter in the hypothalamus. *J Comp Neurol,* 302**,** 1019-37.

EVANS, J. A. & DAVIDSON, A. J. 2013. Health consequences of circadian disruption in humans and animal models. *Prog Mol Biol Transl Sci,* 119**,** 283-323.

FOSTER, R. G., PEIRSON, S. N., WULFF, K., WINNEBECK, E., VETTER, C. & ROENNEBERG, T. 2013. Sleep and circadian rhythm disruption in social jetlag and mental illness. *Prog Mol Biol Transl Sci,* 119**,** 325-46.

FREEMAN, G. M., JR., KROCK, R. M., ATON, S. J., THABEN, P. & HERZOG, E. D. 2013. GABA networks destabilize genetic oscillations in the circadian pacemaker. *Neuron,* 78**,** 799-806.

GEKAKIS, N., STAKNIS, D., NGUYEN, H. B., DAVIS, F. C., WILSBACHER, L. D., KING, D. P., TAKAHASHI, J. S. & WEITZ, C. J. 1998. Role of the CLOCK protein in the mammalian circadian mechanism. *Science,* 280**,** 1564-9.

GRANADOS-FUENTES, D., NORRIS, A. J., CARRASQUILLO, Y., NERBONNE, J. M. & HERZOG, E. D. 2012. I(A) channels encoded by Kv1.4 and Kv4.2 regulate neuronal firing in the suprachiasmatic nucleus and circadian rhythms in locomotor activity. *J Neurosci,* 32**,** 10045-52.

GRIFFIN, E. A., JR., STAKNIS, D. & WEITZ, C. J. 1999. Light-independent role of CRY1 and CRY2 in the mammalian circadian clock. *Science,* 286**,** 768-71.

GUILDING, C., HUGHES, A. T., BROWN, T. M., NAMVAR, S. & PIGGINS, H. D. 2009. A riot of rhythms: neuronal and glial circadian oscillators in the mediobasal hypothalamus. *Mol Brain,* 2**,** 28.

GUILDING, C. & PIGGINS, H. D. 2007. Challenging the omnipotence of the suprachiasmatic timekeeper: are circadian oscillators present throughout the mammalian brain? *Eur J Neurosci,* 25**,** 3195-216.

GUILLAUMOND, F., DARDENTE, H., GIGUERE, V. & CERMAKIAN, N. 2005. Differential control of Bmal1 circadian transcription by REV-ERB and ROR nuclear receptors. *J Biol Rhythms,* 20**,** 391-403.

ITRI, J. N., VOSKO, A. M., SCHROEDER, A., DRAGICH, J. M., MICHEL, S. & COLWELL, C. S. 2010. Circadian regulation of a-type potassium currents in the suprachiasmatic nucleus. *J Neurophysiol,* 103**,** 632-40.

KETTNER, N. M., MAYO, S. A., HUA, J., LEE, C., MOORE, D. D. & FU, L. 2015. Circadian Dysfunction Induces Leptin Resistance in Mice. *Cell Metab,* 22**,** 448-59.

KO, C. H. & TAKAHASHI, J. S. 2006. Molecular components of the mammalian circadian clock. *Hum Mol Genet,* 15 Spec No 2**,** R271-7.

KONDRATOV, R. V., KONDRATOVA, A. A., GORBACHEVA, V. Y., VYKHOVANETS, O. V. & ANTOCH, M. P. 2006. Early aging and age-related pathologies in mice deficient in BMAL1, the core componentof the circadian clock. *Genes Dev,* 20**,** 1868-73.

KONG, D., TONG, Q., YE, C., KODA, S., FULLER, P. M., KRASHES, M. J., VONG, L., RAY, R. S., OLSON, D. P. & LOWELL, B. B. 2012. GABAergic RIP-Cre neurons in the arcuate nucleus selectively regulate energy expenditure. *Cell,* 151**,** 645-57.

KONOPKA, R. J. & BENZER, S. 1971. Clock mutants of Drosophila melanogaster. *Proc Natl Acad Sci U S A,* 68**,** 2112-6.

KRASHES, M. J., KODA, S., YE, C., ROGAN, S. C., ADAMS, A. C., CUSHER, D. S., MARATOS-FLIER, E., ROTH, B. L. & LOWELL, B. B. 2011. Rapid, reversible activation of AgRP neurons drives feeding behavior in mice. *J Clin Invest,* 121**,** 1424-8.

KRASHES, M. J., SHAH, B. P., KODA, S. & LOWELL, B. B. 2013. Rapid versus delayed stimulation of feeding by the endogenously released AgRP neuron mediators GABA, NPY, and AgRP. *Cell Metab,* 18**,** 588-95.

KUHLMAN, S. J. & MCMAHON, D. G. 2004. Rhythmic regulation of membrane potential and potassium current persists in SCN neurons in the absence of environmental input. *Eur J Neurosci,* 20**,** 1113-7.

LAMIA, K. A., STORCH, K. F. & WEITZ, C. J. 2008. Physiological significance of a peripheral tissue circadian clock. *Proc Natl Acad Sci U S A,* 105**,** 15172-7.

LI, A. J., WIATER, M. F., OOSTROM, M. T., SMITH, B. R., WANG, Q., DINH, T. T., ROBERTS, B. L., JANSEN, H. T. & RITTER, S. 2012. Leptin-sensitive neurons in the arcuate nuclei contribute to endogenous feeding rhythms. *Am J Physiol Regul Integr Comp Physiol,* 302**,** R1313-26.

LOWREY, P. L. & TAKAHASHI, J. S. 2004. Mammalian circadian biology: elucidating genome-wide levels of temporal organization. *Annu Rev Genomics Hum Genet,* 5**,** 407-41.

MADISEN, L., ZWINGMAN, T. A., SUNKIN, S. M., OH, S. W., ZARIWALA, H. A., GU, H., NG, L. L., PALMITER, R. D., HAWRYLYCZ, M. J., JONES, A. R., LEIN, E. S. & ZENG, H. 2010. A robust and high-throughput Cre reporting and characterization system for the whole mouse brain. *Nat Neurosci,* 13**,** 133-40.

MCHUGH, T. J., BLUM, K. I., TSIEN, J. Z., TONEGAWA, S. & WILSON, M. A. 1996. Impaired hippocampal representation of space in CA1-specific NMDAR1 knockout mice. *Cell,* 87**,** 1339-49.

MEISTER, B., CECCATELLI, S., HOKFELT, T., ANDEN, N. E., ANDEN, M. & THEODORSSON, E. 1989. Neurotransmitters, neuropeptides and binding sites in the rat mediobasal hypothalamus: effects of monosodium glutamate (MSG) lesions. *Exp Brain Res,* 76**,** 343-68.

MENDONCA, P. R. F., KYLE, V., YEO, S. H., COLLEDGE, W. H. & ROBINSON, H. P. C. 2018. Kv4.2 channel activity controls intrinsic firing dynamics of arcuate kisspeptin neurons. *J Physiol,* 596**,** 885-899.

MIEDA, M., HASEGAWA, E., KESSARIS, N. & SAKURAI, T. 2017. Fine-Tuning Circadian Rhythms: The Importance of Bmal1 Expression in the Ventral Forebrain. *Front Neurosci,* 11**,** 55.

MIEDA, M. & SAKURAI, T. 2011. Bmal1 in the nervous system is essential for normal adaptation of circadian locomotor activity and food intake to periodic feeding. *J Neurosci,* 31**,** 15391-6.

MUKHERJI, A., KOBIITA, A. & CHAMBON, P. 2015. Shifting the feeding of mice to the rest phase creates metabolic alterations, which, on their own, shift the peripheral circadian clocks by 12 hours. *Proc Natl Acad Sci U S A,* 112**,** E6683-90.

NAGOSHI, E., SAINI, C., BAUER, C., LAROCHE, T., NAEF, F. & SCHIBLER, U. 2004. Circadian gene expression in individual fibroblasts: cell-autonomous and self-sustained oscillators pass time to daughter cells. *Cell,* 119**,** 693-705.

OISHI, K., MIYAZAKI, K., KADOTA, K., KIKUNO, R., NAGASE, T., ATSUMI, G., OHKURA, N., AZAMA, T., MESAKI, M., YUKIMASA, S., KOBAYASHI, H., IITAKA, C., UMEHARA, T., HORIKOSHI, M., KUDO, T., SHIMIZU, Y., YANO, M., MONDEN, M., MACHIDA, K., MATSUDA, J., HORIE, S., TODO, T. & ISHIDA, N. 2003. Genome-wide expression analysis of mouse liver reveals CLOCK-regulated circadian output genes. *J Biol Chem,* 278**,** 41519-27.

PANDA, S., ANTOCH, M. P., MILLER, B. H., SU, A. I., SCHOOK, A. B., STRAUME, M., SCHULTZ, P. G., KAY, S. A., TAKAHASHI, J. S. & HOGENESCH, J. B. 2002. Coordinated transcription of key pathways in the mouse by the circadian clock. *Cell,* 109**,** 307-20.

PREITNER, N., DAMIOLA, F., LOPEZ-MOLINA, L., ZAKANY, J., DUBOULE, D., ALBRECHT, U. & SCHIBLER, U. 2002. The orphan nuclear receptor REV-ERBalpha controls circadian transcription within the positive limb of the mammalian circadian oscillator. *Cell,* 110**,** 251-60.

RAUCH, M., RIEDIGER, T., SCHMID, H. A. & SIMON, E. 2000. Orexin A activates leptin-responsive neurons in the arcuate nucleus. *Pflugers Arch,* 440**,** 699-703.

REPPERT, S. M. & WEAVER, D. R. 2002. Coordination of circadian timing in mammals. *Nature,* 418**,** 935-41.

ROGAN, S. C. & ROTH, B. L. 2011. Remote control of neuronal signaling. *Pharmacol Rev,* 63**,** 291-315.

SAEB-PARSY, K., LOMBARDELLI, S., KHAN, F. Z., MCDOWALL, K., AU-YONG, I. T. & DYBALL, R. E. 2000. Neural connections of hypothalamic neuroendocrine nuclei in the rat. *J Neuroendocrinol,* 12**,** 635-48.

SAKHI, K., BELLE, M. D., GOSSAN, N., DELAGRANGE, P. & PIGGINS, H. D. 2014a. Daily variation in the electrophysiological activity of mouse medial habenula neurones. *J Physiol,* 592**,** 587-603.

SAKHI, K., WEGNER, S., BELLE, M. D., HOWARTH, M., DELAGRANGE, P., BROWN, T. M. & PIGGINS, H. D. 2014b. Intrinsic and extrinsic cues regulate the daily profile of mouse lateral habenula neuronal activity. *J Physiol,* 592**,** 5025-45.

SATO, T. K., PANDA, S., MIRAGLIA, L. J., REYES, T. M., RUDIC, R. D., MCNAMARA, P., NAIK, K. A., FITZGERALD, G. A., KAY, S. A. & HOGENESCH, J. B. 2004. A functional genomics strategy reveals Rora as a component of the mammalian circadian clock. *Neuron,* 43**,** 527-37.

SATO, T. K., YAMADA, R. G., UKAI, H., BAGGS, J. E., MIRAGLIA, L. J., KOBAYASHI, T. J., WELSH, D. K., KAY, S. A., UEDA, H. R. & HOGENESCH, J. B. 2006. Feedback repression is required for mammalian circadian clock function. *Nat Genet,* 38**,** 312-9.

SMYLLIE, N. J., CHESHAM, J. E., HAMNETT, R., MAYWOOD, E. S. & HASTINGS, M. H. 2016. Temporally chimeric mice reveal flexibility of circadian period-setting in the suprachiasmatic nucleus. *Proc Natl Acad Sci U S A,* 113**,** 3657-62.

STORCH, K. F., PAZ, C., SIGNOROVITCH, J., RAVIOLA, E., PAWLYK, B., LI, T. & WEITZ, C. J. 2007. Intrinsic circadian clock of the mammalian retina: importance for retinal processing of visual information. *Cell,* 130**,** 730-741.

SUJINO, M., MASUMOTO, K. H., YAMAGUCHI, S., VAN DER HORST, G. T., OKAMURA, H. & INOUYE, S. T. 2003. Suprachiasmatic nucleus grafts restore circadian behavioral rhythms of genetically arrhythmic mice. *Curr Biol,* 13**,** 664-8.

TIAN, L., HIRES, S. A., MAO, T., HUBER, D., CHIAPPE, M. E., CHALASANI, S. H., PETREANU, L., AKERBOOM, J., MCKINNEY, S. A., SCHREITER, E. R., BARGMANN, C. I., JAYARAMAN, V., SVOBODA, K. & LOOGER, L. L. 2009. Imaging neural activity in worms, flies and mice with improved GCaMP calcium indicators. *Nat Methods,* 6**,** 875-81.

TSIEN, J. Z., HUERTA, P. T. & TONEGAWA, S. 1996. The essential role of hippocampal CA1 NMDA receptor-dependent synaptic plasticity in spatial memory. *Cell,* 87**,** 1327-38.

VAN DEN TOP, M., LYONS, D. J., LEE, K., CODERRE, E., RENAUD, L. P. & SPANSWICK, D. 2007. Pharmacological and molecular characterization of ATP-sensitive K(+) conductances in CART and NPY/AgRP expressing neurons of the hypothalamic arcuate nucleus. *Neuroscience,* 144**,** 815-24.

VAN DER HORST, G. T., MUIJTJENS, M., KOBAYASHI, K., TAKANO, R., KANNO, S., TAKAO, M., DE WIT, J., VERKERK, A., EKER, A. P., VAN LEENEN, D., BUIJS, R., BOOTSMA, D., HOEIJMAKERS, J. H. & YASUI, A. 1999. Mammalian Cry1 and Cry2 are essential for maintenance of circadian rhythms. *Nature,* 398**,** 627-30.

VAN DER ZEE, E. A., HAVEKES, R., BARF, R. P., HUT, R. A., NIJHOLT, I. M., JACOBS, E. H. & GERKEMA, M. P. 2008. Circadian time-place learning in mice depends on Cry genes. *Curr Biol,* 18**,** 844-8.

VITATERNA, M. H., KING, D. P., CHANG, A. M., KORNHAUSER, J. M., LOWREY, P. L., MCDONALD, J. D., DOVE, W. F., PINTO, L. H., TUREK, F. W. & TAKAHASHI, J. S. 1994. Mutagenesis and mapping of a mouse gene, Clock, essential for circadian behavior. *Science,* 264**,** 719-25.

VONG, L., YE, C., YANG, Z., CHOI, B., CHUA, S., JR. & LOWELL, B. B. 2011. Leptin action on GABAergic neurons prevents obesity and reduces inhibitory tone to POMC neurons. *Neuron,* 71**,** 142-54.

WANG, T. A., YU, Y. V., GOVINDAIAH, G., YE, X., ARTINIAN, L., COLEMAN, T. P., SWEEDLER, J. V., COX, C. L. & GILLETTE, M. U. 2012. Circadian rhythm of redox state regulates excitability in suprachiasmatic nucleus neurons. *Science,* 337**,** 839-42.

WEI, W., PHAM, K., GAMMONS, J. W., SUTHERLAND, D., LIU, Y., SMITH, A., KACZOROWSKI, C. C. & O'CONNELL, K. M. 2015. Diet composition, not calorie intake, rapidly alters intrinsic excitability of hypothalamic AgRP/NPY neurons in mice. *Sci Rep,* 5**,** 16810.

YOO, S. H., KO, C. H., LOWREY, P. L., BUHR, E. D., SONG, E. J., CHANG, S., YOO, O. J., YAMAZAKI, S., LEE, C. & TAKAHASHI, J. S. 2005. A noncanonical E-box enhancer drives mouse Period2 circadian oscillations in vivo. *Proc Natl Acad Sci U S A,* 102**,** 2608-13.

YOO, S. H., YAMAZAKI, S., LOWREY, P. L., SHIMOMURA, K., KO, C. H., BUHR, E. D., SIEPKA, S. M., HONG, H. K., OH, W. J., YOO, O. J., MENAKER, M. & TAKAHASHI, J. S. 2004. PERIOD2::LUCIFERASE real-time reporting of circadian dynamics reveals persistent circadian oscillations in mouse peripheral tissues. *Proc Natl Acad Sci U S A,* 101**,** 5339-46.

ZHANG, L., PTACEK, L. J. & FU, Y. H. 2013. Diversity of human clock genotypes and consequences. *Prog Mol Biol Transl Sci,* 119**,** 51-81.

ZHENG, B., LARKIN, D. W., ALBRECHT, U., SUN, Z. S., SAGE, M., EICHELE, G., LEE, C. C. & BRADLEY, A. 1999. The mPer2 gene encodes a functional component of the mammalian circadian clock. *Nature,* 400**,** 169-73.

Chapter 3

Neuropeptide-Y neurons in ARC do not display a daily rhythm in firing rate

Neuropeptide-Y neurons in ARC do not display a daily rhythm in firing rate

Introduction

Animals must begin feeding in response to negative energy levels in order to maintain appropriate energy homeostasis. Food seeking is a complex behaviour that is regulated by sensory inputs, circulating hormones and social interaction and depends on a physical feeling of hunger (Begg and Woods, 2013, Denis et al., 2015). The biological system which evokes appetite and hunger has been an area of intense research over recent decades. A major component of this system is found in the hypothalamus, where distinct neuronal populations play antagonistic roles in driving appetite and food seeking behaviour (Andermann and Lowell, 2017). In particular, cells in the ARC integrate an array of inputs that convey systemic energy status to either promote satiety or hunger by projecting to downstream brain regions.

Pro-opiomelanocortin (POMC) neurons residing in the ARC promote satiety (Dube et al., 1978). This was first highlighted following central injection of α-melanocyte-stimulating hormone (αMSH), a processed peptide downstream of POMC which potently decreased feeding in rats (Poggioli et al., 1986). The role of αMSH as a satiety signal has been demonstrated in POMC deficient mice, and further validated in profoundly obese humans with an identified αMSH deficiency (Krude et al., 1998, Yaswen et al., 1999). In the brain αMSH evokes its actions via melanocortin 4 receptors (MC4R). The physiological relevance of this interaction can be demonstrated by central injection of MC4R agonists which decreases food intake (Fan et al., 1997). Also, ablation of MC4R in mice and humans leads to overeating and obesity (Huszar et al., 1997, Vaisse et al., 1998, Yeo et al., 1998). Therefore the above lines of evidence highlight the importance of POMC neuron signalling via MC4R in maintaining appropriate caloric consumption.

A separate ARC neuronal population, the so called NPY/AgRP neurons, express Agouti-related peptide (AgRP), Neuropeptide (NPY) and GABA and stimulate appetite directly and through antagonism of the satiety-promoting effect of POMC neurons. The role of

AgRP in stimulating appetite was first demonstrated by overexpression studies in ARC NPY/AgRP neurons which caused marked hyperphagia through antagonism of MC3/4Rs (Graham et al., 1997, Ollmann et al., 1997, Rossi et al., 1998). Both central and hypothalamic injections of NPY potently induce feeding behaviour (Allen et al., 1985, Levine and Morley, 1984, Stanley and Leibowitz, 1984). NPY/AgRP neurons also send GABAergic collaterals to POMC neurons to supress their satiety inducing action (Horvath et al., 1992, Cowley et al., 2001). Genetic ablation of NPY/AgRP neurons in adult rodents evokes reduction in food intake (Gropp et al., 2005, Luquet et al., 2005). The antagonistic functions of ARC neurons can be confirmed under fasting conditions and in cases of leptin deficiency (mimics fasting), which activate NPY/AgRP neurons and inhibit POMC neurons (Hahn et al., 1998, Mizuno et al., 1998, Ollmann et al., 1997, Schwartz et al., 1997, Shutter et al., 1997).

The paraventricular nucleus of the hypothalamus (PVN) first emerged as a key target for energy-sensing ARC neurons because PVN-specific lesions cause obesity (Gold et al., 1977, Leibowitz et al., 1981). Indeed, PVN neurons express an abundancy of MC4Rs (Kishi et al., 2003, Liu et al., 2003, Mountjoy et al., 1994) and they receive projections from both NPY/AgRP and POMC neurons in ARC (Bagnol et al., 1999, Cowley et al., 1999).

Opto- and chemo-genetic activation of NPY/AgRP neurons evokes feeding within minutes to the same extent as that seen in fasted mice (Aponte et al., 2011, Krashes et al., 2011). The high speed component of this effect is mediated by NPY and GABA where as AgRP release increases feeding with a delay of 4hr following activation of NPY/AgRP neurons (Krashes et al., 2013). Associated increases in the reward value of food accompany these changes (Atasoy et al., 2012, Krashes et al., 2011). The antagonistic nature of POMC neurons can be further demonstrated through opto- and chemogenetic activation which inhibits food intake, however in contrast to NPY/AgRP neurons this occurs over a longer time scale of many hours (Aponte et al., 2011, Fenselau et al., 2017, Zhan et al., 2013). Optogenetic stimulation of AgRP terminals in PVN increased food intake (Atasoy et al., 2012).

Aims

Circulating hormones target NPY/AgRP neurons in the ARC to regulate hunger and satiety (Andermann and Lowell, 2017). However, little is known about how the circadian system influences the activity of NPY/AgRP neurons in ARC. From previous studies and the experiments performed in this thesis it is clear that the molecular clock drives daily changes in neuronal excitability in both the SCN and ARC. Therefore, we sought to determine whether similar daily changes in excitability are conserved when targeting ARC NPY/AgRP neurons and not other neuronal subtypes.

To investigate this we used a NPY-Green Fluorescent Protein (-GFP) reporter mouse which allows accurate identification of NPY-expressing neurons that are not distinguishable by morphophology alone (van den Pol et al., 2009). A number of NPY-GFP mouse lines have been generated by different groups (Pinto et al., 2004, Roseberry et al., 2004), however the GFP expression in the line used for the experiments in this chapter is very bright which allows easy targeting during whole-cell experiments (van den Pol et al., 2009). This line was created using a large bacterial artificial chromosome (BAC) sequence which contains the NPY promotor driving the expression of a bright and stable humanised *Renilla* GFP from the sea pansy (hrGFP). These mice display intense fluorescence in a dense plexus of cells in the ventromedial ARC near the third ventricle. The investigators also conducted an in-depth investigation into the electrophysiological properties of NPY-hrGFP-positive neurons in the ARC (van den Pol et al., 2009).

Materials and methods

Animal housing

Experiments for this chapter were conducted on male NPY-hrGFP mice (5-7 weeks old) expressing a humanised *Renilla* GFP driven by an NPY gene promotor sequence. Mice were kindly gifted by Prof. S. Luckman (University of Manchester, UK) and were originally generated by Prof. A. van den Pol (Yale University, USA). All procedures were carried out in accordance with the UK Animals (Scientific Procedures) Act of 1986. Animals were group housed in an area under a controlled 12/12 h light/dark (LD) cycle. Animals had *ad*

libitum access to food and water and the temperature in the housing area was maintained at 20 ± 2 °C and humidity at ~40%.

Whole-cell Electrophysiology

Slices were harvested for whole-cell recordings in accordance with the protocol previously outlined in this thesis. NPY-hrGFP mice (5-7 weeks old) were deeply anaesthetised and decapitated at ZT1 for daytime recordings (ZT4-10) or ZT11 for night recordings (ZT14-20). Brains were removed and transferred into cutting solution containing (in mM): 0.5 NaCl, 1.8 KCl, 1.2 KH_2PO_4, 7 $MgSO_4$, 26 $NaHCO_3$, 15 Glucose and 50 Sucrose (300-310 $mosmol^{-1}$; pregassed with 95% O_2/ 5% CO_2).

300μm slices containing ARC were prepared using a vibroslicer (Campden Instruments, Loughborough, UK) and transferred into an incubation chamber filled with cutting solution to rest at room temperature. Slices were then transferred to aCSF, comprising of (in mM): 127 NaCl, 1.8 KCl, 1.2 KH_2PO_4, 1.3 $MgSO_4$, 26 $NaHCO_3$, 5 Glucose, 5 Sucrose and 2.4 $CaCl_2$.

Intracellular solution was identical to that previously described in Results chapter 1 and 2 and contained (in mM): 130 K-gluconate, 10 KCl, 2mM $MgCl_2$, 10 Hepes, 0.5 EGTA, 2 K_2ATP and 0.5 NaGTP (Belle et al., 2009). Visually guided whole-cell recordings were performed while targeting ARC NPY-hrGFP neurons by epifluorescence. Location was recorded by capturing live images with a Hamamatsu Orca R^2 camera system (Hamamatsu Photonics, Tohoku, Japan) during recordings and by filling cells with biocytin for post-recording immunohistochemistry. An npi BA-03X amplifier in bridge configuration (npi electronics, Tamm, Germany), compensating for the transient capacitance of the pipette, and a CED 1401 mark II A/D data acquisition interface (Cambridge Electronic Design, Cambridge, United Kingdom) were used to record current clamp data.

Recordings were sampled (30kHz) and analysed in Spike 2 Version 7 (Cambridge Electronic Design, Cambridge, United Kingdom). Microsoft Excel was used to store data and Origin version 9.0 was used for statistical analysis and figures (OriginLab Corporation, Ma, USA). Representative traces displayed in figures were exported directly from Spike 2 as image files.

Basic electrical states of NPY-hrGFP neurons were defined as either depolarised silent, firing or hyperpolarised silent. Firing cells generate APs whereas depolarised silent and hyperpolarised silent cells rest above and below (respectively) the threshold AP formation. Variation in the proportion of electrical states or firing regularity (coefficient of variance (C.V.) <0.35 for regular firing) were analysed by Fisher's exact-test ($p<0.05$).

Ghrelin 100nM (Tocris Bioscience, Bristol, UK) was bath applied for 1min. Responses were defined as a ±2mV change in RMP between a 10s window of baseline prior to application and 10s of stable activity 30s or 90s after the end of the application. Individual responses to ghrelin were quantified in Spike 2 and compiled to calculate average responses in Origin 9.

Synaptic event frequency was measured using an Axopatch 200b amplifier (Molecular Devices, Cal, USA). The internal solution was identical to the one used in current clamp recordings, except for 120mM K-gluconate and 20KCl mM causing a positive shift in the Cl- reversal potential. All postsynaptic currents (PSCs) appeared as inward current at -70mV therefore receptor antagonists (AP5 at 50µM/CNQX at 10µM, Tocris Bioscience, Bristol, UK) for the glutamate receptors and $GABA_A$ receptor (Gabazine, Tocris) were applied to calculate respective frequency offline in pClamp 10.2 (Clampex and Clampfit). TTX (1µM, Tocris) was applied to discriminate between PSCs arising from AP-dependent synaptic communication and spontaneous quantal release of neurotransmitter (miniature PSCs). Signals were acquired using pClamp 10.2 (Clampex and Clampfit) in conjunction with a Digidata 1440A interface (Molecular Devices). Day-night changes in PSC frequency and amplitude were statistically analysed in Origin 9.

Immunohistochemistry

After the recording session, slices were post-fixed in ice-cold 4% paraformaldehyde diluted in fresh 0.1M PBS (pH 7.4). After 24h the slices were then transferred to 0.1M PBS alone for storage prior to immunohistochemistry (max. 3days). Slices were then transferred to a fresh culture plate and washed with PBS prior to incubation in Triton-X 100 (0.6% in PBS;10% normal donkey serum) for 3h at room temperature. Slices were then placed into a solution containing Cy3-conjugated Extravidin (1:250 in PBS, Sigma-Aldrich, USA) and rabbit anti-GFP primary antibody (1:1000, Abcam, UK) in PBS, 2% NDS

and 0.3% Triton-X 100 and incubated at 4°C in darkness for 1-3 days. Following this, slices were transferred to a secondary antibody solution containing a CY5 anti-rabbit antibody (1:800, Jackson ImmunoResearch, USA) and incubated at 4°C overnight. The following morning, slices were washed in PBS and mounted onto gelatine-coated slides for image capture. Images were captured using a Leica SP5 Upright confocal microscope at 20x or 63x magnification (Leica systems, Wetzlar, Germany).

Results

The ARC of NPY-hrGFP mice consistently displayed anti-GFP fluorescence in cells clustered in the medial portion of ARC near to the wall of the third ventricle. Intense fluorescence was evident throughout the cell soma and in proximal dendritic projections (Fig1). NPY-hrGFP cells were also sparely distributed throughout the VMH but not in the DMH. The brightness of the NPY-hrGFP cells was particularly useful during whole-cell recordings as single GFP-positive neurons were clearly distinguishable from GFP-negative cells. To further examine the morphology of NPY-hrGFP cells, recording pipettes used for whole-cell recording were filled with biocytin which diffuses into the soma and proximal processes. Between 2-3 proximal dendritic appendages per cell were labelled by biocytin. Intriguingly, unilateral recording and filling of GFP-negative cells resulted in multiple faintly stained cells as far as 200µm from neurons which were originally filled (Fig1C,H). This phenomenon was not observed in unilateral ARC when NPY-hrGFP neurons were filled with biocytin (Fig1C,D). Biocytin is well-known to transfer at gap junctions after somal filling (Bennett and Zukin, 2004), therefore these faint cells likely represent ARC neurons or glial cells which are electrically coupled to GFP-negative cells. The merged image clearly shows that these secondary cells are not NPY-hrGFP neurons.

Electrophysiological characteristics of NPY-hrGFP neurons

Targeted whole-cell recordings were performed on ARC NPY-hrGFP neurons during the day and night, at ZT4-10 and ZT14-20 respectively. The electrical behaviours exhibited by these neurons can be divided into three categories: depolarised silent, firing and hyperpolarised silent (Fig2A). Depolarised silent and hyperpolarised NPY-hrGFP neurons do not fire APs and rest at less negative (mean RMP, -30.2mV, n=4) and more negative (-

58mV, n=7) potentials than are required for AP generation respectively. A small proportion of all NPY-hrGFP neurons exhibited the depolarised silent state at rest across the daily cycle (4/35, 11%). However, manual hyperpolarisation with current injection was able to elicit AP firing in depolarised silent NPY-hrGFP neurons. NPY-hrGFP electrophysiology can be further subdivided at the level of firing neurons (mean RMP -38.3mV), which can be categorised as regular firing, irregular firing without bursts and burst firing (Fig2A,B). These bursting neurons were characterised by short and irregular increases in firing rate every few seconds and have previously been described in NPY-hrGFP neurons (van den Pol et al., 2009).

Firing regularity was determined by calculating the coefficient of variance (C.V.) of the interspike interval (ISI). NPY-hrGFP neurons with a baseline C.V. of <0.35 were considered regular firing. Neurons that generated APs with a regular pattern (Day, 1/16; Night, 1/19, Fig2F) typically fired with a high frequency (>3.5Hz) relative to the population mean firing rate during the day or night (<2Hz, Fig2D). Of the three firing phenotypes, the highest proportion was occupied by those that generate APs with an irregular pattern without bursting (Day, 6/16, 38%; Night, 8/19, 42%) followed by burst firing neurons which made up approximately a quarter of the total cells (Day, 4/16, 25%; Night, 4/19, 21%). Based on the population mean SFR during the day and night (n=11/16, 1.12 ± 0.28Hz; n=13/19, 1.85 ± 0.55Hz respectively) ARC NPY-hrGFP neurons did not show a daily variation in SFR (two-sample t-test, p=0.28). We postulated that this may be due to heterogeneity of states within the sample, however when just irregular firing cells were taken for analysis no daily variation was detected (p=0.081), although the comparison did show a trend that was near to statistical significance.

From a total of 16 ARC NPY-hrGFP recorded during the day and 19 at night, no daily variation in RMP (Day, -39.92 ± 3.17mV; Night, -36.6mV ± 1.18mV, p=0.33) was observed within our time points. R_{input} also remained consistent between the day (n=8, 1.7 ± 0.45GΩ) and night (n=14, 1.63 ± 0.16mV, p=0.85). The overall proportion of the 5 states was also unchanged between the day and night time epochs (Fisher's exact-test, p=0.56, Fig2F). Collectively, these findings suggest that neither the circadian clock nor other factors within the slice influence the temporal pattern of excitability in NPY-hrGFP neurons.

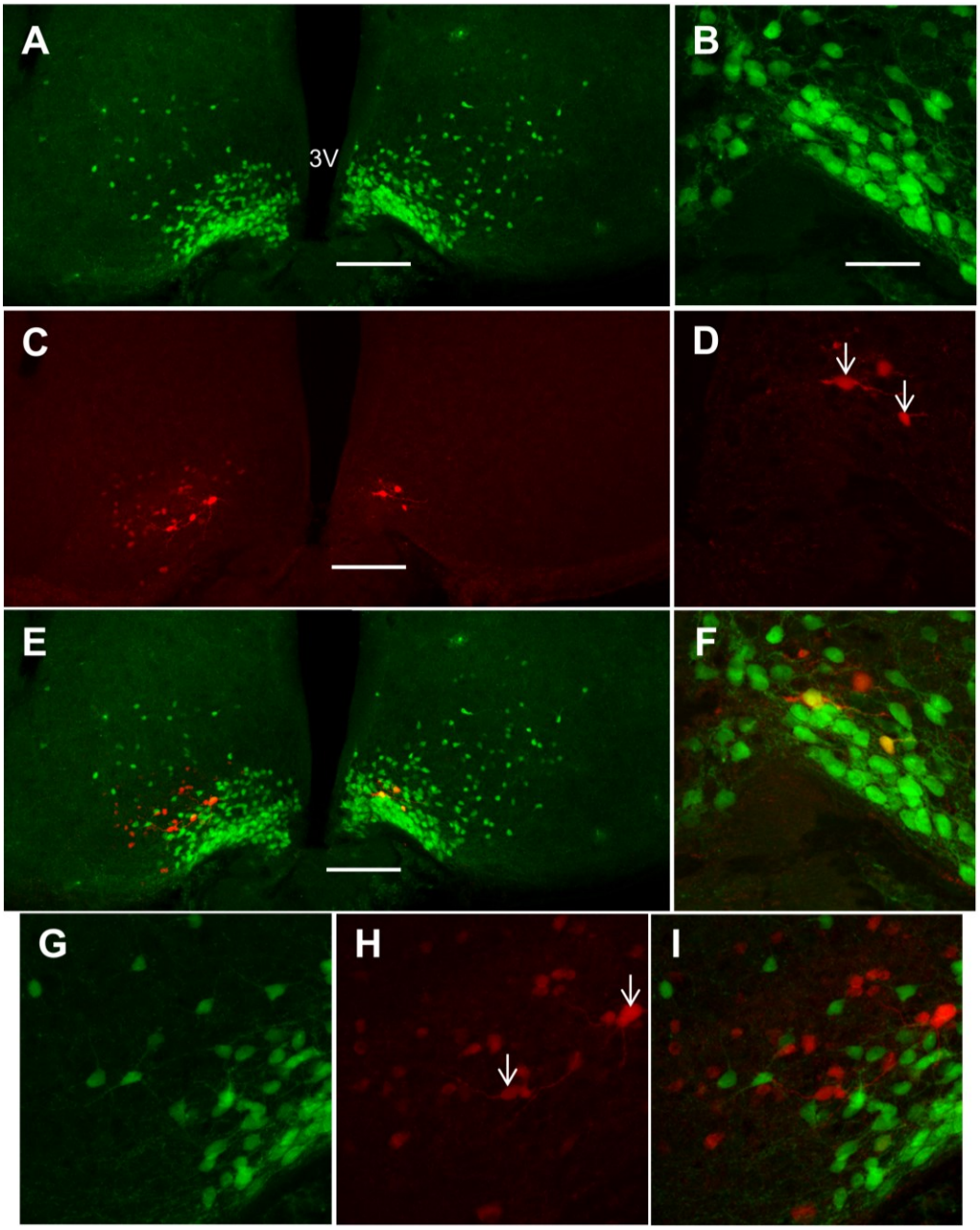

Figure 1: NPY-hrGFP neurons are densely clustered in the ventromedial portion of the ARC: A: Anti-GFP staining reveals a dense plexus of NPY-hrGFP neurons (green) in ARC near the third ventricle (3V). 20x. Scale bar 200µm. **B:** Higher magnification images (63x) of show densely packed NPY-hrGFP neuron soma and processes. Scale bar 50µm **C:** NPY-hrGFP neurons were filled with biocytin and labelled with conjugated extravidin-CY3. A few GFP-ve neurons (left side of 3V) were also targeted and filled for comparison. **D:** Biocytin staining demarcates the soma, axonal and dendritic processes of two NPY-hrGFP neurons. Those marked by arrows were targeted for whole-cell recording of electrical activity. A single GFP-ve cell that was not recorded from was filled, located between and dorsal to the two NPY-hrGFP neurons. **E:** Composite image of NPY-hrGFP neurons (green) and biocytin-filled neurons (red). **F:** Yellow indicates overlap between GFP labelling and biocytin. **G-I:** On one side of the ARC recordings were performed on two GFP-ve neurons only (left of 3V). Interestingly, filling of neurons that do not express NPY-hrGFP (arrows) resulted in multiple cells faintly exhibiting biocytin staining in their soma. This phenomenon is likely to occur due to diffusion of biocytin across gap-junctions and was not evident in unilateral ARC following targeting of NPY-hrGFP neurons (D).

Ghrelin depolarises a subset of ARC NPY-hrGFP neurons

Peripheral signals involved in the maintenance of energy homeostasis have long been shown to modulate the electrical activity of ARC NPY neurons. Ghrelin, an orexigenic peptide hormone predominantly produced in the stomach, is also produced by central neurons which contact the cell soma and dendrites of NPY/AgRP neurons in the ARC (Cowley et al., 2003). Here, we tested whether ghrelin (100nM) elicits changes in neuronal excitability when bath-applied onto ARC-slices from NPY-hrGFP mice. For the analysis we pooled data from the day and night epochs giving a total of 10 cells that were tested with ghrelin.

1min application of ghrelin (100nM) evoked sustained depolarisation in a small subset of NPY-hrGFP neurons (3/10) tested in this study. 90s after the end of ghrelin application, responsive neurons reached a steady state of depolarisation (9.4 ± 1.2mV). The excitatory effect of ghrelin was rapid and cells were depolarised 30s after the application was complete (Fig3B). However, while SFR was elevated 30s after ghrelin application, responsive neurons entered depolarisation block and exhibited smaller (~ suprathreshold spikes at a frequency equivalent to that prior to application (Fig3C). Thus *in vitro,* ghrelin produced paradoxical effects that resulted in unchanged spiking frequency. The remaining NPY-hrGFP neurons tested with ghrelin (7/10) did not respond with changes in RMP or SFR (response defined as ±2mV). The concentration of ghrelin used in this study is well in excess of physiologically relevant levels (Bednarek et al., 2000). Thus, our data suggests that the whole animal orexigenic effects of ghrelin such as increased food intake and adiposity are not imposed by a ubiquitous increase in the excitability of ARC NPY neurons.

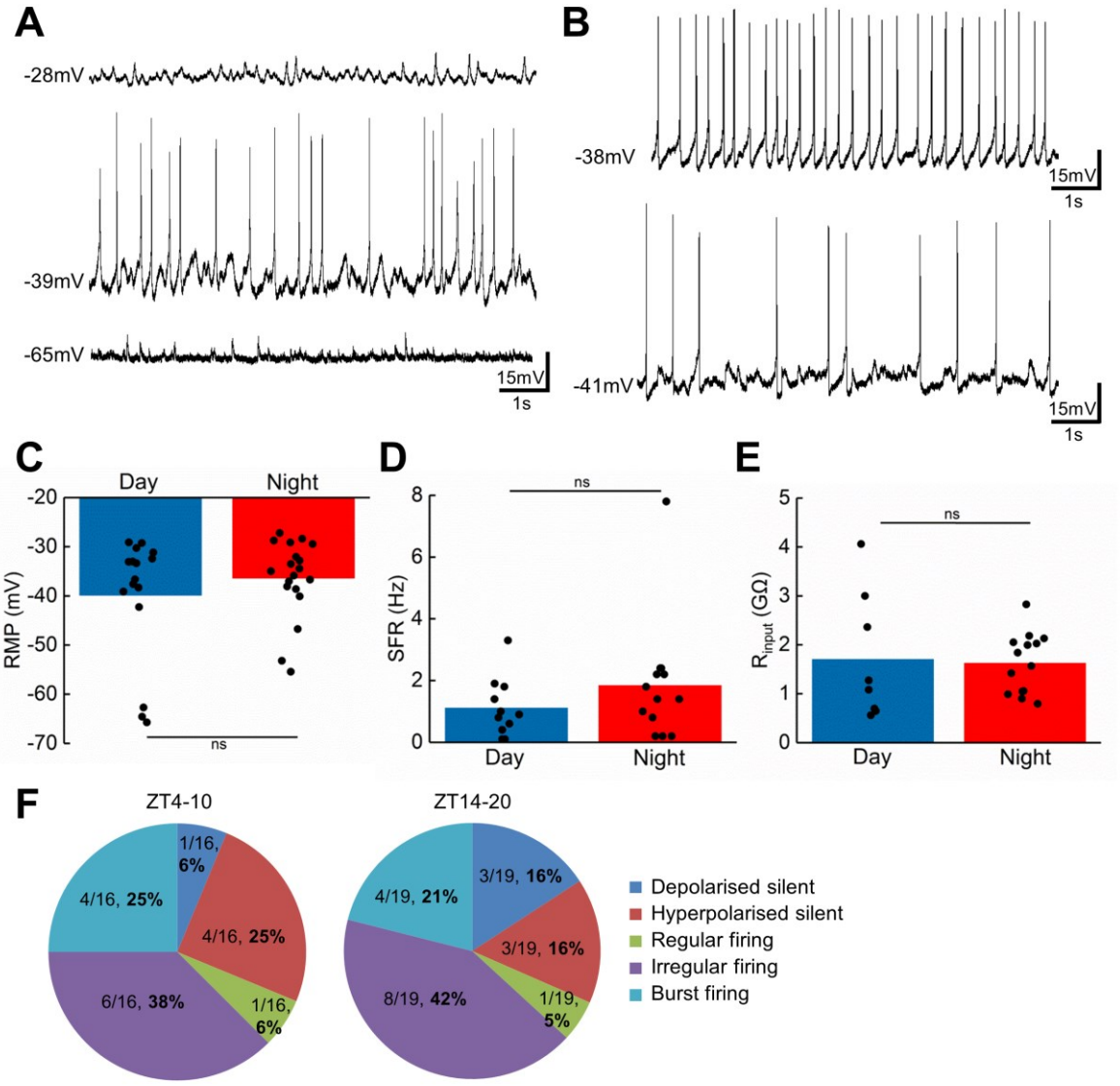

Figure 2: ARC NPY-hrGFP neurons exhibit an array of electrical behaviours. NPY-hrGFP neurons were targeted for whole-cell recordings during the day (ZT4-10) and night (ZT14-20) and displayed 5 distinct electrical behaviours. **A:** NPY-hrGFP neurons exhibit either depolarised silent (top), firing or hyperpolarised silent electrical states. ~25% of NPY-hrGFP neurons recorded during the day or night display bursting behaviour (middle). **B:** Regular firing (top) and irregular firing pattern of NPY-hrGFP neurons without bursting. **C-E:** Membrane parameters RMP, SFR and R_{Input} remain consistent between day and night (two-sample t-test, $p>0.28$). Each dot corresponds to an individual neuron. **F:** The proportion of each electrical behaviour also did not vary across the day-night cycle (Fishers exact test, $p=0.56$).

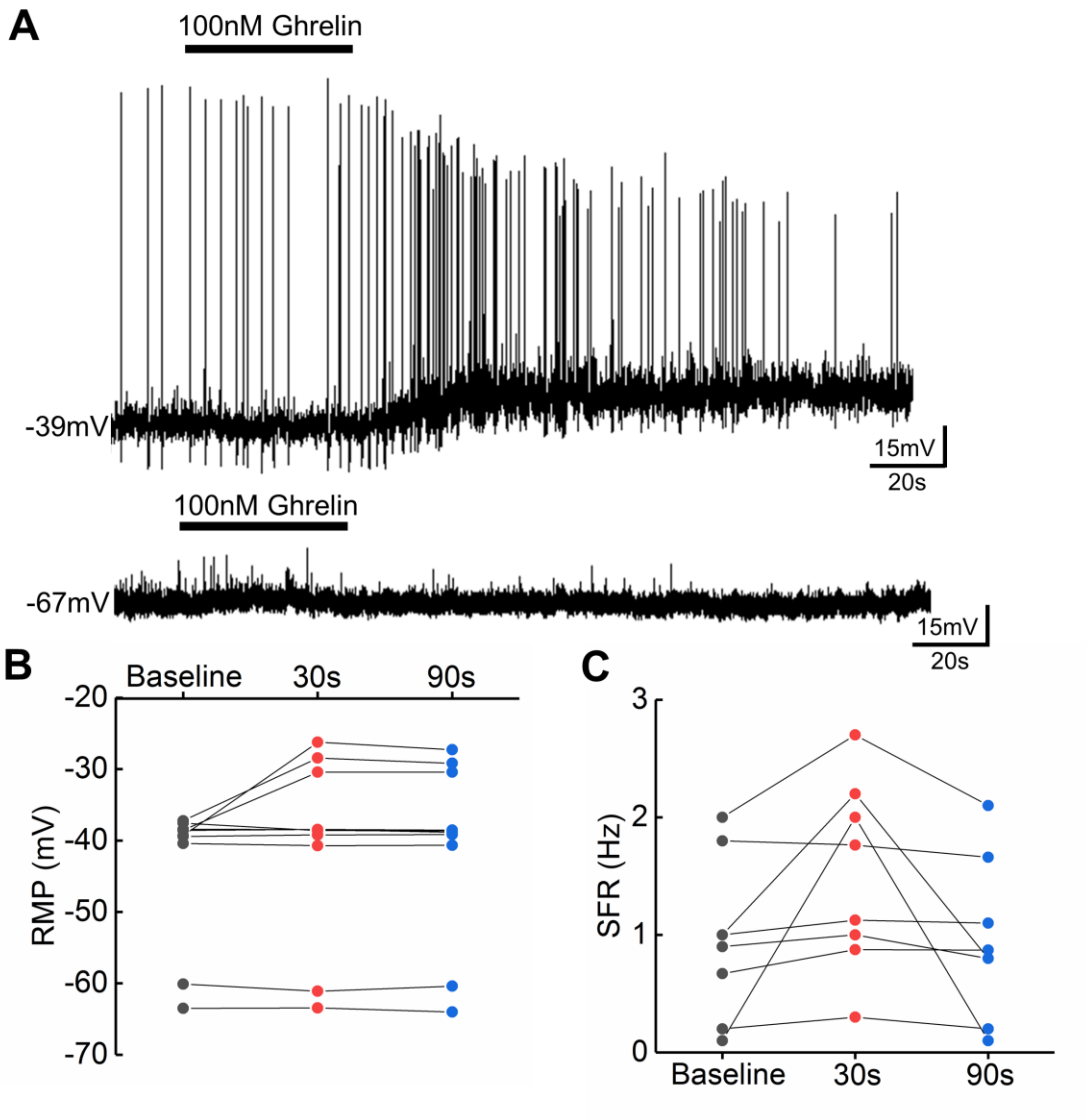

Figure 3: NPY-hrGFP ARC neurons are excited by ghrelin. A: Representative whole-cell recordings made from NPY-hrGFP neurones in the presence of ghrelin (100nM) during both the day and night (ZT4-10 or ZT14-20 respectively). Bath-application (1min) induced excitation of electrical activity in some of the tested neurons (3/10). The remaining 7 neurons did not respond to ghrelin (±2mV). **B:** Line series showing RMP value for each NPY-hrGFP neuron prior to (baseline) and after ghrelin application. 10s recording segments were analysed 30s and 90s after offset of application. RMP was significantly elevated in 3 neurons. **C:** Spontaneous firing rate (SFR) was elevated 30s after the offset of ghrelin application. However after 90s SFR was reduced due to depolarisation of the recorded cell above the threshold for AP firing.

Synaptic communication to NPY-hrGFP neurons *in vitro* does not depend on action potential-evoked neurotransmitter release

To assess whether the extent of network communication to ARC NPY-hrGFP neurons differs across the diurnal cycle we performed synaptic event recordings during the day (ZT4-10) and night (ZT14-20). Recordings were performed at a holding potential of -70mV and in these recordings all events appeared as inward postsynaptic currents (PSCs). The origin of PSCs was determined by application of AP5 (50μM)/CNQX(10μM) or Gabazine (20μM) to block glutamatergic and GABAergic PSCs respectively (Fig4A). In this case, glutamatergic PSCs were assumed excitatory (EPSCs) whereas GABAergic were deemed inhibitory (IPSCs).

NPY-hrGFP neurons received a roughly equivalent number of EPSCs and IPSCs during the day and night (~1Hz). EPSC frequency did not vary across the daily cycle (Day, 1.14 ± 0.32Hz, n=4; Night, 1.23 ± 0.21Hz, n=4 two-sample t-test, p=0.23). Similarly, time of day did not affect the frequency of GABAergic IPSCs, which remained at a similar frequency during the day (0.84 ± 0.21Hz, n=4) and night (0.95 ± 0.32, n=4, p=0.28). After the application of all antagonists all events exceeding 5pA were blocked.

To assess whether PSCs evoked in NPY-hrGFP neurons depend on AP-dependent synaptic communication we performed a comparative analysis between PSC frequency at baseline and following TTX application. 10s segments of data were taken at 30s intervals at baseline, during and after application. Interestingly, TTX did not evoke any changes in overall PSC frequency in two cells which were tested with a 1min bath-application (Fig4C). In both cells, PSC frequency 3min after the end of TTX actually exceeded that prior to application, however this is likely due to natural variation. Therefore, this data suggests that glutamatergic and GABAergic signalling to NPY-hrGFP neurons *in vitro* is solely mediated by spontaneous neurotransmitter release and not by AP-evoked release.

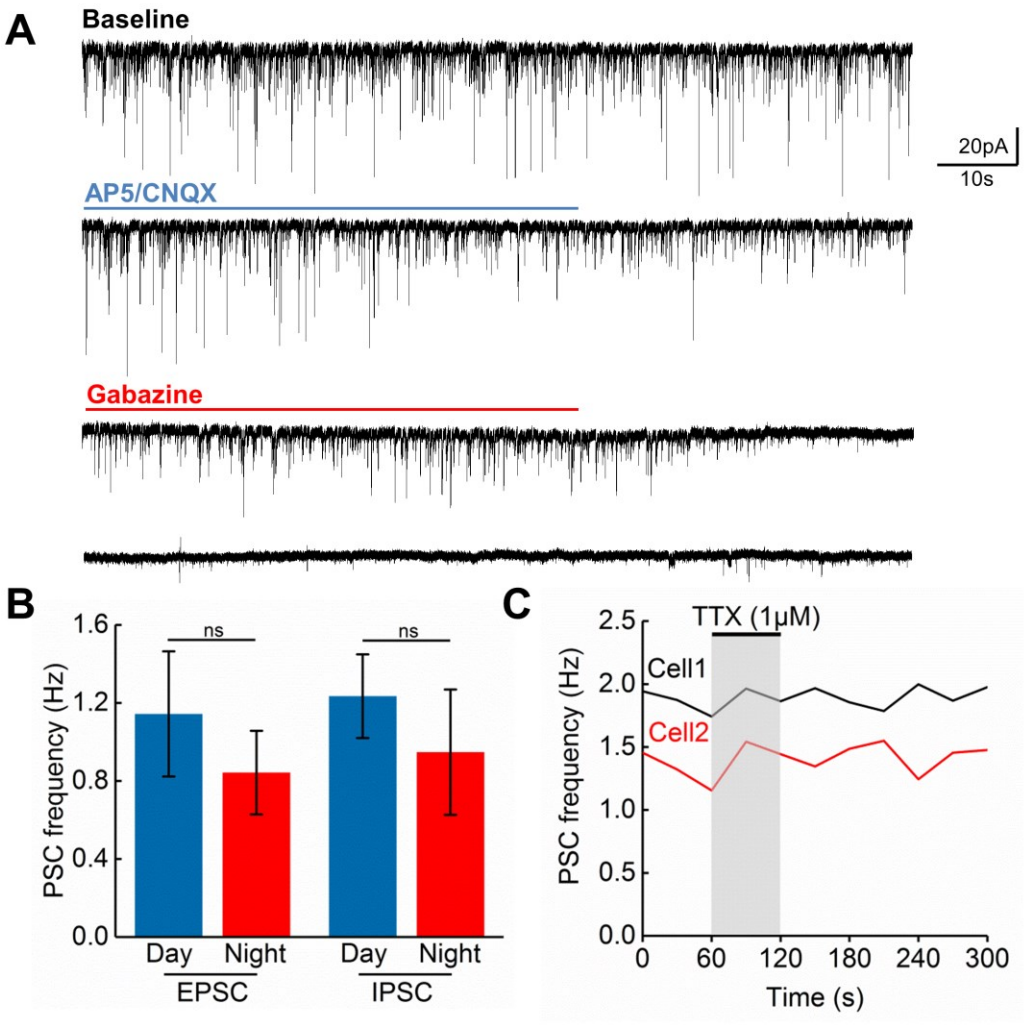

Figure 4: TTX does not influence the frequency of synaptic events received by NPY-hrGFP neurons. A: Representative voltage clamp trace depicting the time course of a typical recording at a holding potential of -70mV. Here, both glutamatergic EPSCs and GABAergic IPSCs appear as inward currents which can be distinguished by application of AP5 (50µM):CNQX(10µM) or Gabazine (20µM). After sufficient data was captured to assess baseline PSC frequency, antagonists were applied in series for 1min. Each cocktail of antagonists were interspersed with at least 30s. Application of all antagonists removed all PSCs (>5pA). **B:** NPY-hrGFP neurons receive approximately the same frequency of EPSCs and IPSCs. The frequency of EPSCs was not changed from day (n=4) to night (n=4, two-sample t-test, p=0.23). IPSC frequency was also unaffected by time of day (p=0.28). Error bars indicate SEM. **C:** TTX (1µM, 1min application across shaded grey area) did not affect PSC frequency of 2 NPY-hrGFP cells tested. This demonstrates that synaptic events were not dependent on the generation of APs.

Discussion

The distribution of NPY neurons here closely matches that reported for adult mice in previous literature, with a dense collection of cells clustered near to the third ventricle (van den Pol et al., 2009, Hassouna et al., 2013, Cains et al., 2017). The fidelity of GFP

expression in NPY neurons in the NPY-hrGFP mouse has been prior tested with antisera against NPY and AgRP peptides, which are exclusively colocalised in ARC NPY/AgRP neurons. Immunostaining for NPY reveals that NPY cell bodies also express GFP in the NPY-hrGFP mouse. AgRP staining also colocalises with GFP therefore demonstrating that NPY-hrGFP neurons in this case, also express AgRP (van den Pol et al., 2009). We successfully filled and stained NPY-hrGFP neurons with biocytin, which diffuses throughout the cell during whole-cell recording. Intriguingly, we found that filling GFP-negative neurons resulted in staining of faint cell bodies throughout the ARC, which in some cases stained cells as far as 200µm from the recording sites. None of these faint cells expressed NPY-hrGFP and filling of NPY-hrGFP in ARC unilaterally did not result in secondary filling and the appearance of faint cells.

Biocytin is a small molecule and is well-known to diffuse across gap junctions which mediate electrical coupling between neighbouring neurons and glia (Bennett and Zukin, 2004). The importance of gap junctions in mediated synchronised electrical activity has been established in several brain regions, yet the hypothalamus has received relatively little attention (Connors and Long, 2004). In rat, a population of ARC neurons that express tyrosine-hydroxylase (TH), the so called hypothalamic tuberoinfundibular dopamine (TIDA) neurons, display highly-synchronised phasic electrical activity which disappears following application of carbenoxolone, a drug which blocks gap junctions (Lyons et al., 2010). Similar oscillations have been reported in mouse TH and NPY/AgRP neurons however these did not depend on gap junctions (Zhang and van den Pol, 2016, van den Top et al., 2004). These results presented here suggest that non-NPY ARC neurons may form a network of electrically coupled cells in ARC. However, the neurochemical phenotype and electrical signatures of these neurons was not investigated here, thus the physiological importance of this finding is currently unclear.

We found 5 distinct electrical behaviours were exhibited by NPY-hrGFP neurons. A subset of NPY-hrGFP neurons were hyperexcitable and rested at such depolarised RMPs that they were unable to generate APs, hence termed depolarised silent. This state has not previously been described in ARC NPY-hrGFP neurons, most likely due to rejection by assumption that these neurons display depolarised silent behaviours due to unhealthy cellular conditions in the slice environment or as a result of the patch-clamp procedure.

Indeed, we found that in some cases 'unhealthy' neurons did rest at depolarised potentials, however these neurons failed to generate APs when manually hyperpolarised. All depolarised silent NPY-hrGFP neurons analysed in this results chapter were able to generate APs upon negative current injection.

Aside from depolarised states, the membrane parameters of ARC NPY-hrGFP neurons presented in this study are broadly consistent with those outlined in previous reports on adult male mice. NPY-hrGFP neurons in the ARC rested from -67 to -29mV however mean RMP (Day, -39.92mV; Night, -36.6mV) was elevated with respect to a number of studies which show firing behaviour in NPY-hrGFP neurons at approximately -60mV (Briggs et al., 2014, van den Pol et al., 2009(Krashes, 2013 #113, Paeger et al., 2017). However, a some studies show mean RMP closer to -40mV, which closely resembles the mean RMP during the day and night in this study (Cains et al., 2017, Huang et al., 2018). The likely explanation for this is variation in the intracellular and extracellular conditions during *in vitro* recordings between each study. Also, here we corrected for the liquid junction potential live during the recording process, where as it is possible that other groups adjusted RMP values for each cell negatively by calculating the potential between the intracellular and extracellular solutions.

The peptide hormone ghrelin is important for homeostatic eating behaviours and exerts its orexigenic actions mainly via binding to the only known ghrelin receptor, growth hormone secretagogue receptor (GHS-R) (Howard et al., 1996, Kojima et al., 1999). The long form of the GHS-R, type 1a, is highly expressed in ARC NPY neurons (Willesen et al., 1999, Mondal et al., 2005), which are essential for ghrelin-induced increases in food intake (Chen et al., 2004, Nakazato et al., 2001, Shintani et al., 2001). Ghrelin is reported to activate NPY neurons via indirect presynaptic stimulation and multiple direct ionic mechanisms, however the ion channels mediating this remain unclear (Hashiguchi et al., 2017).

Here, we found that ghrelin (100nM) evoked sustained (>20mins) depolarising effects which drove NPY-hrGFP neurons to enter depolarisation block. While other studies show that a ubiquitous range of ARC NPY neurons are excited by ghrelin (Cowley et al., 2003, Hashiguchi et al., 2017), we found that 7/10 NPY-hrGFP neurons tested with a high

concentration of ghrelin did not respond with any changes in neuronal excitability. These differences may reflect the complexity of the mechanisms by which ghrelin may activate ARC NPY neurons. Indeed, our findings suggest that a sub-population of ARC NPY neurons may play more dominant roles in regulated the orexigenic actions of ghrelin.

The circadian regulation of ARC NPY/AgRP neuronal activity requires thorough investigation. In awake, freely-feeding mice, NPY/AgRP neurons increase their spike rate during the afternoon compared to the morning, parallel to mounting caloric deficit (Mandelblat-Cerf et al., 2015). AgRP neurons have also been shown to increase firing 4h after lights-off compared to the morning (Krashes et al., 2013). The rate by which ARC NPY-hrGFP neurons generate APs and the presence of burst firing neurons was consistent with previous studies (van den Pol et al., 2009, Cains et al., 2017, Krashes et al., 2013, Takahashi and Cone, 2005). However, we did not observe any daily variation in the frequency of AP generation in NPY-hrGFP neurons. The discrepancy between this and the findings of others is unclear as our recording epochs lie within at equivalent times under light-dark conditions (Krashes et al., 2013). Perhaps, this is due to the fact that we looked at an extended period of the day and night and not solely at a particular hour. RMP and R_{input} also remained constant suggesting that neither circulating clock genes or rhythmic synaptic inputs induce temporal changes in electrical activity of NPY-hrGFP neurons (Guilding et al., 2009).

Glutamatergic and GABAergic synaptic communication to ARC neurons is an essential component of appetite homeostasis (Liu et al., 2012, Vong et al., 2011, Garfield et al., 2016). Consistent with previous reports we found that synaptic signals received by NPY-hrGFP neurons persist in the presence of TTX and therefore do not depend on the presence of APs (Pinto et al., 2004, Baquero et al., 2015). NPY-hrGFP neurons did not receive glutamatergic or GABAergic events with a different frequency from day to night. Therefore, the results presented here suggest that the temporal pattern of NPY-hrGFP neurons is not shaped by the any factor within the slice - that being either the local clock which is internally expressed in ARC NPY/AgRP neurons or input from any other rhythmic region in the slice.

Food intake in rodents is mainly partitioned to the dark phase of the light-dark cycle (Armstrong et al., 1980). Evidence suggests that NPY/AgRP neurons are a critical component in the pathway by which the circadian system regulates the partitioning of feeding to the inactive phase in rodents. Targeted destruction of ARC NPY neurons by injection of a NPY-Saporin conjugate results in loss of feeding rhythms (Wiater et al., 2011). Also, deletion of NPY receptors (Y2 or Y4) results in abnormal daily patterns in locomotor activity and food intake (Edelsbrunner et al., 2009). The SCN communicates with ARC through both direct and indirect neural projections (Saeb-Parsy et al., 2000). Although it is not clear exactly how they interact, here we postulate that SCN to NPY/AgRP neuron connectivity is important for regulating the timing of feeding. However, as ARC NPY/AgRP neurons influence feeding across multiple timescales due to co-release of multiple orexigenic factors (Krashes et al., 2013), and as the SCN is also likely to indirectly interact with NPY/AgRP neurons, it is apparent that the temporal regulation of timing of food intake is a complex process that requires further investigation.

References

ALLEN, L. G., KALRA, P. S., CROWLEY, W. R. & KALRA, S. P. 1985. Comparison of the effects of neuropeptide Y and adrenergic transmitters on LH release and food intake in male rats. *Life Sci,* 37**,** 617-23.

ANDERMANN, M. L. & LOWELL, B. B. 2017. Toward a Wiring Diagram Understanding of Appetite Control. *Neuron,* 95**,** 757-778.

APONTE, Y., ATASOY, D. & STERNSON, S. M. 2011. AGRP neurons are sufficient to orchestrate feeding behavior rapidly and without training. *Nat Neurosci,* 14**,** 351-5.

ARMSTRONG, S., COLEMAN, G. & SINGER, G. 1980. Food and water deprivation: changes in rat feeding, drinking, activity and body weight. *Neurosci Biobehav Rev,* 4**,** 377-402.

ATASOY, D., BETLEY, J. N., SU, H. H. & STERNSON, S. M. 2012. Deconstruction of a neural circuit for hunger. *Nature,* 488**,** 172-7.

BAGNOL, D., LU, X. Y., KAELIN, C. B., DAY, H. E., OLLMANN, M., GANTZ, I., AKIL, H., BARSH, G. S. & WATSON, S. J. 1999. Anatomy of an endogenous antagonist: relationship between Agouti-related protein and proopiomelanocortin in brain. *J Neurosci,* 19**,** RC26.

BAQUERO, A. F., KIRIGITI, M. A., BAQUERO, K. C., LEE, S. J., SMITH, M. S. & GROVE, K. L. 2015. Developmental changes in synaptic distribution in arcuate nucleus neurons. *J Neurosci,* 35**,** 8558-69.

BEDNAREK, M. A., FEIGHNER, S. D., PONG, S. S., MCKEE, K. K., HRENIUK, D. L., SILVA, M. V., WARREN, V. A., HOWARD, A. D., VAN DER PLOEG, L. H. & HECK, J. V. 2000.

Structure-function studies on the new growth hormone-releasing peptide, ghrelin: minimal sequence of ghrelin necessary for activation of growth hormone secretagogue receptor 1a. *J Med Chem,* 43**,** 4370-6.

BEGG, D. P. & WOODS, S. C. 2013. The endocrinology of food intake. *Nat Rev Endocrinol,* 9**,** 584-97.

BELLE, M. D., DIEKMAN, C. O., FORGER, D. B. & PIGGINS, H. D. 2009. Daily electrical silencing in the mammalian circadian clock. *Science,* 326**,** 281-4.

BENNETT, M. V. & ZUKIN, R. S. 2004. Electrical coupling and neuronal synchronization in the Mammalian brain. *Neuron,* 41**,** 495-511.

BRIGGS, D. I., LOCKIE, S. H., BENZLER, J., WU, Q., STARK, R., REICHENBACH, A., HOY, A. J., LEMUS, M. B., COLEMAN, H. A., PARKINGTON, H. C., TUPS, A. & ANDREWS, Z. B. 2014. Evidence that diet-induced hyperleptinemia, but not hypothalamic gliosis, causes ghrelin resistance in NPY/AgRP neurons of male mice. *Endocrinology,* 155**,** 2411-22.

CAINS, S., BLOMELEY, C., KOLLO, M., RACZ, R. & BURDAKOV, D. 2017. Agrp neuron activity is required for alcohol-induced overeating. *Nat Commun,* 8**,** 14014.

CHEN, H. Y., TRUMBAUER, M. E., CHEN, A. S., WEINGARTH, D. T., ADAMS, J. R., FRAZIER, E. G., SHEN, Z., MARSH, D. J., FEIGHNER, S. D., GUAN, X. M., YE, Z., NARGUND, R. P., SMITH, R. G., VAN DER PLOEG, L. H., HOWARD, A. D., MACNEIL, D. J. & QIAN, S. 2004. Orexigenic action of peripheral ghrelin is mediated by neuropeptide Y and agouti-related protein. *Endocrinology,* 145**,** 2607-12.

CONNORS, B. W. & LONG, M. A. 2004. Electrical synapses in the mammalian brain. *Annu Rev Neurosci,* 27**,** 393-418.

COWLEY, M. A., PRONCHUK, N., FAN, W., DINULESCU, D. M., COLMERS, W. F. & CONE, R. D. 1999. Integration of NPY, AGRP, and melanocortin signals in the hypothalamic paraventricular nucleus: evidence of a cellular basis for the adipostat. *Neuron,* 24**,** 155-63.

COWLEY, M. A., SMART, J. L., RUBINSTEIN, M., CERDAN, M. G., DIANO, S., HORVATH, T. L., CONE, R. D. & LOW, M. J. 2001. Leptin activates anorexigenic POMC neurons through a neural network in the arcuate nucleus. *Nature,* 411**,** 480-4.

COWLEY, M. A., SMITH, R. G., DIANO, S., TSCHOP, M., PRONCHUK, N., GROVE, K. L., STRASBURGER, C. J., BIDLINGMAIER, M., ESTERMAN, M., HEIMAN, M. L., GARCIA-SEGURA, L. M., NILLNI, E. A., MENDEZ, P., LOW, M. J., SOTONYI, P., FRIEDMAN, J. M., LIU, H., PINTO, S., COLMERS, W. F., CONE, R. D. & HORVATH, T. L. 2003. The distribution and mechanism of action of ghrelin in the CNS demonstrates a novel hypothalamic circuit regulating energy homeostasis. *Neuron,* 37**,** 649-61.

DENIS, R. G., JOLY-AMADO, A., WEBBER, E., LANGLET, F., SCHAEFFER, M., PADILLA, S. L., CANSELL, C., DEHOUCK, B., CASTEL, J., DELBES, A. S., MARTINEZ, S., LACOMBE, A., ROUCH, C., KASSIS, N., FEHRENTZ, J. A., MARTINEZ, J., VERDIE, P., HNASKO, T. S., PALMITER, R. D., KRASHES, M. J., GULER, A. D., MAGNAN, C. & LUQUET, S. 2015. Palatability Can Drive Feeding Independent of AgRP Neurons. *Cell Metab,* 22**,** 646-57.

DUBE, D., LISSITZKY, J. C., LECLERC, R. & PELLETIER, G. 1978. Localization of alpha-melanocyte-stimulating hormone in rat brain and pituitary. *Endocrinology,* 102**,** 1283-91.

EDELSBRUNNER, M. E., PAINSIPP, E., HERZOG, H. & HOLZER, P. 2009. Evidence from knockout mice for distinct implications of neuropeptide-Y Y2 and Y4 receptors in

the circadian control of locomotion, exploration, water and food intake. *Neuropeptides,* 43**,** 491-7.

FAN, W., BOSTON, B. A., KESTERSON, R. A., HRUBY, V. J. & CONE, R. D. 1997. Role of melanocortinergic neurons in feeding and the agouti obesity syndrome. *Nature,* 385**,** 165-8.

FENSELAU, H., CAMPBELL, J. N., VERSTEGEN, A. M., MADARA, J. C., XU, J., SHAH, B. P., RESCH, J. M., YANG, Z., MANDELBLAT-CERF, Y., LIVNEH, Y. & LOWELL, B. B. 2017. A rapidly acting glutamatergic ARC-->PVH satiety circuit postsynaptically regulated by alpha-MSH. *Nat Neurosci,* 20**,** 42-51.

GARFIELD, A. S., SHAH, B. P., BURGESS, C. R., LI, M. M., LI, C., STEGER, J. S., MADARA, J. C., CAMPBELL, J. N., KROEGER, D., SCAMMELL, T. E., TANNOUS, B. A., MYERS, M. G., JR., ANDERMANN, M. L., KRASHES, M. J. & LOWELL, B. B. 2016. Dynamic GABAergic afferent modulation of AgRP neurons. *Nat Neurosci,* 19**,** 1628-1635.

GOLD, R. M., JONES, A. P. & SAWCHENKO, P. E. 1977. Paraventricular area: critical focus of a longitudinal neurocircuitry mediating food intake. *Physiol Behav,* 18**,** 1111-9.

GRAHAM, M., SHUTTER, J. R., SARMIENTO, U., SAROSI, I. & STARK, K. L. 1997. Overexpression of Agrt leads to obesity in transgenic mice. *Nat Genet,* 17**,** 273-4.

GROPP, E., SHANABROUGH, M., BOROK, E., XU, A. W., JANOSCHEK, R., BUCH, T., PLUM, L., BALTHASAR, N., HAMPEL, B., WAISMAN, A., BARSH, G. S., HORVATH, T. L. & BRUNING, J. C. 2005. Agouti-related peptide-expressing neurons are mandatory for feeding. *Nat Neurosci,* 8**,** 1289-91.

GUILDING, C., HUGHES, A. T., BROWN, T. M., NAMVAR, S. & PIGGINS, H. D. 2009. A riot of rhythms: neuronal and glial circadian oscillators in the mediobasal hypothalamus. *Mol Brain,* 2**,** 28.

HAHN, T. M., BREININGER, J. F., BASKIN, D. G. & SCHWARTZ, M. W. 1998. Coexpression of Agrp and NPY in fasting-activated hypothalamic neurons. *Nat Neurosci,* 1**,** 271-2.

HASHIGUCHI, H., SHENG, Z., ROUTH, V., GERZANICH, V., SIMARD, J. M. & BRYAN, J. 2017. Direct versus indirect actions of ghrelin on hypothalamic NPY neurons. *PLoS One,* 12**,** e0184261.

HASSOUNA, R., LABARTHE, A., ZIZZARI, P., VIDEAU, C., CULLER, M., EPELBAUM, J. & TOLLE, V. 2013. Actions of Agonists and Antagonists of the ghrelin/GHS-R Pathway on GH Secretion, Appetite, and cFos Activity. *Front Endocrinol (Lausanne),* 4**,** 25.

HORVATH, T. L., NAFTOLIN, F., KALRA, S. P. & LERANTH, C. 1992. Neuropeptide-Y innervation of beta-endorphin-containing cells in the rat mediobasal hypothalamus: a light and electron microscopic double immunostaining analysis. *Endocrinology,* 131**,** 2461-7.

HOWARD, A. D., FEIGHNER, S. D., CULLY, D. F., ARENA, J. P., LIBERATOR, P. A., ROSENBLUM, C. I., HAMELIN, M., HRENIUK, D. L., PALYHA, O. C., ANDERSON, J., PARESS, P. S., DIAZ, C., CHOU, M., LIU, K. K., MCKEE, K. K., PONG, S. S., CHAUNG, L. Y., ELBRECHT, A., DASHKEVICZ, M., HEAVENS, R., RIGBY, M., SIRINATHSINGHJI, D. J., DEAN, D. C., MELILLO, D. G., PATCHETT, A. A., NARGUND, R., GRIFFIN, P. R., DEMARTINO, J. A., GUPTA, S. K., SCHAEFFER, J. M., SMITH, R. G. & VAN DER PLOEG, L. H. 1996. A receptor in pituitary and hypothalamus that functions in growth hormone release. *Science,* 273**,** 974-7.

HUANG, Y., HE, Z., GAO, Y., LIEU, L., YAO, T., SUN, J., LIU, T., JAVADI, C., BOX, M., AFRIN, S., GUO, H. & WILLIAMS, K. W. 2018. Phosphoinositide 3-Kinase Is Integral for the

Acute Activity of Leptin and Insulin in Male Arcuate NPY/AgRP Neurons. *J Endocr Soc,* 2**,** 518-532.

HUSZAR, D., LYNCH, C. A., FAIRCHILD-HUNTRESS, V., DUNMORE, J. H., FANG, Q., BERKEMEIER, L. R., GU, W., KESTERSON, R. A., BOSTON, B. A., CONE, R. D., SMITH, F. J., CAMPFIELD, L. A., BURN, P. & LEE, F. 1997. Targeted disruption of the melanocortin-4 receptor results in obesity in mice. *Cell,* 88**,** 131-41.

KISHI, T., ASCHKENASI, C. J., LEE, C. E., MOUNTJOY, K. G., SAPER, C. B. & ELMQUIST, J. K. 2003. Expression of melanocortin 4 receptor mRNA in the central nervous system of the rat. *J Comp Neurol,* 457**,** 213-35.

KOJIMA, M., HOSODA, H., DATE, Y., NAKAZATO, M., MATSUO, H. & KANGAWA, K. 1999. Ghrelin is a growth-hormone-releasing acylated peptide from stomach. *Nature,* 402**,** 656-60.

KRASHES, M. J., KODA, S., YE, C., ROGAN, S. C., ADAMS, A. C., CUSHER, D. S., MARATOS-FLIER, E., ROTH, B. L. & LOWELL, B. B. 2011. Rapid, reversible activation of AgRP neurons drives feeding behavior in mice. *J Clin Invest,* 121**,** 1424-8.

KRASHES, M. J., SHAH, B. P., KODA, S. & LOWELL, B. B. 2013. Rapid versus delayed stimulation of feeding by the endogenously released AgRP neuron mediators GABA, NPY, and AgRP. *Cell Metab,* 18**,** 588-95.

KRUDE, H., BIEBERMANN, H., LUCK, W., HORN, R., BRABANT, G. & GRUTERS, A. 1998. Severe early-onset obesity, adrenal insufficiency and red hair pigmentation caused by POMC mutations in humans. *Nat Genet,* 19**,** 155-7.

LEIBOWITZ, S. F., HAMMER, N. J. & CHANG, K. 1981. Hypothalamic paraventricular nucleus lesions produce overeating and obesity in the rat. *Physiol Behav,* 27**,** 1031-40.

LEVINE, A. S. & MORLEY, J. E. 1984. Neuropeptide Y: a potent inducer of consummatory behavior in rats. *Peptides,* 5**,** 1025-9.

LIU, H., KISHI, T., ROSEBERRY, A. G., CAI, X., LEE, C. E., MONTEZ, J. M., FRIEDMAN, J. M. & ELMQUIST, J. K. 2003. Transgenic mice expressing green fluorescent protein under the control of the melanocortin-4 receptor promoter. *J Neurosci,* 23**,** 7143-54.

LIU, T., KONG, D., SHAH, B. P., YE, C., KODA, S., SAUNDERS, A., DING, J. B., YANG, Z., SABATINI, B. L. & LOWELL, B. B. 2012. Fasting activation of AgRP neurons requires NMDA receptors and involves spinogenesis and increased excitatory tone. *Neuron,* 73**,** 511-22.

LUQUET, S., PEREZ, F. A., HNASKO, T. S. & PALMITER, R. D. 2005. NPY/AgRP neurons are essential for feeding in adult mice but can be ablated in neonates. *Science,* 310**,** 683-5.

LYONS, D. J., HORJALES-ARAUJO, E. & BROBERGER, C. 2010. Synchronized network oscillations in rat tuberoinfundibular dopamine neurons: switch to tonic discharge by thyrotropin-releasing hormone. *Neuron,* 65**,** 217-29.

MANDELBLAT-CERF, Y., RAMESH, R. N., BURGESS, C. R., PATELLA, P., YANG, Z., LOWELL, B. B. & ANDERMANN, M. L. 2015. Arcuate hypothalamic AgRP and putative POMC neurons show opposite changes in spiking across multiple timescales. *Elife,* 4.

MIZUNO, T. M., KLEOPOULOS, S. P., BERGEN, H. T., ROBERTS, J. L., PRIEST, C. A. & MOBBS, C. V. 1998. Hypothalamic pro-opiomelanocortin mRNA is reduced by fasting and [corrected] in ob/ob and db/db mice, but is stimulated by leptin. *Diabetes,* 47**,** 294-7.

MONDAL, M. S., DATE, Y., YAMAGUCHI, H., TOSHINAI, K., TSURUTA, T., KANGAWA, K. & NAKAZATO, M. 2005. Identification of ghrelin and its receptor in neurons of the rat arcuate nucleus. *Regul Pept,* 126**,** 55-9.

MOUNTJOY, K. G., MORTRUD, M. T., LOW, M. J., SIMERLY, R. B. & CONE, R. D. 1994. Localization of the melanocortin-4 receptor (MC4-R) in neuroendocrine and autonomic control circuits in the brain. *Mol Endocrinol,* 8**,** 1298-308.

NAKAZATO, M., MURAKAMI, N., DATE, Y., KOJIMA, M., MATSUO, H., KANGAWA, K. & MATSUKURA, S. 2001. A role for ghrelin in the central regulation of feeding. *Nature,* 409**,** 194-8.

OLLMANN, M. M., WILSON, B. D., YANG, Y. K., KERNS, J. A., CHEN, Y., GANTZ, I. & BARSH, G. S. 1997. Antagonism of central melanocortin receptors in vitro and in vivo by agouti-related protein. *Science,* 278**,** 135-8.

PAEGER, L., KARAKASILIOTI, I., ALTMULLER, J., FROMMOLT, P., BRUNING, J. & KLOPPENBURG, P. 2017. Antagonistic modulation of NPY/AgRP and POMC neurons in the arcuate nucleus by noradrenalin. *Elife,* 6.

PINTO, S., ROSEBERRY, A. G., LIU, H., DIANO, S., SHANABROUGH, M., CAI, X., FRIEDMAN, J. M. & HORVATH, T. L. 2004. Rapid rewiring of arcuate nucleus feeding circuits by leptin. *Science,* 304**,** 110-5.

POGGIOLI, R., VERGONI, A. V. & BERTOLINI, A. 1986. ACTH-(1-24) and alpha-MSH antagonize feeding behavior stimulated by kappa opiate agonists. *Peptides,* 7**,** 843-8.

ROSEBERRY, A. G., LIU, H., JACKSON, A. C., CAI, X. & FRIEDMAN, J. M. 2004. Neuropeptide Y-mediated inhibition of proopiomelanocortin neurons in the arcuate nucleus shows enhanced desensitization in ob/ob mice. *Neuron,* 41**,** 711-22.

ROSSI, M., KIM, M. S., MORGAN, D. G., SMALL, C. J., EDWARDS, C. M., SUNTER, D., ABUSNANA, S., GOLDSTONE, A. P., RUSSELL, S. H., STANLEY, S. A., SMITH, D. M., YAGALOFF, K., GHATEI, M. A. & BLOOM, S. R. 1998. A C-terminal fragment of Agouti-related protein increases feeding and antagonizes the effect of alpha-melanocyte stimulating hormone in vivo. *Endocrinology,* 139**,** 4428-31.

SAEB-PARSY, K., LOMBARDELLI, S., KHAN, F. Z., MCDOWALL, K., AU-YONG, I. T. & DYBALL, R. E. 2000. Neural connections of hypothalamic neuroendocrine nuclei in the rat. *J Neuroendocrinol,* 12**,** 635-48.

SCHWARTZ, M. W., SEELEY, R. J., WOODS, S. C., WEIGLE, D. S., CAMPFIELD, L. A., BURN, P. & BASKIN, D. G. 1997. Leptin increases hypothalamic pro-opiomelanocortin mRNA expression in the rostral arcuate nucleus. *Diabetes,* 46**,** 2119-23.

SHINTANI, M., OGAWA, Y., EBIHARA, K., AIZAWA-ABE, M., MIYANAGA, F., TAKAYA, K., HAYASHI, T., INOUE, G., HOSODA, K., KOJIMA, M., KANGAWA, K. & NAKAO, K. 2001. Ghrelin, an endogenous growth hormone secretagogue, is a novel orexigenic peptide that antagonizes leptin action through the activation of hypothalamic neuropeptide Y/Y1 receptor pathway. *Diabetes,* 50**,** 227-32.

SHUTTER, J. R., GRAHAM, M., KINSEY, A. C., SCULLY, S., LUTHY, R. & STARK, K. L. 1997. Hypothalamic expression of ART, a novel gene related to agouti, is up-regulated in obese and diabetic mutant mice. *Genes Dev,* 11**,** 593-602.

STANLEY, B. G. & LEIBOWITZ, S. F. 1984. Neuropeptide Y: stimulation of feeding and drinking by injection into the paraventricular nucleus. *Life Sci,* 35**,** 2635-42.

TAKAHASHI, K. A. & CONE, R. D. 2005. Fasting induces a large, leptin-dependent increase in the intrinsic action potential frequency of orexigenic arcuate nucleus neuropeptide Y/Agouti-related protein neurons. *Endocrinology,* 146**,** 1043-7.

VAISSE, C., CLEMENT, K., GUY-GRAND, B. & FROGUEL, P. 1998. A frameshift mutation in human MC4R is associated with a dominant form of obesity. *Nat Genet,* 20**,** 113-4.

VAN DEN POL, A. N., YAO, Y., FU, L. Y., FOO, K., HUANG, H., COPPARI, R., LOWELL, B. B. & BROBERGER, C. 2009. Neuromedin B and gastrin-releasing peptide excite arcuate nucleus neuropeptide Y neurons in a novel transgenic mouse expressing strong Renilla green fluorescent protein in NPY neurons. *J Neurosci,* 29**,** 4622-39.

VAN DEN TOP, M., LEE, K., WHYMENT, A. D., BLANKS, A. M. & SPANSWICK, D. 2004. Orexigen-sensitive NPY/AgRP pacemaker neurons in the hypothalamic arcuate nucleus. *Nat Neurosci,* 7**,** 493-4.

VONG, L., YE, C., YANG, Z., CHOI, B., CHUA, S., JR. & LOWELL, B. B. 2011. Leptin action on GABAergic neurons prevents obesity and reduces inhibitory tone to POMC neurons. *Neuron,* 71**,** 142-54.

WIATER, M. F., MUKHERJEE, S., LI, A. J., DINH, T. T., ROONEY, E. M., SIMASKO, S. M. & RITTER, S. 2011. Circadian integration of sleep-wake and feeding requires NPY receptor-expressing neurons in the mediobasal hypothalamus. *Am J Physiol Regul Integr Comp Physiol,* 301**,** R1569-83.

WILLESEN, M. G., KRISTENSEN, P. & ROMER, J. 1999. Co-localization of growth hormone secretagogue receptor and NPY mRNA in the arcuate nucleus of the rat. *Neuroendocrinology,* 70**,** 306-16.

YASWEN, L., DIEHL, N., BRENNAN, M. B. & HOCHGESCHWENDER, U. 1999. Obesity in the mouse model of pro-opiomelanocortin deficiency responds to peripheral melanocortin. *Nat Med,* 5**,** 1066-70.

YEO, G. S., FAROOQI, I. S., AMINIAN, S., HALSALL, D. J., STANHOPE, R. G. & O'RAHILLY, S. 1998. A frameshift mutation in MC4R associated with dominantly inherited human obesity. *Nat Genet,* 20**,** 111-2.

ZHAN, C., ZHOU, J., FENG, Q., ZHANG, J. E., LIN, S., BAO, J., WU, P. & LUO, M. 2013. Acute and long-term suppression of feeding behavior by POMC neurons in the brainstem and hypothalamus, respectively. *J Neurosci,* 33**,** 3624-32.

ZHANG, X. & VAN DEN POL, A. N. 2016. Hypothalamic arcuate nucleus tyrosine hydroxylase neurons play orexigenic role in energy homeostasis. *Nat Neurosci,* 19**,** 1341-7.

General Discussion

General Discussion

Research Context

The body of work undertaken for this thesis has focused on improving understanding of how local oscillation of the circadian molecular clockwork alters the activity of neurons in the arcuate nucleus of the hypothalamus (ARC). Ample research over the last two decades has begun to elucidate the neural circuitry responsible for regulating appetite and food intake, however little is known regarding the circadian control (for review see Andermann and Lowell, 2017). It has been known for some time that the SCN circadian clock plays an important role in setting temporal patterns in feeding. In the majority of mammals, feeding behaviour exhibits a daily rhythm such that animals consume more food when they are active. This rhythm is disrupted by SCN lesions however recent studies have challenged the omnipotence of the master circadian pacemaker. Appetite-involved brain regions in the mediobasal hypothalamus, including ARC, exhibit autonomous oscillations in core clock components, such as PERIOD2 that persist in isolation (Guilding and Piggins, 2007, Guilding et al., 2009, Abe et al., 2002). SCN neurons display rhythmic variation in membrane excitability and firing rate that depend on molecular clock oscillations (Belle et al., 2009, Albus et al., 2002, Diekman et al., 2013). Granted, molecular clock oscillations in the ARC are semi-autonomous and are not sustained for the same duration as in SCN, however given the wealth of studies reinforcing the importance of ARC electrical activity in appetite regulation, any appreciable daily variation in excitability may have a significant impact of feeding. From an evolutionary perspective, it makes sense that the genetic machinery responsible for fine-tuning temporal aspects of feeding regulation are located within first-order neurons. Indeed, studies suggest that ARC neurons are essential for regulating the timing of feeding behaviour (Li et al., 2012, Wiater et al., 2011).

Although this work has relevance in the context of our understanding of extra-SCN oscillators, the primary goal of these investigations was to shed light onto how autonomous and self-sustained molecular clock oscillations that drive electrical rhythms in ARC may influence food intake. Progress in this area also has implications for many of

us that experience persistent daily jetlag due to misalignment between our internal circadian representation of time and a 24h societal clock. Light-driven diurnal behaviour can easily be overcome by alterations in energy supply, such as during restricted feeding schedule (RFS, Mistlberger, 1994). Under RFSs, a multitude of physiological and metabolic functions become entrained to the availability of food, rather than the light-dark cycle. This is reflected in the emergence of food anticipatory activity (FAA), which is still evident in SCN-ablated animals (Stephan et al., 1979). This implies that food entrainable oscillators (FEOs) outside the SCN are capable of aligning behavioural and physiological parameters to the availability of food (e.g. locomotor activity, body temperature and corticosterone release). The mechanism and location of the FEO have been a hot topic of scientific debate and controversy which has been led by extensive lesioning studies in the brain. Targeted disruption of all the major feeding and timing areas does not distinguish the anatomical location of the FEO. Although peripheral clocks rapidly entrain to meal timing (Hara et al., 2001, Damiola et al., 2000), evidence does not support a view that the FEO is located in the periphery (Mieda and Sakurai, 2011, Feillet et al., 2006). Rather, the FEO is likely a network of neural oscillatory sites that interact to govern timing and behavioural entrainment to food. Social jetlag has recently been associated with obesity and metabolic syndrome (Roenneberg et al., 2012). Genetic targeting of the molecular clock in mammals indicates numerous effects on metabolism (Green et al., 2008, Kettner et al., 2015). Thus, it is evident that circadian timing mechanisms regulating feeding are essential for how mammals maintain appropriate energy homeostasis and body weight (Arble et al., 2009, Hatori et al., 2012). However, clock knockout studies do not distinguish whether disrupted circadian clock function is directly causative of metabolic pathology or whether the effects are attributable to genetic ablation of non-circadian components downstream of clock gene regulation. Studies that elucidate the effect of circadian oscillations in brain regions that are important for feeding regulation may help resolve this question. A greater understanding of circadian regulation of appetite is of interest when considering clinical manifestations of clock-disruption and resulting metabolic phenotypes (Evans and Davidson, 2013, Foster et al., 2013, Zhang et al., 2013). Ultimately, progress in this area may lead to the development of targeted chronotherapy in the treatment of metabolic syndromes such as diabetes and obesity.

Major findings and context within the field of research

Use of the *Per1*::Venus reporter mouse to image *Per1*-expressing ARC neurons during electrophysiological experiments has permitted an in-depth study of how the circadian clock influences the excitability of ARC neurons. We found that daily variations in ARC excitability are confined to a particular subregion and are not influenced by a light-dark cycle as they persist in animals from constant darkness. A multi-factorial approach to assess single cells and network activity has demonstrated that ablation of the molecular clockwork has a striking effect on the electrical properties of ARC neurons. Further, we demonstrate that inhibitory GABAergic tone to latARC neurons is increased during the day (relative to the night) when neurons exhibit irregular and low firing.

A population of *Per1*-expressing ARC neurons display depolarisation block

The SCN consists of cells that oscillate with a period of ~24h, which are independent but coupled together to produce a coherent network output. At the single-cell level these oscillations depend on core clock genes such as *Per1, Cry1/2, Clock* and *Bmal1* and their protein products. Rodents have circadian oscillators in other parts of the brain which share similar properties, for example in the ARC. Like SCN, tissue-level oscillations in *Per1/PERIOD2* expression can be observed during bioluminescence recordings from reporter mice and by *in situ* hybridisation (Abe et al., 2002, Guilding et al., 2009, Shieh et al., 2005).

Both SCN and ARC molecular oscillations depend on intact cryptochrome genes for maintaining appropriate period control of molecular clock oscillations. In either oscillator, period is shortened in *Cry1*$^{-/-}$ mice and lengthened in *Cry2*$^{-/-}$ mice (Uchida et al., 2016). In our study we observed that *Per1* expression, assessed by immunohistochemistry and epifluorescence in the *Per1*::Venus reporter mouse, was constitutively expressed in ARC cells. SCN recordings revealed that only some neurons that were visualised during whole-cell recordings appeared to express the *Per1*::Venus construct. A prior study demonstrated that when SCN neurons are cultured at a low density, only 27% of cells expressed PER2 at detectable levels (Webb et al., 2008). When removed from the network-reinforcing environment, robust oscillations appear constrained to a small

proportion of cells that are strongly rhythmic. In slices, targeting of SCN *Per1* neurons with a different reporter line, the *Per1::*eGFP mouse, demonstrated that a subpopulation of cells were putatively *Per1*-negative. These findings suggest that molecular clock distribution amongst SCN cells and/or the magnitude of *Per1* expression may differ between cells. Indeed, given the high strength of intercellular coupling between SCN neurons, perhaps from an evolutionary perspective the clock neuron/non-clock neuron model is more efficient. Not all SCN neurons are rhythmic and these rhythmic cells oscillate with an array of periods within a broadly circadian range (Welsh et al., 1995, Honma et al., 1998). Ubiquitous expression of the molecular clock in ARC neurons may function to drive rhythmic physiology in single cells in the absence of strong network coupling mechanisms. Indeed, while the ARC network possessed many of the attributes required to strong cell-cell coupling, it is clear that PER2:LUC oscillations in single cells is not as strongly phase-aligned to neighbouring cells in the ARC compared to the SCN (Guilding et al., 2009).

A recent study conducted by Campbell et al. demonstrated the complex range of transcriptionally-distinct ARC cell populations using Drop-seq (Campbell et al., 2017). They catalogued 24 molecularly distinct neuron types from a large population of acutely dissociated cells (>20'000) from the ARC-ME complex of adult mice. Electrical characterisation facilitates our understanding of how transcriptionally-distinct neuronal subtypes, and their signalling mechanisms, alter the neuronal circuits they form and whole-organism physiology (van den Top et al., 2004, van den Pol et al., 2009). Our study is the first to perform an in-depth whole-cell electrophysiological assessment of *Per1*-expressing neurons in ARC. These recordings offer higher resolution compared to extracellular techniques which are restricted to recording activity from a population of firing neurons. We found that the firing activity of single cells measured by whole-cell recording was broadly within the range of published values using similar technical conditions (Burdakov and Ashcroft, 2002, Baver et al., 2014, Zhang and van den Pol, 2016, Mendonca et al., 2018, Zhan et al., 2013). The majority of ARC *Per1*::Venus neurons generated APs with either a regular or irregular pattern across the day-night cycle. While signalling through AP firing is an important component of cell-cell signalling in neural networks, it is not the only mechanism which permits neural communication. Notably, we

found that some ARC *Per1*::Venus neurons rest at hyperpolarised RMP values, are unable to fire APs, and therefore undetectable by extracellular recording. We also found a third electrical state, called depolarised silent, was exhibited by *Per1*::Venus ARC neurons (~1/10th of all ARC *Per1*::Venus neurons). These neurons rest at hyperexcited RMP values and enter depolarisation block.

This is the first study to describe physiological depolarisation block in mouse ARC neurons. Depolarised silent neurons rested at membrane potentials of ~25mV and display spikelets. In SCN, similar depolarised states exist that depend on *Per1*-expression and are only observed during the afternoon (Jiang et al., 1997a, Pennartz et al., 2002, Belle et al., 2009). Current theory posits that these states in SCN are part of the molecular clock-mediated timing mechanism that occurs due to rhythmic genetic regulation of ion conductance. Leak potassium current displays a rhythm in clock neurons which is conserved in flies and mammals (Kuhlman and McMahon, 2004, Flourakis et al., 2015). Depolarised states in SCN are thought to depend on a clock-controlled reduction potassium conductance and on L-type Ca^{2+} channels and high daytime levels of intracellular Ca^{2+} (Belle et al., 2009, Diekman et al., 2013).

Similar states have been reported in *Per1*-expressing neurons in both the LHb and MHb (Sakhi et al., 2014a, Sakhi et al., 2014b). However, like in ARC, depolarised states in the Hb are distributed across the day and night. Our data demonstrates that depolarised electrical states displayed by *Per1*::Venus ARC neurons are mediated by glutamatergic postsynaptic signals and not by SCN-like clock regulation of ionic conductance. Further evidence supporting a distinct mechanism to SCN is that ARC neurons do not exhibit depolarised low amplitude membrane oscillations (DLAMO) that occur in SCN neurons (Belle et al., 2009). However, these neurons have potential to exhibit DLAMO behaviour when artificially driven to do so by manual current injection. We propose that glutamatergic signalling in a subpopulation of ARC neurons is sufficient to lock neurons into a quiescent state. The physiological relevance of such behaviours in ARC are unknown, however similar states have been reported in rat ARC, that depend on excitatory drive from glutamate that is released intrinsically by ARC cells (Belousov and van den Pol, 1997). Outside the SCN, Hb, and ARC, depolarisation block occurs in midbrain dopamine neurons *in vivo* as a result of repeated haloperidol administration suggesting

that extrinsic agents may exert therapeutic effects by silencing neurons in this manner (Grace and Bunney, 1986, Valenti et al., 2011). Such depolarised states have also been reported in intrinsically photosensitive retinal ganglion cells in response to bright light conditions, and in cerebellar nucleus neurons (Wong et al., 2005, Raman et al., 2000, Pugh and Raman, 2009). Given the complexity of cell types in ARC, depolarised silent states may function to add an addition computational layer to the integration of metabolic signals. Metabolic cues which evoke hyperpolarising actions, such as leptin, may induce paradoxical firing in depolarised silent neurons. Hyperpolarisation resulted in complex bursting behaviour, reminiscent of that displayed by tyrosine hydroxylase neurons (Zhang and van den Pol, 2016). Classical work has demonstrated that neuropeptide release per AP increases with frequency up to a plateau point (Dreifuss et al., 1971, Gainer et al., 1986). However, spike bursts followed by periodic silence are particularly effective at evoking neuropeptide release (Dutton and Dyball, 1979, Bicknell and Leng, 1981, Cazalis et al., 1985). Thus, depolarised silent electrical states mask complex firing behaviours which are known to functionally underpin neuropeptide release.

Firing rate and GABAergic synaptic transmission exhibit daily variation in ARC

Homeostatic regulation of feeding is governed by the balanced activity of orexigenic and anorexigenic neurons in the hypothalamus. Neurons in the ARC sense peripheral indicators of energy status which rise and fall across the day, because food intake is mostly partitioned to the active phase. However, feeding rhythms are not simply a passive result of other rhythmic behaviour such as the sleep-wake cycle (Bechtold and Loudon, 2013). The SCN sends projections to ARC, and the ARC itself contains an autonomous molecular clock, which continues to tick in isolation (Saeb-Parsy et al., 2000, Guilding et al., 2009). Although the distribution of electrical states did not change across the day-night cycle, we found that the firing rate of night *Per1*::Venus ARC neurons was significantly elevated with respect to those recorded during the daytime. Notably, these variations were specific to neurons located in lateral areas of the ARC, were evident

across a large period of the day and night (6h each), and persisted in neurons from mice that were housed in constant darkness for 72h.

Given that latARC electrical rhythms occur in cells that express *Per1*, in constant dark and in an experimental situation where SCN input and circulating factors are not able to influence ARC excitability, it is clear that the molecular clockwork in ARC neurons is integral to sustaining these rhythms. This finding supports evidence that implicates the ARC as part of an extended neural circadian system (Buijs et al., 2017, Abe et al., 2002, Wiater et al., 2011, Li et al., 2012). Unlike SCN neurons, which are day-active, we found that *Per1*::Venus ARC neurons were more nocturnally active. This finding is in agreement with others which demonstrate that ARC neurons fire more frequently during the night in similar *in vitro* experiments in brain slices (Krashes et al., 2013). Further, *in vivo*-measured multiunit spiking frequency is highest during the projected night in constant darkness (Fifel et al., 2018). Neuronal activity indirectly reported by c-fos staining is higher during the night compared to the day in ARC α-melanocyte stimulating hormone cells (Guzman-Ruiz et al., 2014). These diurnal rhythms occur in parallel with variations in gene expression (Lu et al., 2002). In rats *Per1* rhythms in ARC and SCN are in antiphase, with peak expression occurring during the night and day respectively (Shieh et al., 2005). Our results in ARC are similar to SCN where high electrical output occurs after peak *Per* expression. These findings demonstrate that the collective phase of the molecular clock rhythm is temporally related to firing rate rhythms.

Whole-cell recordings provide a comprehensive outlook of how all cells, not only those that generate AP, contribute to rhythm generation. Also, these recordings allowed us to investigate whether variation in firing activity is accompanied by changes in membrane excitability. Daily variation of spontaneous firing rate in ARC *Per1*::Venus neurons occurred without associated changes in membrane potential and input resistance. Such changes have been previously demonstrated in ARC in a non-circadian context. Under fasting conditions the firing rate of ARC AgRP neurons is elevated without significant changes in RMP, an effect which is mediated by small-conductance potassium channels (SK, He et al., 2016). In rats, latARC neurons were activated by lipopolysaccharide and displayed a 2-fold increase in firing rate with a small but significant change in average membrane potential (~3mV, Reis et al., 2015). It is also possible that inhibitory

neurotransmission to latARC *Per1*::Venus neurons during the day may disrupt firing resulting in reduced rate without overtly altering RMP. Indeed, we found that *Per1*::Venus neurons in latARC receive more frequent $GABA_A$ receptor-mediated synaptic input during the day compared to the night. High GABAergic tone in the ARC occurs in antiphase to high *Per1* expression (Shieh et al., 2005). Multiple studies have demonstrated that GABAergic synaptic transmission in the ARC is inhibitory in nature and supresses the activity of key appetite-regulating neurons.

Spontaneous GABA-mediated inhibitory postsynaptic currents (IPSCs) also exhibit daily variation in the SCN, which peaks during the late day/early night and is sensitive to TTX (Itri et al., 2004). Similar to SCN, we observed that ARC *Per1*::Venus neurons generated APs with both regular and irregular firing patterns based on the interspike interval (ISI) distribution (Thomson et al., 1984). Pharmacological blockade of $GABA_A$ receptors in the SCN converts an irregular firing pattern to a regular one without synaptic input (Kononenko and Dudek, 2004). Thus, in SCN neurons, irregular firing patterns are attributed mainly or exclusively to variations in inhibitory synaptic input. Increased frequency of $GABA_A$-mediated IPSCs correlates with the time when firing rate of latARC *Per1*::Venus neurons is low and firing patterns are irregular, therefore we hypothesise that reduced electrical activity is due to the coordinated activity of an inhibitory GABAergic network.

The origin of this inhibitory GABAergic signal is unclear. The ARC receives long range GABAergic and glutamatergic inputs from multiple hypothalamic nuclei, including the dorsomedial nucleus, which is maintained in the brain slices we used for electrophysiology experiments (Krashes et al., 2014, Garfield et al., 2016). However we have demonstrated that the inhibition of daytime activity occurs by processes regulated by the local clock in ARC itself and can be disrupted by ARC-specific viral disruption of *Bmal1*. Given that the GABA-synthesising enzyme glutamate decarboxylase (GAD) is found in approximately 50% of synaptic terminals in ARC, we propose that daytime inhibition originates from rhythmic GABA which is released intrinsic to ARC onto neurons in the lateral subregion (Decavel and Van den Pol, 1990, Horvath et al., 1997). Most if not all peptidergic hypothalamic neurons are also capable of releasing GABA (Atasoy et al., 2008, Atasoy et al., 2012, Dicken et al., 2012). Neuropeptides are coexpressed with fast

neurotransmitters such as GABA other regions of the hypothalamus including the PVN (Decavel and Van den Pol, 1990). This is also the case in ARC. NPY/AgRP neurons modulate POMC neuron activity by reducing inhibitory tone both directly and from a distinct population of GABAergic neurons (Wang et al., 2002, Cowley et al., 2001, Vong et al., 2011, Acuna-Goycolea et al., 2005). Double-label *in situ* mRNA hybridization for POMC and GAD, revealed colocalisation in one-third of POMC ARC neurons (Hentges et al., 2004). Kisspeptin neurons residing in the ARC also express GAD (Cravo et al., 2011). Optogenetic stimulation of ARC TH neurons evokes GABAergic PSCs in neighbouring dopaminergic neurons (Zhang and van den Pol, 2015). Therefore a seemingly ubiquitous array of well-studied peptidergic ARC neuronal populations also release GABA.

Notably, cells throughout the ARC, and not only the latARC, exhibit rhythmicity of PER2::LUC (Guilding et al., 2009). Therefore, GABAergic neurons in either mARC or latARC may function to drive output from this area in a two-compartment model. Increased daytime GABAergic tone on latARC *Per1*::Venus neurons may arise from peptidergic neurons or a separate population of GABAergic clock neurons within the ARC.

Previous studies demonstrate that release of both glutamate and GABA are the result of spontaneous vesicle fusion that does not depend on the generation of APs (Pinto et al., 2004, Baquero et al., 2015, Fatt and Katz, 1952, Qiu et al., 2014). Indeed, *in vitro* voltage clamp recordings from latARC *Per1*::Venus neurons revealed that the frequency of PSCs was not affected by application of TTX. This mechanism differs from rhythmic network signalling in the SCN as tonic GABA is released when SCN cells become depolarised and generate APs (DeWoskin et al., 2015).

Fast synaptic communication in the brain typically requires synchronous presynaptic vesicle fusion that is mediated by AP-induced Ca^{2+} influx (Kavalali, 2015). The traditional view of spontaneous neurotransmitter release is that of low-probability, random events that depend on conformational changes in the vesicle fusion machinery (Kaeser and Regehr, 2014). However, an increasing number of molecular studies have elucidated mechanisms that promote or supress spontaneous neurotransmitter release that are distinct from AP-evoked release (Ramirez and Kavalali, 2011, Kavalali et al., 2011). For example, alternative vesicular SNAREs may have a specialised function in maintaining

spontaneous synaptic transmission. Synaptobrevin-2 deficient mice have a drastic deficit in Ca^{2+}-dependent release that is evoked by presynaptic APs, however spontaneous neurotransmission is intact (Schoch et al., 2001, Deak et al., 2004). Moreover, while 90% of spontaneous release events are carried out by a canonical synaptobrein2 partnership with SNAP25 and syntaxin, increasing evidence suggests that these components are differentially regulated for spontaneous release compared to evoked release (Schoch et al., 2001). In synaptobrevin-2 knockout mice, expression of a modified synaptobrevin-2 construct was able to rescue spontaneous release but not evoked release (Deak et al., 2006). Therefore, conformational distinctions between the same SNARE machinery may selectively modulate spontaneous versus evoked neurotransmitter release. Currently, it is unknown whether components regulating spontaneous neurotransmitter release are regulated by the circadian molecular clock, however importantly, regulation of these mechanisms may occur without increased presynaptic Ca^{2+} or apparent variation in RMP or firing rate.

Daily rhythms in ARC firing rate depend on a functioning molecular clockwork

A recent study demonstrated that *Cry1*$^{-/-}$*Cry2*$^{-/-}$ mice did not consume more food than wild-type mice, but that they did display a dampened food intake rhythm in LD conditions (Kettner et al.). In this study we found that *Cry1*$^{-/-}$*Cry2*$^{-/-}$ mice appeared to entrain to the LD cycle and displayed a very modest dampening in food intake rhythms which were essentially the same as in wild-type mice. These findings demonstrate that the light-dark cycle has a dominant effect on locomotor activity as well as feeding and drinking. We propose that differences between ours and this other study may reflect differences in lighting conditions. Consistent with locomotor activity rhythms, food and water was rhythmic across the subjective day-night in wild-type mice but not in *Cry1*$^{-/-}$*Cry2*$^{-/-}$ animals became circadianly arrhythmic in constant darkness.

The advantage of experiments in brain slices is that SCN input and the majority of endogenous circulating factors are absent. Similar to those expressing *Per1*, *Cry1*$^{+/+}$*Cry2*$^{+/+}$ latARC neurons were more active during the night compared to the daytime, suggesting

that these two experimental populations are broadly equivalent. Further, we found that *Per1* expression (*Per1*::Venus) was essentially ubiquitous in cells throughout the ARC. Notably, electrical rhythms in latARC were disrupted by *Cry1*$^{-/-}$*Cry2*$^{-/-}$ even though these mice displayed rhythmic food intake, the majority of which (65%) was consumed during the dark phase. This result demonstrates that electrical rhythms in ARC are indeed dependent on an intact molecular clock rather than SCN input, circulating signals or rhythms in feeding. *Cry1*$^{-/-}$*Cry2*$^{-/-}$ mice have similarly disrupted daily electrical rhythms in circadian oscillators of the epithalamus. Both MHb and LHb neurons fire at a low frequency during the early day (ZT0-6) and high at the late day (ZT12) and into the night (Sakhi et al., 2014a, Sakhi et al., 2014b). *Cry1*$^{-/-}$*Cry2*$^{-/-}$ neurons in either area do not show variation in activity throughout the day. *Cry1* and *Cry2* are also indispensable for core molecular clock function in the SCN, as evident from arrhythmic wheel-running behaviour, lack of rhythmic clock gene expression, and ablation of circadian oscillations in firing patterns (Albus et al., 2002).

This study is the first to examine the influence that perturbations in genetic circadian components has on neuronal excitability in ARC. Recordings from *Cry1*$^{-/-}$*Cry2*$^{-/-}$ mice and their wild-type counterparts (*Cry1*$^{+/+}$*Cry2*$^{+/+}$) demonstrate that under LD conditions *Cry*-deficient neurons exhibit high firing rates across the day-night cycle compared to those with an intact molecular clock. Similar recordings of MHb neurons demonstrate that intact cryptochromes supress neuronal activity (Sakhi et al., 2014a). However, an opposite relationship between ablation of the molecular clockwork and neuronal activity is observed in the adjacent LHb; *Cry1*$^{-/-}$*Cry2*$^{-/-}$ neurons express constitutively low firing across the day (Sakhi et al., 2014b). We found that *Cry1*$^{-/-}$*Cry2*$^{-/-}$ neurons in the mARC also fired more frequently with respect to *Cry1*$^{+/+}$*Cry2*$^{+/+}$ neurons during the day. Therefore, removing the molecular clock in ARC has implications not only for electrically rhythmic cells but for the whole network. Targeted knockout of *Bmal1* resulted in similar increases in ARC firing activity during the day, which suggests that suppression of electrical activity is a result of an oscillating TTFL rather than solely due to normal expression of *Cry1* and *Cry2*. Also, as viruses were delivered just to the ARC, this study demonstrates that the TTFL in ARC neurons themselves modulates electrical activity. Dynamic modulation of neuronal activity and spiking is essential to ARC function. Here we provide further

evidence that an intrinsic clock as well as extrinsic factors such as leptin, determine the output of ARC neurons, which are known to play key roles in appetite and feeding regulation.

The VMH does not appear to contain an autonomous clock (Guilding et al., 2009). We observed faint immunostaining for *Per1*::Venus neurons; however fluorescence signal was not detectable in VMH during epifluorescence imaging. Excision of *Bmal1* specifically in SF1 neurons drastically reduces the number of BMAL1-positive cells in the VMH (Orozco-Solis et al., 2016). These mice presented with higher body temperature during the active phase and increased expression of brown adipose tissue (BAT) specific genes. Therefore, *Bmal1* in the VMH influences thermal oscillations in BAT. Clock-driven BAT activation is thought to occur via the sympathetic nervous system. Further, *Bmal1* in the VMH integrates light and feeding inputs to shape basal energy expenditure. It is unclear whether direct synaptic connections between VMH and BAT exist (Cannon and Nedergaard, 2004). However, the changes in energy expenditure following ablation of *Bmal1* in VMH are likely to be independent of daily variation in the spiking of VMH neurons as we did not detect such variation in our study.

Evidence for electrical coupling in ARC networks

Prior studies suggest that electrical synapses have an involvement in SCN cell-cell coupling, however the evidence is not as developed as is for conventional chemical synaptic communication. An early sign that non-chemical synapses may be important was that circadian rhythms in metabolic activity, measured by 2-deoxyglucose uptake, appear robust in rat SCN throughout embryonic day E19 (Reppert and Schwartz, 1984), despite chemical synapse development being at an early stage (Moore and Bernstein, 1989). Similar to our observations in ARC, dyes have been shown to diffuse from SCN cells into neighbouring cells, presumably via gap junctions (Jiang et al., 1997b). This coupling is supressed by hyperpolarisation of the membrane, occurs selectively within either the dorsal or ventral SCN and is lower during the subjective night (Colwell, 2000).

Gap junctions in multiple areas of the brain have been shown to drive synchronous firing activity (Connors and Long, 2004). Synchronous patterns of firing activity can be observed in SCN slices even when synaptic communication is blocked by use of a calcium-free

extracellular solution (Bouskila and Dudek, 1993). There is appreciable synchrony of spiking across SCN neurons within the millisecond scale (Long et al., 2005). Further, mice with a mutation in Connexin36 (Cx36) as $Cx36^{-/-}$ mice have a modest weakening of locomotor activity rhythms (Long et al., 2005). In SCN slices, gap junction blockers halothane and octanol damp circadian rhythms in peptide release and neuronal firing (Prosser et al., 1994, Shinohara et al., 2000). Therefore, these lines of evidence suggest that gap junction-mediated electrical synapses may function to reinforce cell-cell coupling in the SCN. Currently, there is little evidence to suggest that gap junctions in ARC play a role in physiology. A population of ARC neurons that express tyrosine-hydroxylase, the so called hypothalamic tuberoinfundibular dopamine (TIDA) neurons, exhibit highly-synchronised phasic firing which is blocked by application of the gap junction blocker carbenoxolone (Lyons et al., 2010).

We found that latARC neurons (*Per1*::Venus and NPY-hrGFP-negative) appear to form gap junctions with neighbouring cells. Biocytin infusion during whole-cell recording and post-experiment immunohistochemistry revealed faint biocytin staining in neurons (not patched) as far as 200µm away. Notably, recordings in mARC (*Per1*::Venus and NPY-hrGFP) did not result in secondary biocytin staining. Recording of 2/3 latARC neurons resulted in >15 faintly stained cells in ipsilateral ARC. This apparent coupling is more extensive between ARC cells compared to SCN cells; whole-cell recordings in hypothalamic slices with neurobiotin in the recording pipette reveal tracer coupling in 5% of SCN neurons (Rash et al., 2007). The extensive tracer staining in latARC suggests that these cells form an interconnected electrical network with each other, potentially to synchronise spiking activity. Immunostaining for Cx43 and Cx30 showed that these gap junction forming proteins are expressed in rat ARC close to the border of the third ventricle and in the rest of the ARC respectively (Allard et al., 2014). However, Cx43 and Cx30 in the ARC are thought to be expressed in astroglial networks involved in brain glucose sensing. Indeed, diffusion of Alexa Fluor 633 into ARC astroglia which stimulate food intake under physiological conditions resulted in staining of numerous secondary cells up to 200µm away (Chen et al., 2016). We observed dense immunostaining for GFAP in latARC. Our data suggest that ARC neurons that express the molecular clock are coupled via gap junctions to an unknown network of cells. Based on the limited number

of studies examining gap junction physiology in ARC, we propose that these neurons may be electrically coupled to a population of astroglia which are involved in glucose sensing.

Open questions and future directions

Under normal physiological conditions, semiautonomous extra-SCN brain oscillators and peripheral clocks are synchronised by mono- or polysynaptic neuronal projections and SCN-derived rhythmic hormone release (Dibner et al., 2010). In the central nervous system, rhythmically expressed circadian genes combined with direct neuronal projections from the SCN is found in multiple hypothalamic areas including ARC (Huang et al., 2011). The pronounced rhythm in latARC neuronal activity suggests that the local oscillator plays an important role in regulating physiological processing in ARC. Given the non-redundant role the SCN plays in setting feeding rhythms, it is most likely that both the master SCN clock and local clocks in the brain are required for proper functioning. This multi-dimensional view of the circadian system is well demonstrated by studies on the liver clock. Normal rhythmic expression of genes involved in lipid metabolism, gluconeogenesis and oxidative phosphorylation depend on a local hepatic clock (Lamia et al., 2008, Zhang et al., 2010, Panda et al., 2002). However, rhythmic autonomic output from the SCN, via the paraventricular nucleus, is also essential for circadian rhythms in hepatic glucose production (Kalsbeek et al., 2008). Thus, both the SCN and the liver clock are required for optimal glucose control.

This organisation of the circadian system has multiple advantages. Firstly, gene transcription is highly tissue specific, therefore a molecular clock which is integrated locally allows tight orchestration of gene expression patterns. Indeed, there is little overlap in the identity of rhythmic genes between tissues (Oishi et al., 2005, McCarthy et al., 2007, Damiola et al., 2000). Secondly, local clocks allow different brain regions and peripheral clocks subtle flexibility from phase alignment by the SCN, which permits tissues to be optimally aligned across different physiological conditions. Finally, local clocks in tissues with well-established physiological functions are set up to be sensitive to dynamic changes to internal and external time signals, such as food intake, whereas the SCN is more constrained to the light-dark cycle. This function has been demonstrated in studies showing that peripheral clock rhythms and extra-SCN brain clocks will entrain to a feeding

schedule that occurs during the animals normal inactive phase, in opposition to the SCN (Bass and Takahashi, 2010, Damiola et al., 2000).

Given that the local clock modulates the generation of APs in ARC, we propose that the ARC clock functions to optimise the rhythmic features of a behaviour that is directly regulated by the electrical activity of ARC neurons. Different ARC neuronal populations regulate feeding behaviour and appetite over different timescales. Chemo- or optogenetic stimulation of AgRP neurons results in voracious and rapid feeding responses in *ad libitum* fed mice (Aponte et al., 2011, Krashes et al., 2011). Photostimulation of ARC POMC neurons results in upregulated firing activity and sustained reductions in food intake over the course of 24h (Aponte et al., 2011). Stimulation during the initiation of feeding behaviour does not influence intake therefore POMC neurons appear not to influence the onset of feeding behaviour that is regulated by NPY/AgRP neurons. Neurons expressing NPY/AgRP/GABA in ARC are also able to differentially regulate either rapid or sustained feeding by release of either NPY and GABA, which result in short term feeding, and AgRP, which mediates a delayed and sustained feeding response (Krashes et al., 2013).

A key question arising from this study is how circadian information from ARC may be conveyed to important downstream regions in the brain. The downstream projections of ARC neurons can be broadly categorised as intra-ARC or as those targeting other brain regions. GABAergic collaterals from NPY/AgRP neurons contact ARC POMC neurons to decrease their satiety-promoting activity (Cowley et al., 2001, Horvath et al., 1992). Stimulation of mouse ARC TH neurons evokes increases in food intake by synaptic inhibition of POMC neurons (Zhang and van den Pol, 2016). A subset of non-POMC, non-AgRP, GABAergic neurons respond to leptin and reduce inhibitory tone to POMC neurons (Vong et al., 2011). Therefore, ARC POMC neurons are a pathway by which other ARC populations modulate food intake and energy expenditure.

ARC neurons are functionally connected to numerous downstream brain regions including the PVN and DMH, the periaqueductal gray, dorsal raphe nucleus and the nucleus tractus solitarius (NTS, Sim and Joseph, 1991, Bouret et al., 2004). PVN is a major target for ARC neurons. NPY/AgRP neurons project to the PVN where the co-release of NPY and AgRP act

via the Y1 receptor and MC4Rs on orexinergic downstream neurons respectively to increase appetite (Ollmann et al., 1997, Li et al., 1999). ARC NPY/AgRP neurons also make GABAergic inhibitory synaptic contact with a subpopulation of PVN neurons (Krashes et al., 2014, Atasoy et al., 2012). Satiety-promoting POMC neurons release αMSH in the PVN which acts on MC4R to regulate appetite. The PVN neurons that receive this signal are glutamatergic and do not express oxytocin, corticotropin-releasing hormone or vasopressin (Balthasar et al., 2005, Garfield et al., 2015). Stimulation of mouse ARC TH neurons evokes increases in food intake by inhibition of PVN neurons by co-release of dopamine and GABA (Zhang and van den Pol, 2016). GABAergic RIP-Cre neurons also project heavily to the PVN to modulate energy expenditure independently of food intake (Kong et al., 2012, Vong et al., 2011). GABA release from these cells functions in PVN to blunt NPY-induced hyperphagia and reduces post-weaning feeding (Kim et al., 2015). Based on the extensive functional connectivity between ARC and PVN it is highly likely that *Per1*::Venus neurons that exhibit daily rhythms in firing rate send circadian information to this major output area.

Direct stimulation of PVN neurons themselves modulates feeding and appetite. Chemogenetic stimulation or inhibition of PVN neurons that express MC4Rs decreases and increases feeding respectively (Garfield et al., 2015). PVN neurons project heavily to multiple brain regions involved in feeding regulation including the central region of the lateral parabrachial nucleus (LPBN), the dorsal vagal complex (NTS/DMV) and the ME (Andermann and Lowell, 2017). The PVN projection to LPBN is responsible for evoking satiety as demonstrated by optogenetic stimulation of PVN^{MC4R} terminals in the LPBN, which reduces feeding (Garfield et al., 2015). ARC^{AgRP} neurons also project to a number of other brain regions. Stimulation of ARC^{AgRP} terminals in the PVN, bed nucleus of the stria terminalis, lateral hypothalamus, paraventricular thalamus and medial amygdala increases feeding (Aponte et al., 2011, Padilla et al., 2016, Betley et al., 2013). Thus, circadian information generated in ARC can potentially be transmitted to a wide range of downstream brain regions.

Given the fact that autonomous oscillations in PER2::LUC and electrical activity occur both in ARC and SCN, one could presume that a network of coupled hypothalamic oscillators are important for generating circadian rhythmicity. The SCN is ideally situated to receive

feedback through reciprocal connections with the ARC (Saeb-Parsy et al., 2000, Yi et al., 2006). The presence of local rhythms in ARC may function to convey timed non-photic information to the SCN to adjust rhythmic physiology. This view is supported by experiments lesioning ARC cell populations which results in disrupted temperature, feeding and sleep rhythms (Li et al., 2012, Wiater et al., 2011). Interactions between the ARC and SCN outputs to downstream brain areas have been shown to be critical for daily changes in body temperature (Guzman-Ruiz et al., 2015). Severing the reciprocal connections between ARC from SCN by retrochiasmatic knife cuts in rats results in a loss of circadian rhythmicity in locomotor activity, body temperature and corticosterone levels in constant darkness (Buijs et al., 2017). Thus, ARC feedback to SCN is critical for maintaining proper physiological rhythms, and the local clock in ARC may form a component of a large network of oscillators that control homeostasis.

Autonomous molecular clock oscillations in ARC may function to regulate rhythmic physiology that is not relevant under normal feeding conditions or may not be related to feeding and appetite homeostasis at all. Molecular rhythms in some ARC oscillators are shifted in response to anticipation of food under an RFS or to fasting conditions (Mendoza et al., 2010, Guilding et al., 2009). Therefore the ARC clock may be important in maintaining circadian control in conditions of metabolic duress. The ARC also plays a well-established role, not only in gating feeding responses, but also in the reproductive axis. Kisspeptin neurons in ARC are a strong candidate for coordinating GnRH neuron activity and for steroid feedback signalling. In the ARC, kisspeptin is colocalised with neurokinin B and dynorphin, hence called KNDy neurons (Lehman et al., 2010). In adult males, GnRH secretion is key to fertility and is pulsatile in nature and ranges in interval from 30minutes to many hours (Levine et al., 1985, Levine and Duffy, 1988). KNDy neurons exhibit long-term patterns of episodic electrical activity which features successive increase and decreases in firing activity with time (Vanacker et al., 2017). A speculative role of the local ARC clock may be to provide an additional level of control of GnRH neurons across the daily cycle by modulating the activity of KNDy neurons. These neurons are located in the latARC region and exhibit similar irregular firing and spike frequency to *Per1*::Venus neurons we recorded (Mendonca et al., 2018).

The time period covered by the electrophysiology experiments presented in this thesis represent a substantial period of the day and night, however recordings did not overlap with when mice typically initiate feeding at the beginning of the dark phase in LD conditions. Elevated night firing in latARC neuron was sustained across a 6h period suggesting that ARC local clock regulation of feeding behaviour is likely to function either to regulate appetite across a timescale of hours or to provide an additional level of control over SCN-driven regulation of ARC neurons. One approach to determining the physiological output of the ARC clock to identify neuronal populations which display circadian rhythms in firing rate. Appetite-stimulating NPY-hrGFP ARC neurons did not exhibit daily variation in firing rate, and latARC *Per1*::Venus and *Cry1*$^{+/+}$*Cry2*$^{+/+}$ neurons were more active during the night when animals are awake and actively seeking food. Nocturnally-active ARC neurons are generally associated with orexigenic effects on appetite. For example, NPY/AgRP neurons exhibit increased activity during the dark phase or in response to fasting (Krashes et al., 2013, Yang et al., 2011, Liu et al., 2012). However, we did not observe any daily change in NPY-hrGFP neuronal activity across the time epochs selected for recording. Basic examination of the distribution of NPY-hrGFP neurons in ARC demonstrate that rhythmic latARC *Per1*::Venus neurons were predominantly non-NPY-hrGFP expressing. This raises two questions when considering a role of local clock-derived variation in excitability in feeding regulation. Firstly, do latARC neurons that display rhythmic firing overlap with another distinct population of orexigenic neurons that are located in the same area. Appetite-stimulating tyrosine hydroxylase neurons, which are distinct from NPY/AgRP and POMC neurons, reside in an equivalent area to latARC and increase feeding when stimulated optogenetically. Further, selective destruction of ARC TH neurons results in long-term reduced weight gain compared to controls, demonstrating that the influence of these neurons is not transient, but rather is required for age-dependent weight increase.

The importance of the melanocortin system in sculpting circadian rhythms in feeding is well-established. Deletion of the melanocortin 3 receptor (MC3) gene in mice resulted in disruption of clock gene in the cortex, such as *Per1* and *Bmal1*, and attenuated food-anticipation during restricted feeding (Sutton et al., 2008). Further, *Per2* knockout mice are obese and have altered feeding rhythms, which have been attributed to disrupted

diurnal expression of αMSH, a product resulting from cleavage of POMC which is a major effector in appetite regulation (Yang et al., 2009). Despite an apparent role for melanocortin receptor-mediated signalling in shaping feeding rhythms, selective deletion of POMC does not alter circadian rhythms in feeding or activity (Richard et al., 2011). Neurons that express αMSH (presumed POMC) exhibit daily rhythmicity which is dependent on an intact SCN (Guzman-Ruiz et al., 2014). Here, neurons that express daily rhythms in excitability do this without an intact SCN as rhythms are sustained in brain slices.

The results presented in this thesis are the culmination of the first in-depth investigation into the influence of the circadian molecular clock on ARC neuronal activity. We found that a local clockwork in ARC supresses daytime firing activity therefore resulting in a diurnal rhythm which is sustained in constant darkness. Viral knockout of the core clock gene *Bmal1* specifically in ARC resulted in a disinhibition of firing during the day which raised AP frequency to levels similar to the night. However, such changes were not accompanied by any changes in food or water intake, or the distribution of daily consumption. There are a number of explanations for why disruption of the local clock in ARC neurons was not associated with any overt phenotypic changes. Any changes in the neural network resulting from perturbations of the molecular clock may be compensated for by a network of cells which function as a hard-wired homeostat. A possible explanation for the absence of phenotype with ablation of *Bmal1* in ARC is disruption of ARC electrical rhythms in latARC neurons results in network compensation from other cell populations. Single-unit activity across the ARC was increased following cre-dependent knockout of *Bmal1* and the number of spiking neurons per electrode also increased. This finding is indicative of recruitment of additional antagonistic firing neurons following clock disruption which may negate disruption of rhythms in cells that are normally rhythmic. Also, while forced stimulation of ARC neurons may induce changes in feeding, this activation may beyond a physiologically relevant level. Channelrhodopsin-2 stimulation of AgRP neurons results in firing activity (>10Hz, similar for stimulated POMC neurons) which is typically higher frequency than activation evoked by fasting conditions (~2Hz, Aponte et al., 2011, Liu et al., 2012, Baver et al., 2014).

ARC neurons sense a number of circulating factors that convey energy status such as leptin, ghrelin and cholecystokinin (Burdakov and Ashcroft, 2002, Wang et al., 2014, Schwartz et al., 2000). A more subtle circadian variation in firing activity may function not to directly drive behaviour but to shape how ARC neurons respond to circulating metabolic cues. The long isoform leptin receptor (lepRb) is highly expressed throughout the ARC (Chua et al., 1996, Mercer et al., 1996, Elmquist et al., 1998). Indeed, circulating factors such as leptin shape the activity of ARC neurons by modulating ion conductance that are responsible for setting firing rate (Qiu et al., 2010, Spanswick et al., 2000). We found that leptin evoked both excitatory and inhibitory responses in *Per1*::Venus neurons. However, the majority of responses were in a hyperpolarising direction. Thus, increased night firing rate may function to increase the magnitude of response to inhibitory circulating factors when mice are active and feeding.

Future work

The neurochemical phenotype of latARC neurons which exhibit a nocturnal increase in firing rate is unknown. Thus far we have demonstrated that firing rate variation occurs in latARC, an area which is well-known to contain POMC neurons (Guzman-Ruiz et al., 2014). Elevated neuronal firing in ARC is coincident with ascending or maximal levels of peripheral hormones such as leptin and insulin that can act to reduce or terminate ingestive behaviour (Challet, 2015, Baver et al., 2014). Since POMC neurons are more numerous in the latARC than the mARC, this raises the possibility that nocturnal increase in spontaneous firing activity primes responsiveness of latARC including POMC neurons to anorexigenic signals. To investigate the identity of latARC neurons that display daily variation in firing rate, a suitable follow-up experiment would be to perform multielectrode array experiments on slices from mice that specifically express channelrhodopsin-2 (ChR2) in ARC POMC neurons. This could be achieved by injecting AAV-Flex-ChR2 in ARC of POMC-Cre mice (Kong et al., 2012, Zhan et al., 2013). Alternatively, ChR2 DNA could be introduced by mouse genetics, via generation of a line carrying a transgene or targeted insert (Britt et al., 2012). Thus, POMC neurons in ARC could be distinguished from other neurons by using brief light pulses to evoke spiking specifically in POMC neurons. Offline discrimination of the spiking rate of these neurons over the course of the experiment may demonstrate that these neurons do indeed

display rhythmic changes in electrical output. This approach is faster than screening individual neurons by whole-cell patch recording. Furthermore, this set up allows for the repeated application of metabolic cues to test whether the sensitivity of POMC neurons to leptin and insulin depends on the time of day.

The data presented in this thesis may benefit from a more comprehensive investigation into output physiology and behaviour that may be modulated by local molecular clockwork in the ARC. For example, the use of a comprehensive lab animal monitoring system (CLAMs), which has been used to demonstrate that mice with mutations in different clock genes show distinct changes in their metabolism and energy expenditure (Kettner et al., 2013). We found that food intake under *ad libitum* conditions was not influenced by ARC-specific knockout of *Bmal1*. However it is possible that energy expenditure and not intake is affected by the local ARC clock. In this case, telemetry probes may also be used to measure fluctuations in body temperature. However, as we found from the experiments performed for this thesis, such studies are speculative and potentially very time consuming. Therefore, a detailed investigation into neurochemical phenotype of latARC neurons that exhibit high nocturnal firing rate, such as that outlined above, would be a preferential starting point.

Conclusions and future direction of the field

Work on *Per1*-expressing neurons in ARC has provided a multi-level and detailed daily profile of electrical activity. This profiling has revealed novel insights into how circadian pacemaking may alter the daily activity and synaptic communication in the arcuate nucleus of the hypothalamus. Together, this work adds to continuing efforts to increase our understanding of how circadian molecular rhythms translate into variable changes in electrical output. We show that a local intact molecular clock is responsible for driving daily and circadian rhythms in firing rate that bear both similarities and differences to timekeeping mechanisms in the circadian master clock in the suprachiasmatic nucleus. Notably, we demonstrate that the molecular clock has a strong influence over ARC neuronal activity, as ablation of core components result in striking changes in excitability. Elucidating how networks of extra-SCN oscillators contribute to physiological and behavioural facets such as feeding behaviour is essential for our understanding of the role

of biological timing in metabolic disorders. Further, evidence suggests that circadian regulation of feeding centres of the brain is important for food entrainment of circadian rhythms, which may have future implications in jet lag research. Hopefully, the insights from this investigation will have an immediate contribution to our understanding of how circadian brain oscillators are constructed and a long-term value in developing therapeutic strategies.

Recent years has seen increased research attention applied to understand the interaction between circadian regulation and feeding and appetite homeostasis. Metabolic disorders are often associated with circadian disruption. Progress in this area also has implications for many of us that experience persistent daily jetlag due to misalignment between our internal circadian representation of time and a 24h societal clock. The ARC is a region of the hypothalamus which is critical for both feeding and circadian timing. Our studies demonstrate that a molecular clock which ticks locally is critical for circadian rhythms in ARC function. The approach we took relied heavily on electrophysiological methodologies to first investigate whether clock gene rhythms are sufficient to influence the functional output of ARC neurons, that being electrical output and subsequent release of fast neurotransmitters and neuropeptides. From this perspective, recent advances in neurobiological tools such as optogenetics, viral targeting and transgenic lines permit targeted and conditional manipulation of brain regions which form an integrated network that is critical for the circadian regulation of feeding. Clever utilisation of this new advanced toolkit in combination with powerful electrophysiological methods, like those used here, will likely prove essential for disseminating the role of hypothalamic circadian oscillators in behaviour and physiology. Current theory postulates that circadian oscillators in important feeding centres form part of a network food entrainable oscillator. I think this is the most pressing issue that is yet to be answered. What is the functional role of circadian electrical rhythms in ARC? The results presented in this study form a solid foundation from which to build an understanding of how robust functional variations in electrical output translate to influence larger scale networks and downstream behaviours.

References

ABE, M., HERZOG, E. D., YAMAZAKI, S., STRAUME, M., TEI, H., SAKAKI, Y., MENAKER, M. & BLOCK, G. D. 2002. Circadian rhythms in isolated brain regions. *J Neurosci,* 22**,** 350-6.

ACUNA-GOYCOLEA, C., TAMAMAKI, N., YANAGAWA, Y., OBATA, K. & VAN DEN POL, A. N. 2005. Mechanisms of neuropeptide Y, peptide YY, and pancreatic polypeptide inhibition of identified green fluorescent protein-expressing GABA neurons in the hypothalamic neuroendocrine arcuate nucleus. *J Neurosci,* 25**,** 7406-19.

ALBUS, H., BONNEFONT, X., CHAVES, I., YASUI, A., DOCZY, J., VAN DER HORST, G. T. & MEIJER, J. H. 2002. Cryptochrome-deficient mice lack circadian electrical activity in the suprachiasmatic nuclei. *Curr Biol,* 12**,** 1130-3.

ALLARD, C., CARNEIRO, L., GRALL, S., CLINE, B. H., FIORAMONTI, X., CHRETIEN, C., BABA-AISSA, F., GIAUME, C., PENICAUD, L. & LELOUP, C. 2014. Hypothalamic astroglial connexins are required for brain glucose sensing-induced insulin secretion. *J Cereb Blood Flow Metab,* 34**,** 339-46.

ANDERMANN, M. L. & LOWELL, B. B. 2017. Toward a Wiring Diagram Understanding of Appetite Control. *Neuron,* 95**,** 757-778.

APONTE, Y., ATASOY, D. & STERNSON, S. M. 2011. AGRP neurons are sufficient to orchestrate feeding behavior rapidly and without training. *Nat Neurosci,* 14**,** 351-5.

ARBLE, D. M., BASS, J., LAPOSKY, A. D., VITATERNA, M. H. & TUREK, F. W. 2009. Circadian timing of food intake contributes to weight gain. *Obesity (Silver Spring),* 17**,** 2100-2.

ATASOY, D., APONTE, Y., SU, H. H. & STERNSON, S. M. 2008. A FLEX switch targets Channelrhodopsin-2 to multiple cell types for imaging and long-range circuit mapping. *J Neurosci,* 28**,** 7025-30.

ATASOY, D., BETLEY, J. N., SU, H. H. & STERNSON, S. M. 2012. Deconstruction of a neural circuit for hunger. *Nature,* 488**,** 172-7.

BALTHASAR, N., DALGAARD, L. T., LEE, C. E., YU, J., FUNAHASHI, H., WILLIAMS, T., FERREIRA, M., TANG, V., MCGOVERN, R. A., KENNY, C. D., CHRISTIANSEN, L. M., EDELSTEIN, E., CHOI, B., BOSS, O., ASCHKENASI, C., ZHANG, C. Y., MOUNTJOY, K., KISHI, T., ELMQUIST, J. K. & LOWELL, B. B. 2005. Divergence of melanocortin pathways in the control of food intake and energy expenditure. *Cell,* 123**,** 493-505.

BAQUERO, A. F., KIRIGITI, M. A., BAQUERO, K. C., LEE, S. J., SMITH, M. S. & GROVE, K. L. 2015. Developmental changes in synaptic distribution in arcuate nucleus neurons. *J Neurosci,* 35**,** 8558-69.

BASS, J. & TAKAHASHI, J. S. 2010. Circadian integration of metabolism and energetics. *Science,* 330**,** 1349-54.

BAVER, S. B., HOPE, K., GUYOT, S., BJORBAEK, C., KACZOROWSKI, C. & O'CONNELL, K. M. 2014. Leptin modulates the intrinsic excitability of AgRP/NPY neurons in the arcuate nucleus of the hypothalamus. *J Neurosci,* 34**,** 5486-96.

BECHTOLD, D. A. & LOUDON, A. S. 2013. Hypothalamic clocks and rhythms in feeding behaviour. *Trends Neurosci,* 36**,** 74-82.

BELLE, M. D., DIEKMAN, C. O., FORGER, D. B. & PIGGINS, H. D. 2009. Daily electrical silencing in the mammalian circadian clock. *Science,* 326**,** 281-4.

BELOUSOV, A. B. & VAN DEN POL, A. N. 1997. Local synaptic release of glutamate from neurons in the rat hypothalamic arcuate nucleus. *J Physiol,* 499 (Pt 3)**,** 747-61.

BETLEY, J. N., CAO, Z. F., RITOLA, K. D. & STERNSON, S. M. 2013. Parallel, redundant circuit organization for homeostatic control of feeding behavior. *Cell,* 155**,** 1337-50.

BICKNELL, R. J. & LENG, G. 1981. Relative efficiency of neural firing patterns for vasopressin release in vitro. *Neuroendocrinology,* 33**,** 295-9.

BOURET, S. G., DRAPER, S. J. & SIMERLY, R. B. 2004. Formation of projection pathways from the arcuate nucleus of the hypothalamus to hypothalamic regions implicated in the neural control of feeding behavior in mice. *J Neurosci,* 24**,** 2797-805.

BOUSKILA, Y. & DUDEK, F. E. 1993. Neuronal synchronization without calcium-dependent synaptic transmission in the hypothalamus. *Proc Natl Acad Sci U S A,* 90**,** 3207-10.

BRITT J. P. 2012. Use of channelrhodopsin for activation of CNS neurons. Curr Protoc Neurosci. 12, 16.

BUIJS, F. N., GUZMAN-RUIZ, M., LEON-MERCADO, L., BASUALDO, M. C., ESCOBAR, C., KALSBEEK, A. & BUIJS, R. M. 2017. Suprachiasmatic Nucleus Interaction with the Arcuate Nucleus; Essential for Organizing Physiological Rhythms. *eNeuro,* 4.

BURDAKOV, D. & ASHCROFT, F. M. 2002. Cholecystokinin tunes firing of an electrically distinct subset of arcuate nucleus neurons by activating A-Type potassium channels. *J Neurosci,* 22**,** 6380-7.

CAMPBELL, J. N., MACOSKO, E. Z., FENSELAU, H., PERS, T. H., LYUBETSKAYA, A., TENEN, D., GOLDMAN, M., VERSTEGEN, A. M., RESCH, J. M., MCCARROLL, S. A., ROSEN, E. D., LOWELL, B. B. & TSAI, L. T. 2017. A molecular census of arcuate hypothalamus and median eminence cell types. *Nat Neurosci,* 20**,** 484-496.

CANNON, B. & NEDERGAARD, J. 2004. Brown adipose tissue: function and physiological significance. *Physiol Rev,* 84**,** 277-359.

CAZALIS, M., DAYANITHI, G. & NORDMANN, J. J. 1985. The role of patterned burst and interburst interval on the excitation-coupling mechanism in the isolated rat neural lobe. *J Physiol,* 369**,** 45-60.

CHALLET, E. 2015. Keeping circadian time with hormones. *Diabetes, Obesity and Metabolism*, 17, 76-83.

CHEN, N., SUGIHARA, H., KIM, J., FU, Z., BARAK, B., SUR, M., FENG, G. & HAN, W. 2016. Direct modulation of GFAP-expressing glia in the arcuate nucleus bi-directionally regulates feeding. *Elife,* 5.

CHUA, S. C., JR., CHUNG, W. K., WU-PENG, X. S., ZHANG, Y., LIU, S. M., TARTAGLIA, L. & LEIBEL, R. L. 1996. Phenotypes of mouse diabetes and rat fatty due to mutations in the OB (leptin) receptor. *Science,* 271**,** 994-6.

COLWELL, C. S. 2000. Rhythmic coupling among cells in the suprachiasmatic nucleus. *J Neurobiol,* 43**,** 379-88.

CONNORS, B. W. & LONG, M. A. 2004. Electrical synapses in the mammalian brain. *Annu Rev Neurosci,* 27**,** 393-418.

COWLEY, M. A., SMART, J. L., RUBINSTEIN, M., CERDAN, M. G., DIANO, S., HORVATH, T. L., CONE, R. D. & LOW, M. J. 2001. Leptin activates anorexigenic POMC neurons through a neural network in the arcuate nucleus. *Nature,* 411**,** 480-4.

CRAVO, R. M., MARGATHO, L. O., OSBORNE-LAWRENCE, S., DONATO, J., JR., ATKIN, S., BOOKOUT, A. L., ROVINSKY, S., FRAZAO, R., LEE, C. E., GAUTRON, L., ZIGMAN, J. M.

& ELIAS, C. F. 2011. Characterization of Kiss1 neurons using transgenic mouse models. *Neuroscience,* 173**,** 37-56.

DAMIOLA, F., LE MINH, N., PREITNER, N., KORNMANN, B., FLEURY-OLELA, F. & SCHIBLER, U. 2000. Restricted feeding uncouples circadian oscillators in peripheral tissues from the central pacemaker in the suprachiasmatic nucleus. *Genes Dev,* 14**,** 2950-61.

DEAK, F., SCHOCH, S., LIU, X., SUDHOF, T. C. & KAVALALI, E. T. 2004. Synaptobrevin is essential for fast synaptic-vesicle endocytosis. *Nat Cell Biol,* 6**,** 1102-8.

DEAK, F., SHIN, O. H., KAVALALI, E. T. & SUDHOF, T. C. 2006. Structural determinants of synaptobrevin 2 function in synaptic vesicle fusion. *J Neurosci,* 26**,** 6668-76.

DECAVEL, C. & VAN DEN POL, A. N. 1990. GABA: a dominant neurotransmitter in the hypothalamus. *J Comp Neurol,* 302**,** 1019-37.

DEWOSKIN, D., MYUNG, J., BELLE, M. D., PIGGINS, H. D., TAKUMI, T. & FORGER, D. B. 2015. Distinct roles for GABA across multiple timescales in mammalian circadian timekeeping. *Proc Natl Acad Sci U S A,* 112**,** E3911-9.

DIBNER, C., SCHIBLER, U. & ALBRECHT, U. 2010. The mammalian circadian timing system: organization and coordination of central and peripheral clocks. *Annu Rev Physiol,* 72**,** 517-49.

DICKEN, M. S., TOOKER, R. E. & HENTGES, S. T. 2012. Regulation of GABA and glutamate release from proopiomelanocortin neuron terminals in intact hypothalamic networks. *J Neurosci,* 32**,** 4042-8.

DIEKMAN, C. O., BELLE, M. D., IRWIN, R. P., ALLEN, C. N., PIGGINS, H. D. & FORGER, D. B. 2013. Causes and consequences of hyperexcitation in central clock neurons. *PLoS Comput Biol,* 9**,** e1003196.

DREIFUSS, J. J., KALNINS, I., KELLY, J. S. & RUF, K. B. 1971. Action potentials and release of neurohypophysial hormones in vitro. *J Physiol,* 215**,** 805-17.

DUTTON, A. & DYBALL, R. E. 1979. Phasic firing enhances vasopressin release from the rat neurohypophysis. *J Physiol,* 290**,** 433-40.

ELMQUIST, J. K., BJORBAEK, C., AHIMA, R. S., FLIER, J. S. & SAPER, C. B. 1998. Distributions of leptin receptor mRNA isoforms in the rat brain. *J Comp Neurol,* 395**,** 535-47.

EVANS, J. A. & DAVIDSON, A. J. 2013. Health consequences of circadian disruption in humans and animal models. *Prog Mol Biol Transl Sci,* 119**,** 283-323.

FATT, P. & KATZ, B. 1952. Spontaneous subthreshold activity at motor nerve endings. *J Physiol,* 117**,** 109-28.

FEILLET, C. A., ALBRECHT, U. & CHALLET, E. 2006. "Feeding time" for the brain: a matter of clocks. *J Physiol Paris,* 100**,** 252-60.

FIFEL, K., MEIJER, J. H. & DEBOER, T. 2018. Long-term effects of sleep deprivation on neuronal activity in four hypothalamic areas. *Neurobiol Dis,* 109**,** 54-63.

FLOURAKIS, M., KULA-EVERSOLE, E., HUTCHISON, A. L., HAN, T. H., ARANDA, K., MOOSE, D. L., WHITE, K. P., DINNER, A. R., LEAR, B. C., REN, D., DIEKMAN, C. O., RAMAN, I. M. & ALLADA, R. 2015. A Conserved Bicycle Model for Circadian Clock Control of Membrane Excitability. *Cell,* 162**,** 836-48.

FOSTER, R. G., PEIRSON, S. N., WULFF, K., WINNEBECK, E., VETTER, C. & ROENNEBERG, T. 2013. Sleep and circadian rhythm disruption in social jetlag and mental illness. *Prog Mol Biol Transl Sci,* 119**,** 325-46.

GAINER, H., WOLFE, S. A., JR., OBAID, A. L. & SALZBERG, B. M. 1986. Action potentials and frequency-dependent secretion in the mouse neurohypophysis. *Neuroendocrinology,* 43**,** 557-63.

GARFIELD, A. S., LI, C., MADARA, J. C., SHAH, B. P., WEBBER, E., STEGER, J. S., CAMPBELL, J. N., GAVRILOVA, O., LEE, C. E., OLSON, D. P., ELMQUIST, J. K., TANNOUS, B. A., KRASHES, M. J. & LOWELL, B. B. 2015. A neural basis for melanocortin-4 receptor-regulated appetite. *Nat Neurosci,* 18**,** 863-71.

GARFIELD, A. S., SHAH, B. P., BURGESS, C. R., LI, M. M., LI, C., STEGER, J. S., MADARA, J. C., CAMPBELL, J. N., KROEGER, D., SCAMMELL, T. E., TANNOUS, B. A., MYERS, M. G., JR., ANDERMANN, M. L., KRASHES, M. J. & LOWELL, B. B. 2016. Dynamic GABAergic afferent modulation of AgRP neurons. *Nat Neurosci,* 19**,** 1628-1635.

GRACE, A. A. & BUNNEY, B. S. 1986. Induction of depolarization block in midbrain dopamine neurons by repeated administration of haloperidol: analysis using in vivo intracellular recording. *J Pharmacol Exp Ther,* 238**,** 1092-100.

GREEN, C. B., TAKAHASHI, J. S. & BASS, J. 2008. The meter of metabolism. *Cell,* 134**,** 728-42.

GUILDING, C., HUGHES, A. T., BROWN, T. M., NAMVAR, S. & PIGGINS, H. D. 2009. A riot of rhythms: neuronal and glial circadian oscillators in the mediobasal hypothalamus. *Mol Brain,* 2**,** 28.

GUILDING, C. & PIGGINS, H. D. 2007. Challenging the omnipotence of the suprachiasmatic timekeeper: are circadian oscillators present throughout the mammalian brain? *Eur J Neurosci,* 25**,** 3195-216.

GUZMAN-RUIZ, M., SADERI, N., CAZAREZ-MARQUEZ, F., GUERRERO-VARGAS, N. N., BASUALDO, M. C., ACOSTA-GALVAN, G. & BUIJS, R. M. 2014. The suprachiasmatic nucleus changes the daily activity of the arcuate nucleus alpha-MSH neurons in male rats. *Endocrinology,* 155**,** 525-35.

GUZMAN-RUIZ, M. A., RAMIREZ-CORONA, A., GUERRERO-VARGAS, N. N., SABATH, E., RAMIREZ-PLASCENCIA, O. D., FUENTES-ROMERO, R., LEON-MERCADO, L. A., BASUALDO SIGALES, M., ESCOBAR, C. & BUIJS, R. M. 2015. Role of the Suprachiasmatic and Arcuate Nuclei in Diurnal Temperature Regulation in the Rat. *J Neurosci,* 35**,** 15419-29.

HARA, R., WAN, K., WAKAMATSU, H., AIDA, R., MORIYA, T., AKIYAMA, M. & SHIBATA, S. 2001. Restricted feeding entrains liver clock without participation of the suprachiasmatic nucleus. *Genes Cells,* 6**,** 269-78.

HATORI, M., VOLLMERS, C., ZARRINPAR, A., DITACCHIO, L., BUSHONG, E. A., GILL, S., LEBLANC, M., CHAIX, A., JOENS, M., FITZPATRICK, J. A., ELLISMAN, M. H. & PANDA, S. 2012. Time-restricted feeding without reducing caloric intake prevents metabolic diseases in mice fed a high-fat diet. *Cell Metab,* 15**,** 848-60.

HENTGES, S. T., NISHIYAMA, M., OVERSTREET, L. S., STENZEL-POORE, M., WILLIAMS, J. T. & LOW, M. J. 2004. GABA release from proopiomelanocortin neurons. *J Neurosci,* 24**,** 1578-83.

HONMA, S., SHIRAKAWA, T., KATSUNO, Y., NAMIHIRA, M. & HONMA, K. 1998. Circadian periods of single suprachiasmatic neurons in rats. *Neurosci Lett,* 250**,** 157-60.

HORVATH, T. L. 2005. The hardship of obesity: a soft-wired hypothalamus. *Nat Neurosci,* 8**,** 561-5.

HORVATH, T. L., BECHMANN, I., NAFTOLIN, F., KALRA, S. P. & LERANTH, C. 1997. Heterogeneity in the neuropeptide Y-containing neurons of the rat arcuate nucleus: GABAergic and non-GABAergic subpopulations. *Brain Res,* 756**,** 283-6.

HORVATH, T. L., NAFTOLIN, F., KALRA, S. P. & LERANTH, C. 1992. Neuropeptide-Y innervation of beta-endorphin-containing cells in the rat mediobasal hypothalamus: a light and electron microscopic double immunostaining analysis. *Endocrinology,* 131**,** 2461-7.

ITRI, J., MICHEL, S., WASCHEK, J. A. & COLWELL, C. S. 2004. Circadian rhythm in inhibitory synaptic transmission in the mouse suprachiasmatic nucleus. *J Neurophysiol,* 92**,** 311-9.

JIANG, Z. G., YANG, Y., LIU, Z. P. & ALLEN, C. N. 1997a. Membrane properties and synaptic inputs of suprachiasmatic nucleus neurons in rat brain slices. *J Physiol,* 499 (Pt 1)**,** 141-59.

JIANG, Z. G., YANG, Y. Q. & ALLEN, C. N. 1997b. Tracer and electrical coupling of rat suprachiasmatic nucleus neurons. *Neuroscience,* 77**,** 1059-66.

KAESER, P. S. & REGEHR, W. G. 2014. Molecular mechanisms for synchronous, asynchronous, and spontaneous neurotransmitter release. *Annu Rev Physiol,* 76**,** 333-63.

KALSBEEK, A., FOPPEN, E., SCHALIJ, I., VAN HEIJNINGEN, C., VAN DER VLIET, J., FLIERS, E. & BUIJS, R. M. 2008. Circadian control of the daily plasma glucose rhythm: an interplay of GABA and glutamate. *PLoS One,* 3**,** e3194.

KAVALALI, E. T. 2015. The mechanisms and functions of spontaneous neurotransmitter release. *Nat Rev Neurosci,* 16**,** 5-16.

KAVALALI, E. T., CHUNG, C., KHVOTCHEV, M., LEITZ, J., NOSYREVA, E., RAINGO, J. & RAMIREZ, D. M. 2011. Spontaneous neurotransmission: an independent pathway for neuronal signaling? *Physiology (Bethesda),* 26**,** 45-53.

KETTNER, N. M., MAYO, S. A., HUA, J., LEE, C., MOORE, D. D. & FU, L. 2015. Circadian Dysfunction Induces Leptin Resistance in Mice. *Cell Metab,* 22**,** 448-59.

KIM, E. R., WU, Z., SUN, H., XU, Y., MANGIERI, L. R., XU, Y. & TONG, Q. 2015. Hypothalamic Non-AgRP, Non-POMC GABAergic Neurons Are Required for Postweaning Feeding and NPY Hyperphagia. *J Neurosci,* 35**,** 10440-50.

KONG, D., TONG, Q., YE, C., KODA, S., FULLER, P. M., KRASHES, M. J., VONG, L., RAY, R. S., OLSON, D. P. & LOWELL, B. B. 2012. GABAergic RIP-Cre neurons in the arcuate nucleus selectively regulate energy expenditure. *Cell,* 151**,** 645-57.

KONONENKO, N. I. & DUDEK, F. E. 2004. Mechanism of irregular firing of suprachiasmatic nucleus neurons in rat hypothalamic slices. *J Neurophysiol,* 91**,** 267-73.

KRASHES, M. J., KODA, S., YE, C., ROGAN, S. C., ADAMS, A. C., CUSHER, D. S., MARATOS-FLIER, E., ROTH, B. L. & LOWELL, B. B. 2011. Rapid, reversible activation of AgRP neurons drives feeding behavior in mice. *J Clin Invest,* 121**,** 1424-8.

KRASHES, M. J., SHAH, B. P., KODA, S. & LOWELL, B. B. 2013. Rapid versus delayed stimulation of feeding by the endogenously released AgRP neuron mediators GABA, NPY, and AgRP. *Cell Metab,* 18**,** 588-95.

KRASHES, M. J., SHAH, B. P., MADARA, J. C., OLSON, D. P., STROCHLIC, D. E., GARFIELD, A. S., VONG, L., PEI, H., WATABE-UCHIDA, M., UCHIDA, N., LIBERLES, S. D. & LOWELL, B. B. 2014. An excitatory paraventricular nucleus to AgRP neuron circuit that drives hunger. *Nature,* 507**,** 238-42.

KUHLMAN, S. J. & MCMAHON, D. G. 2004. Rhythmic regulation of membrane potential and potassium current persists in SCN neurons in the absence of environmental input. *Eur J Neurosci,* 20**,** 1113-7.

LAMIA, K. A., STORCH, K. F. & WEITZ, C. J. 2008. Physiological significance of a peripheral tissue circadian clock. *Proc Natl Acad Sci U S A,* 105**,** 15172-7.

LEHMAN, M. N., COOLEN, L. M. & GOODMAN, R. L. 2010. Minireview: kisspeptin/neurokinin B/dynorphin (KNDy) cells of the arcuate nucleus: a central node in the control of gonadotropin-releasing hormone secretion. *Endocrinology,* 151**,** 3479-89.

LEVINE, J. E., BETHEA, C. L. & SPIES, H. G. 1985. In vitro gonadotropin-releasing hormone release from hypothalamic tissues of ovariectomized estrogen-treated cynomolgus macaques. *Endocrinology,* 116**,** 431-8.

LEVINE, J. E. & DUFFY, M. T. 1988. Simultaneous measurement of luteinizing hormone (LH)-releasing hormone, LH, and follicle-stimulating hormone release in intact and short-term castrate rats. *Endocrinology,* 122**,** 2211-21.

LI, A. J., WIATER, M. F., OOSTROM, M. T., SMITH, B. R., WANG, Q., DINH, T. T., ROBERTS, B. L., JANSEN, H. T. & RITTER, S. 2012. Leptin-sensitive neurons in the arcuate nuclei contribute to endogenous feeding rhythms. *Am J Physiol Regul Integr Comp Physiol,* 302**,** R1313-26.

LI, C., CHEN, P. & SMITH, M. S. 1999. Morphological evidence for direct interaction between arcuate nucleus neuropeptide Y (NPY) neurons and gonadotropin-releasing hormone neurons and the possible involvement of NPY Y1 receptors. *Endocrinology,* 140**,** 5382-90.

LIU, T., KONG, D., SHAH, B. P., YE, C., KODA, S., SAUNDERS, A., DING, J. B., YANG, Z., SABATINI, B. L. & LOWELL, B. B. 2012. Fasting activation of AgRP neurons requires NMDA receptors and involves spinogenesis and increased excitatory tone. *Neuron,* 73**,** 511-22.

LONG, M. A., JUTRAS, M. J., CONNORS, B. W. & BURWELL, R. D. 2005. Electrical synapses coordinate activity in the suprachiasmatic nucleus. *Nat Neurosci,* 8**,** 61-6.

LU, X. Y., SHIEH, K. R., KABBAJ, M., BARSH, G. S., AKIL, H. & WATSON, S. J. 2002. Diurnal rhythm of agouti-related protein and its relation to corticosterone and food intake. *Endocrinology,* 143**,** 3905-15.

LYONS, D. J., HORJALES-ARAUJO, E. & BROBERGER, C. 2010. Synchronized network oscillations in rat tuberoinfundibular dopamine neurons: switch to tonic discharge by thyrotropin-releasing hormone. *Neuron,* 65**,** 217-29.

MCCARTHY, J. J., ANDREWS, J. L., MCDEARMON, E. L., CAMPBELL, K. S., BARBER, B. K., MILLER, B. H., WALKER, J. R., HOGENESCH, J. B., TAKAHASHI, J. S. & ESSER, K. A. 2007. Identification of the circadian transcriptome in adult mouse skeletal muscle. *Physiol Genomics,* 31**,** 86-95.

MENDONCA, P. R. F., KYLE, V., YEO, S. H., COLLEDGE, W. H. & ROBINSON, H. P. C. 2018. Kv4.2 channel activity controls intrinsic firing dynamics of arcuate kisspeptin neurons. *J Physiol,* 596**,** 885-899.

MENDOZA, J., PEVET, P., FELDER-SCHMITTBUHL, M. P., BAILLY, Y. & CHALLET, E. 2010. The cerebellum harbors a circadian oscillator involved in food anticipation. *J Neurosci,* 30**,** 1894-904.

MERCER, J. G., HOGGARD, N., WILLIAMS, L. M., LAWRENCE, C. B., HANNAH, L. T. & TRAYHURN, P. 1996. Localization of leptin receptor mRNA and the long form splice

variant (Ob-Rb) in mouse hypothalamus and adjacent brain regions by in situ hybridization. *FEBS Lett,* 387**,** 113-6.

MIEDA, M. & SAKURAI, T. 2011. Bmal1 in the nervous system is essential for normal adaptation of circadian locomotor activity and food intake to periodic feeding. *J Neurosci,* 31**,** 15391-6.

MISTLBERGER, R. E. 1994. Circadian food-anticipatory activity: formal models and physiological mechanisms. *Neurosci Biobehav Rev,* 18**,** 171-95.

MOORE, R. Y. & BERNSTEIN, M. E. 1989. Synaptogenesis in the rat suprachiasmatic nucleus demonstrated by electron microscopy and synapsin I immunoreactivity. *J Neurosci,* 9**,** 2151-62.

OISHI, K., AMAGAI, N., SHIRAI, H., KADOTA, K., OHKURA, N. & ISHIDA, N. 2005. Genome-wide expression analysis reveals 100 adrenal gland-dependent circadian genes in the mouse liver. *DNA Res,* 12**,** 191-202.

OLLMANN, M. M., WILSON, B. D., YANG, Y. K., KERNS, J. A., CHEN, Y., GANTZ, I. & BARSH, G. S. 1997. Antagonism of central melanocortin receptors in vitro and in vivo by agouti-related protein. *Science,* 278**,** 135-8.

OROZCO-SOLIS, R., AGUILAR-ARNAL, L., MURAKAMI, M., PERUQUETTI, R., RAMADORI, G., COPPARI, R. & SASSONE-CORSI, P. 2016. The Circadian Clock in the Ventromedial Hypothalamus Controls Cyclic Energy Expenditure. *Cell Metab,* 23**,** 467-78.

PADILLA, S. L., QIU, J., SODEN, M. E., SANZ, E., NESTOR, C. C., BARKER, F. D., QUINTANA, A., ZWEIFEL, L. S., RONNEKLEIV, O. K., KELLY, M. J. & PALMITER, R. D. 2016. Agouti-related peptide neural circuits mediate adaptive behaviors in the starved state. *Nat Neurosci,* 19**,** 734-741.

PANDA, S., ANTOCH, M. P., MILLER, B. H., SU, A. I., SCHOOK, A. B., STRAUME, M., SCHULTZ, P. G., KAY, S. A., TAKAHASHI, J. S. & HOGENESCH, J. B. 2002. Coordinated transcription of key pathways in the mouse by the circadian clock. *Cell,* 109**,** 307-20.

PENNARTZ, C. M., DE JEU, M. T., BOS, N. P., SCHAAP, J. & GEURTSEN, A. M. 2002. Diurnal modulation of pacemaker potentials and calcium current in the mammalian circadian clock. *Nature,* 416**,** 286-90.

PINTO, S., ROSEBERRY, A. G., LIU, H., DIANO, S., SHANABROUGH, M., CAI, X., FRIEDMAN, J. M. & HORVATH, T. L. 2004. Rapid rewiring of arcuate nucleus feeding circuits by leptin. *Science,* 304**,** 110-5.

PROSSER, R. A., EDGAR, D. M., HELLER, H. C. & MILLER, J. D. 1994. A possible glial role in the mammalian circadian clock. *Brain Res,* 643**,** 296-301.

PUGH, J. R. & RAMAN, I. M. 2009. Nothing can be coincidence: synaptic inhibition and plasticity in the cerebellar nuclei. *Trends Neurosci,* 32**,** 170-7.

QIU, J., FANG, Y., RONNEKLEIV, O. K. & KELLY, M. J. 2010. Leptin excites proopiomelanocortin neurons via activation of TRPC channels. *J Neurosci,* 30**,** 1560-5.

QIU, J., ZHANG, C., BORGQUIST, A., NESTOR, C. C., SMITH, A. W., BOSCH, M. A., KU, S., WAGNER, E. J., RONNEKLEIV, O. K. & KELLY, M. J. 2014. Insulin excites anorexigenic proopiomelanocortin neurons via activation of canonical transient receptor potential channels. *Cell Metab,* 19**,** 682-93.

RAMAN, I. M., GUSTAFSON, A. E. & PADGETT, D. 2000. Ionic currents and spontaneous firing in neurons isolated from the cerebellar nuclei. *J Neurosci,* 20**,** 9004-16.

RAMIREZ, D. M. & KAVALALI, E. T. 2011. Differential regulation of spontaneous and evoked neurotransmitter release at central synapses. *Curr Opin Neurobiol,* 21**,** 275-82.

RASH, J. E., OLSON, C. O., POULIOT, W. A., DAVIDSON, K. G., YASUMURA, T., FURMAN, C. S., ROYER, S., KAMASAWA, N., NAGY, J. I. & DUDEK, F. E. 2007. Connexin36 vs. connexin32, "miniature" neuronal gap junctions, and limited electrotonic coupling in rodent suprachiasmatic nucleus. *Neuroscience,* 149**,** 350-71.

REIS, W. L., YI, C. X., GAO, Y., TSCHOP, M. H. & STERN, J. E. 2015. Brain innate immunity regulates hypothalamic arcuate neuronal activity and feeding behavior. *Endocrinology,* 156**,** 1303-15.

REPPERT, S. M. & SCHWARTZ, W. J. 1984. The suprachiasmatic nuclei of the fetal rat: characterization of a functional circadian clock using 14C-labeled deoxyglucose. *J Neurosci,* 4**,** 1677-82.

RICHARD, C. D., TOLLE, V. & LOW, M. J. 2011. Meal pattern analysis in neural-specific proopiomelanocortin-deficient mice. *Eur J Pharmacol,* 660**,** 131-8.

ROENNEBERG, T., ALLEBRANDT, K. V., MERROW, M. & VETTER, C. 2012. Social jetlag and obesity. *Curr Biol,* 22**,** 939-43.

SAEB-PARSY, K., LOMBARDELLI, S., KHAN, F. Z., MCDOWALL, K., AU-YONG, I. T. & DYBALL, R. E. 2000. Neural connections of hypothalamic neuroendocrine nuclei in the rat. *J Neuroendocrinol,* 12**,** 635-48.

SAKHI, K., BELLE, M. D., GOSSAN, N., DELAGRANGE, P. & PIGGINS, H. D. 2014a. Daily variation in the electrophysiological activity of mouse medial habenula neurones. *J Physiol,* 592**,** 587-603.

SAKHI, K., WEGNER, S., BELLE, M. D., HOWARTH, M., DELAGRANGE, P., BROWN, T. M. & PIGGINS, H. D. 2014b. Intrinsic and extrinsic cues regulate the daily profile of mouse lateral habenula neuronal activity. *J Physiol,* 592**,** 5025-45.

SCHOCH, S., DEAK, F., KONIGSTORFER, A., MOZHAYEVA, M., SARA, Y., SUDHOF, T. C. & KAVALALI, E. T. 2001. SNARE function analyzed in synaptobrevin/VAMP knockout mice. *Science,* 294**,** 1117-22.

SCHWARTZ, M. W., WOODS, S. C., PORTE, D., JR., SEELEY, R. J. & BASKIN, D. G. 2000. Central nervous system control of food intake. *Nature,* 404**,** 661-71.

SHIEH, K. R., YANG, S. C., LU, X. Y., AKIL, H. & WATSON, S. J. 2005. Diurnal rhythmic expression of the rhythm-related genes, rPeriod1, rPeriod2, and rClock, in the rat brain. *J Biomed Sci,* 12**,** 209-17.

SHINOHARA, K., FUNABASHI, T., MITUSHIMA, D. & KIMURA, F. 2000. Effects of gap junction blocker on vasopressin and vasoactive intestinal polypeptide rhythms in the rat suprachiasmatic nucleus in vitro. *Neurosci Res,* 38**,** 43-7.

SIM, L. J. & JOSEPH, S. A. 1991. Arcuate nucleus projections to brainstem regions which modulate nociception. *J Chem Neuroanat,* 4**,** 97-109.

SPANSWICK, D., SMITH, M. A., MIRSHAMSI, S., ROUTH, V. H. & ASHFORD, M. L. 2000. Insulin activates ATP-sensitive K+ channels in hypothalamic neurons of lean, but not obese rats. *Nat Neurosci,* 3**,** 757-8.

STEPHAN, F. K., SWANN, J. M. & SISK, C. L. 1979. Entrainment of circadian rhythms by feeding schedules in rats with suprachiasmatic lesions. *Behav Neural Biol,* 25**,** 545-54.

SUTTON, G. M., PEREZ-TILVE, D., NOGUEIRAS, R., FANG, J., KIM, J. K., CONE, R. D., GIMBLE, J. M., TSCHOP, M. H. & BUTLER, A. A. 2008. The melanocortin-3 receptor is required for entrainment to meal intake. *J Neurosci,* 28**,** 12946-55.

THOMSON, A. M., WEST, D. C. & VLACHONIKOLIS, I. G. 1984. Regular firing patterns of suprachiasmatic neurons maintained in vitro. *Neurosci Lett,* 52**,** 329-34.

UCHIDA, H., NAKAMURA, T. J., TAKASU, N. N., TODO, T., SAKAI, T. & NAKAMURA, W. 2016. Cryptochrome-dependent circadian periods in the arcuate nucleus. *Neurosci Lett,* 610**,** 123-8.

VALENTI, O., CIFELLI, P., GILL, K. M. & GRACE, A. A. 2011. Antipsychotic drugs rapidly induce dopamine neuron depolarization block in a developmental rat model of schizophrenia. *J Neurosci,* 31**,** 12330-8.

VAN DEN POL, A. N., YAO, Y., FU, L. Y., FOO, K., HUANG, H., COPPARI, R., LOWELL, B. B. & BROBERGER, C. 2009. Neuromedin B and gastrin-releasing peptide excite arcuate nucleus neuropeptide Y neurons in a novel transgenic mouse expressing strong Renilla green fluorescent protein in NPY neurons. *J Neurosci,* 29**,** 4622-39.

VAN DEN TOP, M., LEE, K., WHYMENT, A. D., BLANKS, A. M. & SPANSWICK, D. 2004. Orexigen-sensitive NPY/AgRP pacemaker neurons in the hypothalamic arcuate nucleus. *Nat Neurosci,* 7**,** 493-4.

VANACKER, C., MOYA, M. R., DEFAZIO, R. A., JOHNSON, M. L. & MOENTER, S. M. 2017. Long-Term Recordings of Arcuate Nucleus Kisspeptin Neurons Reveal Patterned Activity That Is Modulated by Gonadal Steroids in Male Mice. *Endocrinology,* 158**,** 3553-3564.

VONG, L., YE, C., YANG, Z., CHOI, B., CHUA, S., JR. & LOWELL, B. B. 2011. Leptin action on GABAergic neurons prevents obesity and reduces inhibitory tone to POMC neurons. *Neuron,* 71**,** 142-54.

WANG, H., STORLIEN, L. H. & HUANG, X. F. 2002. Effects of dietary fat types on body fatness, leptin, and ARC leptin receptor, NPY, and AgRP mRNA expression. *Am J Physiol Endocrinol Metab,* 282**,** E1352-9.

WANG, Q., LIU, C., UCHIDA, A., CHUANG, J. C., WALKER, A., LIU, T., OSBORNE-LAWRENCE, S., MASON, B. L., MOSHER, C., BERGLUND, E. D., ELMQUIST, J. K. & ZIGMAN, J. M. 2014. Arcuate AgRP neurons mediate orexigenic and glucoregulatory actions of ghrelin. *Mol Metab,* 3**,** 64-72.

WELSH, D. K., LOGOTHETIS, D. E., MEISTER, M. & REPPERT, S. M. 1995. Individual neurons dissociated from rat suprachiasmatic nucleus express independently phased circadian firing rhythms. *Neuron,* 14**,** 697-706.

WIATER, M. F., MUKHERJEE, S., LI, A. J., DINH, T. T., ROONEY, E. M., SIMASKO, S. M. & RITTER, S. 2011. Circadian integration of sleep-wake and feeding requires NPY receptor-expressing neurons in the mediobasal hypothalamus. *Am J Physiol Regul Integr Comp Physiol,* 301**,** R1569-83.

WONG, K. Y., DUNN, F. A. & BERSON, D. M. 2005. Photoreceptor adaptation in intrinsically photosensitive retinal ganglion cells. *Neuron,* 48**,** 1001-10.

YANG, S., LIU, A., WEIDENHAMMER, A., COOKSEY, R. C., MCCLAIN, D., KIM, M. K., AGUILERA, G., ABEL, E. D. & CHUNG, J. H. 2009. The role of mPer2 clock gene in glucocorticoid and feeding rhythms. *Endocrinology,* 150**,** 2153-60.

YANG, Y., ATASOY, D., SU, H. H. & STERNSON, S. M. 2011. Hunger states switch a flip-flop memory circuit via a synaptic AMPK-dependent positive feedback loop. *Cell,* 146**,** 992-1003.

YI, C. X., VAN DER VLIET, J., DAI, J., YIN, G., RU, L. & BUIJS, R. M. 2006. Ventromedial arcuate nucleus communicates peripheral metabolic information to the suprachiasmatic nucleus. *Endocrinology,* 147**,** 283-94.

ZHAN, C., ZHOU, J., FENG, Q., ZHANG, J. E., LIN, S., BAO, J., WU, P. & LUO, M. 2013. Acute and long-term suppression of feeding behavior by POMC neurons in the brainstem and hypothalamus, respectively. *J Neurosci,* 33**,** 3624-32.

ZHANG, E. E., LIU, Y., DENTIN, R., PONGSAWAKUL, P. Y., LIU, A. C., HIROTA, T., NUSINOW, D. A., SUN, X., LANDAIS, S., KODAMA, Y., BRENNER, D. A., MONTMINY, M. & KAY, S. A. 2010. Cryptochrome mediates circadian regulation of cAMP signaling and hepatic gluconeogenesis. *Nat Med,* 16**,** 1152-6.

ZHANG, L., PTACEK, L. J. & FU, Y. H. 2013. Diversity of human clock genotypes and consequences. *Prog Mol Biol Transl Sci,* 119**,** 51-81.

ZHANG, X. & VAN DEN POL, A. N. 2015. Dopamine/Tyrosine Hydroxylase Neurons of the Hypothalamic Arcuate Nucleus Release GABA, Communicate with Dopaminergic and Other Arcuate Neurons, and Respond to Dynorphin, Met-Enkephalin, and Oxytocin. *J Neurosci,* 35**,** 14966-82.

ZHANG, X. & VAN DEN POL, A. N. 2016. Hypothalamic arcuate nucleus tyrosine hydroxylase neurons play orexigenic role in energy homeostasis. *Nat Neurosci,* 19**,** 1341-7.